Master's thesis

NTNU
Norwegian University of Science and Technology
Faculty of Engineering
Department of Marine Technology

Nikolai Hammer

Area Crest Height Extremes Versus Point Extremes

Master's thesis in Marine Technology
Supervisor: Sverre K. Haver
July 2019

NTNU
Norwegian University of
Science and Technology

Nikolai Hammer

Area Crest Height Extremes Versus Point Extremes

Master's thesis in Marine Technology
Supervisor: Sverre K. Haver
July 2019

Norwegian University of Science and Technology
Faculty of Engineering
Department of Marine Technology

NTNU
Norwegian University of
Science and Technology

Master's thesis text

Area Crest Height Extremes Versus Point Extremes

Student: Nikolai Hammer

Background

For a fixed platform e.g., a jacket it is often required that major wave-deck impacts should be avoided. A simple approach for achieving this is to require that the air-gap shall be larger than the 10^{-4} annual probability crest height plus the 10^{-4} annual probability storm surge. Air-gap is height from mean still water level to underside of cellar deck. When estimating the 10^{-4} annual probability crest height a point consideration is usually done. However, the projection of the platform deck on the sea surface could well be an area of 1000 - 1600 m^2. It is the largest crest height inside this area during a 10000-year return period that is of concern. This is likely to be slightly larger than the point estimate. In this thesis the aim is to indicate the difference between a point extreme value and an area extreme corresponding to the same annual exceedance probability.

Focus in this thesis shall be area effect for a fixed platform. For a floater, e.g. a semi-submersible, platform motions and diffraction effects will disturb the wave field under the deck considerably. The size of area of possible extremes may be considerably reduced. A brief discussion of this should be done in the introduction part of the thesis.

Sub tasks

1. Estimate extremes for significant wave height and associated spectral peak period for a Norwegian sea location based on available literature. Select 10^{-2} - and 10^{-4} - annual probability conditions to be used in area effect investigation.
2. Consider a quadratic area 40m x 40m for the introductory investigation. Select a sea state corresponding to a 10^{-2} annual probability of being exceeded. Investigate if the area effect is depending on
   - Gaussian surface versus second order surface using long crested sea.
   - Storm duration of 3 hours versus duration of 1 hour.

   Conclude what is to be preferred for the investigation of area effect.
3. Investigate if area effect depends on significant wave height by comparing results for 10^{-2} and 10^{-4} annual probability significant wave height using the same peak period.
4. Investigate area effect by varying spectral peak period within a 90% band for the 10^{-2} annual probability significant wave height. Investigate robustness of estimated area effect by doing many repeats with different random numbers
5. Investigate effect of spread sea using exponent, n, in cos^n formulation from to 2, 4 and 10.

6. For one of the cases above, show results for two additional deck projections:

   - 40m x 60m
   - 40m x 80m

   Direction of wave propagation is parallel to long side of the projection.

The candidate may of course select another scheme as the preferred approach for solving the requested problem. He may also involve other subjects than those mentioned above if found to be important for answering the area effect.

The work may show to be more extensive than anticipated. Some topics may therefore be left out after discussion with the supervisor without any negative influence on the grading.

The candidate should in his report give a personal contribution to the solution of the problem formulated in this text. All assumptions and conclusions must be supported by mathematical models and/or references to physical effects in a logical manner. The candidate should apply all available sources to find relevant literature and information on the actual problem.

The report should be well organized and give a clear presentation of the work and all conclusions. It is important that the text is well written, and that tables and figures are used to support the verbal presentation. The report should be complete, but still as short as possible.

The final report must contain this text, an acknowledgment, summary, main body, conclusions, suggestions for further work, symbol list, references and appendices. All figures, tables and equations must be identified by numbers. References should be given by author and year in the text and presented alphabetically in the reference list. The report must be submitted in two copies unless otherwise has been agreed with the supervisor/department.

The supervisor may require that the candidate should give a written plan that describes the progress of the work mid-semester. The plan may contain a table of content for the report. A planned scheme for the remaining work should also be included. For this thesis, such a plan should be available by Easter.

From the report it should be possible to identify the work carried out by the candidate and what has been found in the available literature. It is important to give references to the original source for theories and experimental results.

The report must be signed by the candidate, include this text, appear as a paperback, and - if needed - have a separate enclosure (binder, diskette or CD-ROM) with additional material.

Supervisor: Sverre K. Haver, NTNU.

Preface

This master thesis have been conducted at the Department of Marine Technology at the Norwegian University of Science and Technology (NTNU) in Trondheim. The writing of this master thesis have been done during the spring semester and the summer of 2019. The topic and the scope for this thesis have been formulated by Professor Sverre Haver. The choice of this topic was made based on my own personal interest.

I would like to specially thank my supervisor Professor Sverre K. Haver for all good help and guidance during this thesis work. Professor Sverre K. Haver has shown great interest in the topic of this thesis, and he has through regular meeting activity and discussions with me shared his knowledge and ideas, and made it possible to have good progress in the thesis work. I wish you the best for your retirement.

Trondheim
July 6, 2019

Nikolai Hammer

Abstract

In this thesis, the area effect for crest heights is investigated. That is, the relationship between the largest crest height within an area and the largest crest height at a single point within that same area during a given time period. For the investigation of the area effect, a MATLAB program is made for time domain simulation of Gaussian and second order surface elevation processes. A thorough verification procedure and convergence studies is performed on the MATLAB program, and the maximum crest heights obtained from simulations. Simulations using both deterministic and Rayleigh distributed random wave amplitudes are performed and compared to probability functions.

The sea state used as a basis for all simulations is a sea state corresponding to a 10^{-2} annual probability of being exceeded at Statfjord oil field, outside the west coast of Norway. The sea state is found as the worst sea state regarding crest heights along the 100-year contour line. The JONSWAP wave spectrum, which is a wave spectrum for growing wind sea is found to be the best wave spectrum to describe this sea state, and is therefore used in all simulations.

The first analysis is this thesis is a comparison analysis of the area effect from Gaussian and second order simulations. Long crested sea is used for the analysis. Results for the area effect as a function of percentile value are presented for both simulation methods and for different sea state durations. The results for the mean area effect and the mean area effect from the 75th percentile value to the 100th percentile value are presented and compared between the two simulation methods. Based on the results from this analysis, a choice of surface elevation process is made for the main analysis of this thesis. Due to extensive simulation time for second order simulations, Gaussian simulations are chosen for the main analysis. It is also concluded that the results obtained for the area effect using Gaussian simulations are expected to be credible.

The main analysis in this thesis is an analysis to investigate the area effect with variations in different sea state parameters. Short crested sea is used in the analysis. Only one parameter will be changed at a time, while all other parameters are fixed. For each variation in parameter, results for the mean area effect and the 90th percentile area effect are presented. The results shows that neither variations in the significant wave height nor variations in the mean wave direction do seem to have any influence on the area effect. The results also shows that variations in the spectral peak period, the directional spectrum shape factor, the sea state duration and the area size clearly do have influence on the area effect.

An additional analysis is also done to complement the results from the main analysis, as well as to look at the locations of the area maximums for the analyzed area. The results concur with the results from the main analysis. The results also show that the area maximums are most probable to occur at the area edges and especially at the corners for the analyzed area.

The results from the analyses clearly indicates that the area effect is an important factor to consider when estimating crest maximums for any area larger than a point. The difference between area maximums and point maximums obtained from simulations are large, even for areas small in size. The results also indicate that the area effect is smaller at a 90th percentile level than when calculated as a mean. This is important, since the higher percentile values such as the 90th percentile value are commonly the values of interest when estimating extremes.

Sammendrag

I denne oppgaven har områdeeffekten for bølgetopper blitt undersøkt. Det vil si, forholdet mellom den største bølgetoppen innenfor et område og den største bølgetoppen ved et enkelt punkt innenfor det samme området i løpet av en gitt tidsperiode. For undersøkelsen av områdeeffekten er et MATLAB-program laget for tidsdomene-simulering av Gaussiske og annenordens overflatehevingsprosesser. En grundig verifiseringsprosedyre og konvergensstudier er gjort for MATLAB-programmet, og de maksimale bølgetoppene fra simuleringer. Simuleringer med både deterministiske og Rayleigh-distribuerte tilfeldige bølgeamplituder er utført og sammenlignet med sannsynlighetsfordelinger.

Grunnsjøtilstanden brukt for alle simuleringer er en sjøtilstand som korresponderer til en 10^{-2} årlig sannsynlighet for å bli oversteget ved Statfjordfeltet, utenfor vestkysten av Norge. Sjøtilstanden er funnet som den verste sjøtilstanden når det gjelder bølgetopper langs 100-års konturlinjen. JONSWAP bølgespekteret, som er et bølgespekter for voksende vindsjø er ansett å være det beste bølgespekteret til å beskrive denne sjøtilstanden, og er derfor benyttet i alle simuleringer.

Den første analysen i denne oppgaven er en sammenligningsanalyse for områdeeffekten fra Gaussiske og annenordens simuleringer. Langkammet sjø er benyttet for analysen. Resultater for områdeeffekten som funksjon av persentil-verdi er presentert for begge simuleringsmetoder, og for forskjellige sjøtilstands varigheter. Resultatene for den gjennomsnittlige områdeeffekten og den gjennomsnittlige områdeeffekten fra 75. persentil-verdi til 100. persentil-verdi er presentert og sammenlignet mellom de to simuleringsmetodene. Basert på resultatene fra denne analysen er et valg gjort for overflatehevingsprosess for hoved-analysen i oppgaven. Det er også konkludert med at resultatene for områdeeffekten ved bruk av Gaussiske simuleringer er forventet å være troverdige.

Hovedanalysen i denne oppgaven er en analyse for å undersøke områdeeffekten med variasjoner i forskjellige sjøtilstands-parametere. Kortkammet sjø er brukt i analysen. Kun en parameter vil bli endret om gangen, mens alle andre parametere er fastsatte. For hver variasjon i parameter er resultater for den gjennomsnittlige områdeeffekten og 90. persentil områdeeffekten presentert. Resultatene viser at hverken varisjoner i den signifikante bølgehøyden eller varisjoner i den gjennomsnittlige bølgeretningen virker å ha innvirkning på områdeeffekten. Resultatene viser også at variasjoner i topp-perioden for spektrumet, formfaktoren til retningsspekteret, sjøtilstandsvarigheten og områdestørrelsen klart har innvirkning på områdeeffekten.

En tilleggsanalyse er også gjort for å komplementere resultatene for hovedanalysen, samt for å se på beliggenheten av områdemaksimumene for det analyserte området. Resultatene samstemmer med resultatene fra hovedanalysen. Resultatene viser også at områdemaksimumene har størst sannsynlighet for å inntreffe ved sidekantene på området og da spesielt på hjørnene for det analyserte området.

Resultatene fra analysene indikerer klart at områdeeffekten er en viktig faktor å ta hensyn til for å estimere toppmaksimumer for ethvert område større enn et punkt. Forskjellen mellom områdemaksimumer og punktmaksimumer fra simuleringer er store, selv for områder av liten størrelse. Resultatene indikerer også at områdeeffekten er mindre på et 90. persentil-nivå enn når regnet ut som et snitt. Dette er viktig, siden de høyere persentil-verdiene slik som 90. persentil-verdien er vanligvis verdiene av interesse når ekstremer skal estimeres.

Contents

List of Tables

List of Figures

Abbreviations

CDF = cumulative distribution function
CPU = Central processing unit
DNV = Det Norske Veritas
HR = High resolution
JONSWAP = Joint North Sea Wave Observation Project
LC = long crested
SC = short crested

Nomenclature

Latin letters

d	Water depth
dt	Time step
dx	Area grid spacing in x-direction
dy	Area grid spacing in y-direction
$d\theta$	Infinitesimal distance between spreading angles
$D(\theta_m)$	Directional spectrum as a function of θ_m
f_{max}	Maximum cutoff frequency for wave spectrum
f_n	Frequency component n
f_p	Peak frequency corresponding to H_s
$F_D(\theta_m)$	CDF for directional spreading of spreading component m
$F_D(\theta_n)$	CDF for directional spreading of wave component n
$F_{\Xi_{An}}(\xi_{An}$	Rayleigh CDF for surface elevation amplitude ξ_{An}
$F_{\Xi^{(1)}_{c,point}}$	Rayleigh CDF for Gaussian zero crossing crest heights
$F_{\Xi^{(2)}_{c,point}}$	Forristall CDF for second order zero crossing crest heights
$F_{\Xi^{(1)}_{max,point,T}}$	Extreme value distribution for maximum Gaussian crest height
$F_{\Xi^{(2)}_{max,point,T}}$	Extreme value distribution for maximum second order crest height
$\hat{F}_{\Xi^{(1)}_{max}}$	Gaussian empirical distribution function
$\hat{F}_{\Xi^{(2)}_{max}}$	Second order empirical distribution function
g	Gravitational constant
H_s	Significant wave height
$H_{s,100}$	Significant wave height with an annual probability of exceedance of 10^-2
$H_{s,10000}$	Significant wave height with an annual probability of exceedance of 10^-4
i	x coordinate number
i_{hr}	High resolution x coordinate number
j	y coordinate number
j_{hr}	High resolution y coordinate number
k	Time parameter number
k_{hr}	High resolution time parameter number
k_n	Wave number for frequency component n
k_{n_1}	Wave number for frequency component n_1
k_{n_2}	Wave number for frequency component n_2
k_s	Number of sorted maximum crest height in sample
k_1	Wave number corresponding to mean wave period T_1
m	Directional component number
m_0	Variance of Gaussian surface elevation process
$m_{0,n}$	Variance in wave component n
$m_{0,input}$	Input variance to wave spectrum
$m_{0,realization}$	Variance from realization of surface elevation process
n	Frequency/wave component number
n_d	Directional spectrum shape parameter
n_1	Second order frequency component number
n_2	Second order frequency component number
N_f	Number of frequency components in wave spectrum
N_{sample}	Size of sample of maximum crest heights

N_{sim}	Number of simulations
N_t	Number time parameter values
$N_{t_{hr}}$	Number of high resolution time parameter values
N_x	Number of x coordinates
$N_{x_{hr}}$	Number of high resolution x coordinates
N_y	Number of y coordinates
$N_{y_{hr}}$	Number of high resolution y coordinates
N_θ	Number of directional components
$N_{\xi^{(1)}_{c,point,T}}$	Number of individual Gaussian zero crossing crest heights
$N_{\xi^{(2)}_{c,point,T}}$	Number of individual second order zero crossing crest heights
$S(f)$	JONSWAP wave spectrum as a function of frequency f
$S(f_n)$	JONSWAP wave spectrum as a function of frequency component f_n
$S(f_n, \theta_m)$	Combined wave and directional spectrum
S_1	Steepness parameter
$S(\omega)$	JONSWAP wave spectrum as a function of angular frequency ω
$S(\omega_n)$	JONSWAP wave spectrum as a function of angular frequency component ω_n
$S(\omega_n, \theta_m)$	Combined wave and directional spectrum
t	Simulation duration
t_k	Time parameter k
$t_{k_{hr}}$	High resolution time parameter k_{hr}
t_{max}	Largest value of time parameter
$t_{max,point}$	Time parameter value at center point maximum
$t_{max,area}$	Time parameter value at area maximum
T	Time period
T_p	Spectral peak period
T_z	Zero up crossing time period
T_1	Mean wave period
U_{rs}	Ursell number
x	Length of area in x direction
x_{center}	Center x coordinate
x_i	Spatial x coordinate i
$x_{i_{hr}}$	High resolution spatial x coordinate i_{hr}
x_{max}	Largest x coordinate
$x_{max,area}$	x coordinate of area maximum
x_{min}	Smallest x coordinate
y	Length of area in y direction
y_{center}	Center y coordinate
y_j	Spatial y coordinate j
$y_{j_{hr}}$	High resolution spatial y coordinate j_{hr}
y_{max}	Largest y coordinate
$y_{max,area}$	y coordinate of area maximum
y_{min}	Smallest y coordinate

Greek letters

α	Area crest height effect
α_{mean}	Mean area crest height effect
α_{90p}	90th percentile area crest height effect

$\alpha^{(1)}$	Gaussian area crest height effect
$\alpha^{(1)}_{mean}$	Gaussian mean area crest height effect
$\alpha^{(1)}_{xp}$	Gaussian x percentile area crest height effect
$\alpha^{(1)}_{75p-100p}$	Gaussian mean area effect from 75th to 100th percentile
$\alpha^{(1)}_{90p}$	Gaussian 90th percentile area crest height effect
$\alpha^{(2)}$	Second order area crest height effect
$\alpha^{(2)}_{mean}$	Second order mean area crest height effect
$\alpha^{(2)}_{xp}$	Second order x percentile area crest height effect
$\alpha^{(2)}_{75p-100p}$	Second order mean area effect from 75th to 100th percentile
$\alpha^{(2)}_{90p}$	Second order 90th percentile area crest height effect
$\alpha_{c,lc}$	Weibull parameter for long crested sea
$\alpha_{c,sc}$	Weibull parameter for short crested sea
$\beta_{c,lc}$	Weibull parameter for long crested sea
$\beta_{c,sc}$	Weibull parameter for short crested sea
β_n	Rayleigh distribution parameter
β_{n_1}	Surface elevation process parameter for frequency component n_1
β_{n_2}	Surface elevation process parameter for frequency component n_2
γ	JONSWAP wave spectrum peak shape parameter
Γ	Gamma function
Δ_f	Distance between frequency components
$\Delta\theta$	Distance between spreading angles
$\Delta\xi^{(2)}$	Second order surface elevation correction
$\Delta\xi^{(2)}_1$	Second order surface elevation correction 1
$\Delta\xi^{(2)}_2$	Second order surface elevation correction 2
$\Delta\xi^{(2)}_3$	Second order surface elevation correction 3
Δ_ω	Distance between angular frequency components
ϵ_n	Random phase parameter
θ_m	Spreading angle number m
θ_n	Spreading angle number n
θ_0	Mean wave direction
$\mu(\xi)$	Mean surface elevation
ξ	Surface elevation process
ξ_{An}	Wave amplitude for frequency component n
ξ_{An_1}	Wave amplitude for frequency component n_1
ξ_{An_2}	Wave amplitude for frequency component n_2
$\xi_{max,area}$	Maximum area crest height
$\xi_{max,point}$	Maximum center point crest height
$\xi^{(1)}$	Gaussian surface elevation process
$\xi^{(1)}_{c,point}$	Gaussian zero crossing crest height
$\xi^{(1)}_{max,area}$	Gaussian maximum area crest height
$\xi^{(1)}_{max,n}$	Sorted Gaussian maximum crest height n
$\xi^{(1)}_{max,point}$	Gaussian maximum point crest height
$\xi^{(1)}_{max,point,90p}$	Gaussian maximum point crest height at 90th percentile level
$\xi^{(2)}$	Second order surface elevation process
$\xi^{(2)}_{c,point}$	Second order zero crossing crest height

$\xi^{(2)}_{max,area}$	Second order maximum area crest height
$\xi^{(2)}_{max,n}$	Sorted second order maximum crest height n
$\xi^{(2)}_{max,point}$	Second order maximum point crest height
$\xi^{(2)}_{max,point,90p}$	Second order maximum point crest height at 90th percentile level
π	Mathematical constant
ρ	Density of sea water
σ	Spectral width parameter
ω_n	Angular frequency component n
ω_p	Angular peak frequency corresponding to H_s

1 Introduction

When doing air gap assessments for fixed platforms, the maximum point crest height at a given annual exceedance probability is commonly used. What is more interesting for the air gap problem, is the maximum crest height within the area of the platform deck at that same annual exceedance probability. The maximum area crest height is the most probable wave crest to hit the underside of the platform deck structure. The maximum area crest height also represent the largest statistical damage potential. Since metocean data usually only contains information for a single point, the maximum area crest height for a given annual exceedance probability cannot be found directly from statistical models such as the maximum point crest height for a given annual exceedance probability.

A well known approach for estimating area maximums is by using time domain simulations of the ocean surface. The simplest way of describing irregular ocean waves is to use Gaussian wave theory. Gaussian time domain simulations of short crested sea states are created by super positioning of multiple sinusoidal free dispersive wave components at different directional angles. Gaussian simulations requires significantly less CPU-time than simulations of higher order wave theories such as second order wave theory. Second order simulations includes a lot more wave components, and therefore, it also requires a lot more CPU-time. Second order simulations are created with both free dispersive and bound waves. The result of this is that the second order waves have narrower and higher wave crests and wider and less negative wave troughs, compared to Gaussian waves.

Maximum crest heights obtained from second order simulations have shown to give close resemblance to maximum crest heights obtained from measurements for both deep and shallow water (Forristall (2000)). Maximum crest heights obtained from Gaussian simulations are significantly smaller than those obtained from measurements. Despite of this, Forristall (2011) and Forristall (2015) showed that using computer simulations of Gaussian surface elevation processes when estimating the area effect for crest heights gave good agreement to measurements made in wave basin tests. Forristall (2006) used Gaussian simulations to calculate the area effect for variations in area size, and stated that using second order simulations to investigate the area effect for crest heights are not necessary. Hagen et al. (2018) simulated extreme sea states for a location on the Norwegian continental shelf, and results showed that the area effect obtained from second order simulations exceeds the area effect obtained from Gaussian simulations for a platform sized area for both short and long crested sea states.

The disturbance of the wave field underneath a platform is determined by the presence and size of under water structural parts such as pontoons or platform legs. When the dimensions of underwater structural parts are large relative to the lengths of incoming waves, diffraction effects become dominant (Greco (2012) and Faltinsen (1993)), and the wave field underneath a platform will be disturbed. Fixed platforms like jackets or jack-ups have small diameter platform legs relative to the wave length when in a storm condition. The diffraction effect in such a case will not cause relevant disturbance in the wave field present. Therefore, neglecting the presence of the platform legs when simulating a sea state, will only lead to minimum errors in the obtained crest heights relative to real conditions. Semi submersible platforms have large diameter legs for stability reasons in addition to underwater pontoons, which causes heavily diffraction effects, and therefore, large disturbances of the wave field underneath the platform will be present. Other types of floating platforms will also have a large body diameter around the water line for stability reasons. Floating platforms will also move when subjected to waves,

which will generate outgoing waves in addition to variating deck elevation relative to mean sea level. Therefore, when doing air gap assessments for floating platforms, diffraction effects, body movement and waves from body movement have to be considered. Advanced hydrodynamic software can be used to account for these effects. However, this is beyond the scope of this thesis work. The scope of this thesis is limited to investigate the area effect for crest heights under undisturbed conditions.

For the investigation of the area effect, a MATLAB program is made for simulation of Gaussian and second order surface elevation processes. A thorough verification procedure and convergence studies is performed to validate the MATLAB program, and the maximum crest heights obtained from simulations. Simulations using both deterministic and Rayleigh distributed random wave amplitudes are performed and compared to probability functions. A comparison analysis of the area effect from Gaussian and second order simulations for a long crested sea state is done. Based on this comparison analysis, a choice of surface process is made for the main analysis of this thesis, which is an analysis to investigate the area effect obtained with variations in different sea state parameters for a short crested sea state corresponding to a 10^{-2} annual probability of being exceeded for a location in the North sea.

2 MATLAB program for simulation of surface elevation process

2.1 JONSWAP wave spectrum

2.1.1 About JONSWAP wave spectrum

When simulating a stationary irregular long created sea state, the sea state can be described solely by a wave spectrum. The wave spectrum is a spectral density function which holds information about the variance in a sea state. Wave amplitudes, at different frequencies are found directly from the wave spectrum. There exists many different standardized wave spectra, and these standardized spectra only describe some form of average fit for a given sea state. A wave spectrum obtained from measurements over a time period will contain random noise. This naturally occurring noise is smoothed out in standardized spectra. Different wave spectra should be used for different geographical areas and for different weather conditions.

The sea states considered in this thesis are pure wind induced extreme sea states without any additionally swell sea. The most preferable wave spectrum to model wind induced extreme sea states is the JONSWAP wave spectrum (NORSOK STANDARD N-003 (2007)). JONSWAP is an abbreviation for Joint North Sea Wave Observation Project, and the spectrum was originally created by Hasselmann et al. (1973) and has been modified since then. The JONSWAP spectrum is based on a Pierson-Moskovitz spectrum but contains an additional peak enhancement factor γ.

2.1.2 Assumptions for JONSWAP wave spectrum

The JONSWAP spectrum is for growing wind sea, which means that the magnitude of the waves will grow over distance and time and therefore, the spectrum will also change over a given time period. The spectrum is however assumed to be stationary over any analyzed time period, and all spectrum properties are independent of spatial coordinates. It is also assumed that the sea conditions of interest can be fully described by the JONSWAP wave spectrum.

2.1.3 Creating JONSWAP wave spectrum

Formulas 1, 2 and 3 are obtained from RP-C205 (2010) and are used to calculate the JONSWAP wave spectrum S as a function of angular frequency components ω_n.

$$S(\omega_n) = \frac{5}{16} H_s^2 \omega_p^4 \omega_n^{-5} exp\Big\{ -\frac{5}{4}(\frac{\omega_n}{\omega_p})^{-4} \Big\} \Big(1 - 0.287 ln(\gamma)\Big) \gamma^{exp\Big\{-0.5(\frac{\omega_n - \omega_p}{\sigma\omega_p})^2\Big\}} \tag{1}$$

$$, where\ \omega_n \geq 0 \quad , for\ n = 1, 2, ..., N_f$$

where H_s is significant wave height and T_p is the mean peak period corresponding to H_s. N_f is the number of frequency components in the wave spectrum. All frequency intervals are of the same magnitude. The spectral width parameter σ has the following two equations

$$\sigma = 0.07\ for\ \omega <= \omega_p \tag{2}$$

$$\sigma = 0.09\ ; for\ \omega > \omega_p \tag{3}$$

The angular peak frequency ω_p and the spectral peak period T_p have the relation

$$\omega_p = \frac{2\pi}{T_p} \tag{4}$$

The non-dimensional peak shape parameter γ is calculated as given in Torsethaugen (1993) for wind dominated sea

$$\gamma = 42.2(\frac{2\pi H_s}{gT_p^2})^{\frac{6}{7}} \tag{5}$$

The relationship between the JONSWAP spectrum for frequencies given in $[hz]$ and for angular frequencies given in $[rad]$ is as for any other wave spectrum, and can be calculated with the following formula.

$$S(f_n) = 2\pi S(\omega_n) \tag{6}$$

$$, where \;\; f_n \geq 0 \;\; , for \;\; n = 1, 2, ..., N_f$$

The relationship between the angular frequency ω_n and the frequency f_n is defined as

$$\omega_n = 2\pi f_n \tag{7}$$

For further calculations, the JONSWAP wave spectrum will be used both as a function of angular frequency ω_n and as a function of frequency f_n, $for\ n = 1, 2, ..., N_f$. Figure 1 shows the JONSWAP wave spectrum $S(f_n)$ as a function of frequency f_n for two different sea states.

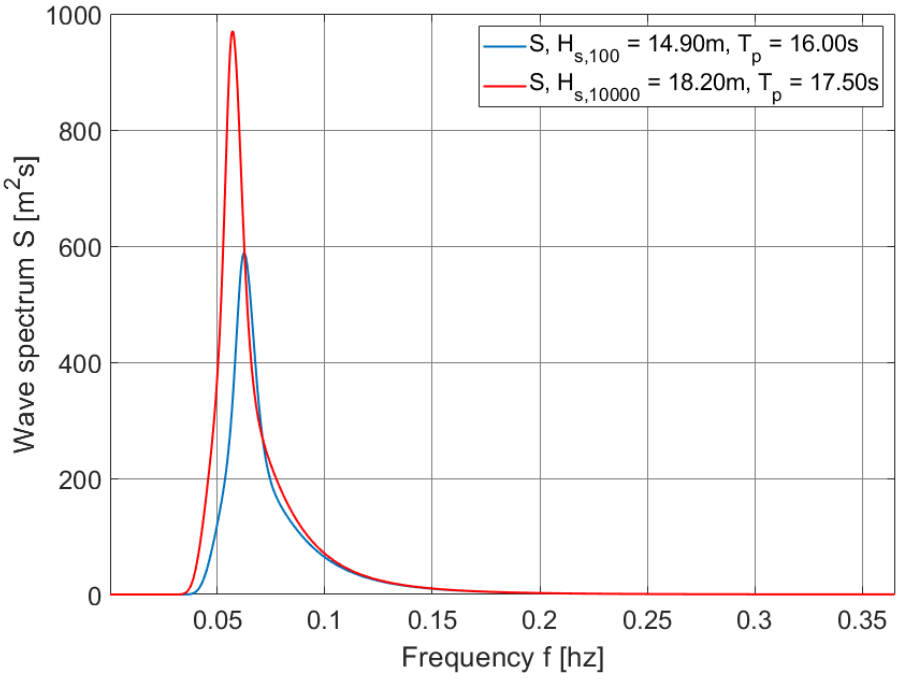

Figure 1: *JONSWAP wave spectrum for two different sea states.*

2.1.4 Simplifications made in MATLAB for JONSWAP wave spectrum

When calculating the JONSWAP wave spectrum, a finite number of frequency components N_f is used. The number N_f affects the calculation time for the surface elevation process which will be used to find area and point maximums. If the number of frequency components is small, the JONSWAP wave spectrum will be jagged when modeled in MATLAB, this will especially affect the shape of the spectrum peak. For the variance of the simulated sea state to be the same as the variance in the wave spectrum, the number of frequency components have to be large. The number of frequency components used, also affects the randomness of the surface elevation process. The number of frequency components used in the wave spectrum will be discussed further in a parameter study for Gaussian and second order simulations in section 6.

The JONSWAP wave spectrum is defined for $f_n \geq 0$. The wave spectrum goes towards zero when f_n goes towards ∞. When modeled in MATLAB, the wave spectrum has to have a maximum frequency for which the wave spectrum is calculated. This maximum boundary frequency for the wave spectrum is denoted f_{max} and will also be discussed further in the parameter study for Gaussian and second order simulations in section 6.

2.2 Directional spectrum

2.2.1 About directional spectrum

The JONSWAP wave spectrum in section 2.1.3 can only be used to simulate long crested sea states. To account for short crestedness of the sea, a directional spectrum have to be implemented. Since wind induced extreme sea states without any additionally swell sea are the sea states of interest, all frequency components in the wave spectrum are assumed to share the same directional spectrum. The directional spectrum is chosen based on recommendations made by RP-C205 (2010) for wind sea conditions. This directional spectrum will be used for all further calculations involving wave directions in this thesis.

2.2.2 Assumptions for directional spectrum

The directional spectrum is assumed independent from frequency. In general, waves around the spectral peak frequency of the wave spectrum will have a narrower distribution of spreading than waves at higher or lower frequencies than the spectral peak frequency of the spectrum. It is further assumed that the mean wave direction θ_0 is constant for all frequencies. Under real wind induced sea conditions the mean wave direction θ_0 is expected to change with frequency (Haver (2017)).

2.2.3 Creating directional spectrum

The equation for the directional spectrum $D(\theta_m)$ as a function of spreading angle θ_m is obtained from RP-C205 (2010) and is given in equation 8.

$$D(\theta_m) = \frac{\Gamma(1+\frac{n_d}{2})}{\sqrt{\pi}\Gamma(\frac{1}{2}+\frac{n_d}{2})} cos^{n_d}(\theta_m - \theta_0) \tag{8}$$

$$where, \ \mid \theta_m - \theta_0 \mid \leq \frac{\pi}{2} \ \ , for\ m = 1, 2, ..., N_\theta$$

,where Γ is the Gamma function, n_d is the shape parameter, θ_0 is the mean wave direction and N_θ is the total number of directional components. When N_θ is large enough, equation 9 will be fulfilled.

$$\sum_{m=1}^{N_\theta} D(\theta_m)\Delta\theta \approx 1 = \int_{-\pi/2}^{\pi/2} D(\theta)d\theta \tag{9}$$

, where $\Delta\theta$ is the distance between calculated spreading angles, $D(\theta)$ is the analytical version of the directional spectrum and $d\theta$ is an infinitesimal distance between spreading angles. When the condition in equation 9 is fulfilled, since all wave components share the same directional spectrum, we can now write the combined wave spectrum and directional spectrum as.

$$S(\omega_n, \theta_m) = S(\omega_n)D(\theta_m) \tag{10}$$

$$, where\ \omega_n \geq 0 \quad , for\ \ n = 1, 2, ..., N_f$$

$$, and \mid \theta_m - \theta_0 \mid \leq \frac{\pi}{2} \quad , for\ m = 1, 2, ..., N_\theta$$

The same holds for the combined wave spectrum and directional spectrum as a function of f_n and θ_m

$$S(f_n, \theta_m) = S(f_n)D(\theta_m) \tag{11}$$

$$, where\ \ f_n \geq 0 \quad , for\ \ n = 1, 2, ..., N_f$$

$$, and \mid \theta_m - \theta_0 \mid \leq \frac{\pi}{2} \quad , for\ m = 1, 2, ..., N_\theta$$

As seen in equation 10 and 11, the combined wave and directional spectrum will now have $N_f N_\theta$ components. The directional spectrum $D(\theta_m)$ for six different values of the shape parameter n_d is shown in figure 2

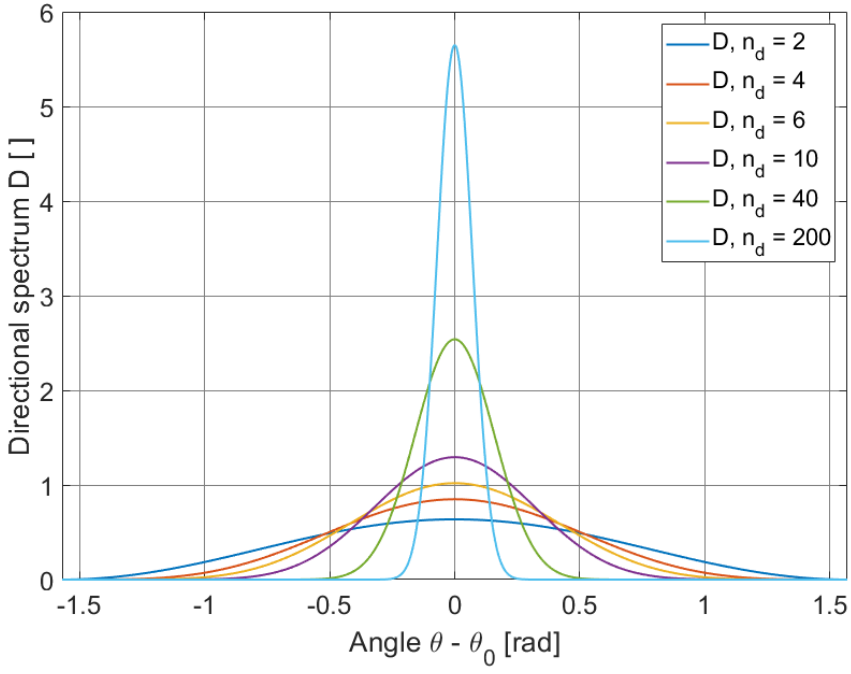

Figure 2: *Directional spectrum for six different shape parameters n_d.*

2.2.4 Probabilistic modeling of wave directions

The way of modeling a short crested sea state with combined wave and directional spectrum as described in section 2.2.3 with the use of equation 10, means that there will be a total number of wave components in the combined spectrum equal to $N_f N_\theta$. Another way of modeling the implementation of directional spreading is to use the directional spectrum as a probabilistic model for the wave direction for each wave component generated from the wave spectrum. This will decrease the total number of wave components to N_f, the same number as when a long crested sea is modeled. Reducing the total number of wave components will substantially decrease computation time in MATLAB later on when the sea surface is to be modeled based on the wave spectrum and the directional spectrum. Using the directional spectrum as a probabilistic model for the direction of each wave component in the wave spectrum is the method that will be used further on in this thesis. Since the integral of the spreading spectrum equals one as seen in equation 9, we can rewrite the equation to model the integral of the directional spectrum as a function of θ_m into a cumulative distribution function $F_D(\theta_m)$ as a function of θ_m. The expression can be found in equation 12. Equation 12 is not solvable analytically with respect to θ for all shape parameters n_d.

$$\int_{-\pi/2}^{\theta_m} D(\theta)d\theta = F_D(\theta_m) \tag{12}$$

$$\mid \theta_m - \theta_0 \mid \leq \frac{\pi}{2} \quad , for\ m = 1, 2, ..., N_\theta$$

The cumulative distribution function $F_D(\theta_m)$ as a function of θ_m for different values of the shape parameter n_d is shown in figure 3.

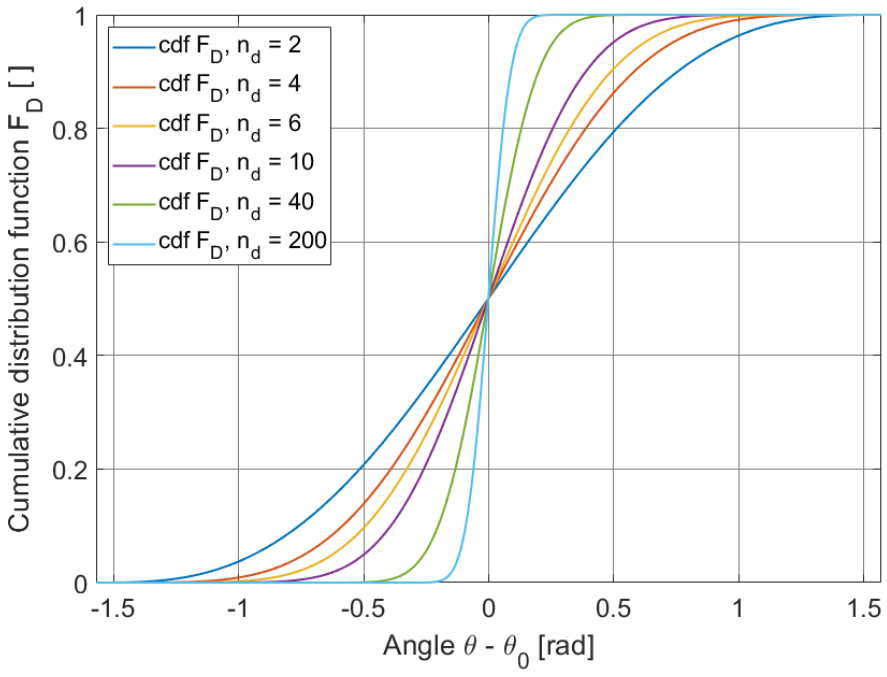

Figure 3: *$F_D(\theta)$ for six different shape parameters n_d.*

Monte Carlo simulation is then used to generate random numbers between zero and one for each frequency component $n = 1, 2, ..., N_f$ in the wave spectrum. This random number is representing the cumulative probability of the wave direction for each frequency component. Once a random number for the cumulative probability of the spreading angle is generated, MATLAB finds the corresponding spreading angle with the use of equation 12. The waves calculated for each frequency component in the wave spectrum now have a predetermined direction θ_n. The pure JONSWAP wave spectrum (not the combined wave and directional spectrum) can then be used for further calculations. The directional angle will instead be implemented into the equation for the surface elevation ξ as will be shown in chapter 2.4 and 2.5. This means we now only have N_f unique wave components in stead of $N_f N_\theta$, which will significantly reduce computing time when the surface elevation ξ is calculated.

2.2.5 Simplifications made in MATLAB for directional spectrum

Both the directional spectrum $D(\theta_m)$ in figure 2, and the cumulative distribution function $F_D(\theta_m)$ in figure 3 is calculated for N_θ values. Since N_θ is a finite value this means that the graphs will not be completely smooth. When a random number between zero and one is generated for each wave component, MATLAB finds the nearest calculated value as seen on the vertical axis in figure 3, and then converts this value into a pre calculated spreading angle on the horizontal axis in figure 3. This is done since equation 12 is not solvable analytically. This will cause some roundoff errors in the calculated wave directions. Since N_θ is not a part of the very time demanding calculations of the surface elevation ξ, N_θ is chosen high enough for this effect to be considered negligible.

2.3 Wave amplitudes

2.3.1 About wave amplitudes

When simulating a sea state, the wave amplitude for each wave component can be calculated from the wave spectrum. The selected JONSWAP wave spectrum will be used further to find an amplitude for each wave component. The wave spectrum contains information about the variance of the sea state at different frequencies, and this information will be used to find each respective wave amplitude. When wave amplitudes are calculated directly from a wave spectrum, there will not be any randomness in wave amplitudes. The wave amplitudes as a function of frequency will be as smooth as the input JONSWAP spectrum in figure 1. This method with a deterministic distribution of wave amplitudes will be described in section 2.3.3. Randomness in wave amplitudes exists under real conditions and a method for implementing this randomness will be described in section 2.3.4.

2.3.2 Assumptions for wave amplitudes

The same assumptions as for the wave spectrum and the directional spectrum made in sections 2.1.2 and 2.2.2 still applies. It is further assumed that the variance of a single Gaussian wave component can be described by the variance properties of the JONSWAP wave spectrum. When using deterministic wave amplitudes, it is assumed that there is no randomness in wave amplitudes. When using random wave amplitude, it is assumed that the randomness of the wave amplitudes can be described by a Rayleigh probability density function.

2.3.3 Creating deterministic wave amplitudes

To simulate a sea surface, the amplitude ξ_{An} of each wave component with frequencies f_n, for $n = 1, 2, ..., N_f$ needs to be obtained. The procedure for calculating deterministic wave amplitudes will be as described in Knut Minsaas (2004). The variance of each wave component $m_{0,n}$ can be described by the following equation

$$m_{0,n} = \frac{1}{2}\xi_{An}^2 \quad , for\ n = 1, 2, ..., N_f \tag{13}$$

The total variance m_0 in a Gaussian sea state ,which is the sum of the variance of all Gaussian wave components is described by equation 14

$$m_0 = \sum_{i=1}^{N_f} \frac{\xi_{An}^2}{2} \quad , for\ n = 1, 2, ..., N_f \tag{14}$$

The wave spectrum S is defined so that the area of the spectrum within a small frequency interval Δf or $\Delta\omega$ is equal to the variance of all wave components within this frequency interval. With summation of all frequency intervals in the wave spectrum, we obtain another equation for the total variance of a sea state. See equation 15.

$$m_0 = \sum_{i=1}^{N_f} S(\omega_n)\Delta\omega \quad , for\ n = 1, 2, ..., N_f \tag{15}$$

When combining equation 14 and 15 we obtain equation 16

$$m_0 = \sum_{i=1}^{N_f} \frac{\xi_{An}^2}{2} = \sum_{i=1}^{N_f} S(\omega_n)\Delta\omega \tag{16}$$

$$for\ \ n = 1, 2, ..., N_f$$

With some rewriting of equation 16, the deterministic wave amplitudes ξ_{An} for all wave components can be found from the JONSWAP wave spectrum S as given in the following equation.

$$\xi_{An} = \sqrt{2S(\omega_n)\Delta\omega} = \sqrt{2S(f_n)\Delta f} \tag{17}$$

$$for\ \ n = 1, 2, ..., N_f$$

Equations 13, 14, 15 and 17 are obtained from Knut Minsaas (2004).

2.3.4 Creating random wave amplitudes

As mentioned is section 2.1.1, when a wave spectrum is created based on measurements from a real life sea state, the wave spectrum will contain a lot of noise. The wave spectrum will not look smooth as the JONSWAP wave spectrum in figure 1. In order to simulate this type of random noise that exists under real conditions, the wave amplitudes can be modeled as a random variable. The method for creating Rayleigh distributed random wave amplitudes as described in Tucker et al. (1984) will be used. Tucker et al. (1984) stated that using random wave amplitudes are necessary for simulating a fully Gaussian process. The random wave amplitudes are changed simultaneously as the random phase angles of the wave components (Tucker et al. (1984)), as described in sections 2.4 and 2.5 when the surface elevation process is created. The Rayleigh distributed random wave amplitudes have the following equation.

$$F_{\Xi_{An}}(\xi_{An}) = 1 - exp\Big[- \Big(\frac{\xi_{An}}{\beta_n}\Big)^2 \Big] \tag{18}$$

$$, where\ \ \xi_{An} \geq 0\ \ \ , for\ n = 1, 2, ..., N_f$$

,where N_f is the number of frequency components in the spectrum. The equation for the Rayleigh parameter β_n is given in Haver (2017) as

$$\beta_n = \sqrt{2S(f_n)\Delta f} \tag{19}$$

,where Δf is the distance between frequency components and S is the wave spectrum. The next step in determining the random wave amplitudes is to use Monte Carlo simulation and generate a sample of evenly distributed random vales between zero and one for each $F_{\Xi_{An}}(\xi_{An})$, representing the Rayleigh CDF value for each wave amplitude ξ_{An}. With some manipulation of equation 18, the following equation is obtained for the random wave amplitudes ξ_{An} for each frequency component.

$$\xi_{An} = \beta_n \sqrt{-ln[1 - F_{\Xi_{An}}(\xi_{An}))]} \tag{20}$$

$$for\ n = 1, 2, ..., N_f$$

When simulating a sea state with random amplitudes, the variance in the simulated sea state will no longer be equal to the variance of the input wave spectrum as in equation 16. The variance in the simulated sea state will vary from simulation to simulation. The mean value from a large number of simulations will however converge towards the variance of the input

spectrum. This variance of the variance in simulated sea states will be investigated further in section 5 when verifying simulations using random amplitudes. Figure 4 shows a wave spectrum obtained from one realization of a surface process with random amplitudes, along with the input JONSWAP wave spectrum.

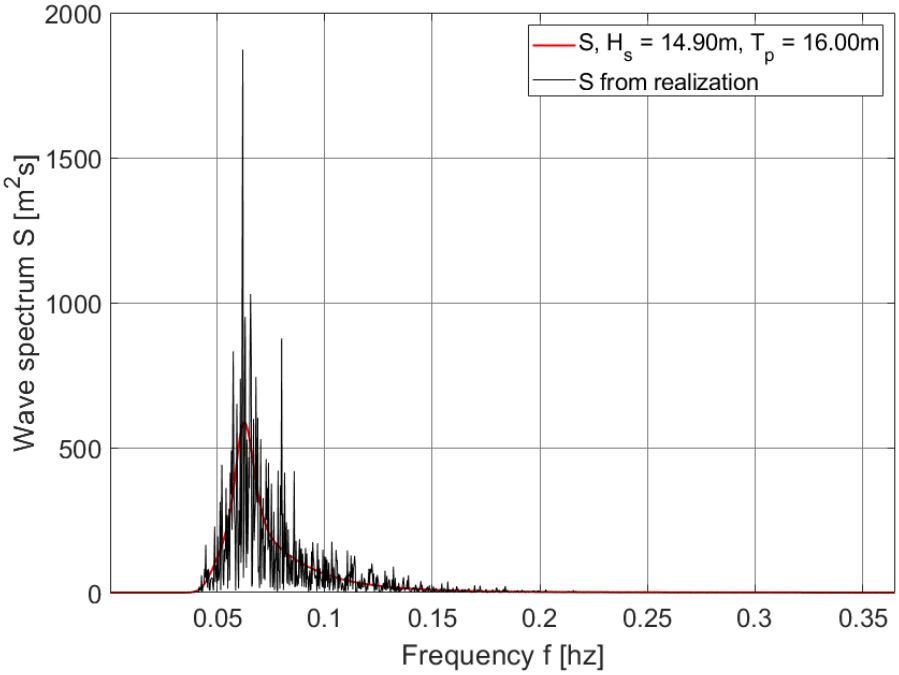

Figure 4: *Wave spectrum obtained from one realization with random wave amplitudes along with input wave spectrum.*

2.3.5 Simplifications made in MATLAB for wave amplitudes

The process for finding the wave amplitudes builds upon the calculations of the wave spectrum. Therefore, the same simplifications done when calculating the wave spectrum and the directional spectrum as described in sections 2.1.4 and 2.2.5 still apply here. There is however no further simplifications done in MATLAB when calculating the wave amplitudes. Neither when calculating deterministic wave amplitudes nor when calculating the randomly distributed wave amplitudes.

2.4 Gaussian surface elevation process

2.4.1 About Gaussian surface elevation process

Gaussian wave theory represents a linear approximation to real ocean waves. The surface elevation is Gaussian distributed with a mean value at the free undisturbed surface. The mean value $\mu(\xi)$ and the variance m_0 of the Gaussian surface process ξ can be found by the following equations.

$$\mu(\xi) = 0 \tag{21}$$

$$m_0 = \int_0^\infty S(\omega)d\omega \approx \sum_{n=1}^{N_f} S(\omega_n)\Delta\omega \tag{22}$$

An irregular Gaussian surface elevation is described by a Fourier series and consists of the surface elevation of a sum of harmonic wave components. For each harmonic wave component the crest and the trough will have the same magnitude. Using Gaussian wave theory is the simplest way of describing irregular ocean waves, and requires a lot less CPU-time than other more accurate methods such as second order wave theory or Stokes wave theory. The shape of waves obtained by Gaussian wave theory will have clear differences from waves observed at a real sea surface and there will be no breaking waves. Real ocean waves will have higher wave crests and less negative wave troughs than Gaussian waves. In spite of being a simplified method, Gaussian wave theory can still give a satisfactory approximation to real conditions in many cases.

2.4.2 Assumptions for Gaussian surface elevation process

The same assumptions done when calculating the wave spectrum, the directional spectrum and the wave amplitudes as described in sections 2.1.2, 2.2.2 and 2.3.2 still applies here. It is assumed that the surface process can be described by a Gaussian process with a mean value of zero and that the process is stationary within each simulation time period. Deep water also is assumed. It is further assumed that the surface process is ergodic.

2.4.3 Creating Gaussian surface elevation process

The Gaussian surface elevation process is described by the properties of the JONSWAP wave spectrum and the directional spectrum through the amplitudes ξ_{An} of the waves components and the direction θ_n of the wave components, for $n = 1, 2, ..., N_f$. Equation 23 describes the Gaussian surface elevation process. The equation is obtained from RP-C205 (2010) and rewritten to describe the Gaussian surface elevation process $\xi^{(1)}(x_i, y_j, t_k)$ for an area.

$$\xi^{(1)}(x_i, y_j, t_k) = \sum_{n=1}^{N_f} \left[\xi_{An} cos\Big(\omega_n t_k - k_n \cos(\theta_n) x_i - k_n \sin(\theta_n) y_j + \epsilon_n\Big) \right] \tag{23}$$

, where ω_n is the angular frequency and ϵ_n is a random phase angle which is evenly distributed with value between 0 and 2π , for $n = 1, 2, ..., N_f$. ϵ_n implements randomness in phases of all wave components. x_i and y_j are spatial coordinates and t_k is the time parameter. The wave number k_n assuming deep water can be found by the following equation

$$k_n = \frac{\omega_n^2}{g} \quad , for\ n = 1, 2, ..., N_f \tag{24}$$

The surface elevation has to be calculated for all x_i, y_j and t_k according to equation 25

$$\begin{gathered} x_{min} \leq x_i \leq x_{max} \quad , for\ i = 1, 2, ..., N_x \\ , and\ \ y_{min} \leq y_j \leq y_{max} \quad , for\ j = 1, 2, ..., N_y \\ , and\ 0 \leq t_k \leq t_{max} \quad , for\ k = 1, 2, ..., N_t \end{gathered} \tag{25}$$

Figure 5 shows a time series for the Gaussian surface elevation obtained by equation 23 at one single point for a short crested sea state. Figure 6 shows a snapshot of the Gaussian surface elevation over an area obtained by equation 23 for the same short crested sea state. The mean wave direction used for the simulations in both figures is along the x-axis.

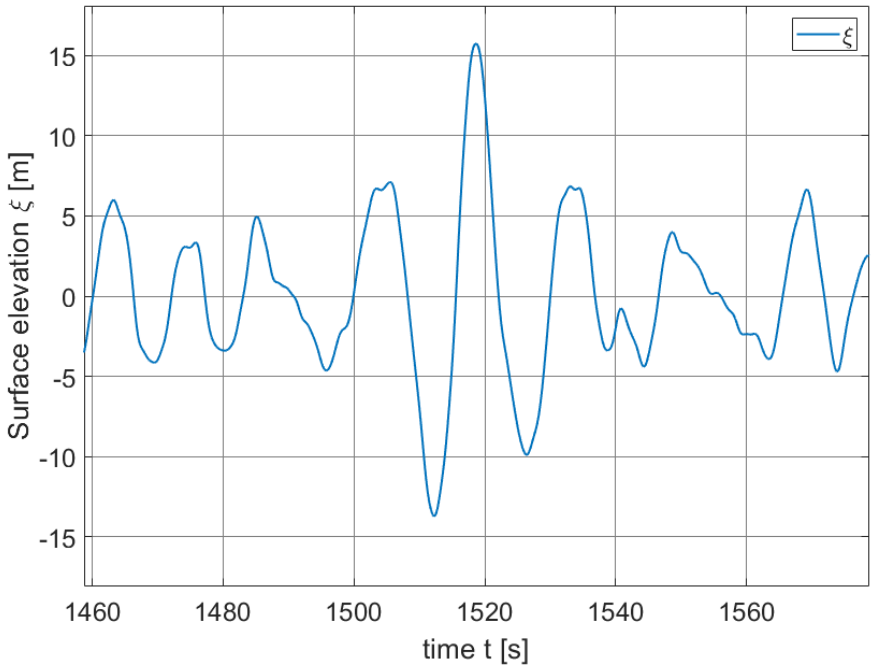

Figure 5: *Gaussian surface process for a short crested sea state at one point in space over a time period of 120 seconds.*

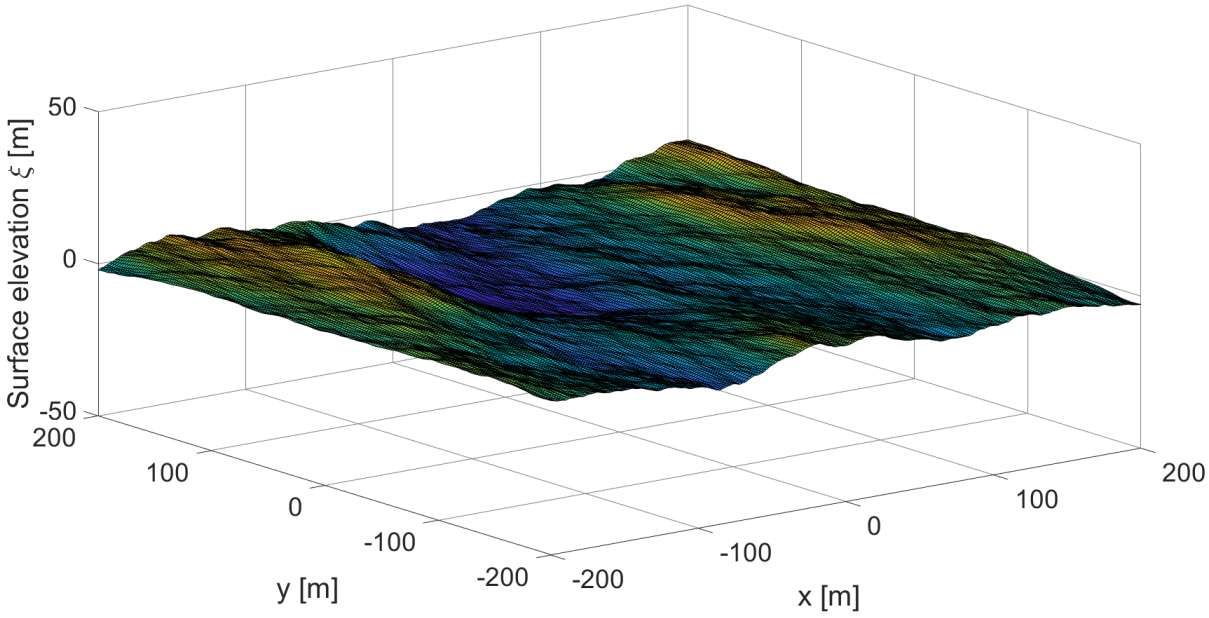

Figure 6: *Snapshot of Gaussian surface process for a short crested sea state over an area. The mean wave direction is along the x-axis*

2.4.4 Simplifications made in MATLAB for Gaussian surface elevation process

There are no further simplifications regarding the resolution of wave components or directional components than already made in calculation of the wave spectrum and the directional spectrum in sections 2.1.4 and 2.2.5. The simplifications made for the calculation of wave amplitudes made in section 2.3.5 also still applies. The resolution for the spatial coordinates and the resolution for the time parameter needs to be determined before calculating the surface elevation. The resolution of the time parameter affects how accurate the wave shape at a single location is calculated. It is therefore important to have this time step between calculated values of the surface elevations small enough so that the wave shape in time is represented in a good way. The resolution of the spatial coordinates does not affect the shape of the waves in time, but how many individual time series of the surface elevation are obtained within the area boundaries. The spatial resolution therefore affects the shape of the waves in space. When the spatial resolution increases, N_x, N_y will increase. When the time step lowers N_t will increase. N_x, N_y and N_t will along with N_f strongly affect calculation time for the Gaussian surface elevation. A thorough parameter study for the resolution for spatial coordinates and for the time parameter for Gaussian simulations can be found in section 6.

2.5 Second order surface elevation process

2.5.1 About second order surface elevation process

Second order waves will have higher wave crests as well as less negative wave troughs than Gaussian waves. The shape of second order waves will therefore be more similar to those observed on a real ocean surface than waves that are obtained by Gaussian wave theory. The crest heights of second order waves will give a closer approximation to the crest heights of real ocean waves. A second order surface process is therefore generally a better model for describing real surface conditions than a Gaussian surface process, but simulating a second order surface process requires a lot more CPU-time than when Gaussian theory is used. A second order surface process is modeled as a superposition of free dispersive harmonic Gaussian wave components and bound harmonic second order corrections. Since the variance from the wave spectrum is maintained when using only Gaussian wave components, the additional variance carried by the bound second order corrections will give excessive variance in a simulated sea state when all the variance from the wave spectrum is implemented. It is therefore necessary to reduce some of the variance in the Gaussian contribution in the simulated second order sea state. The cutoff frequency method recommended in RP-C205 (2010) is chosen for all further calculations involving second order surface elevation.

When using the cutoff frequency method, the JONSWAP wave spectrum will be truncated at frequencies higher than f_{max}. Therefore only lower frequencies than this will be considered when creating the free dispersive Gaussian wave contributions to the total second order surface process. The second order surface corrections will be modeled as bound waves with a maximum frequency of $2f_{max}$. In this way the total variance of the second order sea state will be approximately equal to the variance in the wave spectrum describing the sea state. The cutoff frequency method has proved to fit experimental data reasonably well (Stansberg and Gudmestad (1996), Stansberg et al. (2008) and RP-C205 (2010)). The equation for f_{max} is obtained from RP-C205 (2010).

$$f_{max} = \sqrt{\frac{2g}{H_s}} \tag{26}$$

2.5.2 Assumptions for second order surface elevation process

The same assumptions done for the wave spectrum, the directional spectrum and the wave amplitudes as described in sections 2.1.2, 2.2.2 and 2.3.2 still applies here. It is assumed that the surface process can be described by a second order process with a mean value of zero and that the process is stationary within each simulation time period. Deep water is also assumed. It is further assumed that the surface process is ergodic.

2.5.3 Creating Gaussian surface elevation process truncated at high frequencies

First, the Gaussian surface contribution to the total second order surface elevation has to be calculated. This Gaussian contribution will be truncated at high frequencies according to the cutoff frequency method described in section 2.5.1. Equation 26 gives the cut of frequency. The Gaussian surface elevation process truncated at high frequencies is described by the properties of the JONSWAP wave spectrum and the directional spectrum through the amplitudes ξ_{An} of the wave components and the directions θ_n of the wave components, for $n = 1, 2, ..., N_f$. Equation 27 describes the Gaussian surface elevation process truncated at high frequencies. The equation is obtained from RP-C205 (2010) and rewritten to describe the Gaussian surface elevation process $\xi^{(1)}(x_i, y_j, t_k)$ truncated at high frequencies for an area.

$$\xi^{(1)}(x_i, y_j, t_k) = \sum_{n=1}^{N_f} \left[\xi_{An} cos\Big(\omega_n t_k - k_n \cos(\theta_n) x_i - k_n \sin(\theta_n) y_j + \epsilon_n \Big) \right] \tag{27}$$

, where ω_n is the angular frequency and ϵ_n is a random phase angle which is rectangular distributed with value between 0 and 2π , for $n = 1, 2, ..., N_f$. ϵ_n implements randomness in phases of all wave components. The wave number k_n, assuming deep water can be found in equation 24. x_i and y_j are spatial coordinates and t_k is the time parameter. The surface elevation has to be calculated for all x_i, y_j and t_k according to equation 25.

Figure 7 shows a time series for the Gaussian surface elevation truncated at high frequencies obtained by equation 27 at one single point for a short crested sea state.

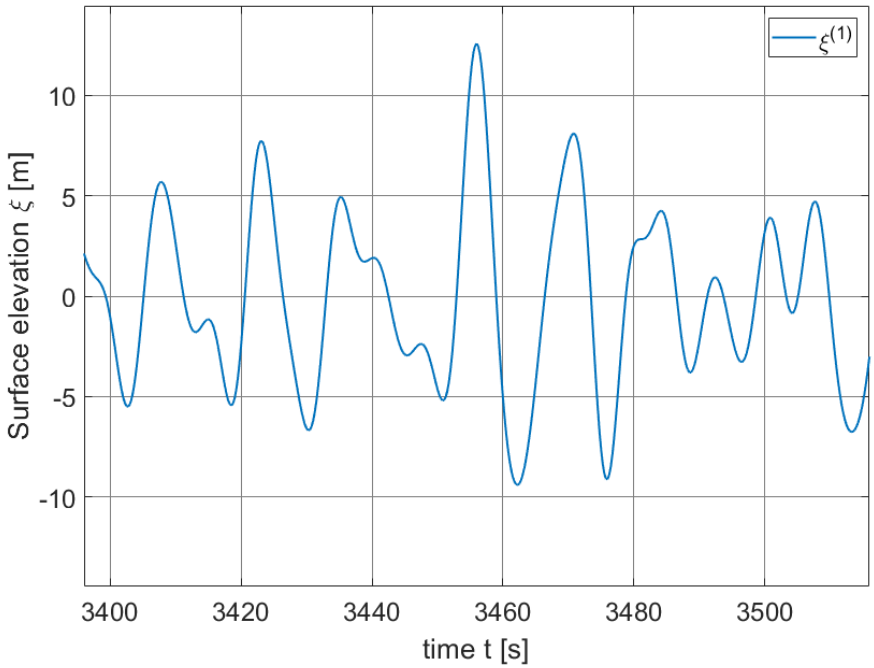

Figure 7: *Gaussian truncated surface process for a short crested sea state at one point in space over a time period of 120 seconds.*

2.5.4 Creating second order surface elevation corrections

Next, the second order surface elevation corrections has to be calculated. The second order model used has its origin from Longuet-Higgins (1963). The second order surface elevation corrections is, like the Gaussian surface elevation process, described by the properties of the JONSWAP wave spectrum and the directional spectrum, through the amplitudes ξ_{An} of the wave components and the directions θ_n of the wave components, for $n = 1, 2, ..., N_f$. Equation 28 describes the second order surface elevation corrections and consists of N_f^2 corrections for all sum frequencies and N_f^2 corrections for all difference frequencies. The second order surface elevation corrections are therefore bound waves of the free dispersive waves calculated for the Gaussian surface elevation process $\xi^{(1)}(x, y, t)$ truncated at high frequencies. The maximum frequency for the second order surface elevation correction is $2f_{max}$. Equation 28 is obtained from RP-C205 (2010) and rewritten to describe the second order surface elevation correction process $\Delta\xi^{(2)}(x_i, y_j, t_k)$ for an area.

$$\begin{aligned}\Delta\xi^{(2)}(x_i, y_j, t_k) = &\frac{1}{4}\sum_{n_1=1}^{N_f}\sum_{n_2=1}^{N_f}\left[\xi_{An_1}\xi_{An_2}\Big(k_{n_1}+k_{n_2}\Big)\cos\Big(\beta_{n_1}+\beta_{n_2}\Big)\right] \\ &-\frac{1}{4}\sum_{n_1=1}^{N_f}\sum_{n_2=1}^{N_f}\left[\xi_{An_1}\xi_{An_2}\Big|k_{n_1}-k_{n_2}\Big|\cos\Big(\beta_{n_1}-\beta_{n_2}\Big)\right]\end{aligned} \tag{28}$$

, where ω_n is the angular frequency and ϵ_n is a random phase angle which is rectangular distributed with value between 0 and 2π , for $n = 1, 2, ..., N_f$. ϵ_n implements randomness in phases of all wave components. β_n is defined as

$$\beta_n = \Big[\omega_n t_k - k_n \cos(\theta_n) x_i - k_n \sin(\theta_n) y_j + \epsilon_n\Big] \quad , for\ n = 1, 2, ..., N_f \tag{29}$$

The wave number k_n, assuming deep water can be found by equation 24. x_i and y_j are spatial coordinates and t_k is the time parameter. The surface elevation has to be calculated for all x_i, y_j and t_k according to equation 25. Equation 28 has a double summation of N_f. Since the summation is symmetric across the diagonal equation 28 can be rewritten, resulting in approximately half the computational time in MATLAB by only summing the diagonal and the upper triangular of the summation in equation 28. The rewritten edition of the second order surface elevation corrections $\Delta\xi_1^{(2)}(x, y, t)$, $\Delta\xi_2^{(2)}(x, y, t)$ and $\Delta\xi_3^{(2)}(x, y, t)$ are given in equations 30, 31 and 32.

$$\Delta\xi_1^{(2)}(x_i, y_j, t_k) = \frac{1}{2} \sum_{n_1=1}^{N_f} \Big[\xi_{An_1}^2 k_{n_1} \cos\Big(2\beta_{n_1}\Big)\Big] \tag{30}$$

$$\Delta\xi_2^{(2)}(x_i, y_j, t_k) = \frac{1}{2} \sum_{n_1=1}^{N_f-1} \sum_{n_2=n_1+1}^{N_f} \Big[\xi_{An_1}\xi_{An_2}\Big(k_{n_1} + k_{n_2}\Big) \cos\Big(\beta_{n_1} + \beta_{n_2}\Big)\Big] \tag{31}$$

$$\Delta\xi_3^{(2)}(x_i, y_j, t_k) = -\frac{1}{2} \sum_{n_1=1}^{N_f-1} \sum_{n_2=n_1+1}^{N_f} \Big[\xi_{An_1}\xi_{An_2}\Big(-k_{n_1} + k_{n_2}\Big) \cos\Big(-\beta_{n_1} + \beta_{n_2}\Big)\Big] \tag{32}$$

Figure 8 shows a time series for the second order surface elevation corrections obtained by equations 30, 31 and 32 at one single point for a short crested sea state.

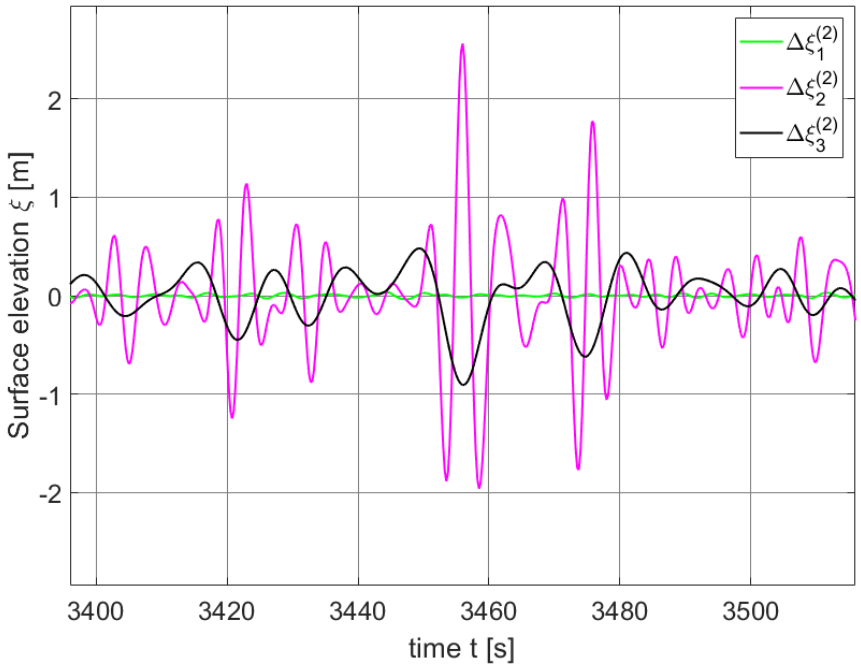

Figure 8: *Second order corrections for a short crested sea state at one point in space over a time period of 120 seconds.*

2.5.5 Creating complete second order surface elevation process

The complete second order surface elevation process $\xi^{(2)}(x_i, y_j, t_k)$ can now be found by super positioning of Gaussian surface elevation $\xi^{(1)}(x, y, t)$ truncated at high frequencies and the second order surface elevation corrections $\Delta\xi^{(2)}(x_i, y_j, t_k)$. This is done according to equation 33.

$$\begin{aligned}\xi^{(2)}(x_i, y_j, t_k) &= \xi^{(1)}(x_i, y_j, t_k) + \Delta\xi^{(2)}(x_i, y_j, t_k) \\ &= \xi^{(1)}(x_i, y_j, t_k) + \Delta\xi_1^{(2)}(x_i, y_j, t_k) + \Delta\xi_2^{(2)}(x_i, y_j, t_k) + \Delta\xi_3^{(2)}(x_i, y_j, t_k)\end{aligned} \tag{33}$$

, where x_i and y_j are spatial coordinates and t_k is the time parameter. The surface elevation has to be calculated for all x_i, y_j and t_k according to equation 25.
Figure 9 shows a time series for the complete second order surface elevation $\xi^{(2)}(x_i, y_j, t_k)$ along with the Gaussian surface elevation $\xi^{(1)}(x_i, y_j, t_k)$ truncated at high frequencies and the second order surface elevation corrections $\Delta\xi_1^{(2)}(x_i, y_j, t_k)$, $\Delta\xi_2^{(2)}(x_i, y_j, t_k)$ and $\Delta\xi_3^{(2)}(x_i, y_j, t_k)$ at one single point for a short crested sea state. Figure 10 shows a snapshot of the complete second order surface elevation $\xi^{(2)}(x, y, t)$ over an area obtained by equation 33 for the same short crested sea state.

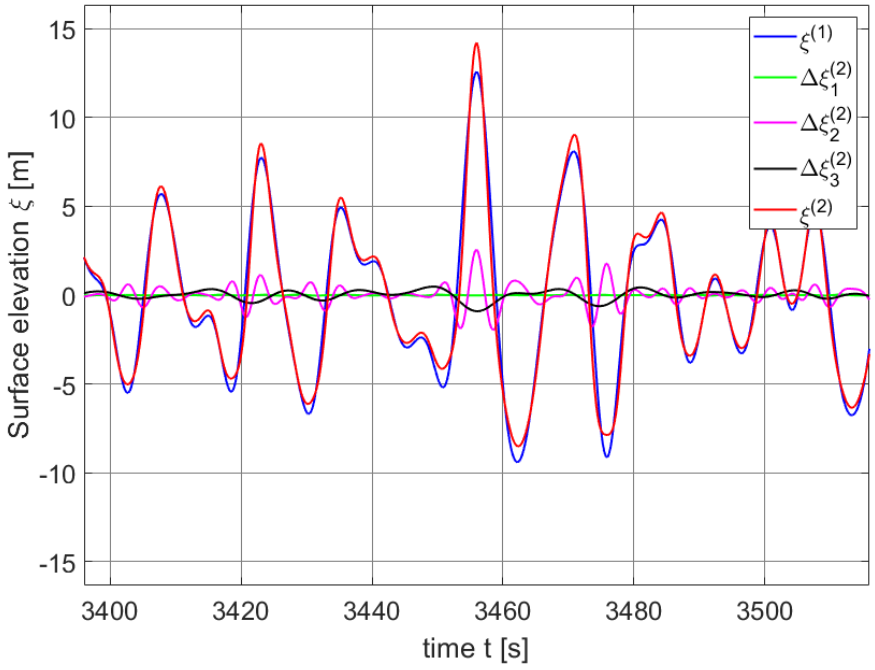

Figure 9: *Second order surface process along with its components for a short crested sea state at one point in space over a time period of 120 seconds.*

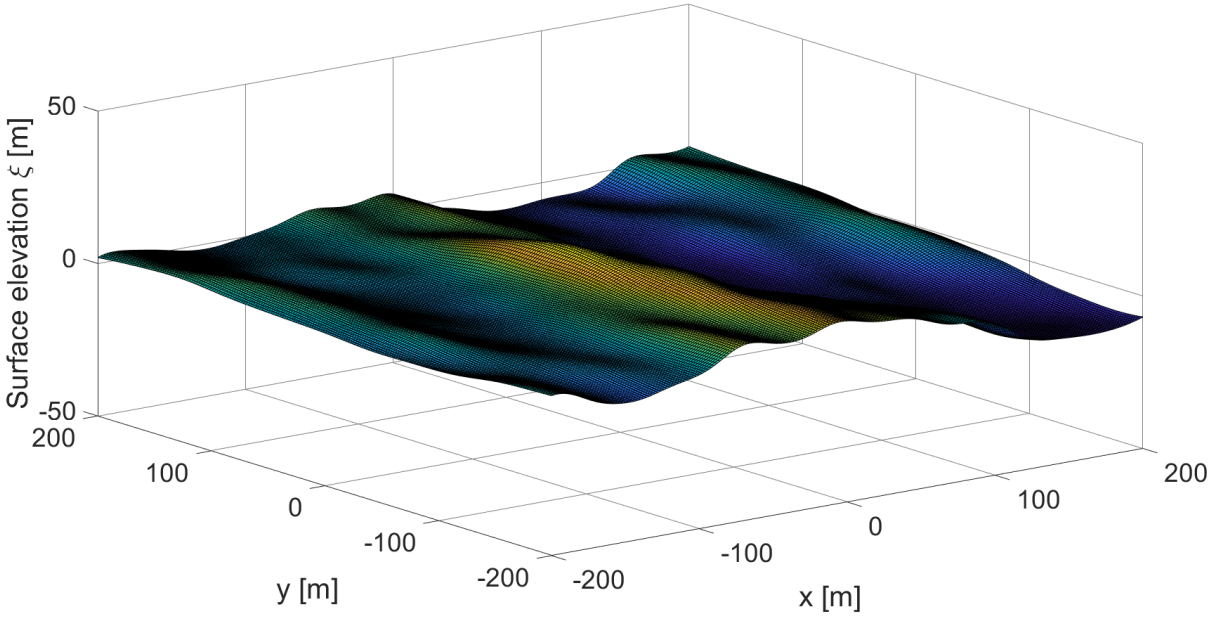

Figure 10: *Snapshot of complete second order surface process for a short crested sea state over an area.*

Note the smoothness of the complete second order surface process in figure 10 compared to Gaussian surface process in figure 6. This smoothness of the surface is due to the cutoff frequency condition. The Gaussian surface process will include free dispersive waves at considerable higher frequencies than f_{max} in order to have the correct variance in the sea state simulated. When the cutoff frequency condition is implemented into the complete second order surface process, there will be no free dispersive waves with frequencies higher than f_{max}.

2.5.6 Simplifications made in MATLAB for second order surface elevation process

There are no further simplifications regarding the resolution of wave components or directional components than already made in calculation of the wave spectrum and the directional spectrum in sections 2.1.4 and 2.2.5. The simplifications made for the calculation of wave amplitudes made in section 2.3.5 also still applies. The resolution for the spatial coordinates and the resolution for the time parameter needs to be determined before calculating the surface elevation. The resolution of the time parameter affects how accurate the wave shape at a single location is calculated. It is therefore important to have this time step between calculated values of the surface elevations small enough so that the wave shape in time is represented in a good way. The resolution of the spatial coordinates does not affect the shape of the waves in time, but how many individual time series of the surface elevation are obtained within the area boundaries. The spatial resolution therefore affects the shape of the waves in space. When the spatial resolution increases, N_x, N_y will increase. When the time step lowers N_t will increase. N_x, N_y and N_t will along with N_f strongly affect calculation time for the second order surface elevation. More about determination of resolution for spatial coordinates and time parameter for calculation of second order surface elevation in section 6.

2.6 Maximum crest heights

2.6.1 About maximum crest heights

The maximum crest heights are found as the maximum value of the surface elevation process after a complete simulation is finished. MATLAB will loop through the array holding the data for the surface elevation process and find the maximum area crest height and the maximum point crest height. The location for finding the maximum point crest height from a simulation will always be at the center of the simulated area. The maximum area crest height and the maximum point crest height will be found in the same way for both Gaussian and second order surface elevation processes. The procedure for finding maximum point crest heights $\xi_{max,point}$ and maximum area crest heights $\xi_{max,area}$ will be described respectively in sections 2.6.2 and 2.6.4.

A high resolution procedure to obtain more accurate values for the maximum point crest heights $\xi_{max,point}$ and the maximum area crest heights $\xi_{max,area}$ near the real top of the simulated crests will be described respectively in sections 2.6.3 and 2.6.5. When using the high resolution procedure, a new simulation of the surface elevation process is done using the same randomly calculated parameters as in the initial simulation. The new high resolution surface elevation process is only calculated for a limited interval in time when finding point maximums. And the new high resolution surface elevation process is only calculated for a limited time interval and over a limited area when finding area maximums. The time step and the area grid size between calculated values of the surface elevation process will then be lowered. The additional CPU-time needed for running an additional high resolution simulation and finding corresponding high resolution maximums is small. The method is in particular effective when finding area maximums, and it therefore allows for simulations with large area grid size to be more accurate relative to not using this high resolution method. The effect on obtained point maximums is not very large when using small time steps, but is included in the MATLAB program for when larger time steps are used.

A parameter study is done for the convergence of obtained area maximums from simulations over an area in section 6.7, and shows the differences when using the high resolution method and using only the initial simulations when obtaining area maximums. To illustrate the procedure for finding maximums, a one hour simulation over a 100m*100m area is done with an area grid size of 5m*5m and time steps of 0.25s. All maximums found in the following four sections, 2.6.2, 2.6.3, 2.6.4 and 2.6.5 are based on this same initial simulation.

2.6.2 Finding point maximum crest height

The point maximum crest heights are found at a specific location for all simulations. The spatial point chosen for finding the point maximum crest height is the center point of the simulated area, and is at coordinates $x_i = 0$ and $y_j = 0$. The maximum center point crest height $\xi_{max,point}$ is obtained by the following equation.

$$\xi_{max,point} = max\Big[\xi(0,0,t_k)\Big] \tag{34}$$

, where ξ is the surface elevation process and t_k is the time parameter. The maximum point crest height is found amongst all t_k for which the surface process is calculated for, according to equation 35

$$0 \leq t_k \leq t_{max} \quad , for\ k = 1, 2, ..., N_t \tag{35}$$

Figures 11 and 12 shows the same maximum point crest height obtained from a one hour surface elevation process. A time step of 0.25 seconds and an area grid size of 5m*5m are used for the simulation. Figure 11 shows the obtained maximum point crest height along with the surface elevation process at the center point over the simulated time period. Figure 12 shows the maximum point crest height along with a snapshot of the surface elevation process at time of maximum. Both figures are from the same simulation of the surface elevation process ξ over an area. The indicated maximum point crest height is the same for both figures, and corresponds in both time and space. The maximum center point crest height is indicated with a blue dot in both figures.

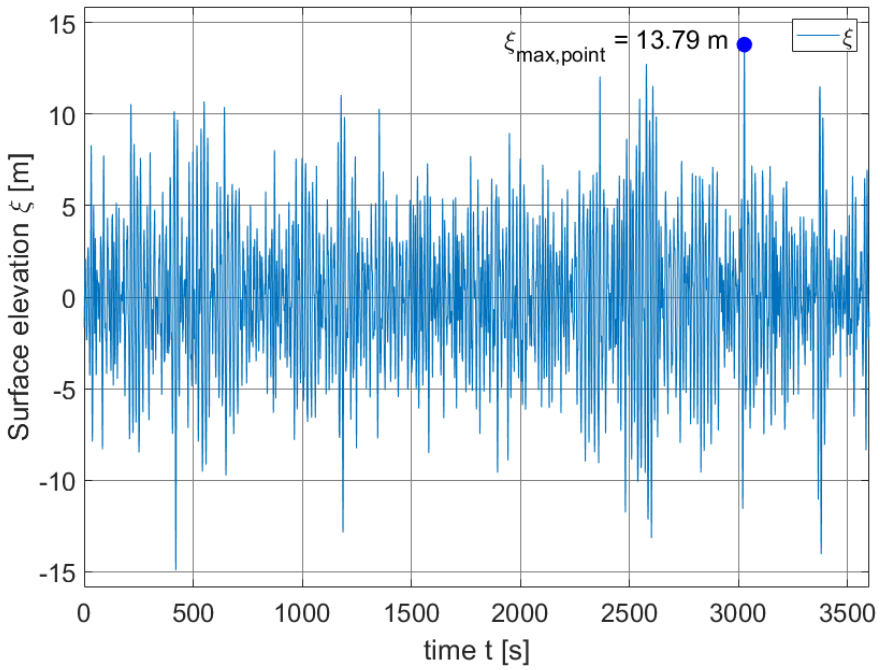

Figure 11: *Surface elevation process at center point over a time period of one hour. The blue dot indicates center point maximum.*

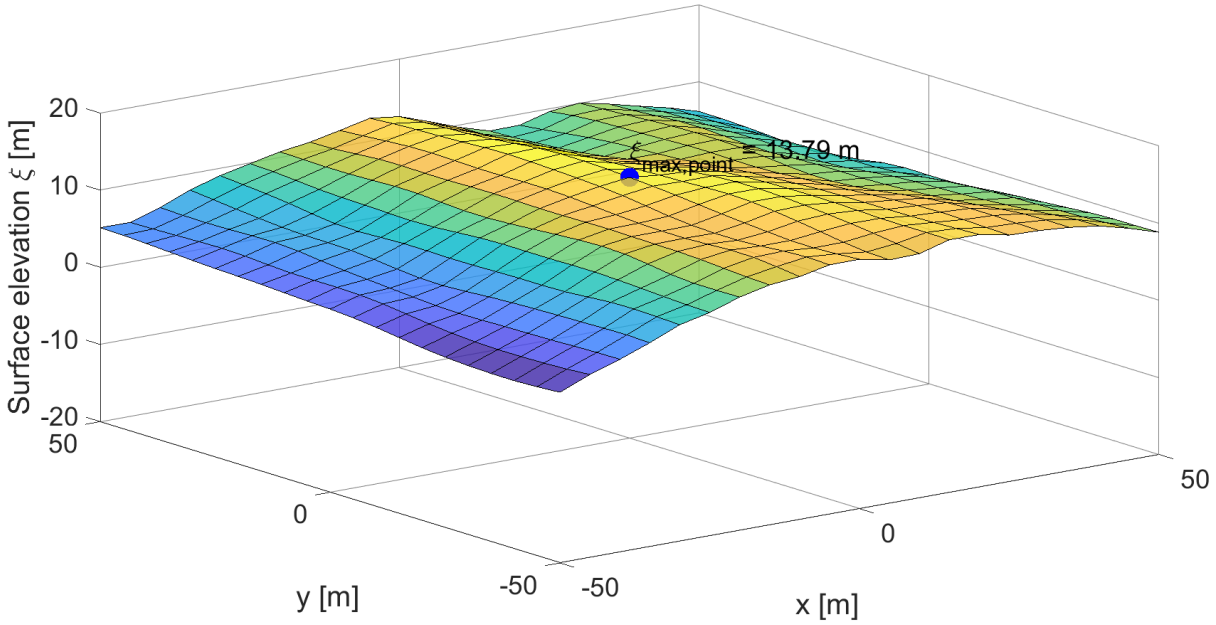

Figure 12: *Snapshot of surface elevation process for simulated area at time of center point maximum during one hour. The blue dot indicates center point maximum.*

2.6.3 Finding high resolution point maximum crest height

To increase the accuracy of the obtained maximum center point crest height, a new simulation of the surface elevation process is done with high resolution of the time parameter at the center point around the time when the maximum center point crest height occurred in the initial simulation. The new high resolution simulation uses the same random input as the initial simulation of the surface elevation process. In this way, a more accurate value for the maximum center point crest height is obtained under the same random conditions as in the initial simulation. The center point is the same as in the initial simulation, and is at coordinates $x_i = 0$ and $y_j = 0$. The new high resolution simulation for the surface elevation is only done for the center point with a very limited time interval to reduce additional CPU-time when using this high resolution method. The new high resolution surface elevation process ξ will be calculated according to Gaussian or second order wave theory as described respectively in section 2.4 and 2.5 as for the initial simulation. The new high resolution surface elevation process will only be calculated for the center point for the high resolution time parameter $t_{k_{hr}}$ over the limited time interval according to the equation

$$, and \;\; t_{max,point} - 2dt \leq t_{k_{hr}} \leq t_{max,point} + 2dt \;\; , for \; k_{hr} = 1, 2, ..., N_{t_{hr}} \tag{36}$$

, where dt is the time step from the initial analysis and $t_{max,point}$ is the point in time when the maximum center point crest height occurred during the initial simulation. If some values of the new high resolution time parameter are located outside the initial time frame, these time parameter values will not be used in the calculation of the new high resolution surface elevation process. The new high resolution time parameter $t_{k_{hr}}$ is set in MATLAB to have time steps five times smaller in size than the time steps of the time parameter t_k used in the initial simulation. This size of high resolution time steps is chosen to obtain a good accuracy for the maximum center point crest height near the real crest of the wave profile without spending to

much CPU-time for the additional high resolution simulation. The high resolution maximum center point crest height $\xi_{max,point}$ is obtained by the following equation

$$\xi_{max,point} = max\Big[\xi(0,0,t_{k_{hr}})\Big] \tag{37}$$

, where ξ is new high resolution surface elevation process. The maximum center point crest height has to be found at the center point from all $t_{k_{hr}}$ for which the new high resolution surface process is calculated for, according to equation 36.

Figure 13 shows both the initial and the new high resolution surface elevation process ξ around the time of center point maximum. The wave profile from the initial surface elevation process has a much more jagged shape than the wave profile from the high resolution surface elevation process. The high resolution method for finding the maximum center point crest height will therefore obtain a value for the maximum center point crest height closer to the true crest of the wave profile than the value obtained for the maximum center point crest height from the initial simulation. The high resolution center point maximum is indicated with a blue dot in figure 13 and is obtained with equation 37. In this case, the initial simulation uses a time step of 0.25 seconds. The difference between the maximum center point crest heights from the initial surface elevation process and from the high resolution surface elevation process will be more profound when the time step between calculated values of the surface elevation process in the initial simulation increases. The high resolution point maximum method will therefore be used for all further calculations in this thesis involving finding the maximum center point crest height $\xi_{max,point}$.

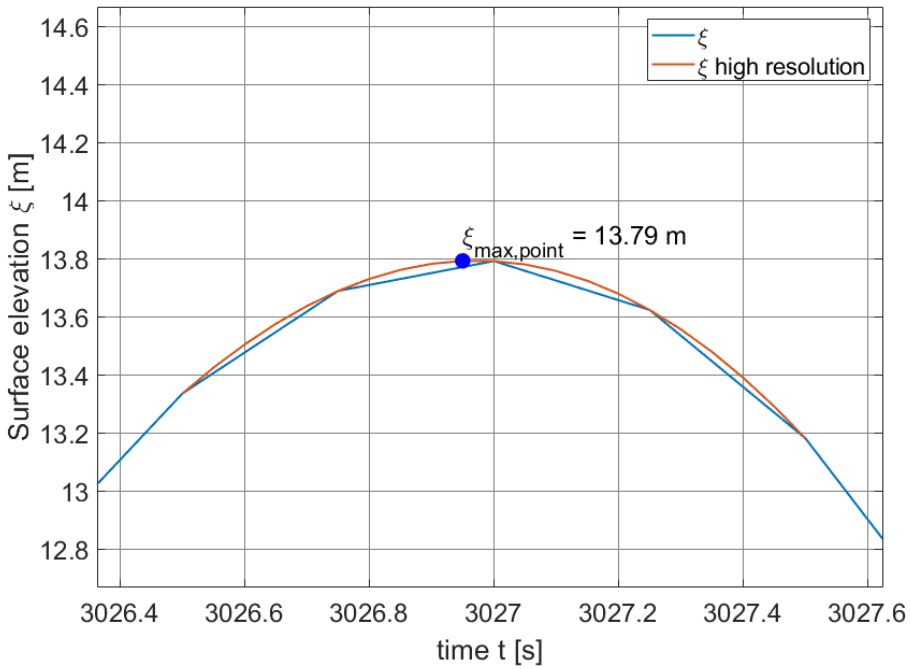

Figure 13: *Surface elevation process at center point around time of center point maximum, along with high resolution surface elevation process at center point. The blue dot indicates high resolution center point maximum.*

2.6.4 Finding area maximum crest height

When finding the area maximum crest height, the surface elevation process at all points across the simulated area have to be accounted for. The maximum area crest height $\xi_{max,area}$ is obtained by the following equation

$$\xi_{max,area} = max\Big[\xi(x_i, y_j, t_k)\Big] \tag{38}$$

, where ξ is the surface elevation process. x_i and y_j are spatial coordinates and t_k is the time parameter. The maximum area crest height has to be found amongst all x_i, y_j and t_k for which the surface process is calculated for, according to equation 25.

Figures 14 and 15 shows the same maximum area crest height obtained from a one hour simulation of a surface elevation process. A time step of 0.25 seconds and an area grid size of 5m*5m are used for the simulation. Figure 14 shows the obtained maximum area crest height along with the surface elevation process at the point of area maximum over the simulated time period. Figure 15 shows the maximum area crest height along with a snapshot of the surface elevation process at time of area maximum. Figure 16 shows a contour plot of the maximum surface elevation at all spatial points during the entire simulation period of the surface elevation process, with both maximum area crest height and maximum center point crest height indicated in the figure. All three figures are from the same one hour simulation of the surface elevation process ξ over an area. The indicated maximum area crest height is the same for all three figures, and corresponds in both time and space. The maximum area crest height is indicated with a red dot in all three figures. The maximum center point crest height from the simulation period is indicated with a blue dot in the contour plot in figure 16.

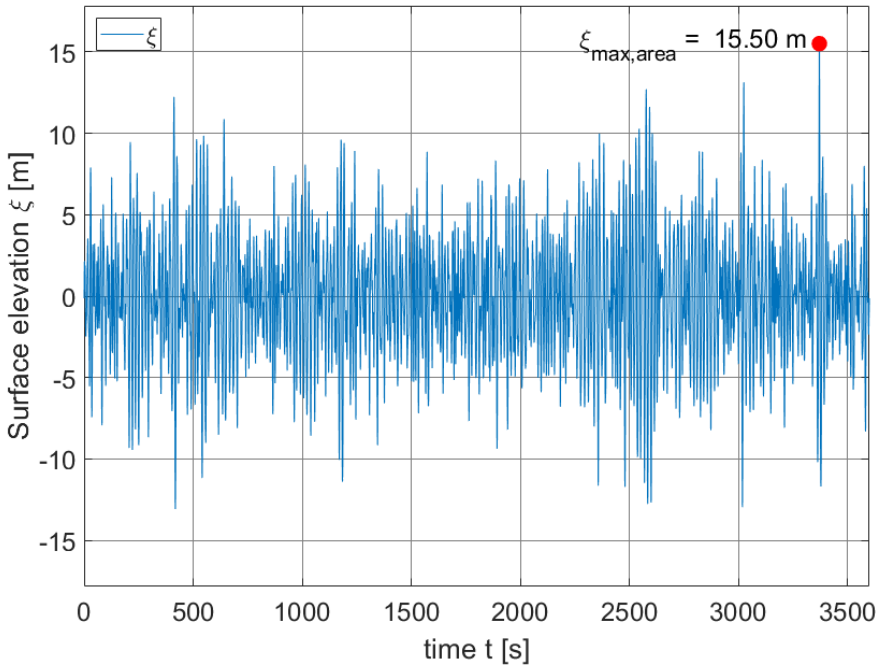

Figure 14: *Surface elevation process at point of area maximum over a time period of one hour. The red dot indicates area maximum.*

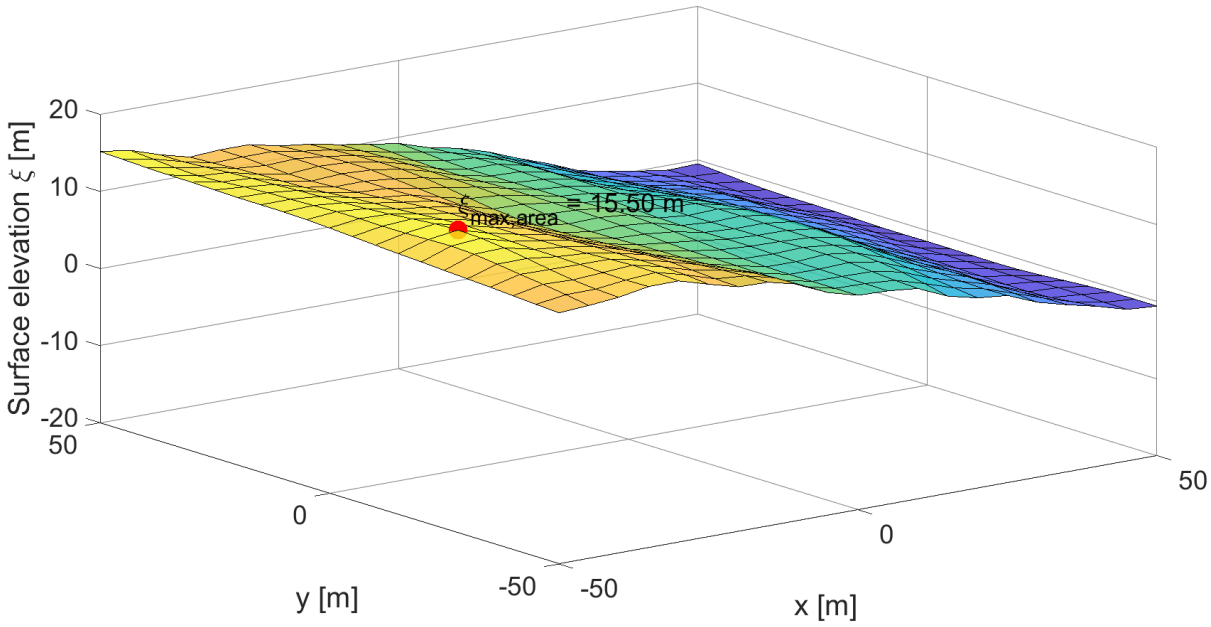

Figure 15: *Snapshot of surface elevation process for simulated area at time of area maximum during one hour. The red dot indicates area maximum.*

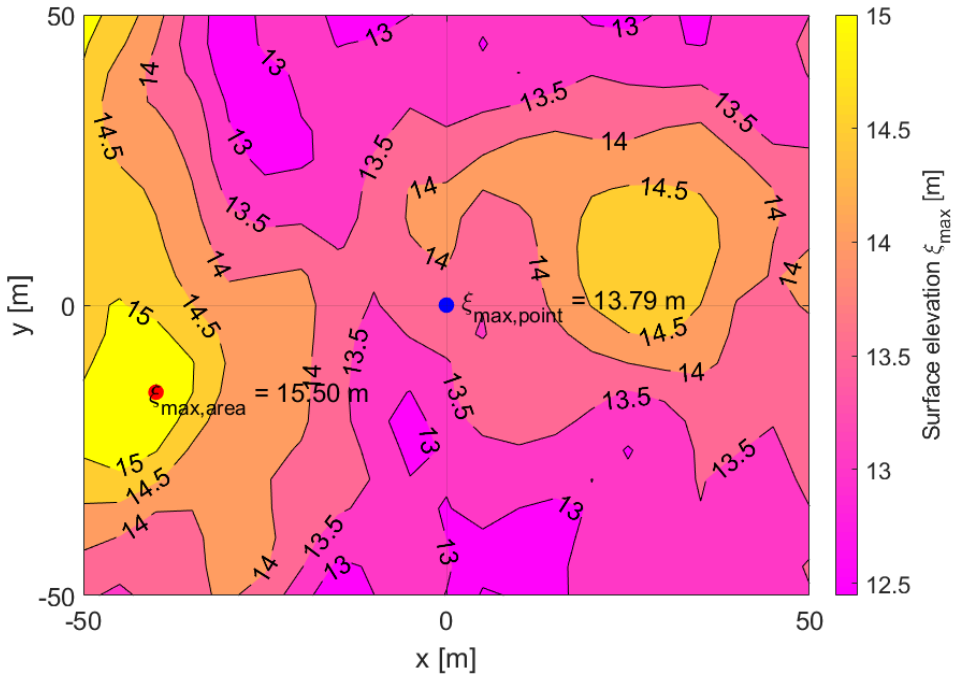

Figure 16: *Contour plot of maximum surface elevation during one hour at all separate points. The blue dot indicates center point maximum and the red dot indicates area maximum.*

2.6.5 Finding high resolution area maximum crest height

To increase the accuracy of the obtained maximum area crest height, a new simulation of the surface elevation process is done with high resolution in both area grid size and in the time

parameter around the spatial coordinates and the time when the area maximum crest height occurred in the initial simulation. The new high resolution simulation uses the same random input as the initial simulation of the surface elevation process. In this way, a more accurate value for the maximum area crest height is obtained under the same random conditions as in the initial simulation. This new simulation for the surface elevation process is only done for very limited intervals in time and space to reduce additional CPU-time with the use of high resolution simulations. The new high resolution surface elevation process ξ will be calculated according to Gaussian wave theory or according to second order wave theory as described in section 2.4 and 2.5 as for the initial simulation. The high resolution surface elevation process will be calculated for all $x_{i_{hr}}$, $y_{j_{hr}}$ and $t_{k_{hr}}$ at the very limited spatial and time intervals according to equation 39

$$x_{max,area} - 2dx \leq x_{i_{hr}} \leq x_{max,area} + 2dx \quad , for\ i_{hr} = 1, 2, ..., N_{x_{hr}}$$

$$, and \quad y_{max,area} - 2dy \leq y_{j_{hr}} \leq y_{max,area} + 2dy \quad , for\ j_{hr} = 1, 2, ..., N_{y_{hr}} \tag{39}$$

$$, and \quad t_{max,area} - 2dt \leq t_{k_{hr}} \leq t_{max,area} + 2dt \quad , for\ k_{hr} = 1, 2, ..., N_{t_{hr}}$$

, where dx, dy and dt are respectively the area grid size and the time step from the initial simulation, and $x_{max,area}$, $y_{max,area}$ and $t_{max,area}$ are respectively the spatial coordinates and the time of the maximum area crest height from the initial simulation. If some of the new high resolution spatial coordinates or new values for the high resolution time parameter are located outside the initial area or outside the initial time frame, these spatial coordinates or time parameter values will not be used in the calculation of the new high resolution surface elevation process. The new high resolution spatial coordinates $x_{i,hr}$ and $y_{j,hr}$ and the time parameter $t_{k_{hr}}$ are set in MATLAB to have area grid size side lengths and time steps five times smaller in size than the spatial coordinates x_i and y_j and the time parameter t_k from the initial simulation. This size of high resolution grid size and time steps are chosen to obtain a good accuracy for the high resolution maximum area crest height near the real crest of the wave profile without spending to much CPU-time for the additional high resolution simulation. The high resolution maximum area crest heights $\xi_{max,area}$ are obtained with the following equation.

$$\xi_{max,area} = max\Big[\xi(x_{i_{hr}}, y_{j_{hr}}, t_{k_{hr}})\Big] \tag{40}$$

, where ξ is the new high resolution surface elevation process. The maximum area crest height has to be found from all $x_{i_{hr}}$, $y_{j_{hr}}$ and $t_{k_{hr}}$ for which the new high resolution surface process is calculated for, according to equation 39.

Figure 17 shows the area and the area grid size used in the initial simulation as explained in section 2.6.5, and the new high resolution area and grid size. The size of the new high resolution area is 20m*20m compared to 100m*100m in the initial simulation. The area grid size used in the new high resolution simulation is 1m*1m compared to 5m*5m in the initial simulation. The new high resolution maximum is in this particular case located at ($x_{i_{hr}}$, $y_{j_{hr}}$) = (-43, -17m), compared to the maximum from the initial simulation at (x_i, y_i) = (-40m, -15m).

Figure 18 shows both the initial and the new high resolution surface elevation process ξ around the time where the area maximum crest heights occurred. Note that the new high resolution surface elevation process has a shift in time with respect to the initial surface elevation process. This is because the new area maximum obtained with the high resolution method is in this case

located at a slightly different spatial coordinates within the initial area than the area maximum from the initial simulation. The wave profile from the initial surface elevation process also has a much more jagged shape than the wave profile from the high resolution surface elevation process. The time step used in the high resolution simulations is 1/5 of the time step used in the initial simulations, which was 0.25 seconds. The high resolution method for finding the maximum area surface elevation will obtain a value for the maximum crest height closer to the true crest of the wave profile within the area of interest, than the area maximum crest height obtained from the initial simulation.

Figure 19 shows a snapshot of the surface profile for the area simulated with the high resolution method, at the time of high resolution area maximum. Figure 20 shows a contour plot of the maximum surface elevation at all high resolution spatial points during the new high resolution simulation. All four figures are from the same high resolution simulation of the surface elevation process ξ over an area. The maximum area crest height from the new high resolution simulation is indicated with a red dot in figures 18, 19 and 20, and correspond in both time and space. The difference between obtained maximum area crest height from the initial surface elevation process and the high resolution surface elevation process will be more profound when the spatial steps and time steps increase in the initial simulation. The high resolution area maximum method will therefore be used for all further calculations in this thesis involving finding the maximum area crest height $\xi_{max,area}$.

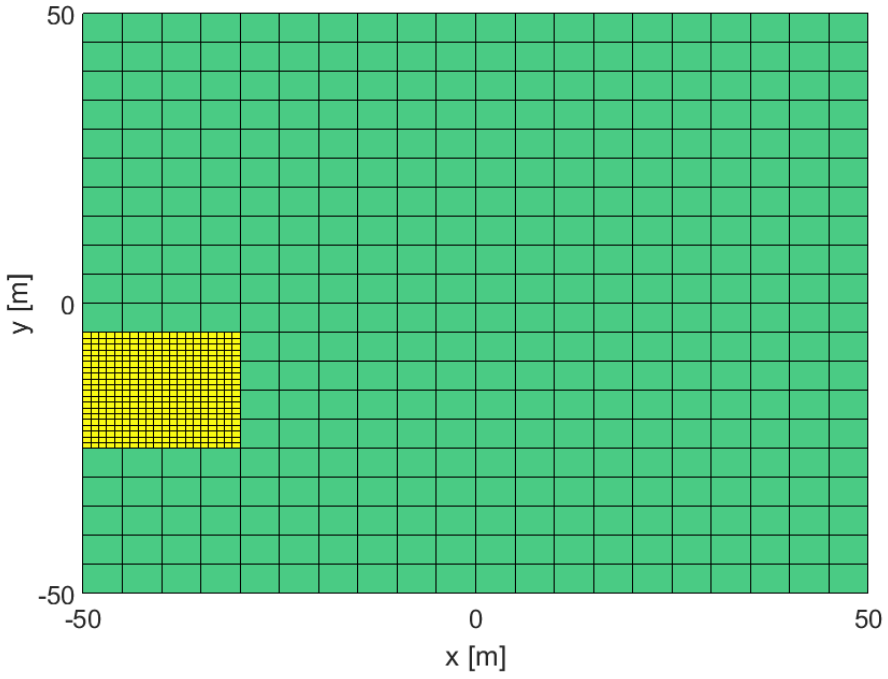

Figure 17: *Area and grid size from initial simulation in green, and area and grid size from high resolution simulation in yellow. The location of the high resolution area is based on the location of the initial area maximum.*

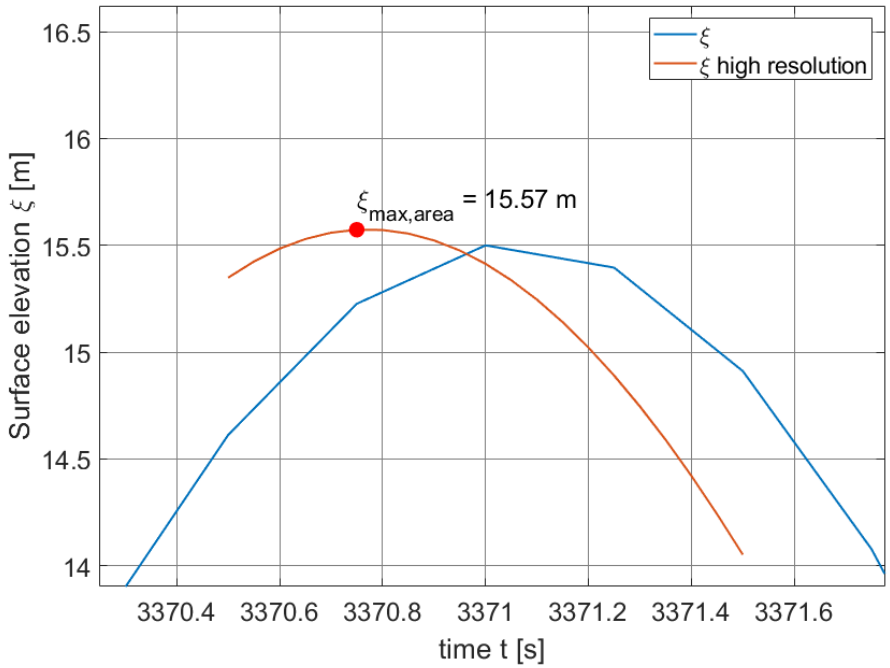

Figure 18: *Surface elevation process at point of area maximum around the time of area maximum, along with high resolution surface elevation process at point of high resolution area maximum. The red dot indicates high resolution area maximum. Note that the two surface elevation processes is in this case not located at the same spatial coordinates, and the maximum area crest heights are therefore also shifted in time.*

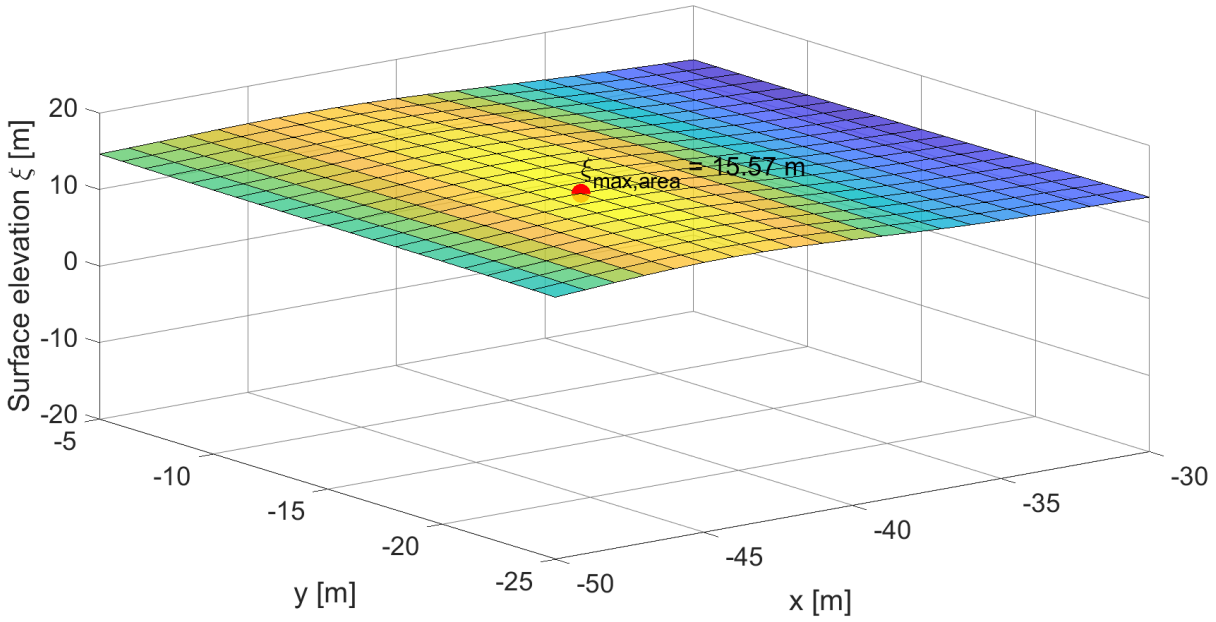

Figure 19: *Snapshot of high resolution surface elevation process for simulated high resolution area at time of high resolution area maximum. The red dot indicates high resolution area maximum.*

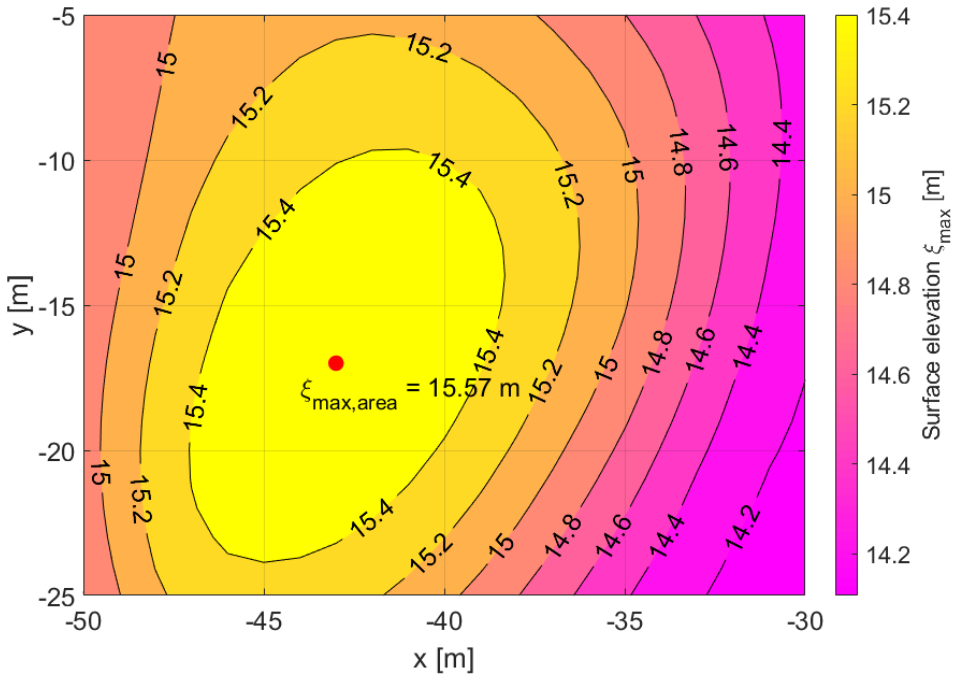

Figure 20: *Contour plot of maximum high resolution surface elevation during high resolution simulation at all separate points. The red dot indicates high resolution area maximum.*

A parameter study for the convergence of area maximums obtained from the high resolution method are done in section 6.7 for variations in the area grid size, and is also compared to the area maximums obtained from the initial simulations to show the effect of using the high resolution method.

2.6.6 Simplifications made in MATLAB for maximum crest heights

There are no further simplifications done in MATLAB when finding the maximum crest heights than the simplifications already done when simulating the surface elevation process. If the time steps between calculated values of the surface elevation process are large, the shapes of the waves in time will not be represented in a good way. The same is true when the area grid size is large. If the area grid size is large, the shapes of the waves in space will not be represented in a good way. Therefore, if the time step and the area grid size are large when a simulation of the surface process is done, it is not sure that the obtained largest crest height is from the real largest crest from the simulation. If the high resolution procedure is then applied, it can be applied at the wrong time and at the wrong location. It is therefore important to have spatial and time steps small enough for the real highest crest to be sampled in the initial simulation of the surface elevation process. The high resolution method can then be applied on that crest to find a value of the maximum crest height close to the top of this crest.

2.7 Comments regarding the MATLAB program for simulation of surface elevation process

Since MATLAB have a deterministic pseudo-random number generator, MATLAB will by default simulate the same surface elevation process every time MATLAB is restarted when using the same input parameters. To avoid this, the random number generator has to be manually

seeded to make sure that all simulations use different random numbers. The random number generator is therefore seeded with the current time at each simulation startup. All results produced will then use a different set of random numbers, and no multiplication of results will occur.

3 Extreme value distributions for maximum crest heights

3.1 Extreme value distribution for Gaussian maximum crest heights

3.1.1 About extreme value distribution for Gaussian maximum crest heights

The Rayleigh distribution function (Longuet-Higgins (1952)) is commonly used as the distribution function for Gaussian wave heights and Gaussian crest heights for small banded processes. The Rayleigh distribution will be used for the Gaussian zero crossing crest heights. The Gaussian zero crossing crest height can be defined as the highest level of a Gaussian surface elevation process between two zero crossings for one point in space. The Rayleigh distribution for crest heights is non conservative for real ocean crest heights.

3.1.2 Assumptions for extreme value distribution for Gaussian maximum crest heights

The assumption is made that all Gaussian crest heights are identically Rayleigh distributed. It is also assumed that all Gaussian crest heights are statistically independent. The first assumption is probably a good one when predicting Gaussian crest heights, while the latter one can be questioned and will probably give predicted Gaussian crest heights slightly on the high side (Knut Minsaas (2004) and Myrhaug (2005)). It is also assumed that the wave spectrum is narrow banded (Knut Minsaas (2004)).

3.1.3 Creating extreme value distribution for Gaussian maximum crest heights

The equation used for the Rayleigh cumulative distribution function (CDF) $F_{\Xi^{(1)}_{c,point}}$ for the Gaussian zero crossing crest heights is

$$F_{\Xi^{(1)}_{c,point}}(\xi^{(1)}_{c,point}) = 1 - exp\Big[-8\Big(\frac{\xi^{(1)}_{c,point}}{H_s}\Big)^2\Big] \tag{41}$$

$$, where\ \xi^{(1)}_{c,point} \geq 0$$

Due to the assumption that all Gaussian crest heights are identically distributed and statistically independent, the extreme value distribution $F_{\Xi^{(1)}_{max,point,T}}$ for the maximum Gaussian crest height during the time period T can be written as

$$F_{\Xi^{(1)}_{max,point,T}}(\xi^{(1)}_{max,point}) = \left[1 - exp\Big[-8\Big(\frac{(\xi^{(1)}_{max,point}}{H_s}\Big)^2\Big]\right]^{N_{\xi^{(1)}_{c,point,T}}} \tag{42}$$

$$, where\ \xi^{(1)}_{max,point} \geq 0$$

, and $N_{\xi^{(1)}_{c,point,T}}$ is the number of individual Gaussian zero crossing crest heights. $N_{\xi^{(1)}_{c,point,T}}$ can be found using the equation

$$N_{\xi^{(1)}_{c,point,T}} = \frac{T}{T_z} \tag{43}$$

, where T_z is the zero up crossing wave period which is given in RP-C205 (2010) as

$$T_z = T_p\Big[0.6673 + 0.05037\gamma - 0.006230\gamma^2 + 0.0003341\gamma^3\Big] \tag{44}$$

The peak enhancement factor γ is the same as used in the calculations for the JONSWAP wave spectrum. The peak enhancement factor γ is calculated as given in equation 5.

$$\gamma = 42.2(\frac{2\pi H_s}{gT_p^2})^{\frac{6}{7}} \tag{5}$$

Figure 21 shows the extreme value distribution obtained by equation 42 for the maximum Gaussian crest height for three different durations T of the Gaussian surface elevation process. When the duration of the Gaussian surface elevation process increases, the extreme value distribution shifts towards higher maximum Gaussian crest heights.

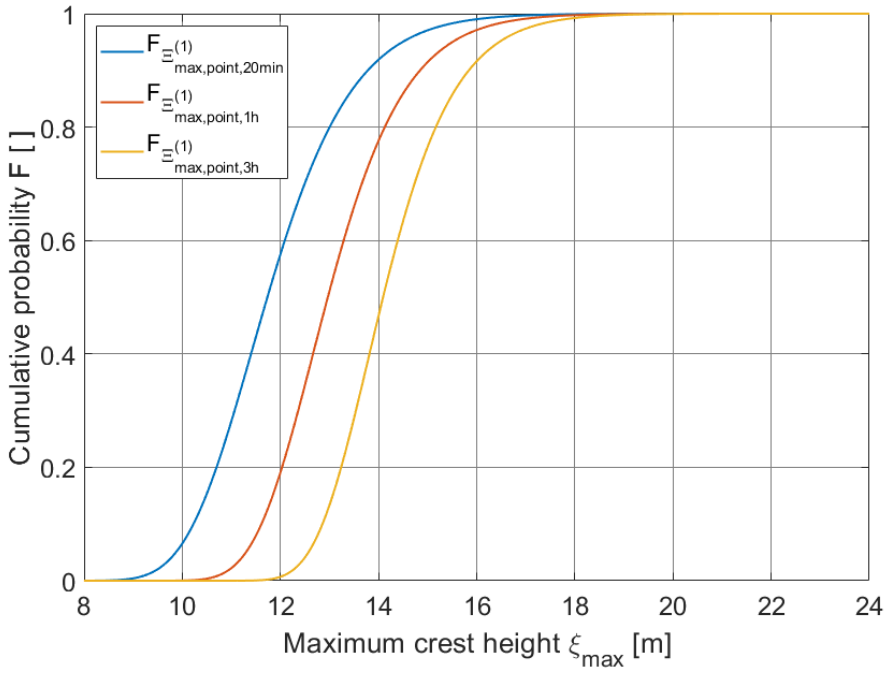

Figure 21: *Extreme value distribution for largest Gaussian crest heights for three different durations.*

3.1.4 Plotting Gaussian maximum crest heights with extreme value distribution

When maximum crest heights are to be considered, the MATLAB program for the Gaussian surface elevation process will obtain a sample of Gaussian maximum crest heights $\xi_{max}^{(1)}$ from many independent simulations of time period T. This sample of Gaussian maximum crest heights can be plotted together with the extreme value distribution from the same sea state for verification of the Gaussian maximum crest heights obtained from simulations. Both samples for the Gaussian point maximum crest heights $\xi_{max,point}^{(1)}$ and for the Gaussian area maximum crest heights $\xi_{max,area}^{(1)}$ will be plotted with the extreme value distribution. Since the extreme value distribution only applies to point maximums, the area maximums will only be plotted for comparison reasons, to see how they distribute compared to the point maximums. The Gaussian point maximum crest heights is expected to be slightly on the low side of the extreme value distribution due to the assumption that all crest heights are statistically independent, but still very close. The Gaussian area maximum crest heights should be on the high side of the extreme value distribution when the area considered is larger than a single point. When the

area of simulation increases, the area maximums are expected to move further to the high side of the extreme value distribution. To plot the sample of Gaussian maximum crest heights with the extreme value distribution, the sample of Gaussian maximum crest heights is sorted from lowest value to highest value $[\xi^{(1)}_{max,1} \leq \xi^{(1)}_{max,2} \leq ... \leq \xi^{(1)}_{max,N_{sample}}]$. The sorted sample of the maximum crest height will then be plotted against the empirical distribution function for the Gaussian maximum crest heights. The empirical distribution function $\hat{F}_{\Xi^{(1)}_{max}}(\xi^{(1)}_{max,k_s})$ is given by the following equation

$$\hat{F}_{\Xi^{(1)}_{max}}(\xi^{(1)}_{max,k_s}) = \frac{k_s}{N_{sample}+1} \tag{45}$$

$$, for\ k_s = 1, 2, ..., N_{sample}$$

,where k_s is the sorted sample number and N_{sample} is the sample size. Figure 22 shows the Gaussian extreme value distribution for a three hour sea state along with a sample of 200 Gaussian maximum point crest heights $\xi^{(1)}_{max,point}$ obtained by simulations in MATLAB for the same time period.

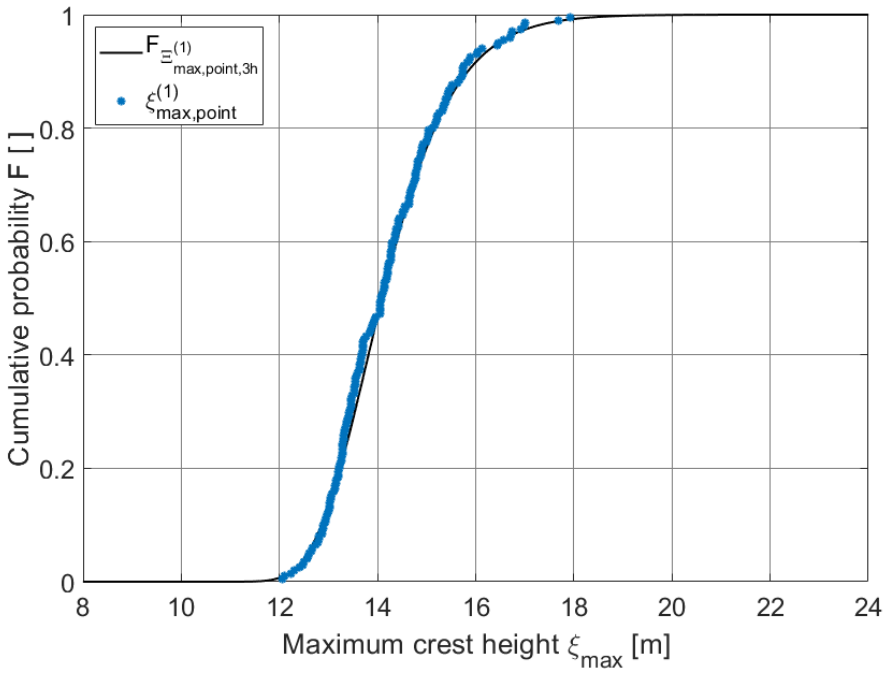

Figure 22: *Three hour extreme value distribution along with 200 Gaussian maximum crest heights obtained by simulations.*

3.2 Extreme value distribution for second order maximum crest heights

3.2.1 About extreme value distribution for second order maximum crest heights

For the second order zero crossing crest heights, the Forristall crest height distribution is used. The Forristall distribution function is recommended by RP-C205 (2010), but was developed by Forristall (2000). The Forristall distribution is a Weibull distribution function and will be used as given in RP-C205 (2010). The second order zero crossing crest height can be defined

as for the Gaussian zero crossing crest heights, as the highest level of a second order surface elevation process between two zero crossings for one point in space. The Forristall distribution exists as a long crested model and as a short crested model. Kvingedal et al. (2018) showed that both the Forristall distributions gave reasonable results when compared to real crest height measurements for a location in the northern North Sea. Gunnar Lian (2015) showed that the short crested Forristall distribution may be slightly conservative in the most severe sea states at a location in the North Sea.

3.2.2 Assumptions for extreme value distribution for second order maximum crest heights

The assumption is made that all second order crest heights are identically Forristall distributed. It is also assumed that all second order crest heights are statistically independent. The first assumption is probably a good one when predicting second crest heights, while the latter one can be questioned and will probably give predicted second order crest heights slightly on the high side (Knut Minsaas (2004) and Myrhaug (2005)). It is also assumed that the wave spectrum is narrow banded (Knut Minsaas (2004)). The deep water assumption made in section 2.4.2 and 2.5.2 is also applied for the Forristall distribution.

3.2.3 Creating extreme value distribution for second order maximum crest heights

Equation 46 shows the Forristall CDF $F_{\Xi^{(2)}_{c,point}}$ for zero crossing crest heights and is obtained from RP-C205 (2010).

$$F_{\Xi^{(2)}_{c,point}}(\xi^{(2)}_{c,point}) = 1 - exp\Bigg[- \Big(\frac{\xi^{(2)}_{c,point}}{\alpha_c H_s}\Big)^{\beta_c}\Bigg] \tag{46}$$

$$, where\ \xi^{(2)}_{c,point} \geq 0$$

Due to the assumption that all second order crest heights are identically distributed and statistically independent, the extreme value distribution $F_{\Xi^{(2)}_{max,point,T}}$ for the maximum second order crest height during the time period T can be written as

$$F_{\Xi^{(2)}_{max,point,T}}(\xi^{(2)}_{max,point}) = \Bigg[1 - exp\Bigg[- \Big(\frac{\xi^{(2)}_{max,point}}{\alpha_c H_s}\Big)^{\beta_c}\Bigg]\Bigg]^{N_{\xi^{(2)}_{c,point,T}}} \tag{47}$$

$$, where\ \xi^{(2)}_{max,point} \geq 0$$

, and $N_{\xi^{(2)}_{c,point,T}}$ is the number of individual second order zero crossing crest heights. $N_{\xi^{(2)}_{c,point,T}}$ can be found using the equation

$$N_{\xi^{(2)}_{c,point,T}} = \frac{T}{T_z} \tag{48}$$

, where T_z is the zero up crossing wave period as given in equation 44. The peak enhancement factor γ is the same as used in the calculations for the JONSWAP wave spectrum and is given in equation 5. The extreme value distribution for second order crest heights is different for short and long crested sea states. The Weibull parameters $\alpha_{c,lc}$ and $\beta_{c,lc}$ for a long crested sea state are obtained from RP-C205 (2010) and are given as

$$\alpha_{c,lc} = 0.3536 + 0.2892S_1 + 0.1060U_{rs} \tag{49}$$

$$\beta_{c,lc} = 2 - 2.1597S_1 + 0.0968U_{rs}^2 \tag{50}$$

The Weibull parameters $\alpha_{c,sc}$ and $\beta_{c,sc}$ for a short crested sea state are obtained from RP-C205 (2010) and are given as

$$\alpha_{c,sc} = 0.3536 + 0.2568S_1 + 0.0800U_{rs} \tag{51}$$

$$\beta_{c,lc} = 2 - 1.7912S_1 - 0.5302U_{rs} + 0.284U_{rs}^2 \tag{52}$$

,where S_1 is the steepness parameter and U_{rs} is the Ursell number. The steepness parameter S_1 has the equation

$$S_1 = \frac{2\pi}{g}\frac{H_s}{T_1^2} \tag{53}$$

,where g is the gravitational constant and H_s is the significant wave height. The mean wave period T_1 can be found in the following equation

$$T_1 = T_p\Big[0.7303 + 0.04936\gamma - 0.006556\gamma^2 + 0.0003610\gamma^3\Big] \tag{54}$$

The Ursell number U_{rs} has the equation

$$U_{rs} = \frac{H_s}{k_1^2 d^3} \tag{55}$$

,where d is the water depth and k_1 is the wave number assuming deep water for the frequency corresponding to the mean wave period T_1. k_1 assuming deep water can be found by the equation

$$k_1 = \frac{4\pi^2}{gT_1^2} \tag{56}$$

Equations 53, 54, 55 and 56 are obtained from RP-C205 (2010). Figure 23 shows the extreme value distribution obtained by equation 47 for the maximum second order crest heights for three different durations T for both short crested and long crested sea states. It is seen from figure 23 that the second order extreme value distribution for short crested sea states predicts smaller maximum crest heights at all probability levels than the second order extreme value distribution for long crested sea states at all three durations. When the duration of the second order surface elevation process increases, the extreme value distribution shifts towards higher expected maximum crest heights.

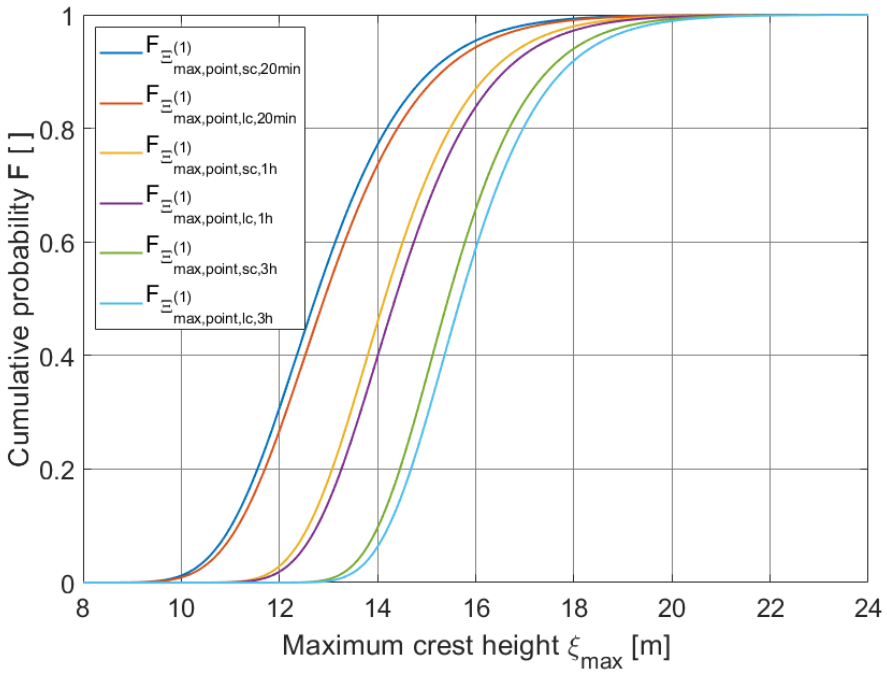

Figure 23: *Extreme value distribution for largest second order crest heights for both short and long crested sea states for three different durations.*

3.2.4 Plotting second order maximum crest heights with extreme value distribution

When plotting a sample of second order maximum crest heights with the second order extreme value distribution, the same procedure as explained for the plotting of Gaussian maximum crest heights along with the Gaussian extreme value distribution in section 3.1.4 will be followed. The second order empirical distribution function $\hat{F}_{\Xi^{(2)}_{max}}(\xi^{(2)}_{max,k_s})$ as a function of second order crest heights will be used in stead. The second order crest heights will be plotted along with the second order extreme value distribution from the same sea state.

Figure 24 shows the second order extreme value distributions for short and long crested three hour sea states along with a sample of 200 second order maximum point crest heights $\xi^{(2)}_{max,point}$ obtained by simulations of a long crested sea state in MATLAB for the same time period.

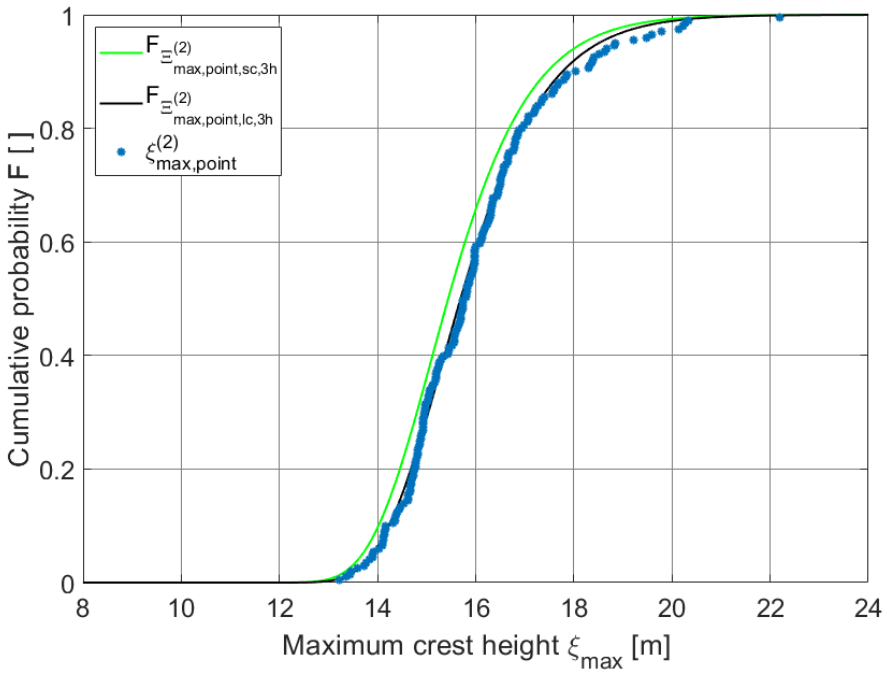

Figure 24: *Three hour extreme value distributions for long and short crested sea states along with 200 second order maximum crest heights obtained by simulations of a long crested sea state.*

4 Metocean data

4.1 Location for simulation

All analyses performed in this thesis are based on an example metocean design basis (Example Metocean Report (2003)) for Statfjord oil field outside the west coast of Norway. Due to later issued metocean reports for Statfjord oil field, this example metocean report is no longer valid. Therefore, the results obtained from analyses using this metocean data are no longer considered valid at Statfjord oil field. The metocean data used to from the example metocean report is collected from both Statfjord and Gullfaks oil fields located outside the west coast of Norway, and also from North Cormorant oil field located into UK territory. The results for the marginal extremes are based on wave measurements within the time period 1983 - 2002 from both Statfjord/Gullfaks and the North Cormorant oil fields (Example Metocean Report (2003)). Figure 25 shows Statfjord oil field and is obtained from Pettersen (2016). Figure 26 shows the location of Statfjord and Gullfaks oil fields and is obtained from Lundberg (2019). North Cormorant oil field is located to the west of Statfjord and Gullfaks into UK territory.

Figure 25: *Statfjord oil field (Pettersen (2016)).*

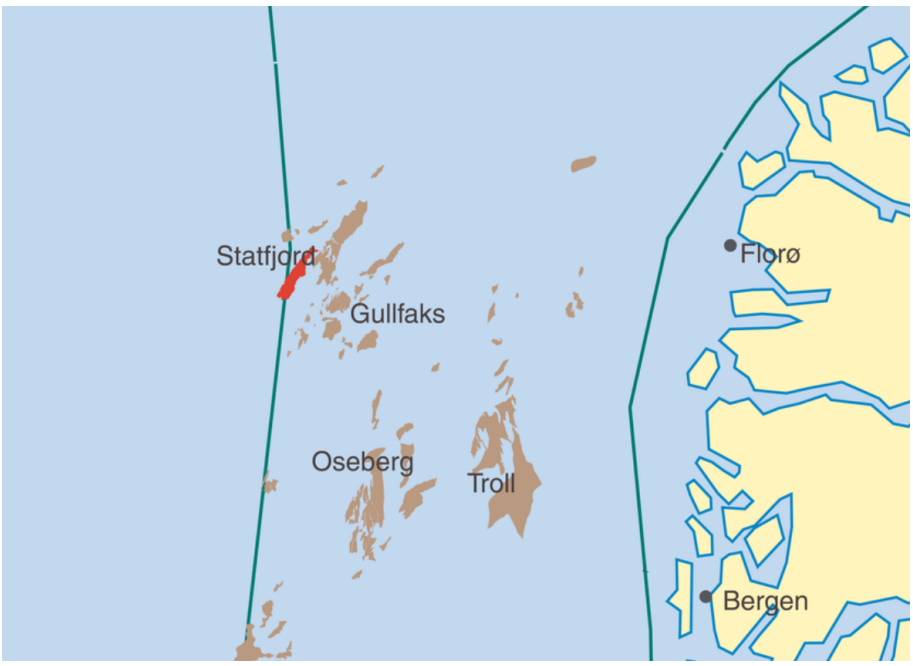

Figure 26: *Map showing Statfjord oil field (Lundberg (2019)).*

4.2 Metocean data from location

The area crest height effect will be analyzed in this thesis for a sea state corresponding to a 10^{-2} annual probability of being exceeded. Figure 27 shows omni directional contour lines for Statfjord oil field obtained from Example Metocean Report (2003). Table 1 shows marginal omni directional extremes for the significant wave height H_s, and corresponding spectral peak period T_p, corresponding to the contour lines in figure 27. All values in table 1 are obtained from Example Metocean Report (2003). Only omni directional data will be used in further calculations.

Table 1: *Marginal omni directional extremes for the significant wave height and corresponding spectral peak periods. The values in the table are obtained from Example Metocean Report (2003).*

Return period	**Extreme sea states**		
(years)	H_s [m]	T_p [s]	90% range of T_p [s]
1	11.0	14.2	12.1 - 16.5
10	13.0	15.1	13.1 - 17.3
100	14.9	16.0	14.0 - 18.2
10000	18.2	17.5	15.5 - 19.7

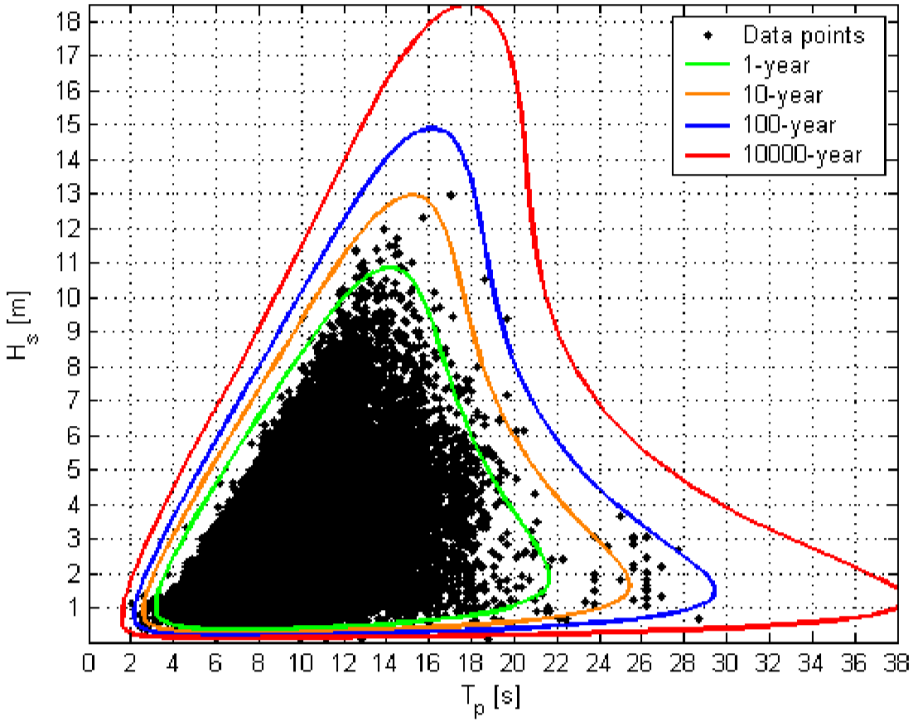

Figure 27: *Contour lines for Statfjord oil field (Example Metocean Report (2003)).*

4.3 Finding worst sea state along contour line

The worst sea state regarding crest heights along the 100 year contour line in figure 27 will be used as the basis sea state for all simulations conducted in this thesis. The worst sea state along the 100 year contour line regarding crest heights can be found by plotting sea states from the contour line in extreme value distributions for second order crest heights, and then comparing a percentile value from the different extreme value distributions, to find the worst sea state along the contour line. It is recommended in NORSOK STANDARD N-003 (2007) to use a percentile value between 0.85th and 0.95th when calculating extreme values for a sea state with an annual exceedance probability of 10^{-2}. The percentile value used for comparing sea states to locate the worst sea state along the 100 year contour line will therefore be set to 90 after recommendations in Example Metocean Report (2003). Sea states around the significant wave height maximum of the 100 year contour line are plotted in extreme value distributions for both long crested and short crested sea states. A full description of the second order extreme value distributions for crest heights used for locating the worst sea state along the contour line for both short and long crested sea can be found in section 3.2.

Figure 28 shows the extreme value distributions for crest heights for different short crested sea states around the marginal maximum of the significant wave height at the 100 year contour line. Figure 29 shows the extreme value distributions for crest heights for different long crested sea states around the marginal maximum of the significant wave height maximum at the 100 year contour line.

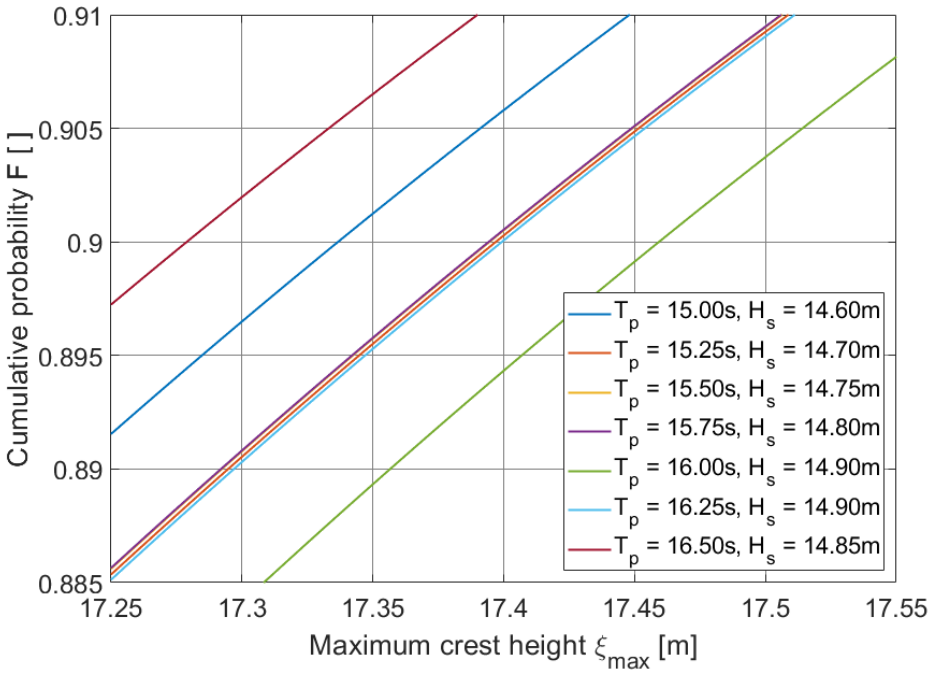

Figure 28: *Extreme value distributions for second order crest heights for different short crested sea states around the marginal maximum of the significant wave height at the 100 year contour line.*

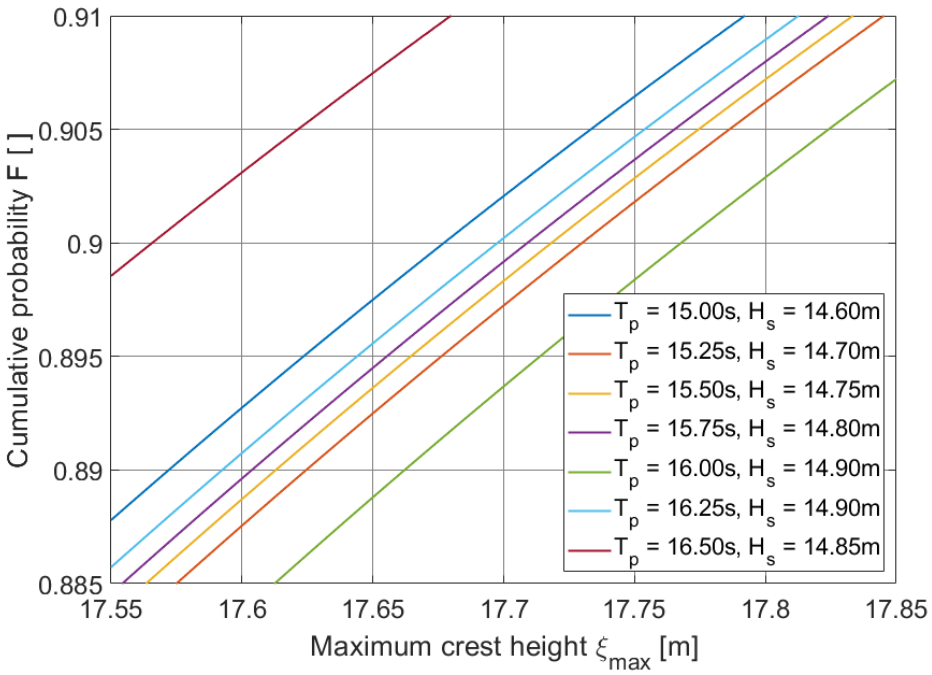

Figure 29: *Extreme value distributions for second order crest heights for different long crested sea states around the marginal maximum of the significant wave height at the 100 year contour line.*

The values used for the significant wave height H_s and the spectral peak period T_p in the extreme value distributions in figures 28 and 29, along with the obtained values for the maximum crest heights $\xi^{(2)}_{max,point}$ for short crested (SC) and for long crested (LC) sea at a 90th percentile level can be found in table 2.

Table 2: *Maximum crest heights calculated from 90th percentile of extreme value distributions for second order crest heights for points along the 100-year contour line.*

T_p [s]	H_s [m]	SC 90th p $\xi^{(2)}_{max,point}$ [m]	LC 90th p $\xi^{(2)}_{max,point}$ [m]
15.00	14.60	17.34	17.68
15.25	14.70	17.40	17.73
15.50	14.75	17.39	17.72
15.75	14.80	17.39	17.71
16.00	14.90	17.46 (max)	17.77 (max)
16.25	14.90	17.40	17.70
16.50	14.85	17.28	17.57

As seen in table 2, the worst sea state regarding crest heights along the 100 year contour line is the same for both short and long crested sea. This sea state also corresponds to the sea state of the marginal extreme for the significant wave height in table 1. The process of reading data from the contour lines in figure 27 is a source of error when finding the worst sea state for an annual exceedance probability of 10^{-2}. However, the results obtained for the significant wave height and the corresponding spectral peak period are assumed valid for further use when analyzing the area crest height effect.

4.4 Sea state obtained for analysis

The results for the significant wave height and the corresponding spectral peak period obtained as the worst sea state regarding crest heights for an annual exceedance probability of 10^{-2} are summed up in table 3. This sea state will be used as a basis for all further analyses performed in this thesis.

Table 3: *Worst sea state along contour line regarding crest heights with an annual exceedance probability of* 10^{-2}*. This sea state is chosen as the basis sea state for all further simulations in this thesis.*

Return period	**Worst 100 year extreme sea state**	
(years)	H_s [m]	T_p [s]
100	14.9	16.0

5 Verification of MATLAB program for simulation of surface elevation process

5.1 Verification of variance from Gaussian simulations

5.1.1 About verification of variance from Gaussian simulations

Under the assumptions made when creating the JONSWAP wave spectrum and the Gaussian surface elevation process, in respectively sections 2.1.2 and 2.4.2, that the surface process is stationary, Gaussian distributed and ergodic, we can write (Knut Minsaas (2004))

$$m_{0,input,Gauss} = \frac{1}{16} H_s^2 \tag{57}$$

,where $m_{0,input,Gauss}$ is the Gaussian input variance and H_s is the significant wave height used for creating the JONSWAP wave spectrum. Equation 57 is valid for the JONSWAP wave spectrum (RP-C205 (2010)) and will be used to calculate the input variance in a Gaussian sea state at a given significant wave height. Since the mean of the Gaussian surface process is zero, we can use the following equation for the variance from Gaussian realizations (Haver (2017)).

$$m_{0,realization,Gauss} = \frac{1}{N_t} \sum_{k=1}^{N_t} \left[\xi^{(1)}(t_k)\right]^2 \tag{58}$$

,where $\xi^{(1)}$ is the Gaussian surface elevation process at any spatial coordinate at time step t_k and N_t is the number of time steps. Since the Gaussian surface process is ergodic, the variance could also be found over multiple locations, or from a combination of time steps and spatial locations. However, in this verification procedure, the variance from realization is found from simulations at one spatial point.

The value obtained by equation 58 should converge to the value obtained by equation 57 when $\Delta\omega \to 0$, $f_{max} \to \infty$ and when $t \to \infty$ (Knut Minsaas (2004)), both for Gaussian simulations using deterministic and random wave amplitudes. The input parameters used in the JONSWAP wave spectrum and in the simulations of the Gaussian surface elevation process when verifying the variance are given in table 4. The variance from realization is calculated for every three hours of simulation time.

Table 4: *Parameters used in Gaussian simulations for verification of variance.*

Parameter	**Value**
Significant wave height H_s [m]	14.90
Spectral peak period T_p [s]	16.00
Directional shape parameter n_d [ ]	∞
Mean wave direction w.r.t x-axis θ_0 [deg]	0.00
Simulation duration t [s]	9*1200
Wave spectrum cutoff frequency f_{max} [hz]	0.3652
Number of frequency components N_f [hz]	1314
Time step dt [s]	0.25
Number of individual simulations N_{sim} [pcs]	10000

The wave spectrum cutoff frequency f_{max} is set to 0.3652 hz in the simulations. The variance of the wave spectrum used in simulations will then be less than 0.08% lower than the variance for the wave spectrum with f_{max} at ∞, as given in equation 57.

5.1.2 Verification of variance in Gaussian simulations using deterministic wave amplitudes

The Gaussian input variance $m_{0,input,Gauss}$ and the variance $m_{0,realization,Gauss}$ calculated from a 30000 hour realization of the Gaussian surface elevation process using deterministic wave amplitudes, along with the deviation between the two are given in table 5. The input variance and the variance from realization are calculated with respectively equations 57 and equation 58. A convergence plot of the variance from simulation as a function of simulation duration, along with the input variance is given in figure 30.

Table 5: *Variance calculated for input to spectrum and variance calculated from a 30000 hour Gaussian realization using deterministic wave amplitudes.*

Calculated variance	**Value**
Variance input to spectrum $m_{0,input,Gauss}$ $[m^2]$	13.8756
Variance from realization $m_{0,realization,Gauss}$ $[m^2]$	13.8619
Deviation in percent [ ]	-0.10%

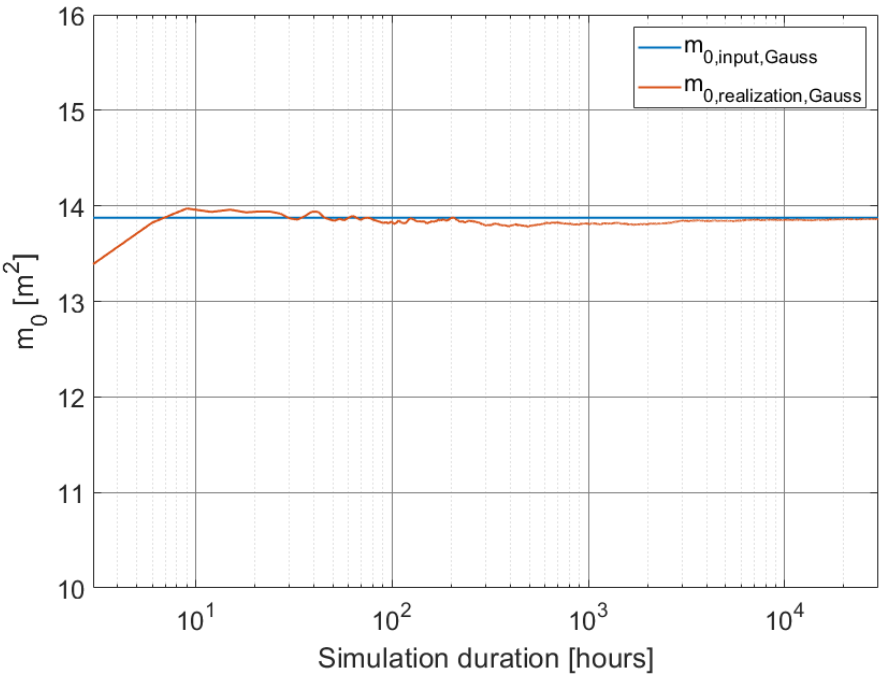

Figure 30: *Variance from Gaussian simulations using deterministic wave amplitudes as a function of simulation duration, along with input variance.*

As seen in table 5, the Gaussian input variance and the variance from the 30000 hour realization of the Gaussian surface elevation process using deterministic wave amplitudes are approximately equal. It is therefore concluded that the variance in simulated Gaussian sea states using deterministic wave amplitudes is correct.

5.1.3 Verification of variance in Gaussian simulations using random wave amplitudes

The Gaussian input variance $m_{0,input,Gauss}$ and the variance $m_{0,realization,Gauss}$ calculated from a 30000 hour realization of the Gaussian surface elevation process using random wave amplitudes, along with the deviation between the two are given in table 6. The input variance and the variance from realization are calculated with respectively equations 57 and equation 58. A convergence plot of the variance from simulation as a function of simulation duration, along with the input variance is given in figure 31.

Table 6: *Variance calculated for input to spectrum and variance calculated from a 30000 hour Gaussian realization using random wave amplitudes.*

Calculated variance	**Value**
Variance input to spectrum $m_{0,input,Gauss}$ $[m^2]$	13.8756
Variance from realization $m_{0,realization,Gauss}$ $[m^2]$	13.8665
Deviation in percent [ ]	-0.07%

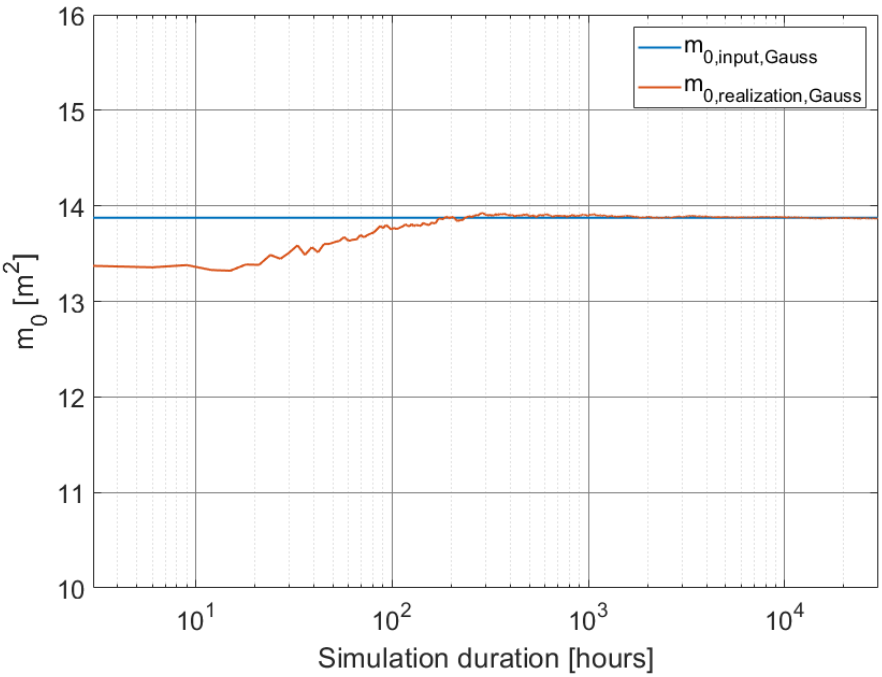

Figure 31: *Variance from Gaussian simulations using random wave amplitudes as a function of simulation duration, along with input variance.*

As seen in table 6, the Gaussian input variance and the variance from the 30000 hour realization of the Gaussian surface elevation process using deterministic wave amplitudes are approximately equal. It is therefore concluded that the variance in simulated Gaussian sea states using deterministic wave amplitudes also is correct.

5.2 Verification of variance in second order simulations

5.2.1 About verification of variance in second order simulations

Since the second order surface process does not have a mean value of zero, the variance from realizations of the second order surface process have to be calculated based on the sample mean. Equation 59 is used to calculate the variance $m_{0,realization,2nd}$ from second order realizations. Equation 60 is used to calculate the sample mean $\bar{\xi}$. Both equations are obtained from Haver (2017).

$$m_{0,realization,2nd} = \frac{1}{(N_t - 1)} \sum_{k=1}^{N_t} \left[\xi^{(2)}(t_k) - \bar{\xi}\right]^2 \tag{59}$$

$$\bar{\xi} = \frac{1}{N_t} \sum_{k=1}^{N_t} \xi^{(2)}(t_k) \tag{60}$$

,where $\xi^{(2)}$ is the second order surface elevation process at any spatial coordinate at time step t_k and N_t is the number of time steps. The variance from second order realizations will be compared to the Gaussian input variance. Due to ergodicity, the variance from second order realizations could also be found over multiple locations, or from a combination of time steps and spatial locations. However, in this verification procedure, the variance from second order realizations is found from simulations at one spatial point.

The input parameters used in the JONSWAP wave spectrum and in the simulations of the second order surface elevation process when verifying the variance are given in table 7. The variance from realization is calculated for every three hours of simulation time.

Table 7: *Parameters used in second order simulations for verification of variance.*

Parameter	**Value**
Significant wave height H_s [m]	14.90
Spectral peak period T_p [s]	16.00
Directional shape parameter n_d [ ]	∞
Mean wave direction w.r.t x-axis θ_0 [deg]	0.00
Simulation duration t [s]	9*1200
Wave spectrum cutoff frequency f_{max} [hz]	0.1826
Number of frequency components N_f [hz]	657
Time step dt [s]	0.50
Number of individual simulations N_{sim} [pcs]	1000

5.2.2 Verification of variance in second order simulations using deterministic wave amplitudes

The Gaussian input variance $m_{0,input,Gauss}$ and the variance $m_{0,realization,2nd}$ calculated from a 3000 hour realization of the second order surface elevation process using deterministic wave amplitudes, along with the deviation between the two are given in table 8. The input variance and the variance from realization are calculated with respectively equations 57 and equation 59. A convergence plot of the variance from simulation as a function of simulation duration, along with the input variance is given in figure 32.

Table 8: *Variance calculated for input to spectrum and variance calculated from a 3000 hour second order realization using deterministic wave amplitudes.*

Calculated variance	**Value**
Variance input to spectrum $m_{0,input,Gauss}$ $[m^2]$	13.8756
Variance from realization $m_{0,realization,2nd}$ $[m^2]$	13.8638
Deviation in percent [ ]	-0.09%

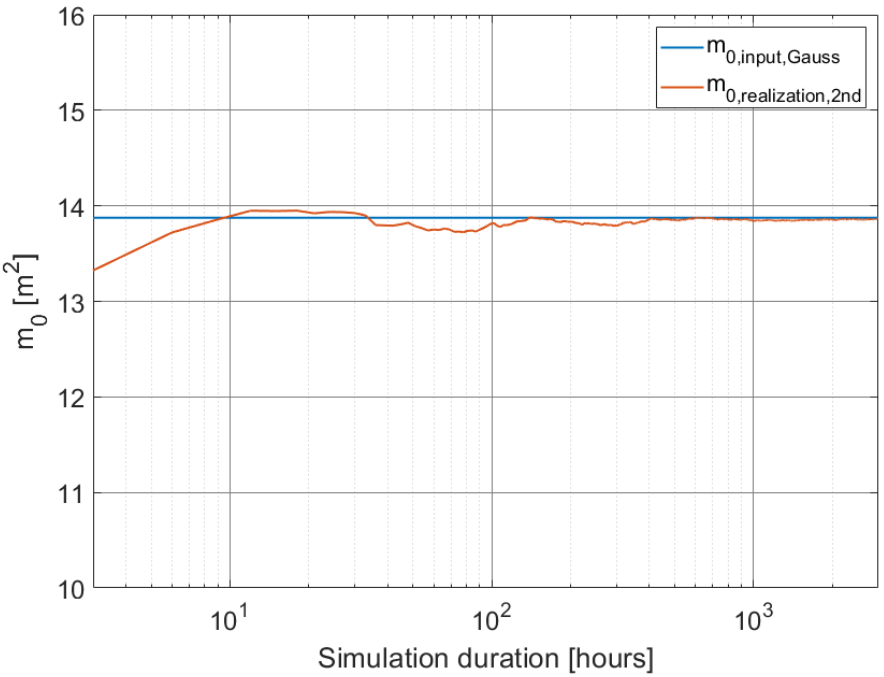

Figure 32: *Variance from second order simulations using deterministic wave amplitudes as a function of simulation duration, along with input variance.*

As seen in table 8 and figure 32, the variance from the 3000 hour realization of the second order surface elevation process using deterministic wave amplitudes is converging towards the Gaussian input variance. It is therefore concluded that the variance in simulated second order sea states using deterministic wave amplitudes is correct.

5.2.3 Verification of variance in second order simulations using random wave amplitudes

The Gaussian input variance $m_{0,input,Gauss}$ and the variance $m_{0,realization,2nd}$ calculated from a 3000 hour realization of the second order surface elevation process using random wave amplitudes, along with the deviation between the two are given in table 9. The input variance and the variance from realization are calculated with respectively equations 57 and equation 59. A convergence plot of the variance from simulation as a function of simulation duration, along with the input variance is given in figure 33.

Table 9: *Variance calculated for input to spectrum and variance calculated from a 3000 hour second order realization using random wave amplitudes.*

Calculated variance	**Value**
Variance input to spectrum $m_{0,input,Gauss}$ $[m^2]$	13.8756
Variance from realization $m_{0,realization,2nd}$ $[m^2]$	13.8649
Deviation in percent [ ]	-0.08%

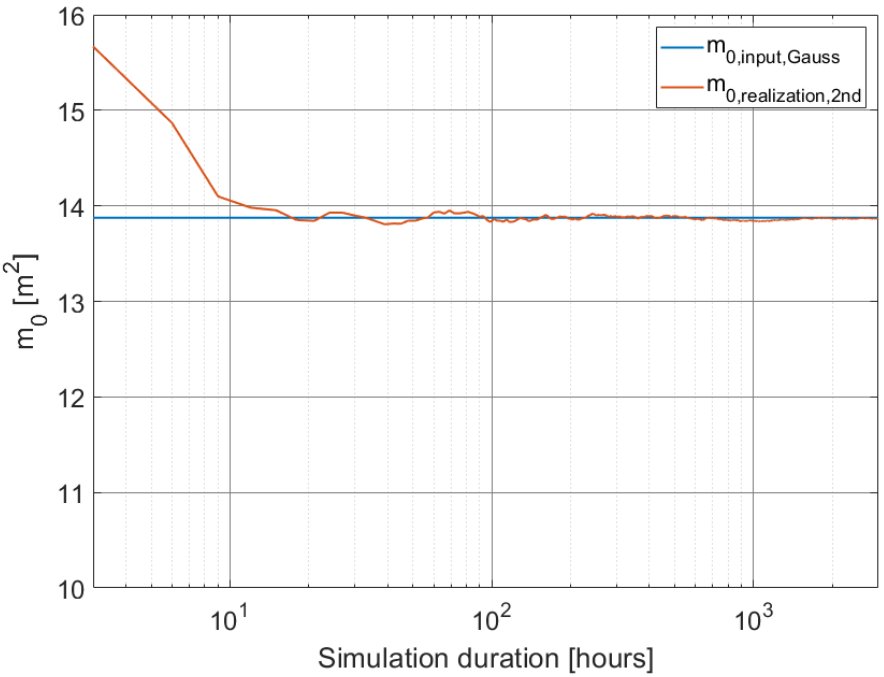

Figure 33: *Variance from second order simulations using random wave amplitudes as a function of simulation duration, along with input variance.*

As seen in table 9 and figure 33, the variance from the 3000 hour realization of the second order surface elevation process using random wave amplitudes is converging towards the Gaussian input variance. It is therefore concluded that the variance in simulated second order sea states using random wave amplitudes is correct.

5.3 Verification of maximum point crest heights from Gaussian simulations

5.3.1 About verification of maximum point crest heights from Gaussian simulations

For verification of the Gaussian maximum point crest heights $\xi^{(1)}_{max,point}$ obtained from simulations in MATLAB, the Gaussian maximum point crest heights will be plotted along with a Rayleigh CDF $F_{\Xi^{(1)}_{max,point,T}}(\xi^{(1)}_{max,point})$ for maximum point crest heights for the same sea state. A description of the Rayleigh CDF used for verification can be found in section 3.1. If the maximum point crest heights obtained from simulations in MATLAB lies close to the Rayleigh CDF for the maximum point crest heights, this will be a good indication that the maximum point crest heights obtained from simulations are calculated correctly. Due to the assumption that the wave spectrum is narrow banded made in section 3.1.2 when creating the Rayleigh CDF, the maximum point crest heights obtained from simulations in MATLAB are expected to be on the low side of the calculated Rayleigh CDF.

When a simulation is done for a time duration of one hour, the Gaussian maximum point crest height obtained from the simulation will be obtained as the maximum from three individual 20 minutes simulations. When a three hour simulation is done, the Gaussian maximum point crest height obtained from the simulation will be obtained as the maximum from nine individual 20 minutes simulations. The reason for this is so that the wave amplitudes are recalculated for every 20 minutes of simulation time. This will give closer resemblance to real conditions when using random wave amplitudes, than if the same random wave amplitudes are used for the entire simulation period when simulating for more than 20 minutes. The same procedure are done both for deterministic and random wave amplitudes. Table 10 shows the parameters used in simulations for the verification of Gaussian maximum point crest heights using both deterministic and random amplitudes.

Table 10: *Parameters used in simulation for verification of maximum point crest heights from Gaussian simulations.*

Parameter	**Value**
Significant wave height H_s [m]	14.90
Spectral peak period T_p [s]	16.00
Directional shape parameter n_d [ ]	∞
Mean wave direction w.r.t x-axis θ_0 [deg]	0.00
Simulation duration t [s]	1200, 3*1200 and 9*1200
Wave spectrum cutoff frequency f_{max} [hz]	0.3652
Number of frequency components N_f [hz]	1314
Time step dt [s]	0.25
Number of individual simulations N_{sim} [pcs]	2000

5.3.2 Verification of maximum point crest heights from Gaussian simulations using deterministic wave amplitudes

The verification of Gaussian maximum point crest heights $\xi^{(1)}_{max,point}$ from simulations using deterministic wave amplitudes are done for the three different time durations of 20min, 3*20min

and 9*20min. For each time duration, 2000 individual Gaussian maximum crest heights using deterministic wave amplitudes are obtained from simulations in MATLAB. Figure 34 shows maximum point crest heights obtained from 2000 20 minutes simulations, along with the corresponding Gaussian extreme value distribution. Figure 35 shows maximum point crest heights obtained from 2000 one hour simulations, along with the corresponding Gaussian extreme value distribution. Figure 36 shows maximum point crest heights obtained from 2000 three hour simulations, along with the corresponding Gaussian extreme value distribution. The parameters used in the simulations for verification of Gaussian simulations using deterministic wave amplitudes are found in table 10.

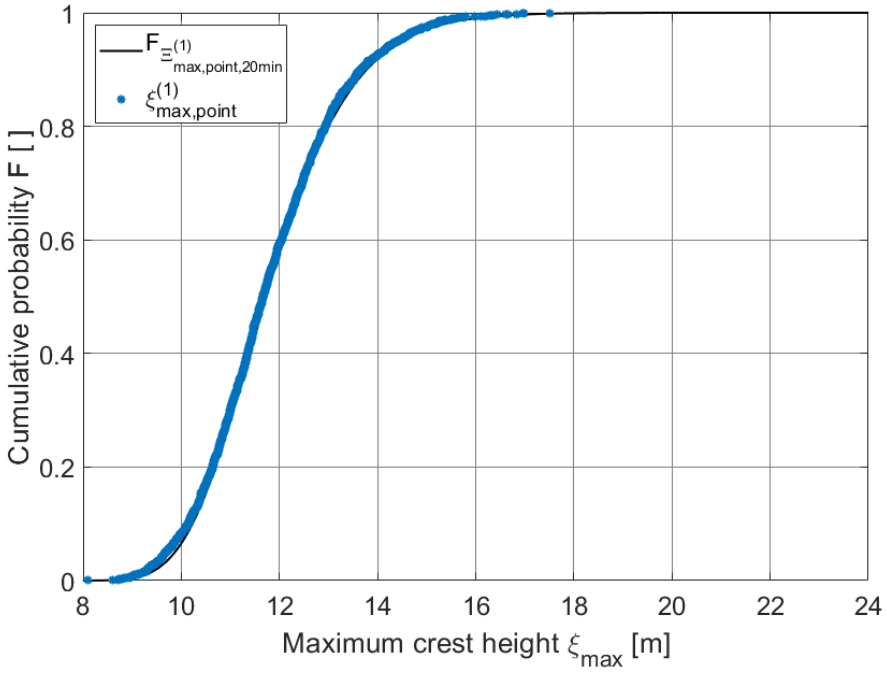

Figure 34: *Gaussian maximum point crest heights from 2000 20 minutes simulations using deterministic wave amplitudes, along with Gaussian extreme value distribution.*

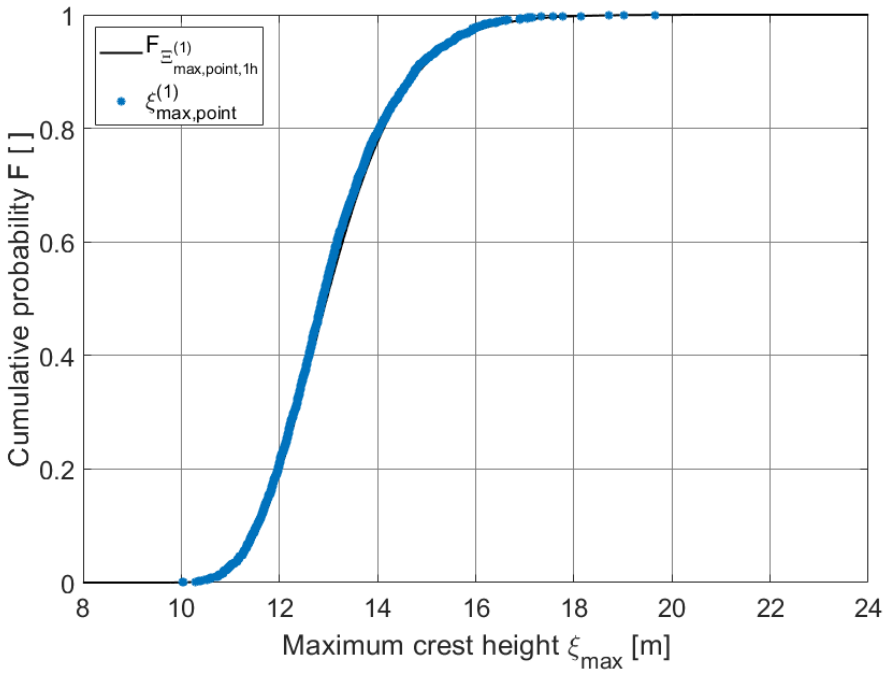

Figure 35: *Gaussian maximum point crest heights from 2000 one hour simulations using deterministic wave amplitudes, along with Gaussian extreme value distribution.*

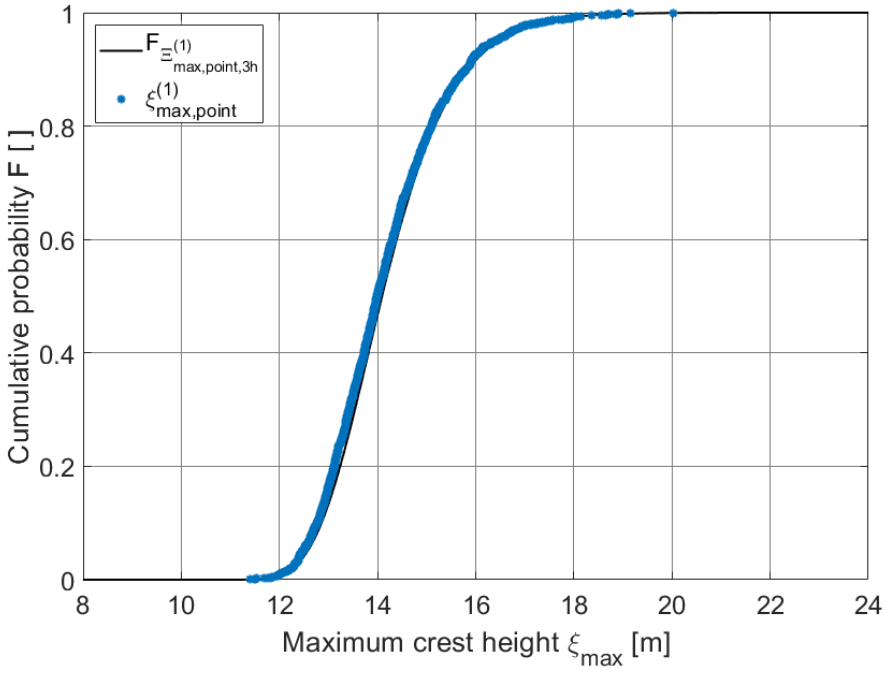

Figure 36: *Gaussian maximum point crest heights from 2000 three hour simulations using deterministic wave amplitudes, along with Gaussian extreme value distribution.*

The values obtained for the Gaussian maximum point crest heights using deterministic wave

amplitudes from simulations in MATLAB shown in figure 34, 35 and 36 gives a close fit to the corresponding Gaussian extreme value distributions. It is therefore concluded that the Gaussian maximum point crest heights $\xi^{(1)}_{max,point}$ obtained from simulations in MATLAB using deterministic wave amplitudes are valid according to Gaussian wave theory.

5.3.3 Verification of maximum point crest heights from Gaussian simulations using random wave amplitudes

The verification of Gaussian maximum point crest heights $\xi^{(1)}_{max,point}$ from simulations using random wave amplitudes are done for the three different time durations of 20min, 3*20min and 9*20min. For each time duration, 2000 individual Gaussian maximum crest heights using random wave amplitudes are obtained from simulations in MATLAB. Figure 37 shows maximum point crest heights obtained from 2000 20 minutes simulations, along with the corresponding Gaussian extreme value distribution. Figure 38 shows maximum point crest heights obtained from 2000 one hour simulations, along with the corresponding Gaussian extreme value distribution. Figure 39 shows maximum point crest heights obtained from 2000 three hour simulations, along with the corresponding Gaussian extreme value distribution. The parameters used in the simulations for verification of Gaussian simulations using random wave amplitudes are found in table 10.

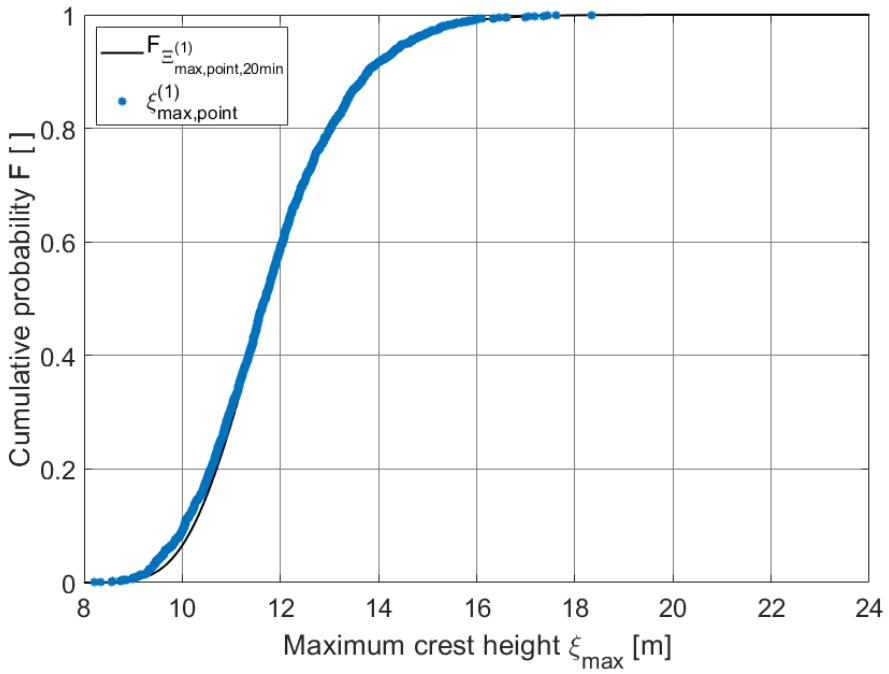

Figure 37: *Gaussian maximum point crest heights from 2000 20 minutes simulations using random wave amplitudes, along with Gaussian extreme value distribution.*

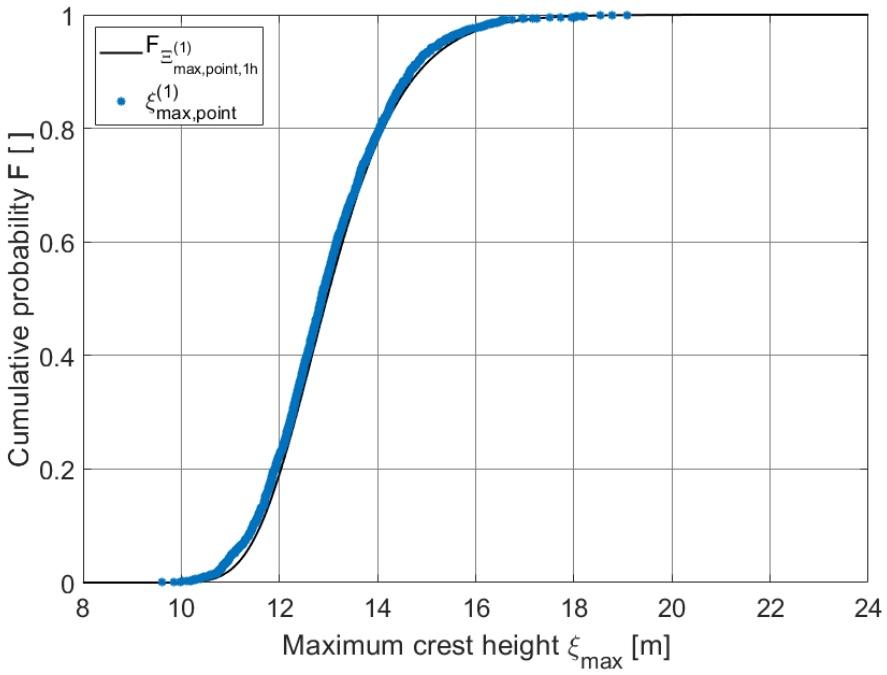

Figure 38: *Gaussian maximum point crest heights from 2000 one hour simulations using random wave amplitudes, along with Gaussian extreme value distribution.*

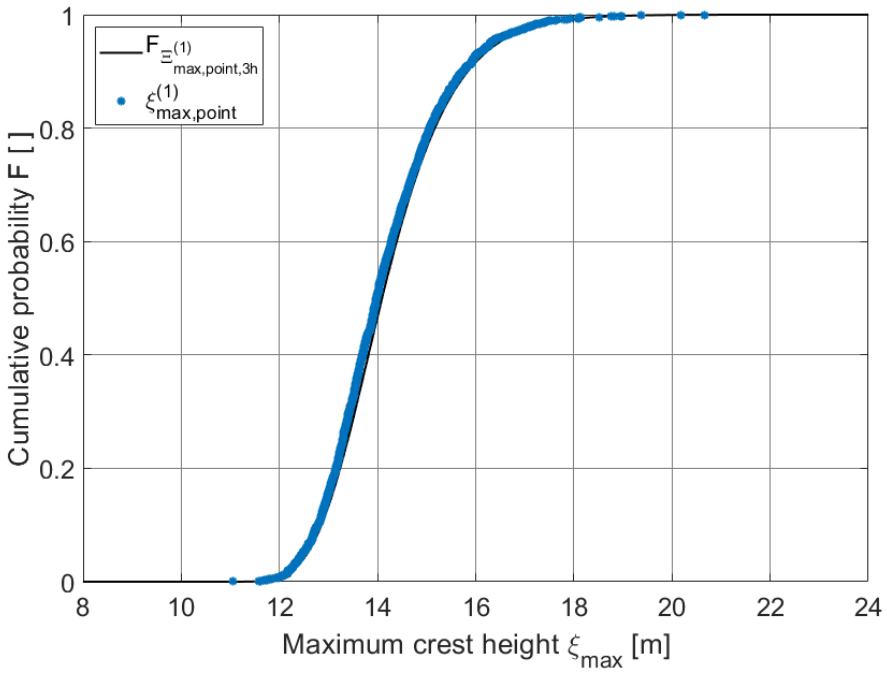

Figure 39: *Gaussian maximum point crest heights from 2000 three hour simulations using random wave amplitudes, along with Gaussian extreme value distribution.*

The values obtained for the Gaussian maximum point crest heights using random wave am-

plitudes from simulations in MATLAB shown in figure 37, 38 and 39 gives a close fit to the corresponding Gaussian extreme value distributions. It is therefore concluded that the Gaussian maximum point crest heights $\xi^{(1)}_{max,point}$ obtained from simulations in MATLAB using random wave amplitudes are valid according to Gaussian wave theory.

5.4 Verification of maximum point crest heights from second order simulations

5.4.1 About verification of maximum point crest heights from second order simulations

For verification of the second order maximum point crest heights $\xi^{(2)}_{max,point}$ obtained from simulations in MATLAB, the second order maximum point crest heights will be plotted along with second order extreme value distributions for maximum crest heights from the same sea state. $F_{\Xi^{(2)}_{max,point,lc,T}}(\xi^{(2)}_{max,point})$ and $F_{\Xi^{(2)}_{max,point,sc,T}}(\xi^{(2)}_{max,point})$ are respectively the extreme value distributions for long and short crested second order sea states. A description of the second order extreme value distributions used for the verification can be found in section 3.2. If the maximum point crest heights obtained from simulations in MATLAB lies close to the corresponding second order extreme value distribution for the maximum point crest heights, this will be a good indication that the maximum point crest heights obtained from simulations are calculated correctly. Due to the assumption that the wave spectrum is narrow banded made in section 3.2.2 when creating the second order extreme value distributions, the maximum point crest heights obtained from simulations in MATLAB are expected to be on the low side of the corresponding second order extreme value distribution.

When a simulation is done for a time duration of one hour, the second order maximum point crest height obtained from the simulation will be obtained as the maximum from three individual 20 minutes simulations. When a three hour simulation is done, the second order maximum point crest height obtained from the simulation will be obtained as the maximum from nine individual 20 minutes simulations. The reason for this is so that the wave amplitudes are recalculated for every 20 minutes of simulation time. This will give closer resemblance to real conditions when using random wave amplitudes, than if the same random wave amplitudes are used for the entire simulation period when simulating for more than 20 minutes. The same procedure are done, both for deterministic and random wave amplitudes. Table 11 shows the parameters used in simulations for the verification of second order maximum point crest heights using both deterministic and random amplitudes. All second order simulations done in the analysis part of this thesis are long crested. Therefore, only crest heights obtained from second order simulations will be verified.

Table 11: *Parameters used in simulation for verification of maximum point crest heights from second order simulations.*

Parameter	**Value**
Significant wave height H_s [m]	14.90
Spectral peak period T_p [s]	16.00
Directional shape parameter n_d [ ]	∞
Mean wave direction w.r.t x-axis θ_0 [deg]	0.00
Simulation duration t [s]	1200, 3*1200 and 9*1200
Wave spectrum cutoff frequency f_{max} [hz]	0.1826
Number of frequency components N_f [hz]	657
Time step dt [s]	0.25
Number of individual simulations N_{sim} [pcs]	200

5.4.2 Verification of maximum point crest heights from second order simulations using deterministic wave amplitudes

The verification of second order maximum point crest heights $\xi^{(2)}_{max,point}$ from long crested simulations using deterministic wave amplitudes are done for the three different time durations of 20min, 3*20min and 9*20min. For each time duration, 200 individual second order maximum crest heights using deterministic wave amplitudes are obtained from simulations in MATLAB. Figure 40 shows maximum point crest heights obtained from 200 20 minutes long crested simulations, along with the second order extreme value distributions for short and long crested sea. Figure 41 shows maximum point crest heights obtained from 200 one hour long crested simulations, along with the second order extreme value distributions for short and long crested sea. Figure 42 shows maximum point crest heights obtained from 200 three hour long crested simulations, along with the second order extreme value distributions for short and long crested sea. The parameters used in the simulations for verification of second order simulations using deterministic wave amplitudes are found in table 11.

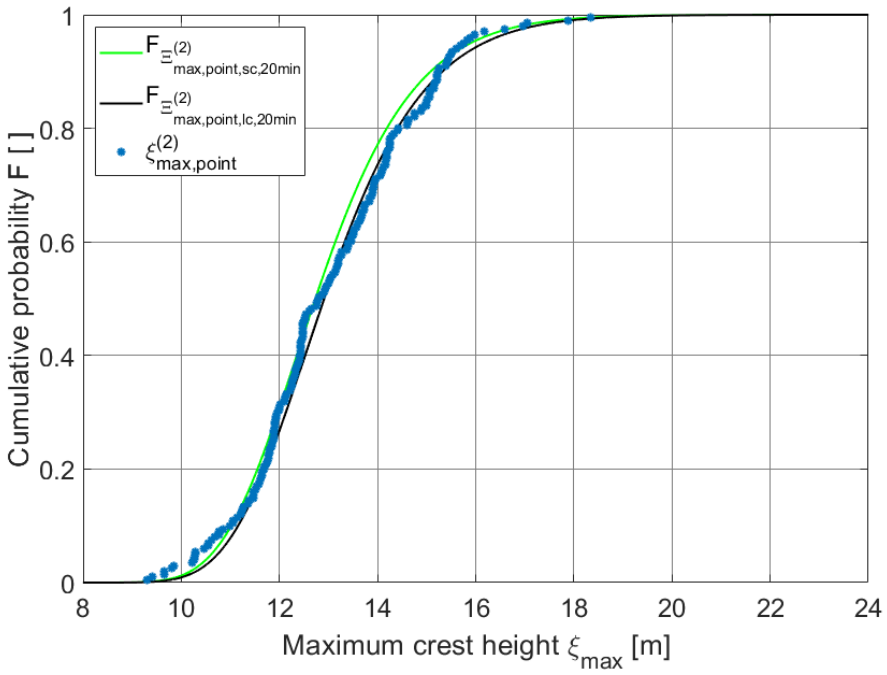

Figure 40: *Second order maximum point crest heights from 200 20 minutes long crested simulations using deterministic wave amplitudes, along with second order extreme value distributions for short and long crested sea.*

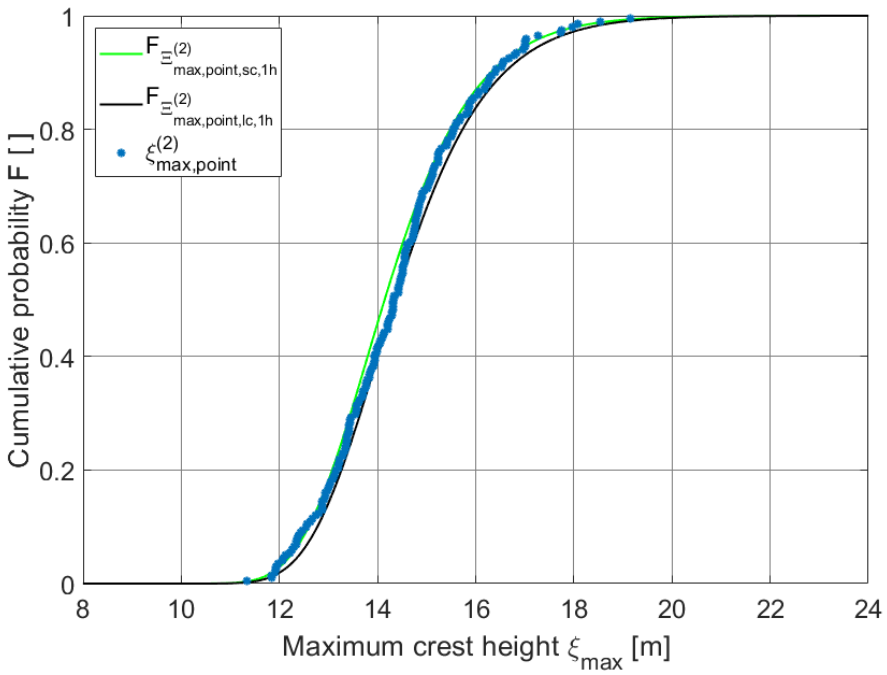

Figure 41: *Second order maximum point crest heights from 200 one hour long crested simulations using deterministic wave amplitudes, along with second order extreme value distributions for short and long crested sea.*

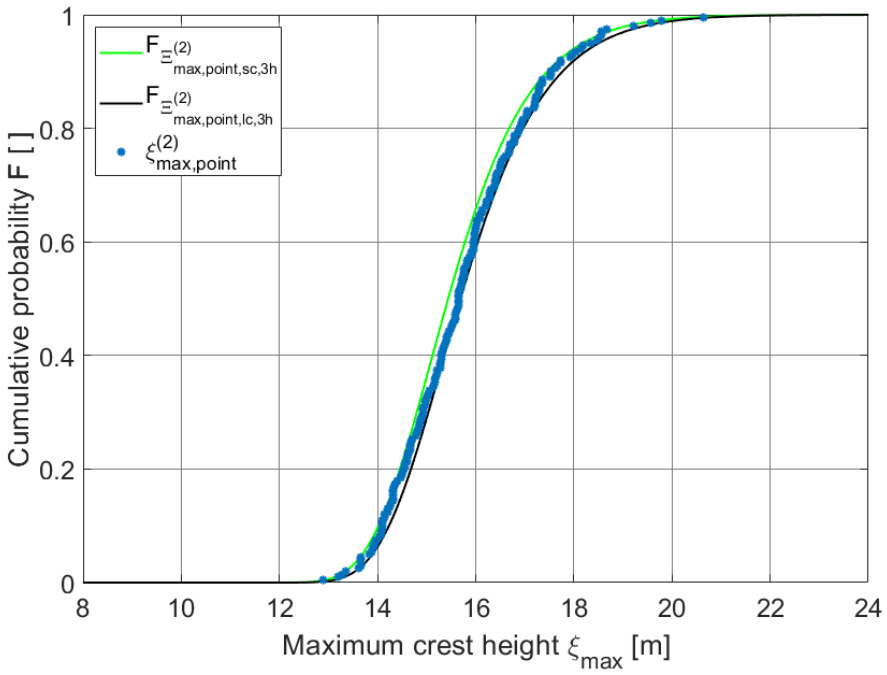

Figure 42: *Second order maximum point crest heights from 200 three hour long crested simulations using deterministic wave amplitudes, along with second order extreme value distributions for short and long crested sea.*

The values obtained for the second order maximum point crest heights using deterministic wave amplitudes from simulations in MATLAB shown in figure 40, 41 and 42 gives a good fit to the corresponding long crested Forristall CDF's. Although, there exists some deviation from the long crested extreme value distributions. This is expected to be solely due to the randomness that exists in the distribution of second order maximum point crest heights in a sample of size 200. It is therefore concluded that the second order maximum point crest heights $\xi^{(2)}_{max,point}$ obtained from simulations in MATLAB using deterministic wave amplitudes are valid according to second order wave theory.

5.4.3 Verification of maximum point crest heights from second order simulations using random wave amplitudes

The verification of second order maximum point crest heights $\xi^{(2)}_{max,point}$ from long crested simulations using random wave amplitudes are done for the three different time durations of 20min, 3*20min and 9*20min. For each time duration, 200 individual second order maximum crest heights using random wave amplitudes are obtained from simulations in MATLAB. Figure 43 shows maximum point crest heights obtained from 200 20 minutes long crested simulations, along with second order extreme value distributions for short and long crested sea. Figure 44 shows maximum point crest heights obtained from 200 one hour long crested simulations, along with second order extreme value distributions for short and long crested sea. Figure 45 shows maximum point crest heights obtained from 200 three hour long crested simulations, along with second order extreme value distributions for short and long crested sea. The parameters used in the simulations for verification of second order simulations using deterministic wave amplitudes are found in table 11.

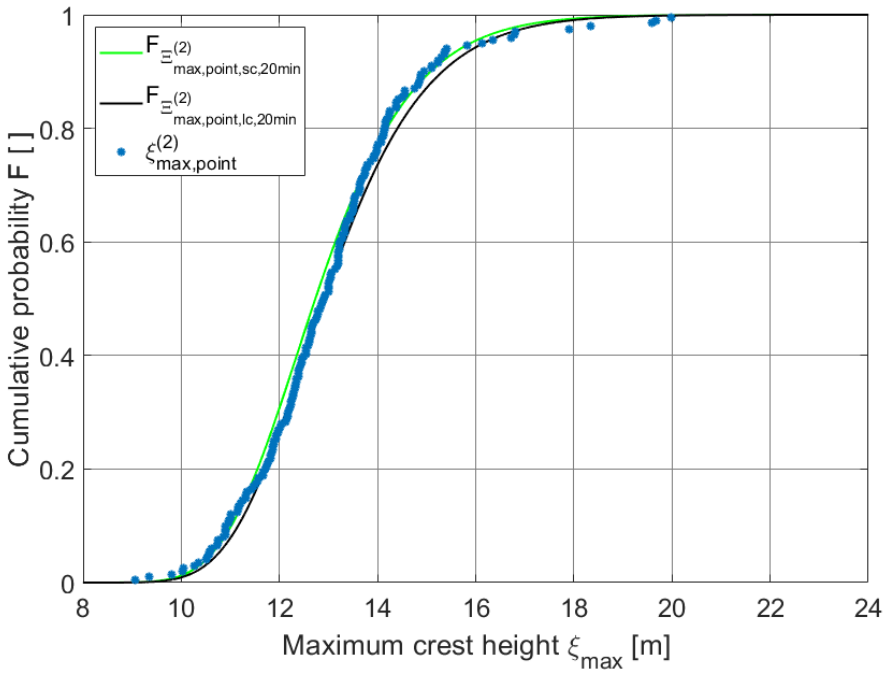

Figure 43: *Second order maximum point crest heights from 200 20 minutes long crested simulations using random wave amplitudes, along with second order extreme value distributions for short and long crested sea.*

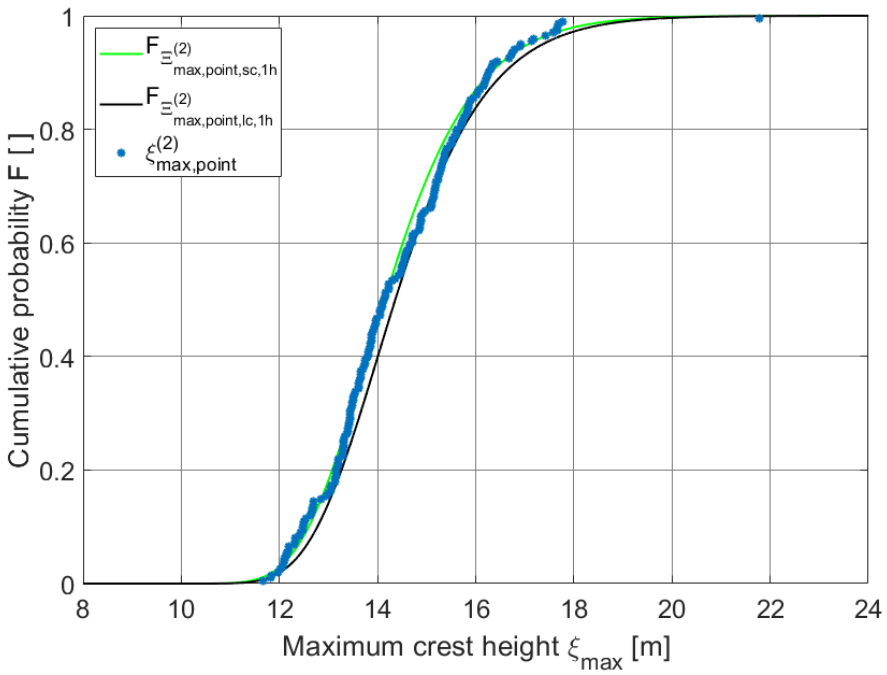

Figure 44: *Second order maximum point crest heights from 200 one hour long crested simulations using random wave amplitudes, along with second order extreme value distributions for short and long crested sea.*

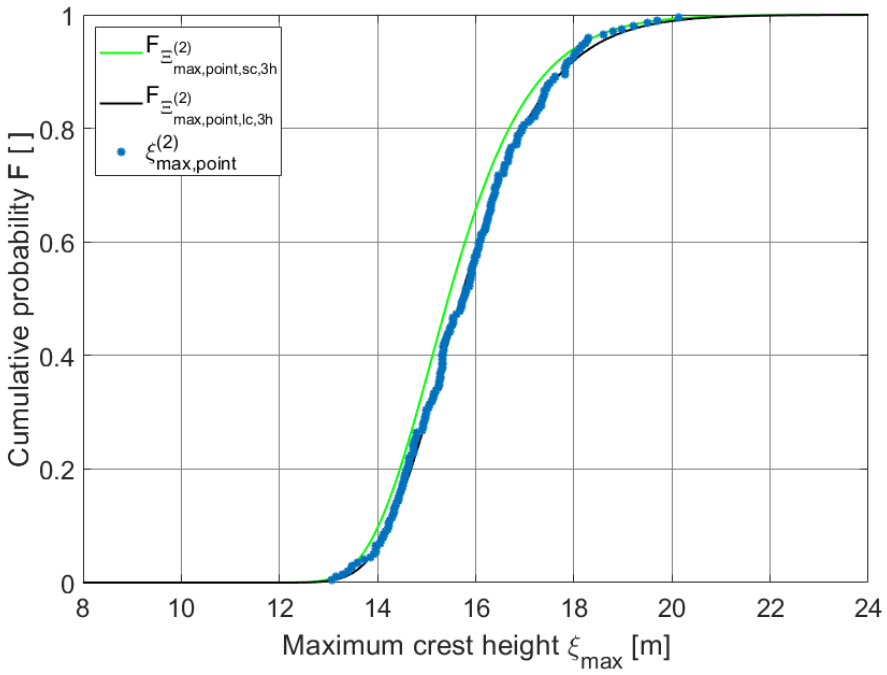

Figure 45: *Second order maximum point crest heights from 200 three hour long crested simulations using random wave amplitudes, along with second order extreme value distributions for short and long crested sea.*

The values obtained for the second order maximum point crest heights using random wave amplitudes from simulations in MATLAB are shown in figure 43, 44 and 45 gives a good fit to the corresponding long crested second order extreme value distributions. Although, there exists some deviation from the long crested second order extreme value distributions. This is expected to be solely due to the randomness that exists in the distribution of second order maximum point crest heights in a sample of size 200. It is therefore concluded that the second order maximum point crest heights $\xi^{(2)}_{max,point}$ obtained from simulations in MATLAB using random wave amplitudes are valid according to second order wave theory.

6 Parameter study for MATLAB program for simulation of surface elevation process

6.1 Parameter study for Gaussian simulations

6.1.1 About parameter study for Gaussian simulations

The MATLAB program for simulation of Gaussian surface elevation process is tested with variations in different parameters to check for convergence of maximum point crest heights. The maximum point crest heights obtained from simulations are plotted along with the Gaussian extreme value distribution from the same sea state for convergence checking. A description of the Gaussian extreme value distribution used when plotting the maximum point crest obtained from Gaussian simulations can be found in section 3.1. Table 12 shows the fixed parameters used for all Gaussian simulations in this parameter study. The parameter study is based on simulations of three hour sea states. A total of 2000 three hour sea states are simulated for each variation in parameters.

Tables including the parameters tested for convergence are given in each section of the respective parameter study. The parameters that will be tested for convergence are the wave spectrum cutoff frequency, the number of frequency components used when creating the wave spectrum, and the time step between calculations of the surface elevation process. All three parameters that are tested for convergence affects the accuracy of the simulated surface elevation process, but all three parameters also affects the computation time for simulations. Both the value of the cutoff frequency and the number of frequency components are approximately proportional to the calculation time of a Gaussian surface elevation process. The value of the time step is approximately inversely proportional to the calculation time. To select the correct parameters in a Gaussian simulation is important to obtain trustworthy results, while simultaneously keep the computation time at a proper level.

Table 12: *Fixed parameters used in parameter study for Gaussian simulations.*

Parameters	**Value**
Significant wave height H_s [m]	14.90
Spectral peak period T_p [s]	16.00
Shape parameter of directional spectrum n_d [ ]	∞
Mean wave direction w.r.t side edge of square area θ_0 [deg]	0.00
Simulation duration t [s]	9*1200
Number of simulations for each variation in parameter N_{sim} [pcs]	2000

This parameter study is performed to create a basis for selecting proper parameters when using the MATLAB program for simulation of Gaussian surface elevation processes. When assessing the results from the parameter study, the fit of the plotted Gaussian maximum crest heights to the corresponding Gaussian extreme value distribution is important. The 90th percentile Gaussian maximum crest heights from simulations are also given in the results, and compared to the 90th percentile value from the Gaussian extreme value distribution. The 90th percentile values are calculated as described in section 8.1. The results for the 90th percentile values may show some ambiguity when close to converging, due to the natural variance in the 90th percentile values from simulations, even at a total number of simulations of 2000 for each variation in

parameter. Parameter studies are conducted both for Gaussian processes using deterministic wave amplitudes, and for Gaussian processes using random wave amplitudes. Convergence is expected to be different for deterministic and random wave amplitudes. It is therefore important to distinguish between the two Gaussian parameter studies when using the results as basis for an analysis.

6.2 Parameter study for Gaussian simulations using deterministic wave amplitudes

6.2.1 Variations in the cutoff frequency in Gaussian simulations using deterministic wave amplitudes

Convergence of maximum point crest heights obtained from Gaussian simulations using deterministic wave amplitudes are tested with variations in the cutoff frequency for the wave spectrum. Table 13 shows the four different values used for the wave spectrum cutoff frequency f_{max}, along with the number of frequency components N_f and the time step dt used in the convergence test. The number of frequency components and the time step are fixed for all variations in the wave spectrum cutoff frequency. The lowest value used for the cutoff frequency corresponds to the cutoff frequency used for the second order surface elevation process, as described in section 2.5.1. The higher values used for the cutoff frequency are respectively the second, third and fourth multiple of the second order cutoff frequency.

Table 13: *Parameters used in Gaussian simulations using deterministic wave amplitudes with variations in the wave spectrum cutoff frequency.*

Parameters used in simulations	**Value**
Wave spectrum cutoff frequency f_{max} [hz]	0.1826, 0.3652, 0.5478, 0.7304
Number of frequency components N_f [pcs]	1314
Time step dt [s]	0.25

Figure 46 shows the maximum point crest heights obtained from 4*2000 three hour Gaussian simulations using deterministic wave amplitudes with variations in the wave spectrum cutoff frequency. The 90th percentile maximum point crest heights $\xi^{(1)}_{max,point,90p}$ from simulations and the 90th percentile maximum point crest height $\xi^{(1)}_{max,point,90p}$ from the Gaussian extreme value distribution are summed up in table 14, along with the deviation between the two. The order of the results presented in table 14 corresponds to the order of f_{max} in table 13.

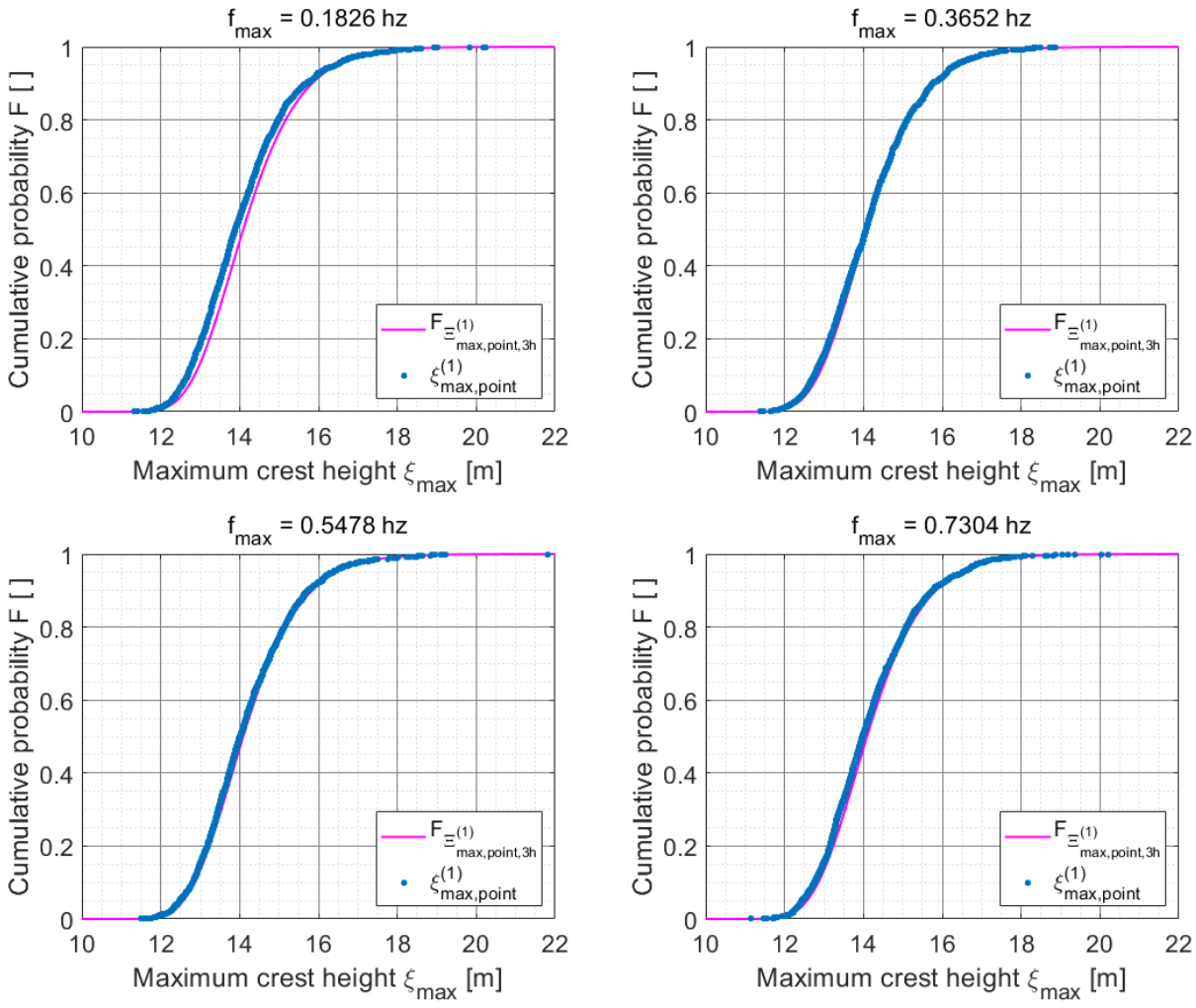

Figure 46: *Gaussian maximum point crest heights from three hour simulations using deterministic wave amplitudes with four different cutoff frequencies, along with Gaussian extreme value distribution.*

Table 14: *90th percentile values for the maximum point crest heights from simulations and from Gaussian extreme value distribution, along with the deviation between the two.*

Results from simulations	**Value**
90th percentile value from distribution $\xi^{(1)}_{max,point,90p}$ [m]	15.84
90th percentile value from simulations $\xi^{(1)}_{max,point,90p}$ [m]	15.70, 15.77, 15.74, 15.77
Deviation in $\xi^{(1)}_{max,point,90p}$ [m]	-0.14, -0.07, -0.10, -0.07

6.2.2 Variations in the number of frequency components in Gaussian simulations using deterministic wave amplitudes

Convergence of maximum point crest heights obtained from Gaussian simulations using deterministic wave amplitudes are tested with variations in the number of frequency components used when creating the wave spectrum. Table 15 shows the four different numbers of frequency components N_f used, along with the wave spectrum cutoff frequency f_{max} and the time step dt used in the convergence test. The wave spectrum cutoff frequency and the time step are fixed for all variations in the number of frequency components. The lowest number of frequency components tested corresponds to a frequency resolution which will cause a repetitions of the surface elevation process after 20 minutes. The higher numbers of frequency components used will respectively cause a repetition of the surface elevation process after 30 minutes, 1 hour and 3 hours.

Table 15: *Parameters used in Gaussian simulations using deterministic wave amplitudes with variations in the number of frequency components.*

Parameters used in simulations	**Value**
Wave spectrum cutoff frequency f_{max} [hz]	0.3652
Number of frequency components N_f [pcs]	438, 657, 1314, 3944
Time step dt [s]	0.25

Figure 47 shows the maximum point crest heights obtained from 4*2000 three hour Gaussian simulations using deterministic wave amplitudes with variations in the number of frequency components. The 90th percentile maximum point crest heights $\xi^{(1)}_{max,point,90p}$ from simulations and the 90th percentile maximum point crest height $\xi^{(1)}_{max,point,90p}$ from the Gaussian extreme value distribution are summed up in table 16, along with the deviation between the two. The order of the results presented in table 16 corresponds to the order of N_f in table 15.

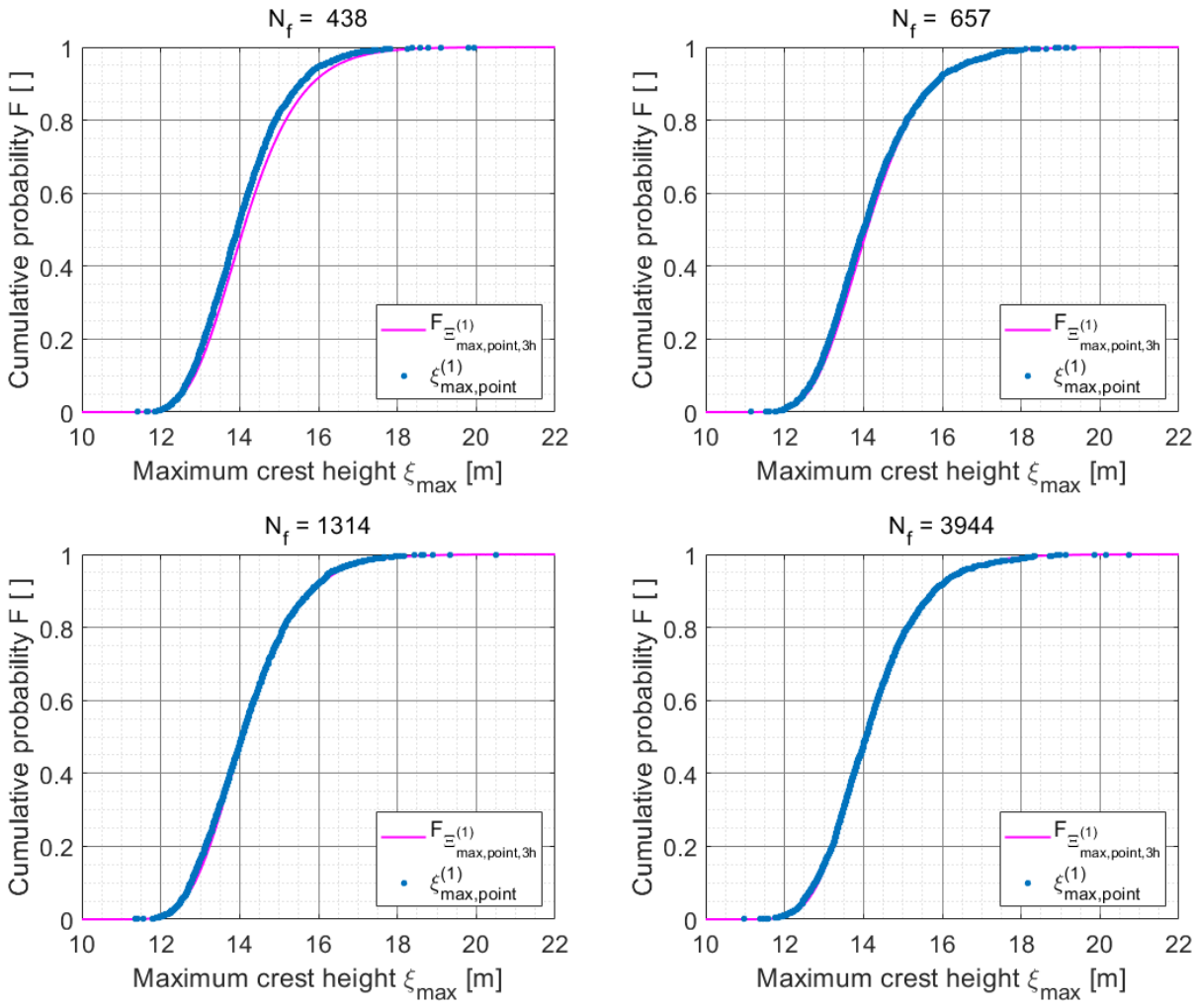

Figure 47: *Gaussian maximum point crest heights from three hour simulations using deterministic wave amplitudes with four different numbers of frequency components, along with Gaussian extreme value distribution.*

Table 16: *90th percentile values for the maximum point crest heights from simulations and from Gaussian extreme value distribution, along with the deviation between the two.*

Results from simulations	**Value**
90th percentile value from distribution $\xi^{(1)}_{max,point,90p}$ [m]	15.84
90th percentile value from simulations $\xi^{(1)}_{max,point,90p}$ [m]	15.54, 15.80, 15.81, 15.78
Deviation in $\xi^{(1)}_{max,point,90p}$ [m]	-0.30, -0.04, -0.03, -0.06

6.2.3 Variations in the time step in Gaussian simulations using deterministic wave amplitudes

Convergence of maximum point crest heights obtained from Gaussian simulations using deterministic wave amplitudes are tested with variations in the time step between calculations of the surface elevation process. Table 17 shows the four different values of the time step dt that are tested, along with the wave spectrum cutoff frequency f_{max} and the number of frequency components N_f used in the convergence test. The wave spectrum cutoff frequency and the number of frequency components are fixed for all variations in the time step. The values of the time step varies from two seconds to a quarter of a second.

Table 17: *Parameters used in Gaussian simulations using deterministic wave amplitudes with variations in the time step.*

Parameters used in simulations	**Value**
Wave spectrum cutoff frequency f_{max} [hz]	0.3652
Number of frequency components N_f [pcs]	1314
Time step dt [s]	2.00, 1.00, 0.50, 0.25

Figure 48 shows the maximum point crest heights obtained from 4*2000 three hour Gaussian simulations using deterministic wave amplitudes with variations in the time step. The 90th percentile maximum point crest heights $\xi^{(1)}_{max,point,90p}$ from simulations and the 90th percentile maximum point crest height $\xi^{(1)}_{max,point,90p}$ from the Gaussian extreme value distribution are summed up in table 18, along with the deviation between the two. The order of the results presented in table 18 corresponds to the order of dt in table 17.

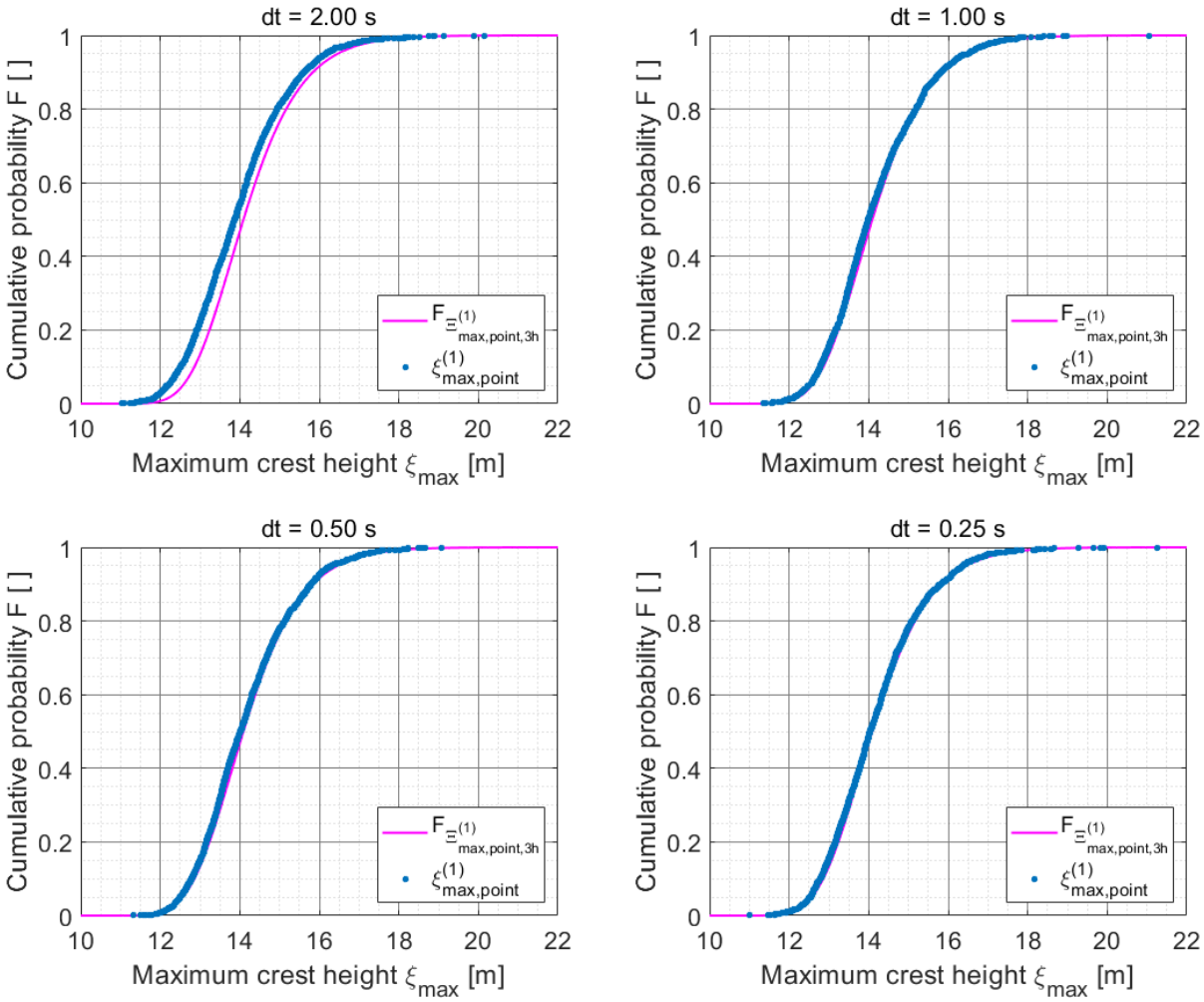

Figure 48: *Gaussian maximum point crest heights from three hour simulations using deterministic wave amplitudes with four different time steps, along with Gaussian extreme value distribution.*

Table 18: *90th percentile values for the maximum point crest heights from simulations and from Gaussian extreme value distribution, along with the deviation between the two.*

Results from simulations	**Value**
90th percentile value from distribution $\xi^{(1)}_{max,point,90p}$ [m]	15.84
90th percentile value from simulations $\xi^{(1)}_{max,point,90p}$ [m]	15.62, 15.82, 15.79, 15.82
Deviation in $\xi^{(1)}_{max,point,90p}$ [m]	-0.22, -0.02, -0.05, -0.02

6.3 Parameter study for Gaussian simulations using random wave amplitudes

6.3.1 Variations in the cutoff frequency in Gaussian simulations using random wave amplitudes

Convergence of maximum point crest heights obtained from Gaussian simulations using random wave amplitudes are tested with variations in the cutoff frequency for the wave spectrum. Table 19 shows the four different values used for the wave spectrum cutoff frequency f_{max}, along with the number of frequency components N_f and the time step dt used in the convergence test. The number of frequency components and the time step are fixed for all variations in the wave spectrum cutoff frequency. The lowest value used for the cutoff frequency corresponds to the cutoff frequency used for the second order surface elevation process, as described in section 2.5.1. The higher values used for the cutoff frequency are respectively the second, third and fourth multiple of the second order cutoff frequency.

Table 19: *Parameters used in Gaussian simulations using random wave amplitudes with variations in the wave spectrum cutoff frequency.*

Parameters used in simulations	**Value**
Wave spectrum cutoff frequency f_{max} [hz]	0.1826, 0.3652, 0.5478, 0.7304
Number of frequency components N_f [pcs]	1314
Time step dt [s]	0.25

Figure 49 shows the maximum point crest heights obtained from 4*2000 three hour Gaussian simulations using random wave amplitudes with variations in the wave spectrum cutoff frequency. The 90th percentile maximum point crest heights $\xi^{(1)}_{max,point,90p}$ from simulations and the 90th percentile maximum point crest height $\xi^{(1)}_{max,point,90p}$ from the Gaussian extreme value distribution are summed up in table 20, along with the deviation between the two. The order of the results presented in table 20 corresponds to the order of f_{max} in table 19.

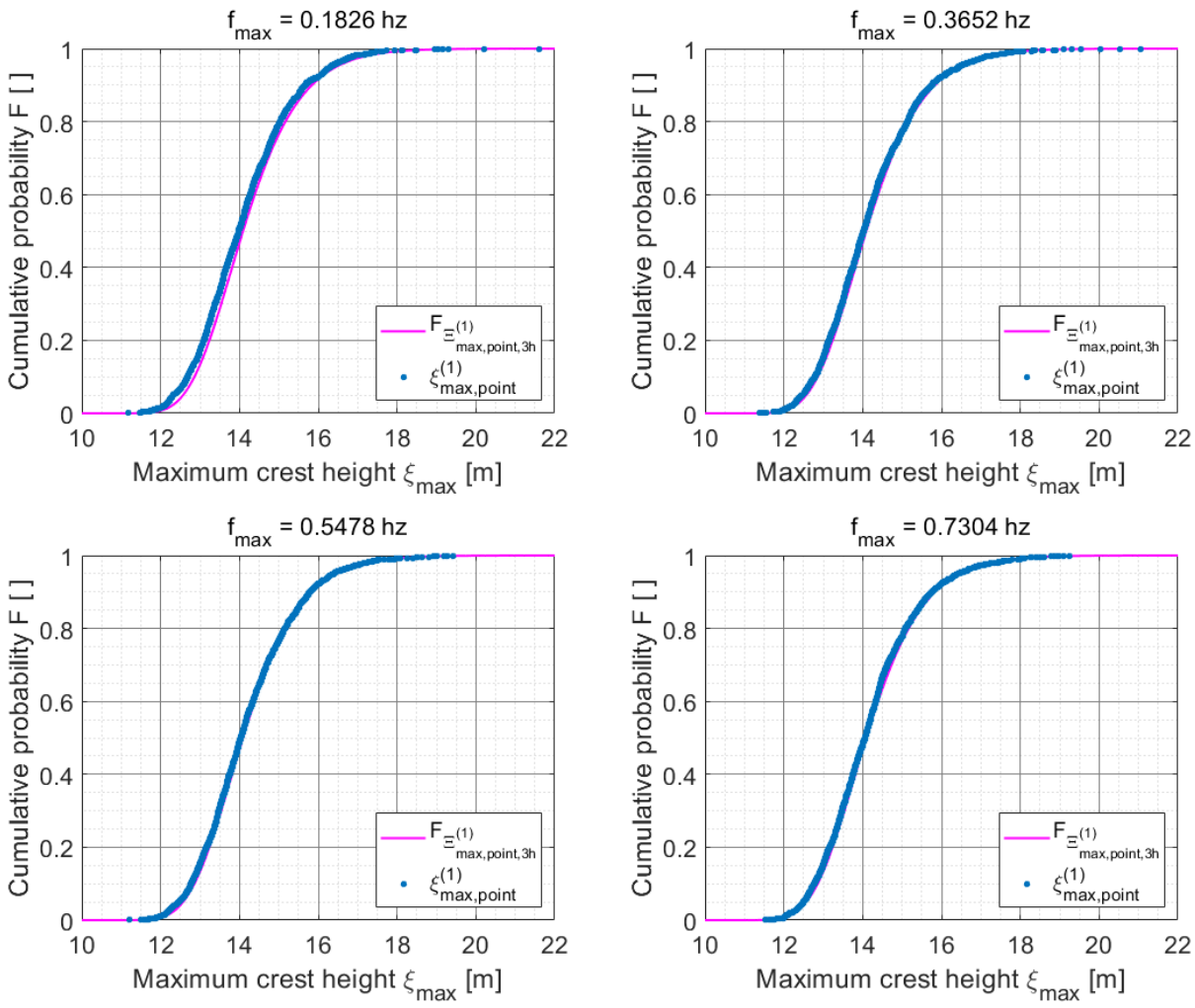

Figure 49: *Gaussian maximum point crest heights from three hour simulations using deterministic wave amplitudes with four different cutoff frequencies, along with Gaussian extreme value distribution.*

Table 20: *90th percentile values for the maximum point crest heights from simulations and from Gaussian extreme value distribution, along with the deviation between the two.*

Results from simulations	**Value**
90th percentile value from distribution $\xi^{(1)}_{max,point,90p}$ [m]	15.84
90th percentile value from simulations $\xi^{(1)}_{max,point,90p}$ [m]	15.67, 15.75, 15.79, 15.77
Deviation in $\xi^{(1)}_{max,point,90p}$ [m]	-0.17, -0.09, -0.05, -0.07

6.3.2 Variations in the number of frequency components in Gaussian simulations using random wave amplitudes

Convergence of maximum point crest heights obtained from Gaussian simulations using random wave amplitudes are tested with variations in the number of frequency components used when creating the wave spectrum. Table 21 shows the four different numbers of frequency components N_f used, along with the wave spectrum cutoff frequency f_{max} and the time step dt used in the convergence test. The wave spectrum cutoff frequency and the time step are fixed for all variations in the number of frequency components. The lowest number of frequency components tested corresponds to a frequency resolution which will cause a repetitions of the surface elevation process after 20 minutes. The higher numbers of frequency components used will respectively cause a repetition of the surface elevation process after 30 minutes, 1 hour and 3 hours.

Table 21: *Parameters used in Gaussian simulations using random wave amplitudes with variations in the number of frequency components.*

Parameters used in simulations	**Value**
Wave spectrum cutoff frequency f_{max} [hz]	0.3652
Number of frequency components N_f [pcs]	438, 657, 1314, 3944
Time step dt [s]	0.25

Figure 50 shows the maximum point crest heights obtained from 4*2000 three hour Gaussian simulations using random wave amplitudes with variations in the number of frequency components. The 90th percentile maximum point crest heights $\xi^{(1)}_{max,point,90p}$ from simulations and the 90th percentile maximum point crest height $\xi^{(1)}_{max,point,90p}$ from the Gaussian extreme value distribution are summed up in table 22, along with the deviation between the two. The order of the results presented in table 22 corresponds to the order of N_f in table 21.

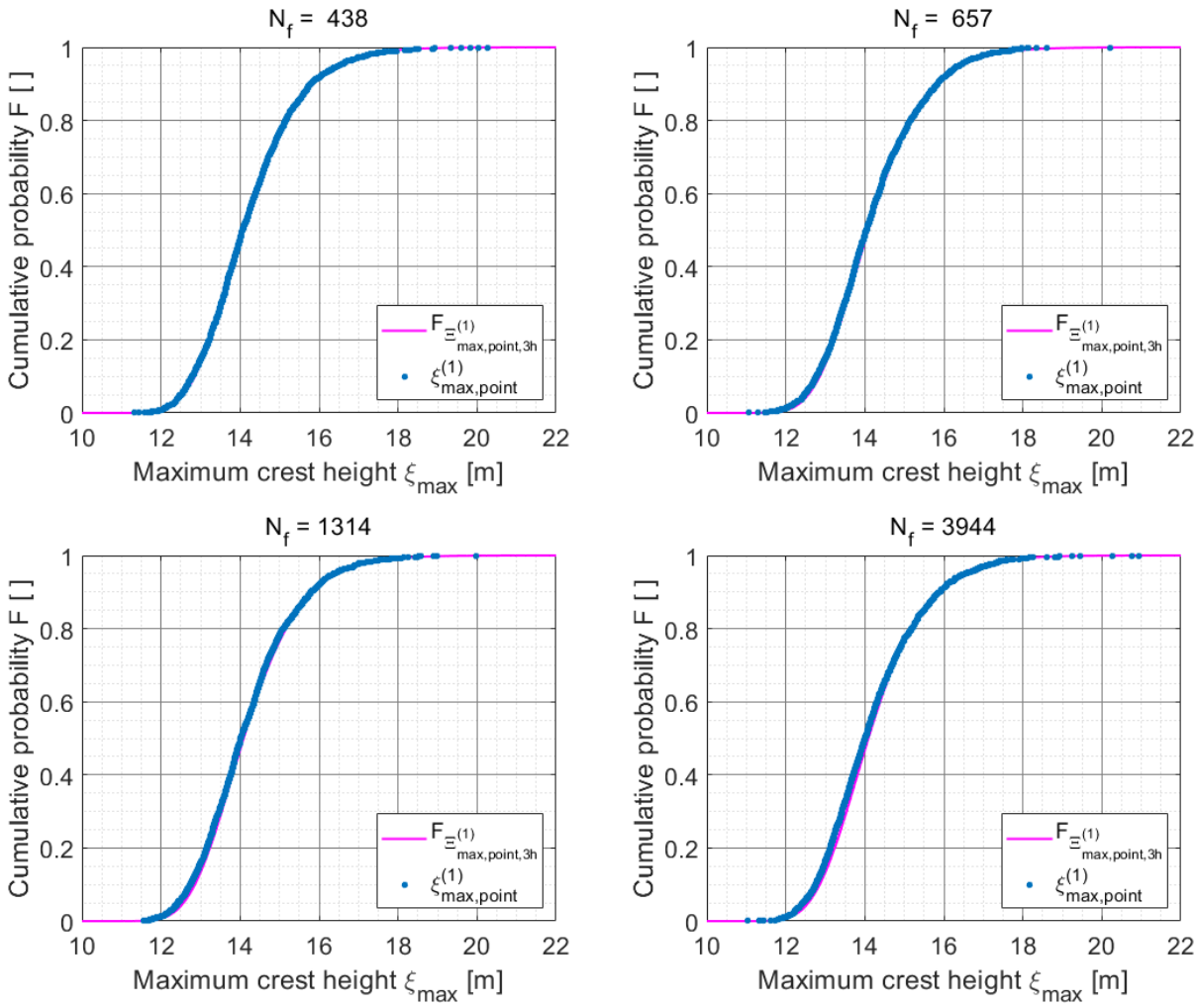

Figure 50: *Gaussian maximum point crest heights from three hour simulations using random wave amplitudes with four different numbers of frequency components, along with Gaussian extreme value distribution.*

Table 22: *90th percentile values for the maximum point crest heights from simulations and from Gaussian extreme value distribution, along with the deviation between the two.*

Results from simulations	**Value**
90th percentile value from distribution $\xi^{(1)}_{max,point,90p}$ [m]	15.84
90th percentile value from simulations $\xi^{(1)}_{max,point,90p}$ [m]	15.80, 15.84, 15.79, 15.90
Deviation in $\xi^{(1)}_{max,point,90p}$ [m]	-0.04, 0.00, -0.05, 0.06

6.3.3 Variations in the time step in Gaussian simulations using random wave amplitudes

Convergence of maximum point crest heights obtained from Gaussian simulations using random wave amplitudes are tested with variations in the time step between calculations of the surface elevation process. Table 23 shows the four different values of the time step dt that are tested, along with the wave spectrum cutoff frequency f_{max} and the number of frequency components N_f used in the convergence test. The wave spectrum cutoff frequency and the number of frequency components are fixed for all variations in the time step. The values of the time step varies from two seconds to a quarter of a second.

Table 23: *Parameters used in Gaussian simulations using random wave amplitudes with variations in the time step.*

Parameters used in simulations	**Value**
Wave spectrum cutoff frequency f_{max} [hz]	0.3652
Number of frequency components N_f [pcs]	1314
Time step dt [s]	2.00, 1.00, 0.50, 0.25

Figure 51 shows the maximum point crest heights obtained from 4*2000 three hour Gaussian simulations using random wave amplitudes with variations in the time step. The 90th percentile maximum point crest heights $\xi^{(1)}_{max,point,90p}$ from simulations and the 90th percentile maximum point crest height $\xi^{(1)}_{max,point,90p}$ from the Gaussian extreme value distribution are summed up in table 24, along with the deviation between the two. The order of the results presented in table 24 corresponds to the order of dt in table 23.

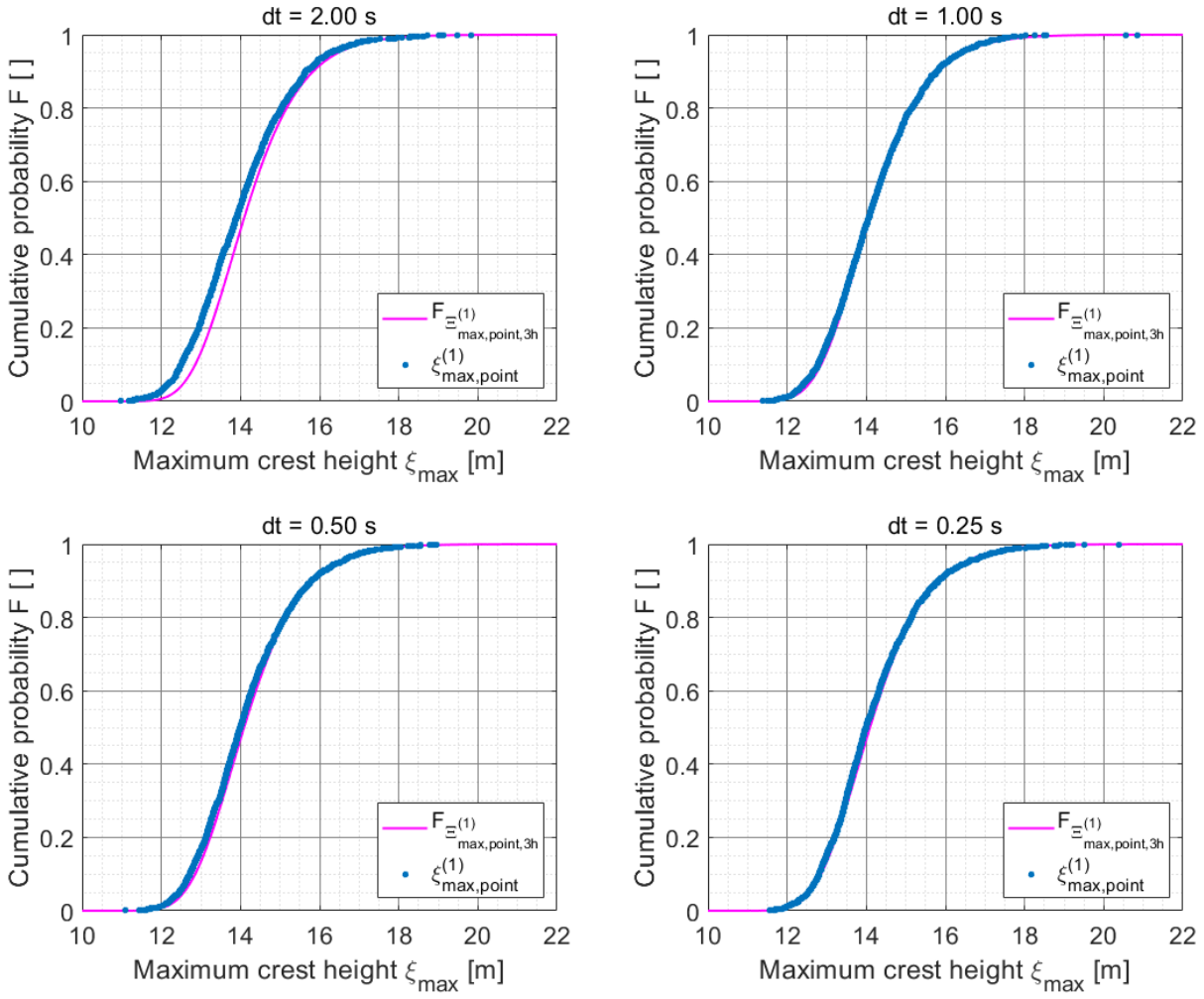

Figure 51: *Gaussian maximum point crest heights from three hour simulations using random wave amplitudes with four different time steps, along with Gaussian extreme value distribution.*

Table 24: *90th percentile values for the maximum point crest heights from simulations and from Gaussian extreme value distribution, along with the deviation between the two.*

Results from simulations	**Value**
90th percentile value from distribution $\xi^{(1)}_{max,point,90p}$ [m]	15.84
90th percentile value from simulations $\xi^{(1)}_{max,point,90p}$ [m]	15.64, 15.79, 15.79, 17.84
Deviation in $\xi^{(1)}_{max,point,90p}$ [m]	-0.20, -0.05, -0.05, 0.00

6.4 Parameter study for second order simulations

6.4.1 About parameter study for second order simulations

The MATLAB program for simulation of second order surface elevation process is tested with variations in different parameters to check for convergence of maximum point crest heights. The maximum point crest heights obtained from simulations are plotted along with the second order extreme value distribution from the same sea state for convergence checking. A description of the second order extreme value distribution used when plotting the maximum point crest obtained from second order simulations can be found in section 3.2. Long crested sea is used for all simulations, and comparisons are therefore made to the second order extreme value distribution for long crested sea. Table 25 shows the fixed parameters used for all second order simulations in this parameter study. The parameter study is based on simulations of three hour sea states. A total of 200 three hour sea states are simulated for each variation in parameters.

Tables including the parameters tested for convergence are given in each section of the respective parameter study. The parameters that will be tested for convergence are the number of frequency components used when creating the wave spectrum, and the time step between calculations of the surface elevation process. The wave spectrum cutoff frequency f_{max} is fixed for all second order simulations as described in section 2.5 (RP-C205 (2010)). Both parameters that are tested for convergence affects the accuracy of the simulated surface elevation process, but both parameters also affects the computation time for simulations. The calculation time for a second order surface elevation process is approximately proportional to the number of frequency components squared, and approximately inversely proportional to the value of the time step used in calculations. To select the correct parameters in a second order simulation is therefore important to obtain trustworthy results, while simultaneously keep the computation time at a proper level.

Table 25: *Fixed parameters used in parameter study for second order simulations.*

Parameters	**Value**
Significant wave height H_s [m]	14.90
Spectral peak period T_p [s]	16.00
Shape parameter of directional spectrum n_d [ ]	∞
Mean wave direction w.r.t side edge of square area θ_0 [deg]	0.00
Simulation duration t [s]	9*1200
Number of simulations for each variation in parameter N_{sim} [pcs]	200
Wave spectrum cutoff frequency f_{max} [hz]	0.1826

This parameter study is performed to create a basis for selecting proper parameters when using the MATLAB program for simulation of second order surface elevation processes. When assessing the results from the parameter study, the fit of the plotted second order maximum crest heights to the corresponding second order extreme value distribution is important. The 90th percentile second order maximum crest heights from simulations are also given in the results, and compared to the 90th percentile value from the second order extreme value distribution. The 90th percentile values are calculated as described in section 8.1. The results for the 90th percentile values may show some ambiguity due to the large variance in the simulated 90th percentile maximum point crest heights when only 200 simulations for each variation in parameter

are used. Parameter studies are conducted for both second order process using deterministic wave amplitudes, and for second order process using random wave amplitudes. Convergence is expected to be different for deterministic and random wave amplitudes. It is therefore important to distinguish between the two second order parameter studies when using the results as basis for an analysis.

6.5 Parameter study for second order simulations using deterministic wave amplitudes

6.5.1 Variations in the number of frequency components in second order simulations using deterministic wave amplitudes

Convergence of maximum point crest heights obtained from second order long crested simulations using deterministic wave amplitudes are tested with variations in the number of frequency components used when creating the wave spectrum. Table 26 shows the three different numbers of frequency components N_f used, along with the time step dt used in the convergence test. The time step is fixed for all variations in the number of frequency components. The lowest number of frequency components tested corresponds to a frequency resolution which will cause a repetitions of the surface elevation process after 20 minutes. The higher numbers of frequency components used will respectively cause a repetition of the surface elevation process after 30 minutes and 1 hour.

Table 26: *Parameters used in second order simulations using deterministic wave amplitudes with variations in the number of frequency components.*

Parameters used in simulations	**Value**
Number of frequency components N_f [pcs]	219, 328, 657
Time step dt [s]	0.25

Figure 52 shows the maximum point crest heights obtained from 3*200 three hour second order simulations using deterministic wave amplitudes with variations in the number of frequency components. The 90th percentile maximum point crest heights $\xi^{(2)}_{max,point,90p}$ from simulations and the 90th percentile maximum point crest height $\xi^{(2)}_{max,point,90p}$ from the second order extreme value distribution are summed up in table 27, along with the deviation between the two. The order of the results presented in table 27 corresponds to the order of N_f in table 26.

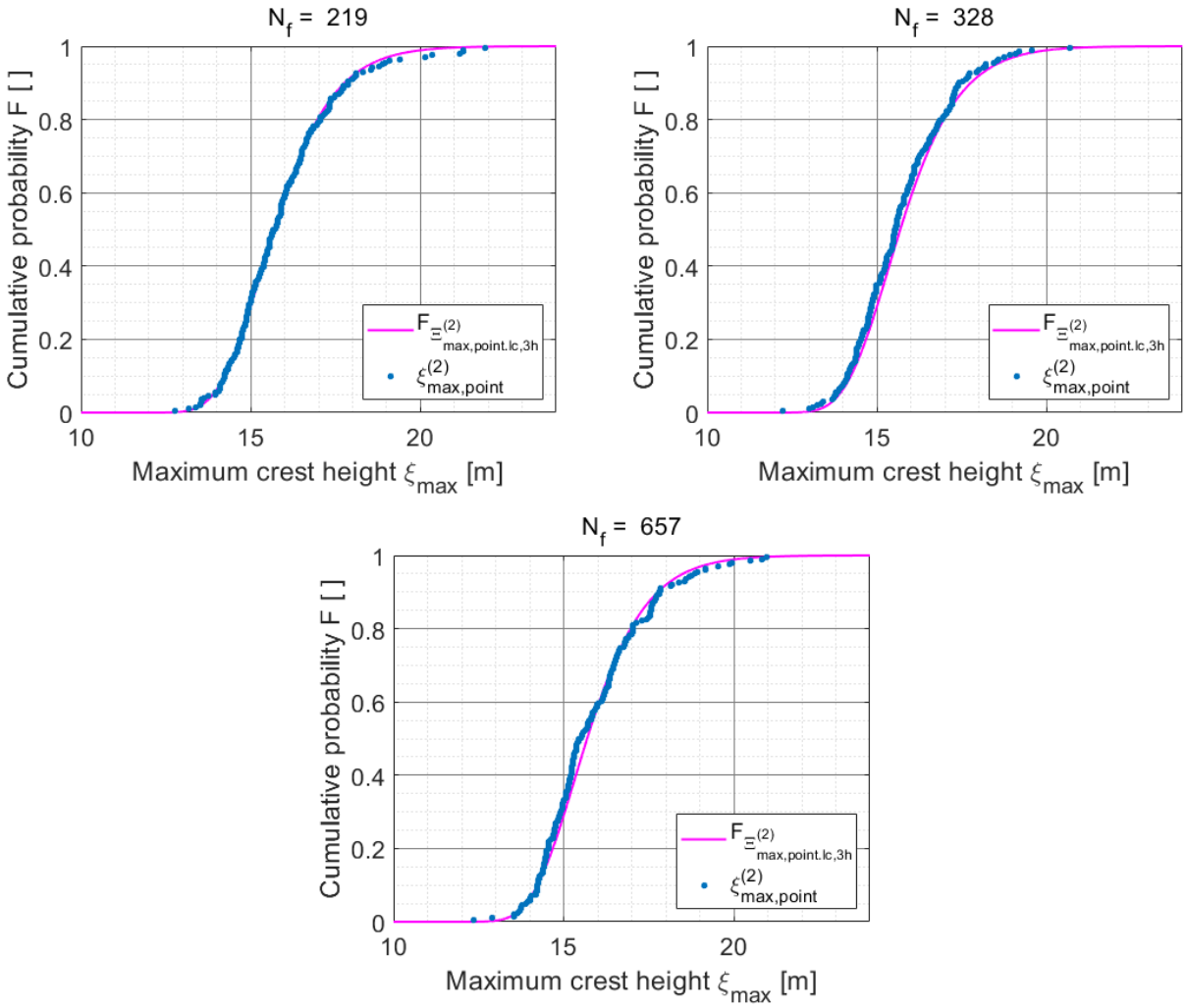

Figure 52: *Second order maximum point crest heights from three hour long crested simulations using deterministic wave amplitudes with three different numbers of frequency components, along with second order extreme value distribution for long crested sea.*

Table 27: *90th percentile values for the maximum point crest heights from simulations and from second order extreme value distribution, along with the deviation between the two.*

Results from simulations	**Value**
90th percentile value from distribution $\xi^{(2)}_{max,point,90p}$ [m]	17.77
90th percentile value from simulations $\xi^{(2)}_{max,point,90p}$ [m]	17.86, 17.42, 17.82
Deviation in $\xi^{(2)}_{max,point,90p}$ [m]	0.09, -0.35, 0.05

6.5.2 Variations in the time step in second order simulations using deterministic wave amplitudes

Convergence of maximum point crest heights obtained from second order long crested simulations using deterministic wave amplitudes are tested with variations in the time step between calculations of the surface elevation process. Table 28 shows the four different values of the time step dt that are tested, along with the number of frequency components N_f used in the convergence test. The number of frequency components are fixed for all variations in the time step. The values of the time step varies from two seconds to a quarter of a second.

Table 28: *Parameters used in second order simulations using deterministic wave amplitudes with variations in the time step.*

Parameters used in simulations	**Value**
Number of frequency components N_f [pcs]	657
Time step dt [s]	2.00, 1.00, 0.50, 0.25

Figure 53 shows the maximum point crest heights obtained from 4*200 three hour second order simulations using deterministic wave amplitudes with variations in the time step. The 90th percentile maximum point crest heights $\xi^{(2)}_{max,point,90p}$ from simulations and the 90th percentile maximum point crest height $\xi^{(2)}_{max,point,90p}$ from the second order extreme value distribution are summed up in table 29, along with the deviation between the two. The order of the results presented in table 29 corresponds to the order of dt in table 28.

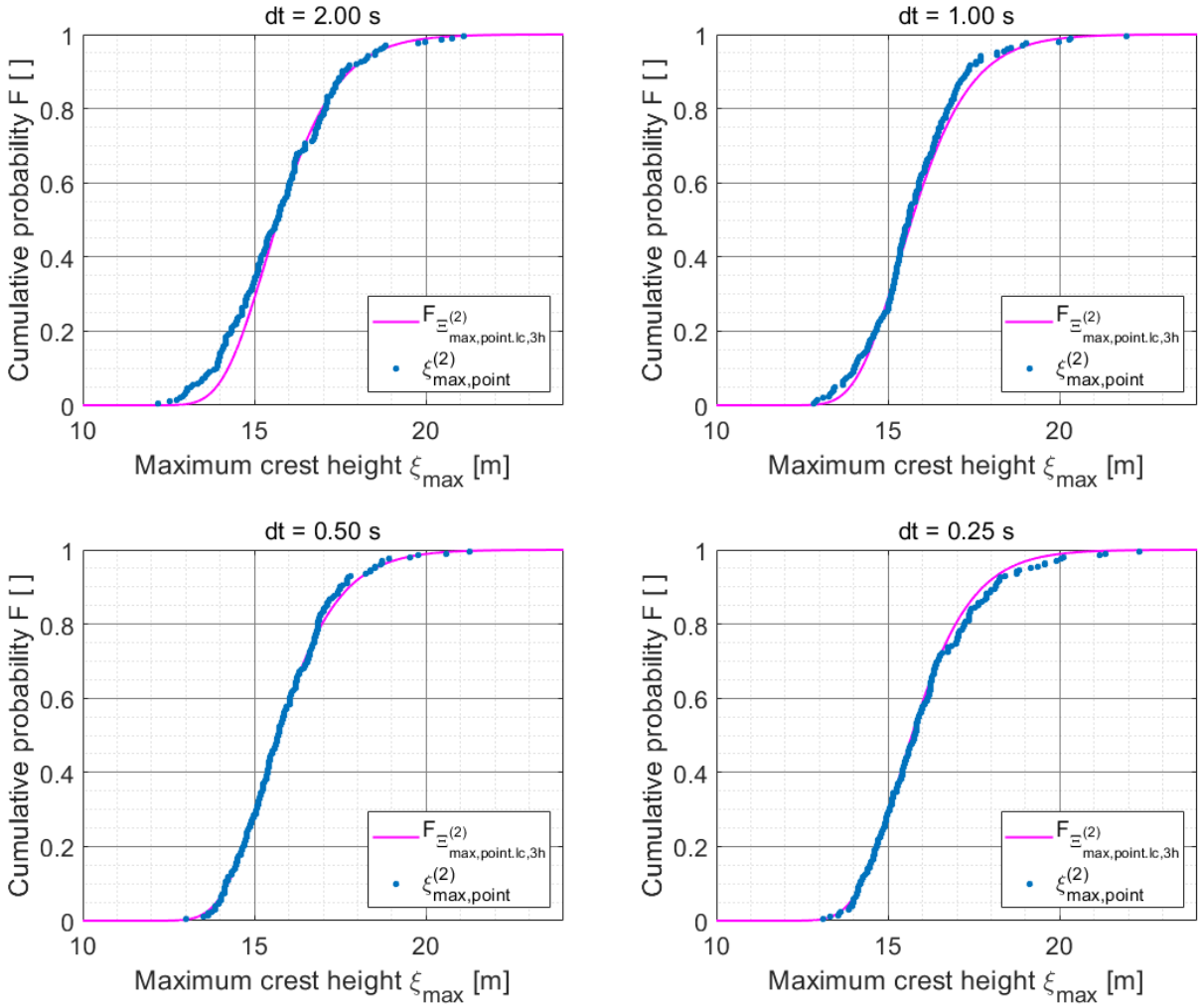

Figure 53: *Second order maximum point crest heights from three hour long crested simulations using deterministic wave amplitudes with four different time steps, along with second order extreme value distribution for long crested sea.*

Table 29: *90th percentile values for the maximum point crest heights from simulations and from second order extreme value distribution, along with the deviation between the two.*

Results from simulations	**Value**
90th percentile value from distribution $\xi^{(2)}_{max,point,90p}$ [m]	17.77
90th percentile value from simulations $\xi^{(2)}_{max,point,90p}$ [m]	17.57, 17.31, 17.50, 18.14
Deviation in $\xi^{(2)}_{max,point,90p}$ [m]	-0.20, -0.46, -0.27, 0.37

6.6 Parameter study for second order simulations using random wave amplitudes

6.6.1 Variations in the number of frequency components in second order simulations using random wave amplitudes

Convergence of maximum point crest heights obtained from second order long crested simulations using random wave amplitudes are tested with variations in the number of frequency components used when creating the wave spectrum. Table 30 shows the three different numbers of frequency components N_f used, along with the time step dt used in the convergence test. The time step is fixed for all variations in the number of frequency components. The lowest number of frequency components tested corresponds to a frequency resolution which will cause a repetitions of the surface elevation process after 20 minutes. The higher numbers of frequency components used will respectively cause a repetition of the surface elevation process after 30 minutes and 1 hour.

Table 30: *Parameters used in second order simulations using random wave amplitudes with variations in the number of frequency components.*

Parameters used in simulations	**Value**
Number of frequency components N_f [pcs]	219, 328, 657
Time step dt [s]	0.25

Figure 54 shows the maximum point crest heights obtained from 3*200 three hour second order simulations using random wave amplitudes with variations in the number of frequency components. The 90th percentile maximum point crest heights $\xi^{(2)}_{max,point,90p}$ from simulations and the 90th percentile maximum point crest height $\xi^{(2)}_{max,point,90p}$ from the second order extreme value distribution are summed up in table 31, along with the deviation between the two. The order of the results presented in table 31 corresponds to the order of N_f in table 30.

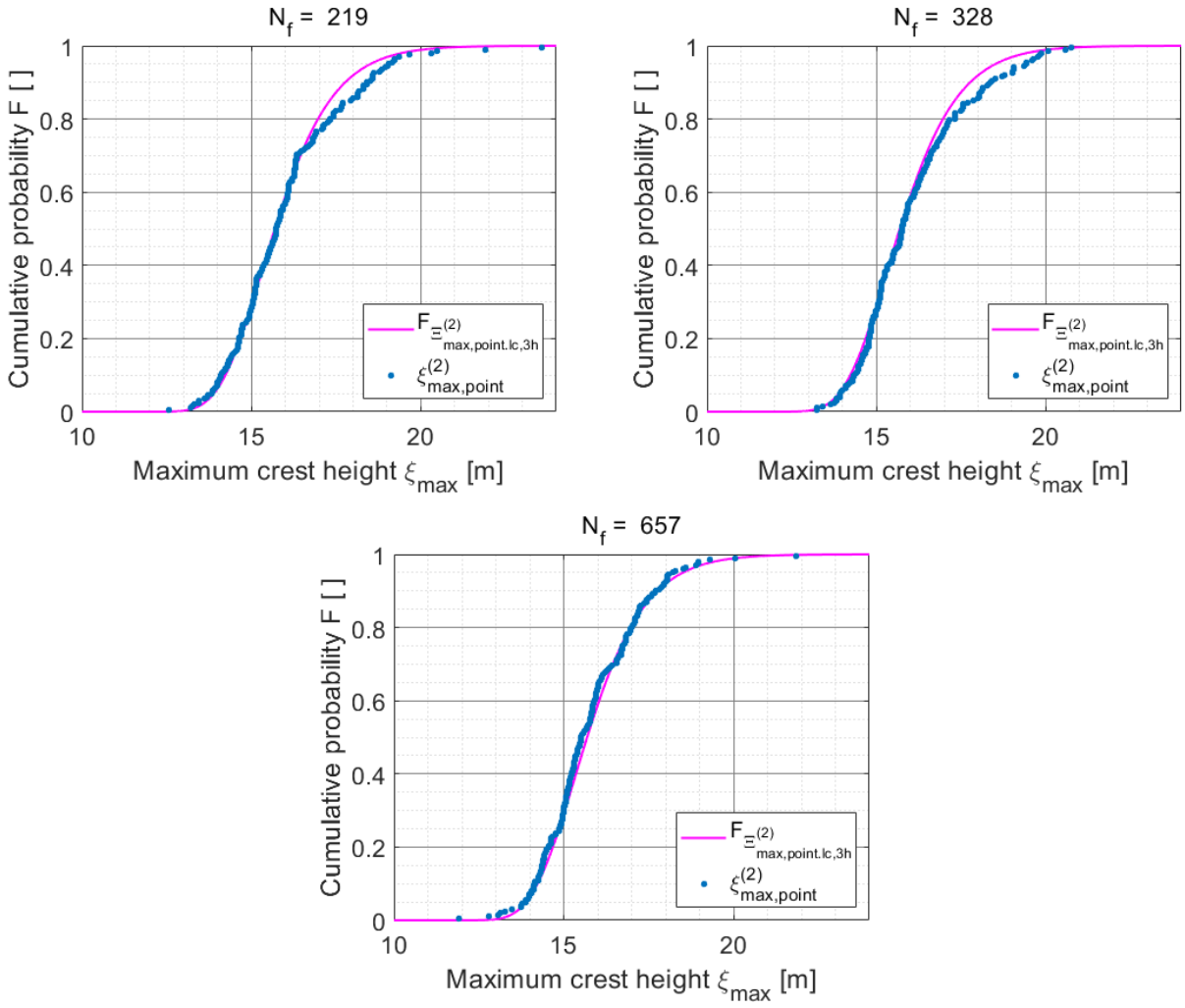

Figure 54: *Second order maximum point crest heights from three hour long crested simulations using random wave amplitudes with three different numbers of frequency components, along with second order extreme value distribution for long crested sea.*

Table 31: *90th percentile values for the maximum point crest heights from simulations and from second order extreme value distribution, along with the deviation between the two.*

Results from simulations	**Value**
90th percentile value from distribution $\xi^{(2)}_{max,point,90p}$ [m]	17.77
90th percentile value from simulations $\xi^{(2)}_{max,point,90p}$ [m]	18.42, 18.39, 17.70
Deviation in $\xi^{(2)}_{max,point,90p}$ [m]	0.65, 0.62, -0.07

6.6.2 Variations in the time step in second order simulations using random wave amplitudes

Convergence of maximum point crest heights obtained from second order long crested simulations using random wave amplitudes are tested with variations in the time step between calculations of the surface elevation process. Table 32 shows the four different values of the time step dt that are tested, along with the number of frequency components N_f used in the convergence test. The number of frequency components are fixed for all variations in the time step. The values of the time step varies from two seconds to a quarter of a second.

Table 32: *Parameters used in second order simulations using random wave amplitudes with variations in the time step.*

Parameters used in simulations	**Value**
Number of frequency components N_f [pcs]	657
Time step dt [s]	2.00, 1.00, 0.50, 0.25

Figure 55 shows the maximum point crest heights obtained from 4*200 three hour second order simulations using random wave amplitudes with variations in the time step. The 90th percentile maximum point crest heights $\xi^{(2)}_{max,point,90p}$ from simulations and the 90th percentile maximum point crest height $\xi^{(2)}_{max,point,90p}$ from the second order extreme value distribution are summed up in table 33, along with the deviation between the two. The order of the results presented in table 33 corresponds to the order of dt in table 32.

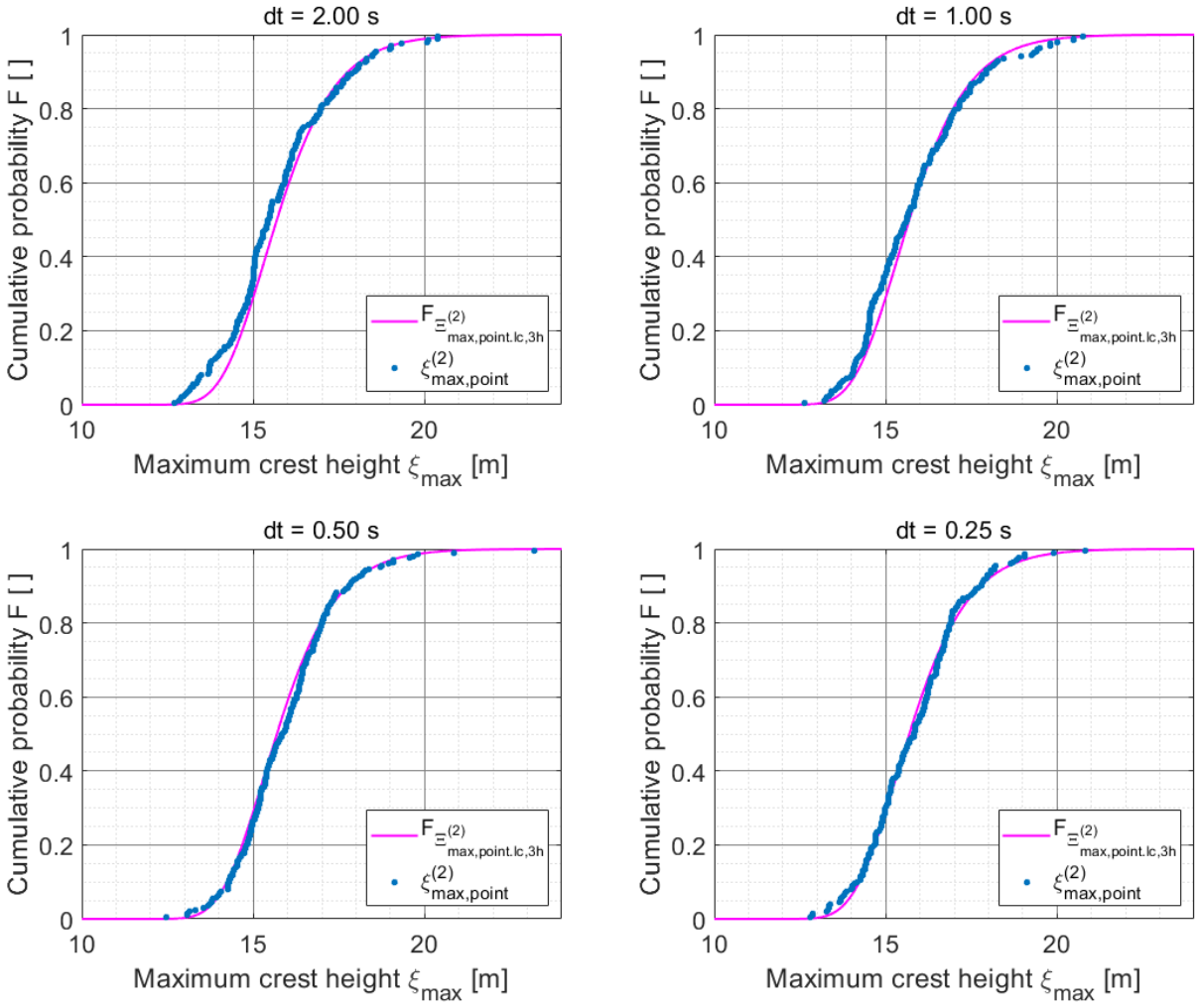

Figure 55: *Second order maximum point crest heights from three hour long crested simulations using random wave amplitudes with four different time steps, along with second order extreme value distribution for long crested sea.*

Table 33: *90th percentile values for the maximum point crest heights from simulations and from second order extreme value distribution, along with the deviation between the two.*

Results from simulations	**Value**
90th percentile value from distribution $\xi^{(2)}_{max,point,90p}$ [m]	17.77
90th percentile value from simulations $\xi^{(2)}_{max,point,90p}$ [m]	17.97, 17.93, 17.80, 17.78
Deviation in $\xi^{(2)}_{max,point,90p}$ [m]	0.20, 0.16, 0.03, 0.01

6.7 Parameter study for area grid size

6.7.1 About parameter study for area grid size

A parameter study is performed for the area grid size of a simulated area. The area grid size is given by the horizontal distances dx and dy between spatial points where the surface elevation process is calculated. When area grid size is to large, the true largest crest height over an area may be located at some distance from the spatial points where the surface elevation process is calculated. Therefore, when estimating the area effect for crest heights, it is essential that the area grid size is small enough so that the surface elevation process is calculated at points near the locations of the true maximum crest heights within an area. Both the MATLAB program for the Gaussian surface elevation process and the second order surface elevation process use the high resolution procedure for finding largest maximum area crest height, as described in section 2.6.5. In this parameter study, both the maximums obtained from the initial simulation, and the maximums obtained from the high resolution method will be tested for convergence.

Since this parameter study is very time demanding due to the large number of area coordinates, the random number generator in MATLAB is reset for every variation in grid size. In this way, the same 200 surface elevation processes are simulated for each variation in area grid size. This is done to avoid random fluctuations in the convergence. Therefore, 200 simulations of 20 minutes duration is considered good enough to estimate the mean of the maximum area crest heights. This mean of the 200 maximum area crest heights obtained from simulations is the value used for convergence checking. A 40m*40m area is selected for all simulations in this parameter study. The calculation times for both Gaussian and second order surface elevation processes are approximately inversely proportional to the product of the horizontal distances dx and dy for a square grid.

The parameter study for area grid size is performed to create a basis for selecting a proper area grid size when using the MATLAB program for simulation for both Gaussian and second order surface elevation processes. Convergence of the maximum area crest heights obtained from analysis are assumed have little variation whether Gaussian or second order, with deterministic or random wave amplitudes are used. Convergence of maximum area crest heights is therefore only tested for Gaussian simulations using random wave amplitudes. Table 34 shows the parameters used in the parameter study for the area grid size. The horizontal distances dx and dy used in simulations are varied from 20m*20m to 1m*1m.

Table 34: *Parameters used in parameter study for area grid size.*

Parameters	**Value**
Significant wave height H_s [m]	14.90
Spectral peak period T_p [s]	16.00
Shape parameter of directional spectrum n_d [ ]	10.00
Mean wave direction w.r.t side edge of square area θ_0 [deg]	0.00
Simulation duration t [s]	1*1200
Side length of area x [m]	40.00
Side length of area y [m]	40.00
Wave spectrum cutoff frequency f_{max} [hz]	0.3652
Number of frequency components N_f [pcs]	1314
Time step dt [s]	0.25
Area grid spacing dx [m]	20, 10, 6.67, 5, 4, 2, 1
Area grid spacing dy [m]	20, 10, 6.67, 5, 4, 2, 1
Number of simulations for each variation in parameter N_{sim} [pcs]	200

6.7.2 Variations in area grid size

Figure 56 shows the results obtained from the area grid size parameter study. For each variation in area grid size, the mean of 200 maximum area crest heights obtained from 20 minutes simulations are plotted against the horizontal grid size side lengths dx and dy for a square grid. Both the mean from high resolution (HR) area maximums and the mean from standard area maximums are plotted in the figure. The maximum area crest heights obtained from the high resolution procedure is expected to converge at a slightly higher value, due to the reduction of the time steps between calculations, in addition to the reduction in area grid size. The values from the convergence test are summed up in table 35. The convergence study for area grid size is assumed to be equally valid for Gaussian and second order simulations, using deterministic or random wave amplitudes.

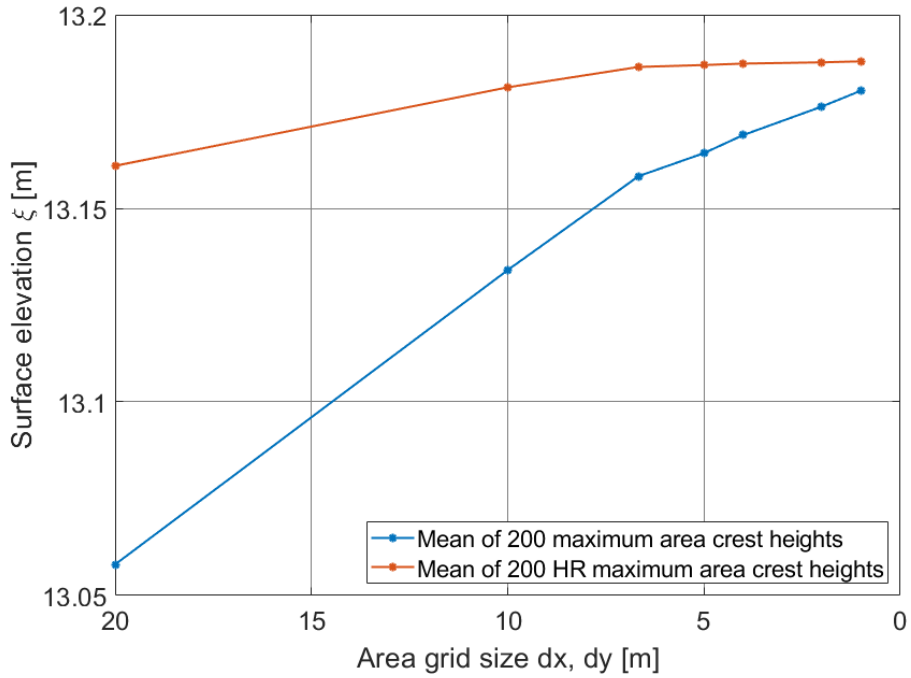

Figure 56: *Mean of maximum area crest heights obtained from simulations as a function of area grid size for a 40m*40m square area.*

Table 35: *Results for HR mean and mean of 200 maximum crest heights from simulations with variations in area grid size.*

	dx, dy [m] 20.00	dx, dy [m] 10.00	dx, dy [m] 6.67	dx, dy [m] 5.00	dx, dy [m] 4.00	dx, dy [m] 2.00	dx, dy [m] 1.00
HR mean $\xi^{(1)}_{max,area}$ [m]	13.161	13.181	13.187	13.187	13.187	13.188	13.188
Mean $\xi^{(1)}_{max,area}$ [m]	13.058	13.134	13.158	13.164	13.169	13.176	13.180

7 Analysis of Gaussian and second order area effect

7.1 About analysis of Gaussian and second order area effect

Differences in area the area effect for crest heights from Gaussian and second order simulations are investigated in this analysis. Both one hour, and three hour sea states is simulated for the comparison analysis. The sea state used for both the one hour and the three hour simulations is a three hour sea state corresponding to a 10^{-2} annual probability of being exceeded at Statfjord oil field (Example Metocean Report (2003) as given in section 4.4 and in table 3. The difference is in the duration of the simulations. Long crested sea is used for all simulations, and the area used is a square area with side edges of 40m*40m. Random wave amplitudes is used both for Gaussian and second order simulations, based on the recommendations given in Tucker et al. (1984). According to Tucker et al. (1984), using random wave amplitudes is the only way to simulate a fully Gaussian process. Random amplitudes are used for the second order simulations to create the most similar conditions between the two simulation methods.

Since the crest heights obtained from simulations of long crested sea states are the same for any line with equal length, parallel to the incoming wave direction and at the same length coordinates, simulations for the 40m*40m square area are done only for a line with length of 40m parallel to the incoming wave direction. This reduces the computational time for the simulations in MATLAB to about 10% of its initial value for the 40m*40m square area with the parameters used in this analysis. Table 36 shows the parameters used in the comparison analysis for crest heights.

Table 36: *Parameters used in analysis of Gaussian and second order area effect.*

Parameters	**Value**
Significant wave height H_s [m]	14.90
Spectral peak period T_p [s]	16.00
Shape parameter of directional spectrum n_d [ ]	∞
Mean wave direction w.r.t side edge of square area θ_0 [deg]	0.00
Simulation duration t [s]	3*1200, 9*1200
Side length of area x [m]	40.00
Side length of area y [m]	40.00
Wave spectrum cutoff frequency f_{max} [hz] (Gaussian)	0.3652
Wave spectrum cutoff frequency f_{max} [hz] (second order)	0.1826
Number of linear frequency components N_f [pcs] (Gaussian)	1314
Number of linear frequency components N_f [pcs] (second order)	657
Time step dt [s]	0.50
Area grid spacing dx [m]	5
Area grid spacing dy [m]	5
Number of simulations for each variation in simulation duration N_{sim} [pcs]	200

The value for the wave spectrum cutoff frequency f_{max} for the Gaussian simulations is chosen based on the parameter study for Gaussian simulation using random wave amplitudes in section 6.3. This approach is recommended by RP-C205 (2010). The value for the wave spectrum cutoff frequency f_{max} for the second order simulations is chosen based on the cutoff frequency method

as recommended in RP-C205 (2010) as described in section 2.5.

The numbers of linearly spaced frequency components N_f for the Gaussian and second order simulations are chosen based on the parameter studies for Gaussian and second order simulations using random wave amplitudes as described in sections 6.3 and 6.6, along with the recommendations made by RP-C205 (2010), that the number of frequency components used in Gaussian simulations of short term sea states should be at least 1000. The number of frequency components used in the second order simulations is less than 1000, since computational time would exceed what is acceptable. Reduced number of frequency components for the second order simulations is considered satisfactory. The frequency step between linearly spaced frequency components are equal for Gaussian and second order simulations.

The value for the time step dt is also based on the same parameter studies for the Gaussian and second order simulations using random wave amplitudes. Forristall (2006) uses a time step of 0.25 seconds in his analysis of the area effect. However, the parameter studies conducted in sections 6.3 and 6.6 shows little difference to the value chosen for the time step in this analysis. The value chosen for the time step is considered satisfactory, given the impact on the computational time.

The value for the area grid spacings dx and dy are chosen based on the parameter study performed in section 6.7 and on the recommendations given in Forristall (2006). The number of individual simulations N_{sim} for each variation in parameter is set to 200 due to time limitations. Forristall (2006) used 100 individual simulations for his area effect investigation using Gaussian simulations. 200 simulations for each variation in parameters is therefore considered adequate for estimating the mean area effect, although a larger number would be preferred for the area effect for sorted crest heights as a function of percentile value.

The results from the comparison analysis of area effect for crest heights are presented as the Gaussian area effect for crest heights as a function of percentile value, and as the second order area effect for crest heights as a function of percentile value. In addition, the mean area effect from both Gaussian and second order simulations will be presented. As will the mean area effect from percentile value 75th to percentile value 100th. To calculate the area effect at each percentile value, the samples of maximum area crest heights and maximum point crest heights obtained from the 200 simulations of each sea state duration are sorted from lowest value to highest value. The maximum area crest heights are sorted according to $[\xi_{max,area,1} \leq \xi_{max,area,2} \leq ... \leq \xi_{max,area,200}]$ and the maximum point crest heights are sorted according to $[\xi_{max,point,1} \leq \xi_{max,point,2} \leq ... \leq \xi_{max,point,200}]$, where $\xi_{max,area,1}$ is the lowest maximum area crest height and $\xi_{max,point,1}$ is the lowest maximum point crest height. The area effect for the Gaussian crest heights $\alpha^{(1)}$ at percentile value xp is calculated using the equation

$$\alpha_{xp}^{(1)} = \frac{\xi_{max,area,xp}^{(1)}}{\xi_{max,point,xp}^{(1)}} \tag{61}$$

,where $\xi_{max,area,xp}^{(1)}$ and $\xi_{max,point,xp}^{(1)}$ are respectively the Gaussian maximum area crest height and the Gaussian maximum point crest height at percentile value xp. The area effect for the second order crest heights $\alpha^{(2)}$ at percentile value xp is calculated using the equation

$$\alpha_{xp}^{(2)} = \frac{\xi_{max,area,xp}^{(2)}}{\xi_{max,point,xp}^{(2)}} \tag{62}$$

,where $\xi^{(2)}_{max,area,xp}$ and $\xi^{(2)}_{max,point,xp}$ are respectively the second order maximum area crest height and the second order maximum point crest height at percentile value xp. The percentile value for the Gaussian and second order crest heights are calculated as described respectively in sections 3.1.4 and 3.2.4. The Gaussian mean area effect $\alpha^{(1)}_{mean}$ is calculated as the mean of the area effect obtained from the 200 Gaussian simulations for a given time duration according to equation 63

$$\alpha^{(1)}_{mean} = \frac{1}{200}\sum_{i_1=1}^{200}\left[\frac{\xi^{(1)}_{max,area,i_1}}{\xi^{(1)}_{max,point,i_1}}\right] \tag{63}$$

,where i_1 is the unsorted Gaussian simulation number and $\xi^{(1)}_{max,area,i_1}$ and $\xi^{(1)}_{max,point,i_1}$ are respectively the Gaussian maximum area crest height and the Gaussian maximum point crest height from the same unsorted simulation number. The second order mean area effect $\alpha^{(2)}_{mean}$ is calculated as the mean of the area effect obtained from the 200 second order simulations for a given time duration according to equation 64

$$\alpha^{(2)}_{mean} = \frac{1}{200}\sum_{i_2=1}^{200}\left[\frac{\xi^{(2)}_{max,area,i_2}}{\xi^{(2)}_{max,point,i_2}}\right] \tag{64}$$

,where i_2 is the unsorted second order simulation number and $\xi^{(2)}_{max,area,i_2}$ and $\xi^{(2)}_{max,point,i_2}$ are respectively the second order maximum area crest height and the second order maximum point crest height from the same unsorted simulation number. The mean area effects from percentile value 75th to percentile value 100th $\alpha^{(1)}_{mean,75p-100p}$ and $\alpha^{(2)}_{mean,75p-100p}$ from respectively Gaussian and second order simulations will be calculated as for the mean area effect, but they will be sorted first, and have a lower boundary at the 75th percentile value.

Plots of the Gaussian and second order maximum crest heights obtained from simulations are also given in the results. The Gaussian and second order maximum crest heights are sorted and plotted along with respectively the Gaussian extreme value distribution and the second order extreme value distribution for maximum point crest heights from the same sea states. The results obtained from one hour simulations are presented in section 7.2 and the results obtained from three hour simulations are presented in section 7.3.

7.2 Results from analysis of one hour sea states

The results from the analysis of the area effect for crest heights comparing Gaussian and second order one hour simulations of a long crested sea state are presented in this section. The area effect has been analyzed for the worst three hour sea state corresponding to a 10^{-2} annual probability of being exceeded at Statfjord oil field (Example Metocean Report (2003), table 3). The analysis has been performed for a square area of 40m*40m, and 200 simulations using random amplitudes are used for both Gaussian and second order simulations. The parameters used in the simulations are given in table 36. The results obtained from the analysis are given in table 37 and figures 57, 58 and 59. Table 37 shows the mean area effects and the mean area effects from percentile value 75th to percentile value 100th obtained from simulations. Figure 57 shows the area effects $\alpha^{(1)}$ and $\alpha^{(2)}$ for respectively the Gaussian and the second order maximum crest heights as a function of percentile value. Figure 58 shows the maximum point crest heights $\xi^{(1)}_{max,point}$ and the maximum area crest heights $\xi^{(1)}_{max,area}$ obtained from Gaussian simulations. Figure 59 shows the maximum point crest heights $\xi^{(2)}_{max,point}$ and the maximum area crest heights $\xi^{(2)}_{max,area}$ obtained from second order simulations.

Table 37: *Area effect obtained from one hour simulations.*

Results from analysis	**Value**
Gaussian mean area effect $\alpha^{(1)}_{mean}$ [ ]	1.0449
Second order mean area effect $\alpha^{(2)}_{mean}$ [ ]	1.0384
Gaussian mean area effect from 75th to 100th percentile $\alpha^{(1)}_{mean,75p-100p}$	1.0397
Second order mean area effect from 75th to 100th percentile $\alpha^{(1)}_{mean,75p-100p}$	1.0313

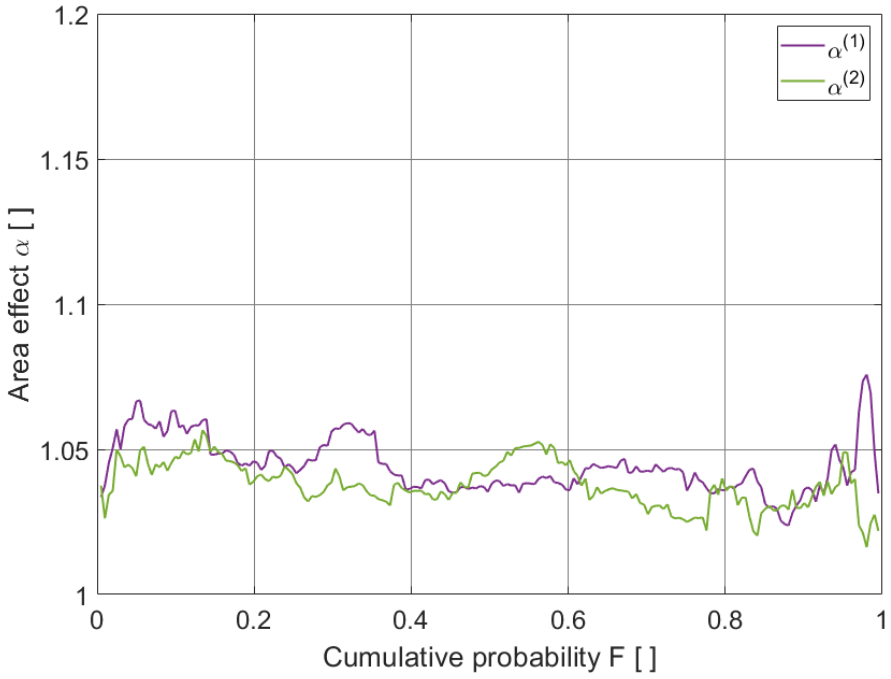

Figure 57: *Area effect at each percentile value obtained from 200 one hour Gaussian and 200 one hour second order simulations using random wave amplitudes.*

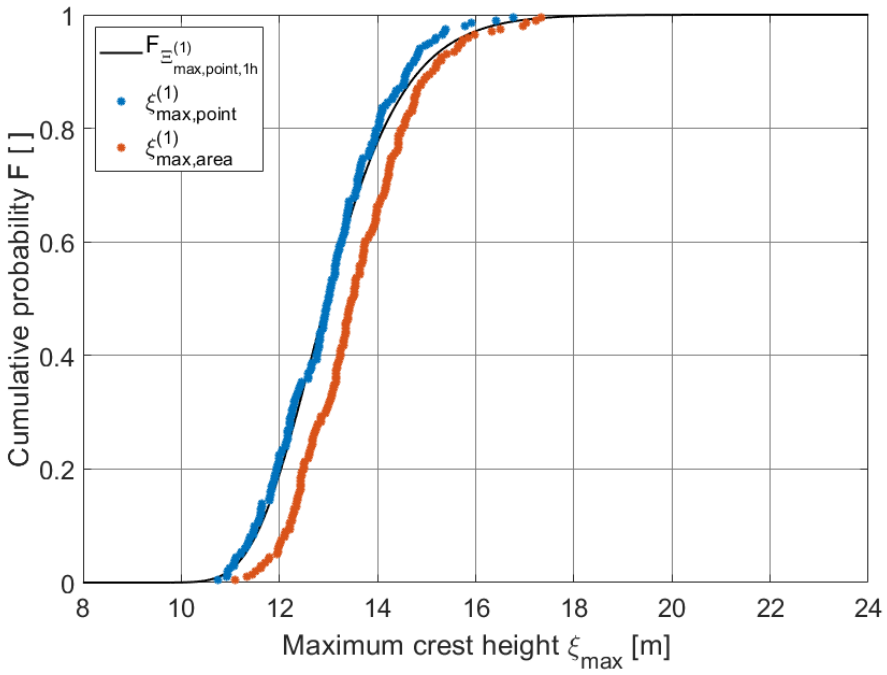

Figure 58: *Point and area maximum crest heights obtained from 200 one hour Gaussian simulations using random wave amplitudes, along with Gaussian extreme value distribution.*

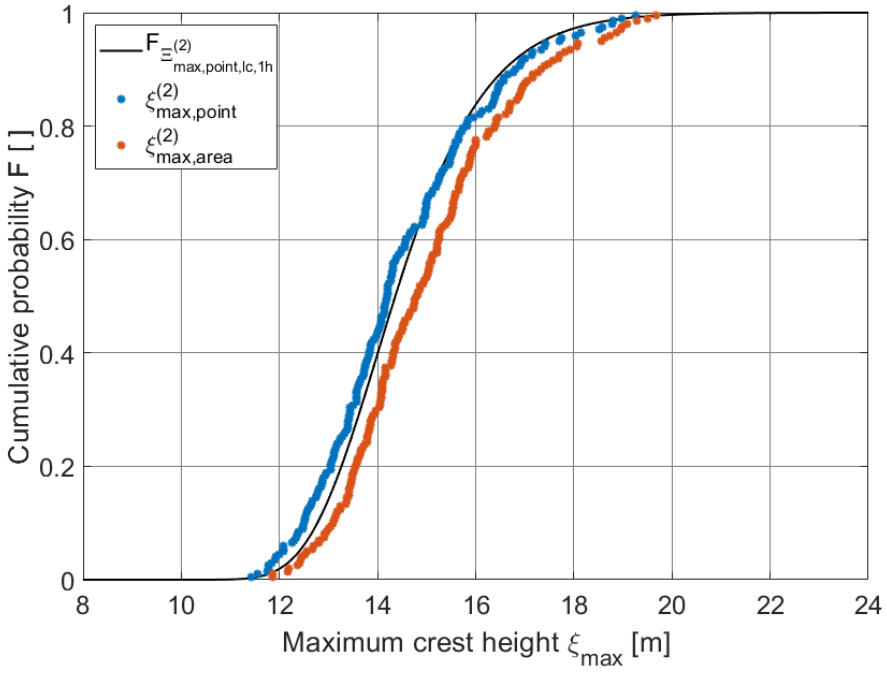

Figure 59: *Point and area maximum crest heights obtained from 200 one hour second order simulations using random wave amplitudes, along with long crested second order extreme value distribution.*

Both the mean area effect and the mean area effects from percentile value 75th to percentile value 100th obtained from Gaussian simulations is higher than the respective values obtained from second order simulations for a simulation duration of one hour. The variance of the area effect at a given percentile value is clearly high at the limited number of simulations done for this comparison analysis.

7.3 Results from analysis of three hour sea states

The results from the analysis of the area effect for crest heights comparing Gaussian and second order three hour simulations of a long crested sea state are presented in this section. The area effect has been analyzed for the worst three hour sea state corresponding to a 10^{-2} annual probability of being exceeded at Statfjord oil field (Example Metocean Report (2003), table 3). The analysis has been performed for a square area of 40m*40m, and 200 simulations using random amplitudes are used for both Gaussian and second order simulations. The parameters used in the simulations are given in table 36. The results obtained from the analysis are given in table 38 and figures 60, 61 and 62. Table 38 shows the mean area effects and the mean area effects from percentile value 75th to percentile value 100th obtained from simulations. Figure 60 shows the area effects $\alpha^{(1)}$ and $\alpha^{(2)}$ for respectively the Gaussian and the second order maximum crest heights as a function of percentile value. Figure 61 shows the maximum point crest heights $\xi^{(1)}_{max,point}$ and the maximum area crest heights $\xi^{(1)}_{max,area}$ obtained from Gaussian simulations. Figure 59 shows the maximum point crest heights $\xi^{(2)}_{max,point}$ and the maximum area crest heights $\xi^{(2)}_{max,area}$ obtained from second order simulations.

Table 38: *Area effect obtained from three hour simulations.*

Results from analysis	**Value**
Gaussian mean area effect $\alpha^{(1)}_{mean}$ [ ]	1.0492
Second order mean area effect $\alpha^{(2)}_{mean}$ [ ]	1.0327
Gaussian mean area effect from 75th to 100th percentile $\alpha^{(1)}_{mean,75p-100p}$	1.0490
Second order mean area effect from 75th to 100th percentile $\alpha^{(1)}_{mean,75p-100p}$	1.0269

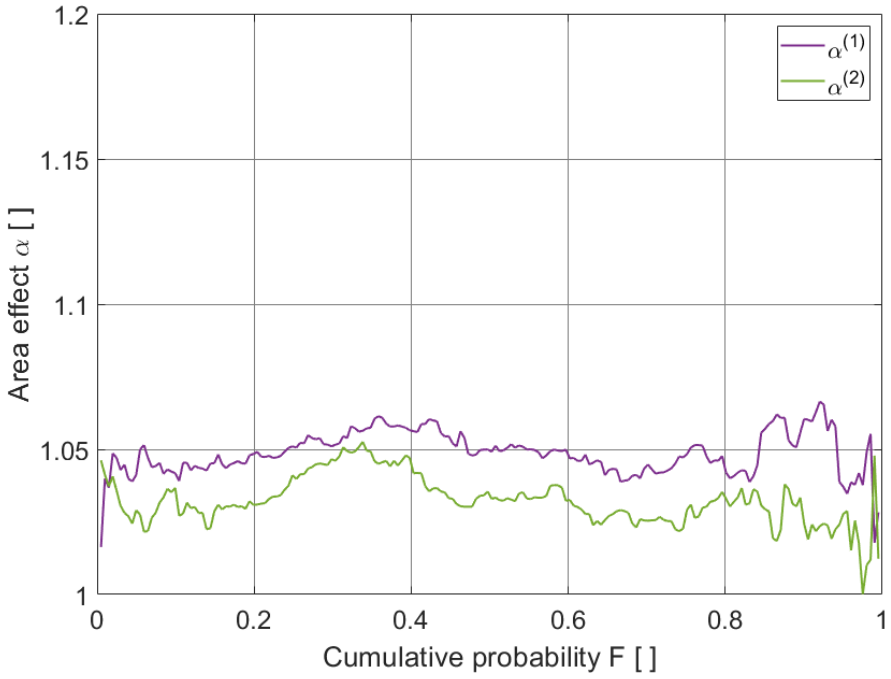

Figure 60: *Area effect at each percentile value obtained from 200 three hour Gaussian and 200 three hour second order simulations using random wave amplitudes.*

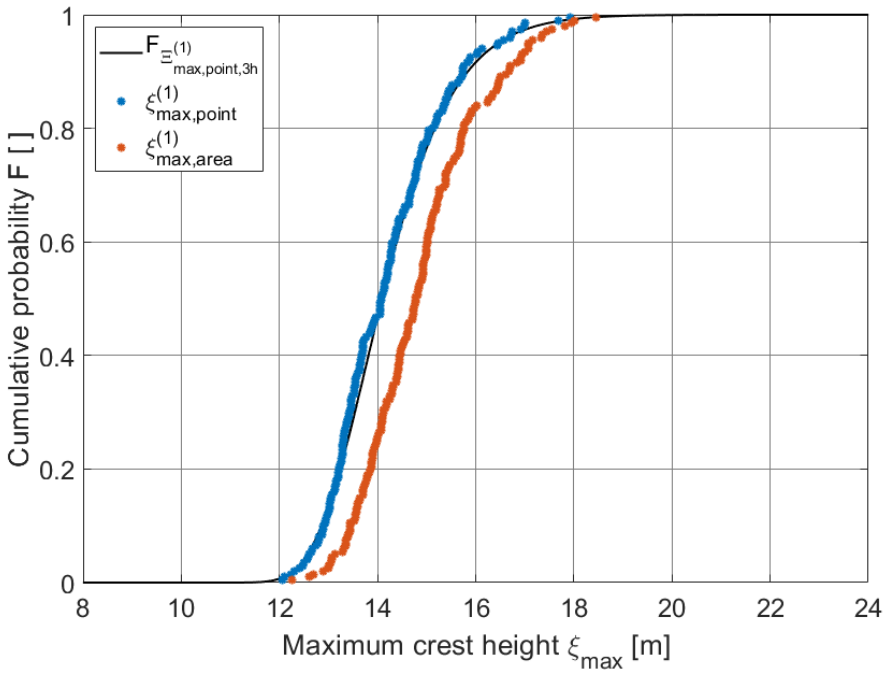

Figure 61: *Point and area maximum crest heights obtained from 200 three hour Gaussian simulations using random wave amplitudes, along with Gaussian extreme value distribution.*

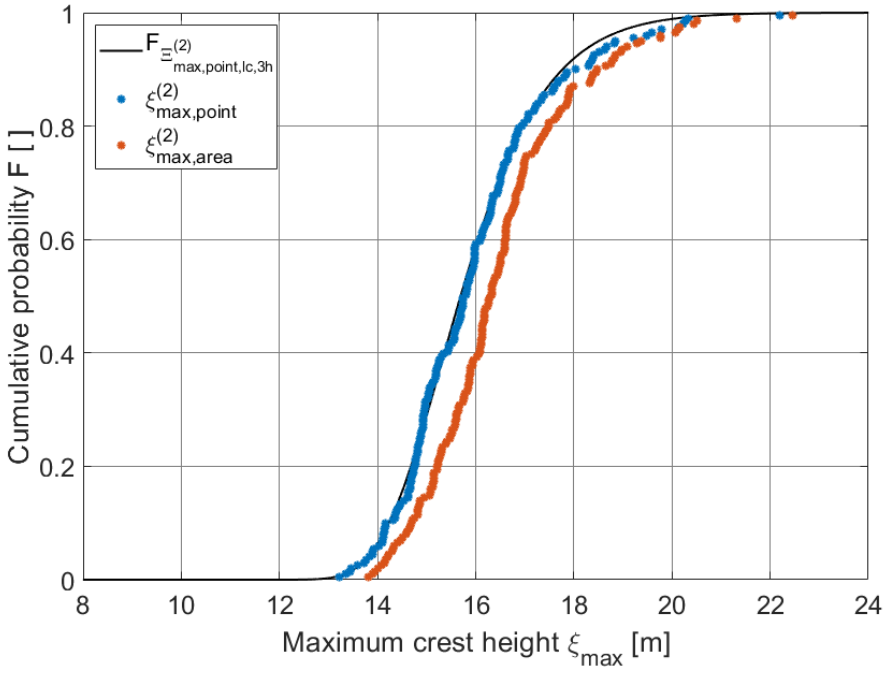

Figure 62: *Point and area maximum crest heights obtained from 200 three hour second order simulations using random wave amplitudes, along with long crested second order extreme value distribution.*

Both the mean area effect and the mean area effects from percentile value 75th to percentile value 100th obtained from Gaussian simulations is higher than the respective values obtained from second order simulations for a simulation duration of three hours. The variance of the area effect at a given percentile value is clearly high at the limited number of simulations done for this comparison analysis.

7.4 Discussion of results and conclusion for further analysis of area effect

The results from the analysis shows that the Gaussian mean area effect is larger than the second order mean area effect obtained from both one hour and three hour simulations. For the mean area effect from 75th percentile value to the 100th percentile value, the results show that the Gaussian simulations gave higher values compared to the second order simulations, both for the one hour case, and from the three hour case. Both the Gaussian and the second order simulations gave higher results for the mean area effect than for the mean area effect from 75th percentile value to the 100th percentile value, both from the one hour case, and from the three hour case.

The Gaussian mean area effect obtained from the one hour simulations is smaller than the Gaussian mean area effect obtained from the three hour simulations. The Gaussian mean area effect from 75th percentile value to the 100th percentile value obtained from the one hour simulations is also smaller than the Gaussian mean area effect from 75th percentile value to the 100th percentile value obtained from the three hour simulations.

The second order mean area effect obtained from the one hour simulations is larger than the second order mean area effect obtained from the three hour simulations. The second order mean area effect from 75th percentile value to the 100th percentile value obtained from the one hour simulations is also larger than the second order mean area effect from 75th percentile value to the 100th percentile value obtained from the three hour simulations.

Based on the results of the analysis of Gaussian and second order area effect for crest heights using long crested sea, there is no reason to believe that using second order simulations would produce higher values of the area effect than if Gaussian simulations are used. A considerably larger number of simulations have to be done to state this for sure. Hagen et al. (2018) used simulations based on the Torsethaugen wave spectrum, and showed that the area effect obtained from second order simulations exceeded the area effect obtained from Gaussian simulations for a platform sized area for both short and long crested extreme sea states. All simulations done in this thesis uses the JONSWAP wave spectrum.

The second order simulations done in this comparison analysis have, with the parameters used, a computational time of approximately 290 times the computational time of the Gaussian simulations when using random wave amplitudes. With a state of the art laptop at the time of writing, the computational time for the 200 three hour second order simulations in section 7.3 is 8 days. The equivalent computational time for the 200 three hour Gaussian simulations in section 7.3 is 40 minutes. Since this comparison analysis is based on a long crested sea state, it has been possible to simulate surface elevation processes over a line and obtain equivalent results as if simulations were done for the entire area. For simulations of the equivalent short crested sea state, the entire area needs to be simulated. The computational time for both Gaussian and second order simulations will then rise by a factor of approximately 9, when still using the same parameters. 200 three hour second order simulations for the entire area using the

equivalent short crested sea state will then have a computational time of approximately 72 days.

Since all further analysis exclusively includes short crested sea states over areas, the only real option for further analysis of the area effect for crest heights is by using Gaussian simulations of the surface elevation process. Using Gaussian simulations will also give the possibility of producing a much larger number of samples of crest heights, and therefore, the results produced will be much more stable than if second order simulations are used.

Forristall (2006) used Gaussian simulations based on the JONSWAP wave spectrum for his investigation of the area effect, and states that second order simulations are not necessary for the investigation. Forristall (2015) compares Gaussian simulations based on the JONSWAP wave spectrum with a single directional spreading spectrum over an area to measurements in a wave basin, and finds that the area effect for crest heights from simulations and from measurements agrees well. Forristall (2011)) and (Forristall (2015) states that using Gaussian simulations is adequate for finding the area effect. Therefore, it is decided that Gaussian simulations will be used for all further analysis of the area effect for crest heights. The results obtained for the area effect using Gaussian simulations are also expected to be credible.

The sea state obtained for analyzing the area effect, the worst sea state regarding crest heights for an annual exceedance probability of 10^{-2} at Statfjord oil field (Example Metocean Report (2003)) is a three hour sea state. Three hour is also the standard duration for registrations of sea states in the Norwegian Sea (RP-C205 (2010)). Due to this, three hour sea states are chosen as a standard for further analyzing of the area effect for crest heights.

8 Analysis of area effect with variation in parameters

8.1 About analysis of area effect with variation in parameters

Simulations are done to analyze how the area crest height effect varies with variations in parameters. The sea state used as a standard in the analysis is a three hour short crested sea state corresponding to a 10^{-2} annual probability of being exceeded at Statfjord oil field (Example Metocean Report (2003) as given in section 4.4 and in table 3. The standard area for the analysis is a square area with 40m*40m side edges. A Gaussian surface elevation process using random wave amplitudes is chosen for the analysis, based on the recommendations given in Tucker et al. (1984). According to Tucker et al. (1984), using random wave amplitudes is the only way to simulate a fully Gaussian process. Table 39 shows the parameters chosen for the analysis of the area effect with variation in parameters.

Table 39: *Parameters used in area effect analysis with variation in parameters.*

Parameters	**Value**
Wave spectrum cutoff frequency f_{max} [hz]	0.3652
Number of frequency components N_f [pcs]	1314
Time step dt [s]	0.25
Area grid spacing dx [m]	5.00
Area grid spacing dy [m]	5.00
Number of simulations for each variation in parameter N_{sim} [pcs]	200

The value for the wave spectrum cutoff frequency f_{max} is chosen based on the parameter study for Gaussian simulation using random wave amplitudes in section 6.3. This approach is recommended by RP-C205 (2010). The number of frequency components N_f is chosen based on the same parameter study along with the recommendations made by RP-C205 (2010), that the number of frequency components used for simulations of short term sea states should be at least 1000. The value for the time step dt is based on the same parameter study. This time step is the same as used in the area effect investigation performed by Forristall (2006). The value for the area grid spacings dx and dy are chosen based on the parameter study performed in section 6.7 and on the recommendations given in Forristall (2006). The number of individual simulations N_{sim} for each variation in parameter is set to 200 due to time limitations. This is considered good enough for estimating the mean area effect. Forristall used 100 individual simulations for his area effect investigation using Gaussian simulations in Forristall (2006). The area effect for crest heights is analyzed for variations in the following parameters:

- Significant wave height H_s
- Spectral peak period T_p
- Directional spectrum shape parameter n_d
- Mean wave direction w.r.t side edge of square area θ_0
- Sea state duration t
- Length of side edges in square area x and y

Only one parameter will be changed at a time, while all other parameters are fixed. For each variation in parameter, results for the mean area effect and the 90th percentile area effect will be presented. The 90th percentile area effect is expected to have large variance at 200 individual simulations, but is still included in the analysis.

The mean area effect $\alpha^{(1)}_{mean}$ for each variation in parameter is calculated with equation 63 as described in section 7.1. To calculate the 90th percentile area effect for each variation in parameter, the samples of maximum area crests and maximum point crest heights obtained from the 200 simulations have to be sorted from lowest value to highest value. The Gaussian maximum area crest heights are sorted according to $[\xi^{(1)}_{max,area,1} \leq \xi^{(1)}_{max,area,2} \leq ... \leq \xi^{(1)}_{max,area,90p} \leq ... \leq \xi^{(1)}_{max,area,200}]$ and the Gaussian maximum point crest heights are sorted according to $[\xi^{(1)}_{max,point,1} \leq \xi^{(1)}_{max,point,2} \leq ... \leq \xi^{(1)}_{max,point,90p} \leq ... \leq \xi^{(1)}_{max,point,200}]$, where $\xi^{(1)}_{max,area,90p}$ and $\xi^{(1)}_{max,point,90p}$ are respectively the Gaussian maximum area crest height and the Gaussian maximum point crest height closest to the 90th percentile value. The percentile value is calculated as described in section 3.1.4 for Gaussian maximum crest heights. The 90th percentile area effect $\xi^{(1)}_{\alpha,90p}$ is calculated according to equation 65

$$\xi^{(1)}_{\alpha,90p} = \frac{\xi^{(1)}_{max,area,90p}}{\xi^{(1)}_{max,point,90p}} \tag{65}$$

The results from the analysis of the area crest height effect with variations in significant wave height H_s, spectral peak period T_p, directional spectrum shape parameter n_d, mean wave direction w.r.t side edge of square area θ_0, sea state duration t and length of side edges in square area x and y are found respectively in sections 8.2, 8.4, 8.6, 8.8, 8.10 and 8.12. The directional spectrum shape factor n_d is set to a standard value of 10, the same value as used in Hagen et al. (2018) for area effect simulations for a location in the northern North Sea. The actual maximum crest heights obtained for this analysis can be found in appendix A.

At a given sea state duration, the Gaussian area effect is expected to depend on the number of individual crests within the area, and also whether the actual top of the crest is inside the area or not. The Gaussian area effect is also expected to change when the sea state duration changes.

8.2 Results from analysis with variation in significant wave height

The results from the analysis of the area effect for crest heights with variation in significant wave height are presented in this section. The area effect for crest heights has been analyzed for the worst three hour short crested sea state corresponding to a 10^{-2} annual probability of being exceeded at Statfjord oil field (Example Metocean Report (2003), table 3). The analysis has been performed for an area of 40m*40m, and 200 Gaussian simulations using random amplitudes are done for each variation in parameter. The parameters used in the simulations are given in table 41. The significant wave height has been varied from a significant wave height corresponding to a 10^{-2} annual probability of being exceeded, to a significant wave height corresponding to a 10^{-4} annual probability of being exceeded (table 1). All other parameters, including the spectral peak period T_p have been held constant during the simulations. The results obtained from the analysis, along with the corresponding values used for the significant wave height H_s are given in table 40 and figure 63. Both the mean area effect $\alpha^{(1)}_{mean}$ and the 90th percentile area effect $\alpha^{(1)}_{90p}$ are included in the results.

Table 40: *Results from area effect analysis with variation in significant wave height.*

	H_s [m] 14.90	H_s [m] 15.70	H_s [m] 16.50	H_s [m] 17.30	H_s [m] 18.20
Mean area effect $\alpha^{(1)}_{mean}$ [ ]	1.0774	1.0784	1.0733	1.0714	1.0751
90th percentile area effect $\alpha^{(1)}_{90p}$ [ ]	1.0748	1.0707	1.0675	1.0712	1.0569

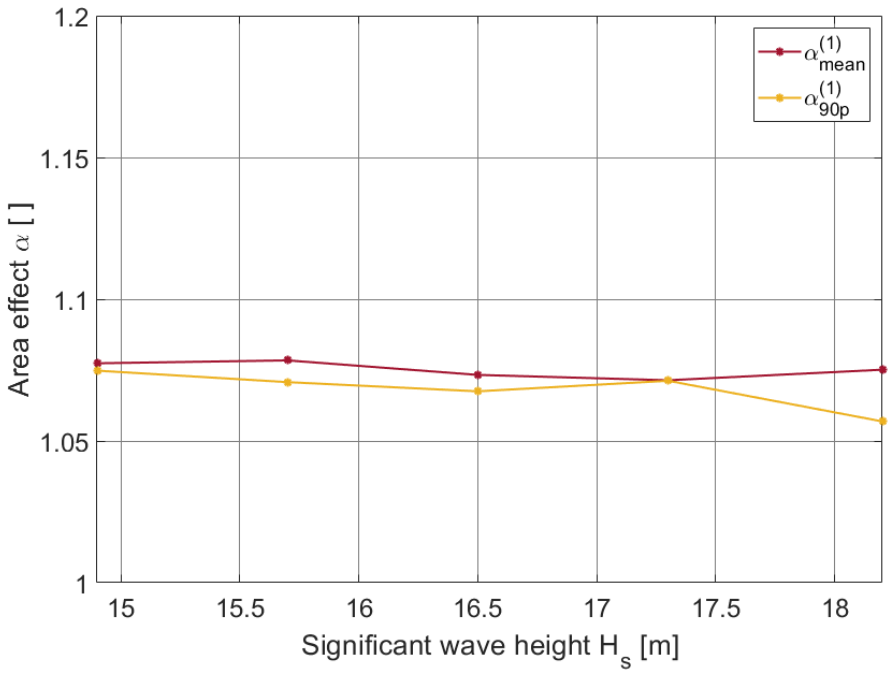

Figure 63: *Results from area effect analysis with variation in significant wave height.*

Table 41: *Parameters used in area effect analysis with variation in significant wave height.*

Parameter varied in analysis	**Value**
Significant wave height H_s [m]	14.90, 15.70, 16.50, 17.30, 18.20
Fixed parameters	**Value**
Spectral peak period T_p [s]	16.00
Shape parameter of directional spectrum n_d [ ]	10.00
Mean wave direction w.r.t side edge of square area θ_0 [deg]	0.00
Simulation duration t [s]	9*1200
Side length of area x [m]	40.00
Side length of area y [m]	40.00

8.3 Discussion

There seem to be no notable trend in the mean area crest height effect $\alpha^{(1)}_{mean}$ for the analyzed sea state when varying the significant wave height. The 90th percentile area crest height effect $\alpha^{(1)}_{90p}$ seems to have a slightly descending trend when the significant wave height increases, but the variance of the 90th percentile area crest height effect is expected to be high. The 90th percentile area crest height effect is lower than the mean area crest height effect for five out of five variations in significant wave height.

The crest heights themselves will change when varying the significant wave height, but the ratio between the area maximums and the point maximums is still the same. When changing the significant wave height, the number of individual crests within the area boundaries will not change. Nor will the fraction of sampled crest heights with the actual top within the area boundaries. Therefore, variations in the significant wave height, without varying any other parameters, will not cause any changes in the area effect. The results for the area effect are in accordance with the results presented in Teigland (2018).

8.4 Results from analysis with variation in spectral peak period

The results from the analysis of the area effect for crest heights with variation in spectral peak period within a 90% confidence interval are presented in this section. The area effect for crest heights has been analyzed for the worst three hour short crested sea state corresponding to a 10^{-2} annual probability of being exceeded at Statfjord oil field (Example Metocean Report (2003), table 3. The analysis has been performed for an area of 40m*40m, and 200 Gaussian simulations using random amplitudes are done for each variation in parameter. The parameters used in the simulations are given in table 43. The spectral peak period has been varied from a spectral peak period corresponding to the bottom of the 90% range, to a spectral peak period corresponding to the top of the 90% range (table 1). All other parameters have been held constant during the simulations. The results obtained from the analysis, along with the corresponding values used for the spectral peak period T_p are given in table 42 and figure 64. Both the mean area effect $\alpha^{(1)}_{mean}$ and the 90th percentile area effect $\alpha^{(1)}_{90p}$ are included in the results.

Table 42: *Results from area effect analysis with variation in spectral peak period.*

	T_p [s] 14.00	T_p [s] 15.00	T_p [s] 16.00	T_p [s] 17.10	T_p [s] 18.20
Mean area effect $\alpha^{(1)}_{mean}$ [ ]	1.0874	1.0791	1.0775	1.0705	1.0698
90th percentile area effect $\alpha^{(1)}_{90p}$ [ ]	1.0554	1.0837	1.0633	1.0699	1.0718

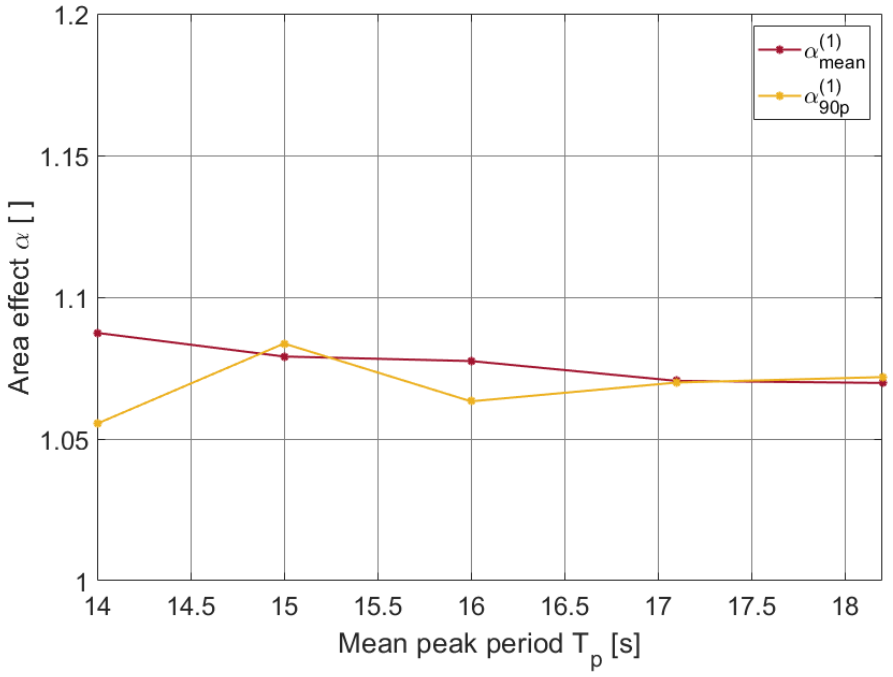

Figure 64: *Results from area effect analysis with variation in spectral peak period.*

Table 43: *Parameters used in area effect analysis with variation in spectral peak period.*

Parameter varied in analysis	**Value**
Spectral peak period T_p [s]	14.00, 15.00, 16.00, 17.10, 18.20
Fixed parameters	**Value**
Significant wave height H_s [m]	14.90
Shape parameter of directional spectrum n_d [ ]	10.00
Mean wave direction w.r.t side edge of square area θ_0 [deg]	0.00
Simulation duration t [s]	9*1200
Side length of area x [m]	40.00
Side length of area y [m]	40.00

8.5 Discussion

The mean area crest height effect $\alpha^{(1)}_{mean}$ have a decreasing trend for the analyzed sea state when the spectral peak period increases. The 90th percentile area crest height effect $\alpha^{(1)}_{90p}$ does not seem to have a notable trend when the mean peak period varies, but the variance of the 90th percentile area crest height effect is expected to be high. The 90th percentile area crest height effect is lower than the mean area crest height effect for three out of five variations in spectral peak period.

When reducing the spectral peak period, the number of individual crests within the area boundaries will increase. The fraction of sampled crest heights with the actual top within the area boundaries will also increase. Therefore, lowering the spectral peak period, without varying any other parameters, will cause an increase in the mean area effect. The results for the mean area effect are in accordance with the results presented in Teigland (2018) and Forristall (2006).

8.6 Results from analysis with variation in directional spectrum shape factor

The results from the analysis of the area effect for crest heights with variation in directional spectrum shape factor are presented in this section. The area effect for crest heights has been analyzed for the worst three hour short crested sea state corresponding to a 10^{-2} annual probability of being exceeded at Statfjord oil field (Example Metocean Report (2003), table 3). The analysis has been performed for an area of 40m*40m, and 200 Gaussian simulations using random amplitudes are done for each variation in parameter. The parameters used in the simulations are given in table 45. The directional spectrum shape factor has been varied from a directional spectrum shape factor of two, to a directional spectrum shape factor of ten. All other parameters have been held constant during the simulations. The results obtained from the analysis, along with the corresponding values used for the directional spectrum shape factor n_d are given in table 44 and figure 65. Both the mean area effect $\alpha^{(1)}_{mean}$ and the 90th percentile area effect $\alpha^{(1)}_{90p}$ are included in the results.

Table 44: *Results from area effect analysis with variation in directional spectrum shape factor.*

	n_d [ ] 2.00	n_d [ ] 4.00	n_d [ ] 6.00	n_d [ ] 8.00	n_d [ ] 10.00
Mean area effect $\alpha^{(1)}_{mean}$ [ ]	1.0951	1.0871	1.0845	1.0803	1.0752
90th percentile area effect $\alpha^{(1)}_{90p}$ [ ]	1.0530	1.0758	1.0789	1.0607	1.0673

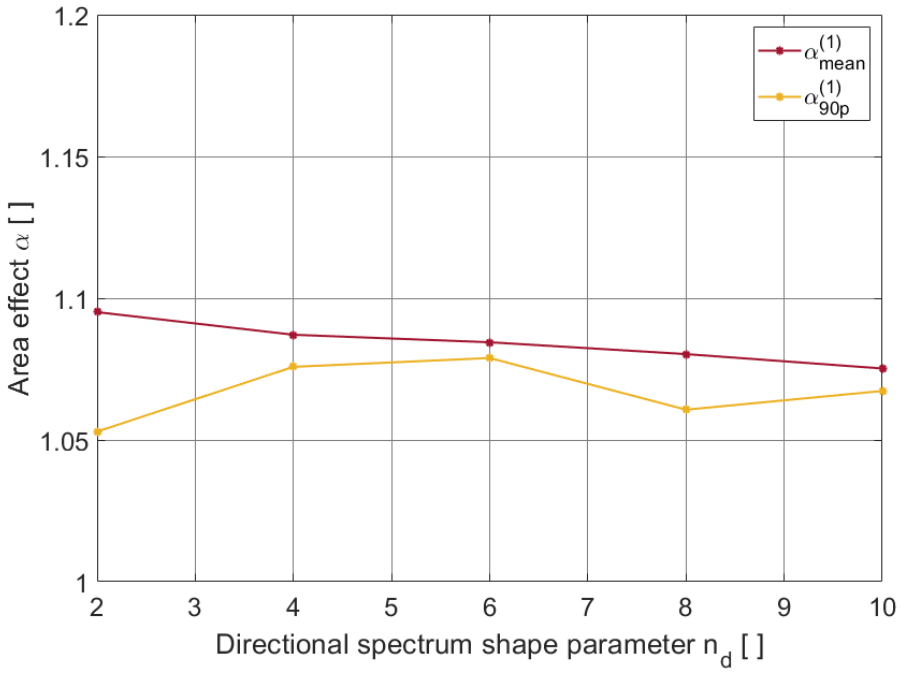

Figure 65: *Results from area effect analysis with variation in directional spectrum shape factor.*

Table 45: *Parameters used in area effect analysis with variation in directional spectrum shape factor.*

Parameter varied in analysis	**Value**
Shape parameter of directional spectrum n_d [ ]	2.00, 4.00, 6.00, 8.00, 10.00
Fixed parameters	**Value**
Significant wave height H_s [m]	14.90
Spectral peak period T_p [s]	16.00
Mean wave direction w.r.t side edge of square area θ_0 [deg]	0.00
Simulation duration t [s]	9*1200
Side length of area x [m]	40.00
Side length of area y [m]	40.00

8.7 Discussion

The mean area crest height effect $\alpha^{(1)}_{mean}$ have a descending trend for the analyzed sea state when the directional spectrum shape parameter increases. The 90th percentile area crest height effect $\alpha^{(1)}_{90p}$ does not seem to have a notable trend when the directional spectrum shape parameter increases, but the variance of the 90th percentile area crest height effect is expected to be high. The 90th percentile area crest height effect is lower than the mean area crest height effect for five out of five variations in directional spectrum shape parameter.

When lowering the directional spectrum shape factor, the number of individual crests within the area boundaries will increase. The fraction of sampled crest heights with the actual top within the area boundaries will also increase. Therefore, lowering the directional spectrum shape factor, without varying any other parameters, will cause an increase in the mean area effect. The results for the mean area effect are in accordance with the results presented in Teigland (2018) and Hagen et al. (2018).

8.8 Results from analysis with variation in mean wave direction

The results from the analysis of the area effect for crest heights with variation in mean wave direction are presented in this section. The area effect for crest heights has been analyzed for the worst three hour short crested sea state corresponding to a 10^{-2} annual probability of being exceeded at Statfjord oil field (Example Metocean Report (2003), table 3). The analysis has been performed for an area of 40m*40m, and 200 Gaussian simulations using random amplitudes are done for each variation in parameter. The parameters used in the simulations are given in table 47. The mean direction for the wave propagation has been varied with respect to one of the side edges of the square area, from a mean wave direction of zero degrees (along side edge), to a mean wave direction of 45 degrees (45 degrees w.r.t all edges). All other parameters have been held constant during the simulations. The results obtained from the analysis, along with the corresponding values used for the mean direction θ_0 are given in table 46 and figure 66. Both the mean area effect $\alpha^{(1)}_{mean}$ and the 90th percentile area effect $\alpha^{(1)}_{90p}$ are included in the results.

Table 46: *Results from area effect analysis with variation in mean wave direction.*

	θ_0 [deg] 0.00	θ_0 [deg] 11.25	θ_0 [deg] 22.50	θ_0 [deg] 37.75	θ_0 [deg] 45.00
Mean area effect $\alpha^{(1)}_{mean}$ [ ]	1.0782	1.0770	1.0788	1.0783	1.0770
90th percentile area effect $\alpha^{(1)}_{90p}$ [ ]	1.0732	1.0563	1.0702	1.0609	1.0593

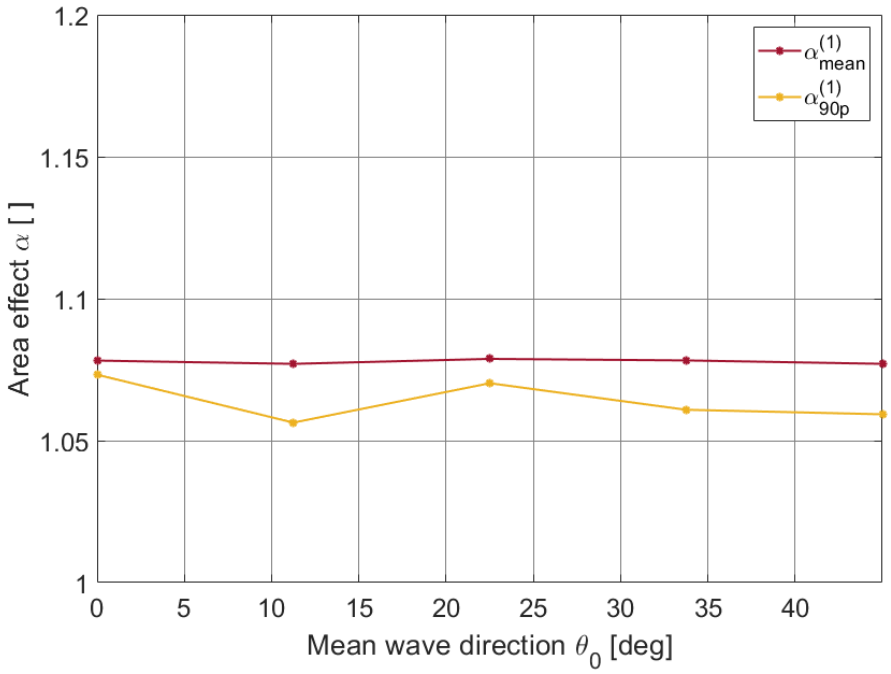

Figure 66: *Results from area effect analysis with variation in mean wave direction.*

Table 47: *Parameters used in area effect analysis with variation in mean wave direction.*

Parameter varied in analysis	**Value**
Mean wave direction w.r.t side edge of square area θ_0 [deg]	0.00, 11.25, 22.50, 37.75, 45.00
Fixed parameters	**Value**
Significant wave height H_s [m]	14.90
Spectral peak period T_p [s]	16.00
Shape parameter of directional spectrum n_d [ ]	10.00
Simulation duration t [s]	9*1200
Side length of area x [m]	40.00
Side length of area y [m]	40.00

8.9 Discussion

There seem to be no notable trend in the mean area crest height effect $\alpha^{(1)}_{mean}$ for the analyzed sea state when varying the mean wave direction. The 90th percentile area crest height effect $\alpha^{(1)}_{90p}$ does not seem to have any notable trend either when the mean wave direction varies, but the variance of the 90th percentile area crest height effect is expected to be high. The 90th percentile area crest height effect is lower than the mean area crest height effect for five out of five variations in mean wave direction.

In a perfectly short crested sea state, the number of individual crests within the area boundaries will not change with variations in the mean wave direction. Nor will the fraction of sampled crest heights with the actual top within the area boundaries. In a long crested sea state, the area effect will change with variations in the mean wave direction. Since the crests of the waves are still very long relative to the area size with a directional spectrum shape factor of 10, it would not be surprising if the mean wave direction had some influence on the area effect. However, it seems like variations in the mean wave direction, without varying any other parameters, will not cause any changes in the area effect. The results for the mean area effect are in accordance with the results presented in Forristall (2006).

8.10 Results from analysis with variation in sea state duration

The results from the analysis of the area effect for crest heights with variation in sea state duration are presented in this section. The area effect for crest heights has been analyzed for the worst three hour short crested sea state corresponding to a 10^{-2} annual probability of being exceeded at Statfjord oil field (Example Metocean Report (2003), table 3). The analysis has been performed for an area of 40m*40m, and 200 Gaussian simulations using random amplitudes are done for each variation in parameter. The parameters used in the simulations are given in table 49. The sea state duration has been varied from a sea state duration of 1*1200 seconds to a sea state duration of 9*1200 seconds. All other parameters have been held constant during the simulations. The results obtained from the analysis, along with the corresponding values used for the sea state duration t are given in table 48 and figure 67. Both the mean area effect $\alpha^{(1)}_{mean}$ and the 90th percentile area effect $\alpha^{(1)}_{90p}$ are included in the results.

Table 48: *Results from area effect analysis with variation in sea state duration.*

	t [s] 1*1200	t [s] 3*1200	t [s] 5*1200	t [s] 7*1200	t [s] 9*1200
Mean area effect $\alpha^{(1)}_{mean}$ [ ]	1.0997	1.0861	1.0886	1.0787	1.0777
90th percentile area effect $\alpha^{(1)}_{90p}$ [ ]	1.0898	1.0638	1.0767	1.0628	1.0764

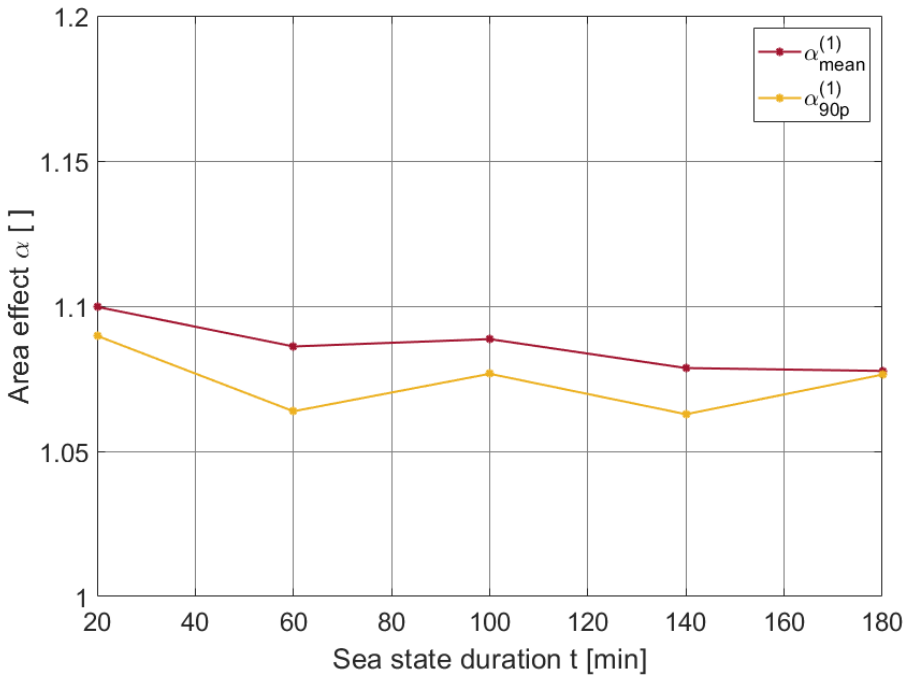

Figure 67: *Results from area effect analysis with variation in sea state duration.*

Table 49: *Parameters used in area effect analysis with variation in sea state duration.*

Parameter varied in analysis	**Value**
Simulation duration t [s]	[1, 3, 5, 7, 9]*1200
Fixed parameters	**Value**
Significant wave height H_s [m]	14.90
Spectral peak period T_p [s]	16.00
Shape parameter of directional spectrum n_d [ ]	10.00
Mean wave direction w.r.t side edge of square area θ_0 [deg]	0.00
Side length of area x [m]	40.00
Side length of area y [m]	40.00

8.11 Discussion

The mean area crest height effect $\alpha^{(1)}_{mean}$ have a decreasing trend for the analyzed sea state when the sea state duration increases. The 90th percentile area crest height effect $\alpha^{(1)}_{90p}$ also seem to have a descending trend when the sea state duration increases, but the variance of the 90th percentile area crest height effect is expected to be high. The 90th percentile area crest height effect is lower than the mean area crest height effect for five out of five variations in variation in sea state duration.

The reason for the decrease of the area effect with increasing sea state durations is as follows. The area maximums and the point maximums both increase as the sea state duration increase. However, the ratio between the area maximums and the point maximums decrease as the sea state duration increases, resulting in a decrease in the area effect when the sea state duration increases. The results for the mean area effect are in accordance with the results presented in Teigland (2018).

A separate analysis with an illustration and further explanations into why the area effect changes with sea state duration is given in appendix C. The separate analysis is meant to complement the discussion given in this section, and to help understand why the sea state duration has effect on the area effect.

8.12 Results from analysis with variation in square area size

The results from the analysis of the area effect for crest heights with variation in square area size are presented in this section. The area effect for crest heights has been analyzed for the worst three hour short crested sea state corresponding to a 10^{-2} annual probability of being exceeded at Statfjord oil field (Example Metocean Report (2003), table 3). The analysis has been performed with 200 Gaussian simulations using random amplitudes for each variation in parameter. The parameters used in the simulations are given in table 51. The square area size has been varied from one point to a square area size with side lengths of 100 meters. All other parameters have been held constant during the simulations. The results obtained from the analysis, along with the corresponding values used for the side lengths x and y for the square area are given in table 50 and figure 68. Both the mean area effect $\alpha^{(1)}_{mean}$ and the 90th percentile area effect $\alpha^{(1)}_{90p}$ are included in the results.

Table 50: *Results from area effect analysis with variation in area size.*

	x, y[m] 0.00	x, y[m] 10.00	x, y[m] 20.00	x, y[m] 40.00	x, y[m] 60.00	x, y[m] 80.00	x, y[m] 100.00
Mean area effect $\alpha^{(1)}_{mean}$ [ ]	1.0000	1.0259	1.0435	1.0703	1.1050	1.1228	1.1414
90th percentile area effect $\alpha^{(1)}_{90p}$ [ ]	1.0000	1.0238	1.0419	1.0574	1.1038	1.1111	1.1324

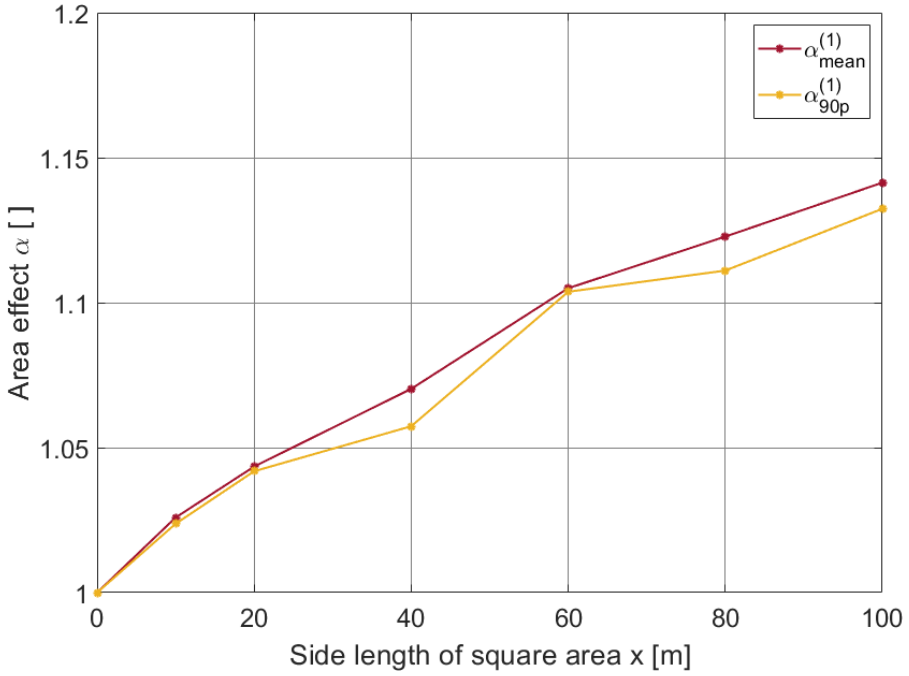

Figure 68: *Results from area effect analysis with variation in area size.*

Table 51: *Parameters used in area effect analysis with variation in area size.*

Parameter varied in analysis	**Value**
Side length of area x [m]	0, 10, 20, 40, 60, 80, 100
Side length of area y [m]	0, 10, 20, 40, 60, 80, 100
Fixed parameters	**Value**
Significant wave height H_s [m]	14.90
Spectral peak period T_p [s]	16.00
Shape parameter of directional spectrum n_d [ ]	10.00
Mean wave direction w.r.t side edge of square area θ_0 [deg]	0.00
Simulation duration t [s]	9*1200

8.13 Discussion

The mean area crest height effect $\alpha^{(1)}_{mean}$ have a clear increasing trend for the analyzed sea state when the area size increases. The 90th percentile area crest height effect $\alpha^{(1)}_{90p}$ also have a clear increasing trend when the area size increases. The variance of the 90th percentile area crest height effect is high. The 90th percentile area crest height effect is lower than the mean area crest height effect for six out of six variations in variation in area size larger than a point.

When increasing the area size, the number of individual crests within the area boundaries will increase. The fraction of sampled crest heights with the actual top within the area boundaries will also increase. Forristall (2006) shows that the number of individual crests within a square area is proportional to the area side lengths for small areas, and not to the area size. For large areas, typically larger than 200m*200m, the number of individual crests within a square area will proportional to the area size (Forristall (2006)). Therefore, increasing the square area side lengths, without varying any other parameters, will cause an increase in the area effect. The results for the area effect are in accordance with the results presented in Forristall (2006), Forristall (2011), Forristall (2015), Teigland (2018) and Hagen et al. (2018).

9 Additional analysis of area effect

9.1 About additional analysis of area effect

For this additional analysis of the area effect, sea states from figure 27 showing the contour lines at Statfjord oil field (Example Metocean Report (2003) as given in section 4.4 are still used. An investigation is done for the area effect with variations in the significant wave height and in the spectral peak period, with sea states from within the boundaries of the contour line corresponding to a 10^{-2} annual probability of being exceeded are used. This opens the possibility of analyzing the area effect with much wider variations in the significant wave height and in the spectral peak period. An investigation of the position of area maximums will also be done for the worst sea state corresponding to a 10^{-2} annual probability of being exceeded. This is the same sea state as used for the analysis in section 8. All sea states used in the simulations are three hour short crested sea states. The area used in the analysis is a square area with 40m*40m side edges. A Gaussian surface elevation process using random wave amplitudes is chosen for the analysis, based on the recommendations given in Tucker et al. (1984). According to Tucker et al. (1984), using random wave amplitudes is the only way to simulate a fully Gaussian process. Table 52 shows the parameters used in the analysis. The values for the significant wave height, the spectral peak period and the number of simulation done are given with the results from the analysis.

Table 52: *Parameters used in additional analysis of the area effect, and for analysis of area maximum location.*

Parameters	**Value**
Shape parameter of directional spectrum n_d [ ]	10.00
Mean wave direction w.r.t x-axis θ_0 [deg]	0.00
Simulation duration t [s]	9*1200
Side length of area x [m]	40.00
Side length of area y [m]	40.00
Number of frequency components N_f [pcs]	1314
Time step dt [s]	0.25
Area grid spacing dx [m]	5.00
Area grid spacing dy [m]	5.00

The values used for the number of frequency components N_f, the time step dt and the area grid spacings dx and dy are the same as used in the analysis of the area effect with variation in parameters in section 8. The value for the wave spectrum cutoff frequency is given in each respective analysis. There is not done any new parameter study for the sea states used in this analysis. The JONSWAP wave spectrum is still used for this analysis. All sea states analyzed does not fit well under the description of growing wing sea for the JONSWAP wave spectrum. It is therefore expected that the results produced include some bias at extreme combinations of the significant wave height and the spectral peak period. The results for the area effect are given as the mean area effect $\alpha^{(1)}_{mean}$ and as the 90th percentile area effect $\alpha^{(1)}_{90p}$, as described in section 8.1. The results from the analysis of locations for area maximums will be given as a plots of the locations for the individual area maximums, and also by a table of locations. The results from the analysis of the area crest height effect with variations in significant wave height

H_s are given in section 9.2. The results from the analysis of the area crest height effect with variations in spectral peak period T_p are given in section 9.4. The results from the analysis of the locations for the area maximums are given in section 9.6. The directional spectrum shape factor n_d is set to a value of 10 for all simulations in this section, the same value as used in Hagen et al. (2018) for area effect simulations for a location in the northern North Sea. The actual maximum crest heights obtained for this analysis can be found in appendix B.

9.2 Results from additional analysis with variation in significant wave height

The results from the additional analysis of the area effect for crest heights with variation in significant wave height are presented in this section. The area effect for crest heights has been analyzed for sea states within the boundaries of the contour line corresponding to a 10^{-2} annual probability of being exceeded at Statfjord oil field (Example Metocean Report (2003), figure 27). The analysis has been performed for an area of 40m*40m, and 200 Gaussian simulations using random amplitudes are done for each variation in significant wave height. The parameters used in the simulations are given in table 54. The significant wave height has been varied from the bottom of the 100-year contour line to the top of the 100-year contour line for a spectral peak period of 16 seconds. All other parameters have been held constant during the simulations. The results obtained from the analysis, along with the corresponding values used for the significant wave height H_s are given in table 53 and figure 69. Both the mean area effect $\alpha^{(1)}_{mean}$ and the 90th percentile area effect $\alpha^{(1)}_{90p}$ are included in the results.

Table 53: *Results from additional area effect analysis with variation in significant wave height.*

	H_s [m] 0.40	H_s [m] 4.00	H_s [m] 8.00	H_s [m] 12.00	H_s [m] 14.90
Mean area effect $\alpha^{(1)}_{mean}$ [ ]	1.0883	1.0868	1.0779	1.0752	1.0774
90th percentile area effect $\alpha^{(1)}_{90p}$ [ ]	1.0630	1.0655	1.0642	1.0667	1.0653

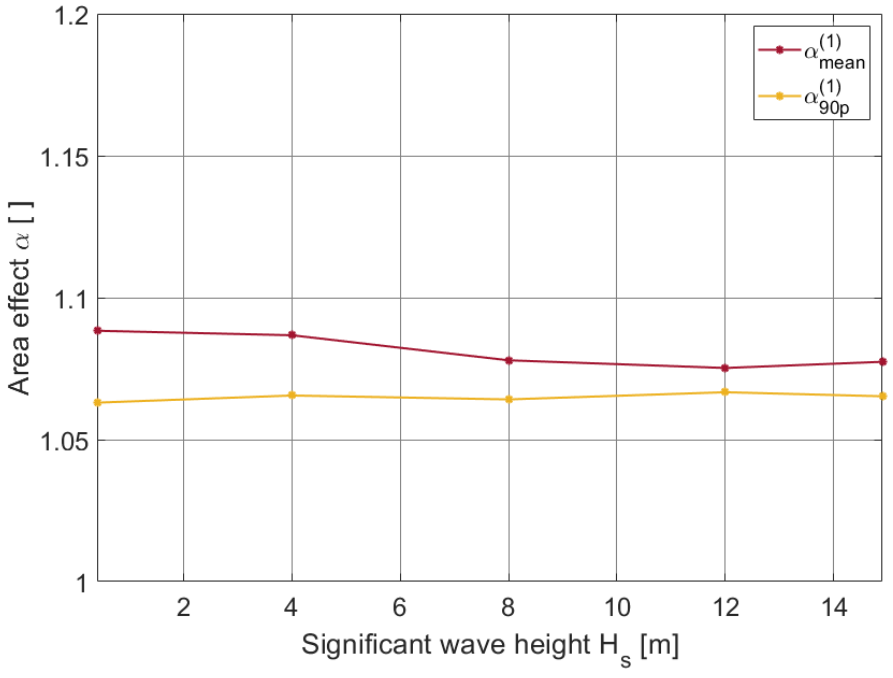

Figure 69: *Results from additional area effect analysis with variation in significant wave height.*

Table 54: *Parameters used in additional area effect analysis with variation in significant wave height.*

Parameter varied in analysis	**Value**
Significant wave height H_s [m]	0.40, 4.00, 8.00, 12.00, 14.90
Fixed parameters	**Value**
Spectral peak period T_p [s]	16.00
Wave spectrum cutoff frequency f_{max} [hz]	0.7304
Number of simulations for each variation in parameter N_{sim} [pcs]	200

9.3 Discussion

There seem to be no notable trend in the mean area crest height effect $\alpha^{(1)}_{mean}$ for the analyzed sea state when varying the significant wave height. Even though the variations in the significant wave height are large. The 90th percentile area crest height effect $\alpha^{(1)}_{90p}$ does not seem to have any notable trend either when the significant wave height varies. The 90th percentile area crest height effect is lower than the mean area crest height effect for five out of five variations in significant wave height. Since the analysis is performed with simulations using the JONSWAP spectrum, some biasness may be included in the results due to the large variations in the significant wave height.

When changing the significant wave height, the number of individual crests within the area boundaries will not change. Nor will the fraction of sampled crest heights with the actual top within the area boundaries. Therefore, variations in the significant wave height, without varying any other parameters, will not cause any changes in the area effect. This agrees well with the results obtained from the analysis. The large variations done for the significant wave heigh in this section does not seem to have any influence on the area effect. The results for the area effect are in accordance with the results presented in Teigland (2018).

9.4 Results from additional analysis with variation in spectral peak period

The results from the additional analysis of the area effect for crest heights with variation in spectral peak period are presented in this section. The area effect for crest heights has been analyzed for sea states within the boundaries of the contour line corresponding to a 10^{-2} annual probability of being exceeded at Statfjord oil field (Example Metocean Report (2003), figure 27). The analysis has been performed for an area of 40m*40m, and 200 Gaussian simulations using random amplitudes are done for each variation in spectral peak period. The parameters used in the simulations are given in table 56. The spectral peak period has been varied from the left side of the 100-year contour line to the right side of the 100-year contour line for a significant wave height of 4 meters. All other parameters have been held constant during the simulations. The results obtained from the analysis, along with the corresponding values used for the spectral peak period T_p are given in table 55 and figure 70. Both the mean area effect $\alpha^{(1)}_{mean}$ and the 90th percentile area effect $\alpha^{(1)}_{90p}$ are included in the results.

Table 55: *Results from additional area effect analysis with variation in spectral peak period.*

	T_p [s] 4.40	T_p [s] 9.00	T_p [s] 14.00	T_p [s] 19.00	T_p [s] 24.80
Mean area effect $\alpha^{(1)}_{mean}$ [ ]	1.2137	1.1567	1.1116	1.0760	1.0561
90th percentile area effect $\alpha^{(1)}_{90p}$ [ ]	1.2078	1.1435	1.1025	1.0704	1.0562

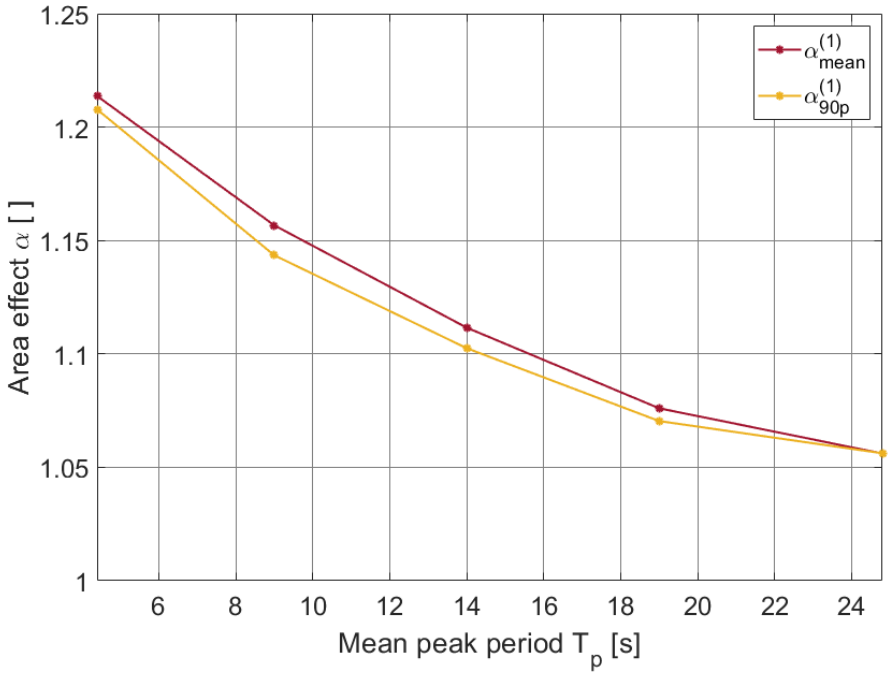

Figure 70: *Results from additional area effect analysis with variation in spectral peak period.*

Table 56: *Parameters used in additional area effect analysis with variation in spectral peak period.*

Parameter varied in analysis	**Value**
Spectral peak period T_p [s]	4.40, 9.00, 14.00, 19.00, 24.80
Fixed parameters	**Value**
Significant wave height H_s [m]	4.00
Wave spectrum cutoff frequency f_{max} [hz]	0.7304
Number of simulations for each variation in parameter N_{sim} [pcs]	200

9.5 Discussion

Both the mean area crest height effect $\alpha^{(1)}_{mean}$ and the 90th percentile area crest height effect $\alpha^{(1)}_{90p}$ have clear decreasing trends for the analyzed sea state when the spectral peak period increases. The 90th percentile area crest height effect is lower than the mean area crest height effect for four out of five variations in the spectral peak period. Since the analysis is performed with simulations using the JONSWAP spectrum, some biasness may be included in the results due to the large variations in the spectral peak period.

When reducing the spectral peak period, the number of individual crests within the area boundaries will increase. The fraction of sampled crest heights with the actual top within the area boundaries will also increase. Therefore, lowering the spectral peak period, without varying any other parameters, will cause an increase in the mean area effect. The large variations done in the spectral peak period clearly have a large influence on the area effect. The results for the mean area effect are in accordance with the results presented in Teigland (2018) and Forristall (2006).

9.6 Results from additional analysis of area maximum location

The results from the analysis of the locations of area crest heights are presented in this section. The locations of area crest heights has been analyzed for the worst three hour short crested sea state corresponding to a 10^{-2} annual probability of being exceeded at Statfjord oil field (Example Metocean Report (2003), table 3). The analysis has been performed for an area of 40m*40m, and 1000 Gaussian simulations using random amplitudes are done. The parameters used in the simulations are given in table 58. All parameters have been held constant during the simulations. The results obtained from the analysis are given in table 57, figure 71 and figure 72. Figure 71 shows positions where area maximum occurred and figure 72 shows number of area maximum at each position. The mean wave direction is along with the x-axis in the figures.

Table 57: *Results from additional area effect analysis of area maximum location.*

Results	**Value**
Percentage of area maximums at longitudinal edges (corners excluded) [%]	31.50
Percentage of area maximums at transverse edges (corners excluded) [%]	16.50
Percentage of area maximums at corners [%]	18.10
Percentage of area maximums at all edges (corners included) [%]	66.10
Percentage of area maximums inside all edges [%]	33.90
Percentage of area maximums at center point [%]	0.00

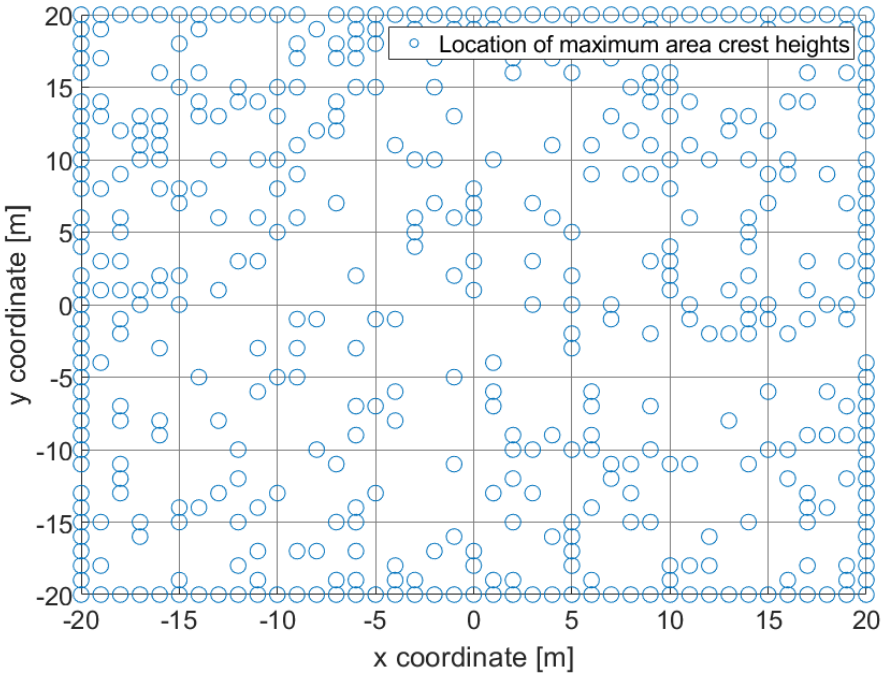

Figure 71: *Positions where area maximum occurred during 1000 simulations. Some of the locations have multiple occurrences of area maximum.*

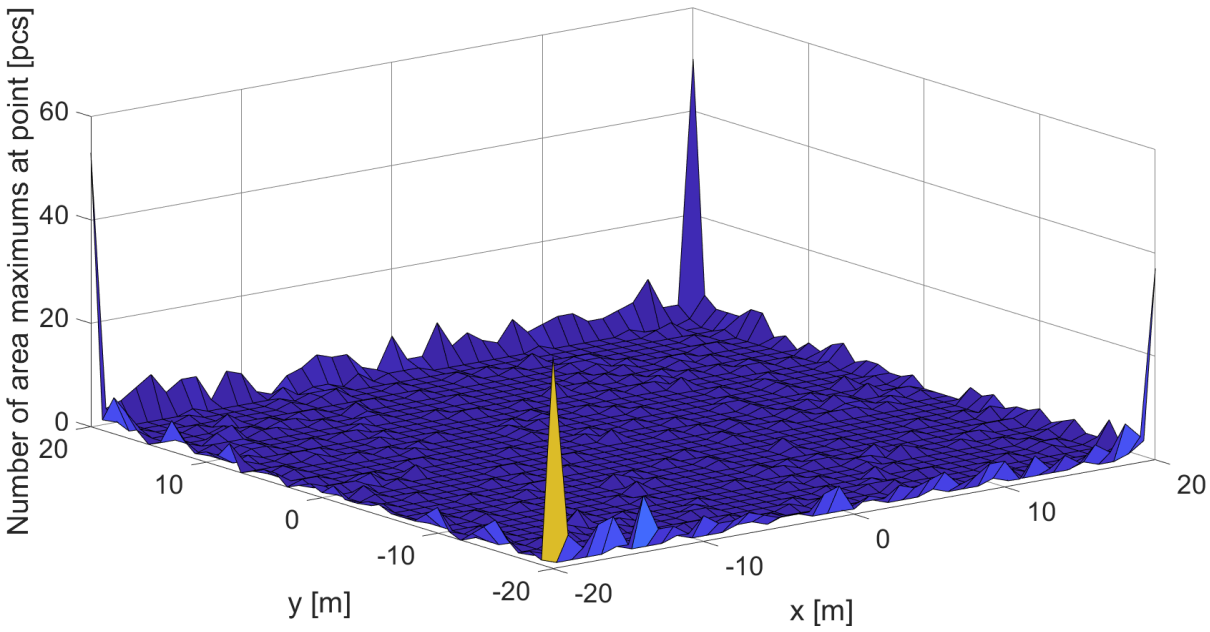

Figure 72: *Number of area maximums at each position during 1000 simulations.*

Table 58: *Parameters used in additional analysis for location of area extreme location*

Parameters	**Value**
Significant wave height H_s [m]	14.90
Spectral peak period T_p [s]	16.00
Wave spectrum cutoff frequency f_{max} [hz]	0.3652
Number of simulations N_{sim} [pcs]	1000

All simulations are run on the same parameters. The area grid size used in the simulations are 5m*5m. Due to the high resolution maximum procedure when finding maximums, as explained in section 2.6.5 for area maximums, the final grid size for the area maximums is 1m*1m. This gives a total of 1681 points of possible area maximum occurrence. 160 of these point lie on the area edge, and four of these points lie in the corners of the area.

9.7 Discussion

It is seen from the results that area maximums clearly happens more frequently on the area edges, and specially at the area corners, than inside the area boundaries, in spite of the low number of boundary points of possible occurrence. Forristall (2006) states that for areas with side lengths smaller than one wave length, which is the case for this analysis, it is likely that the real maximum of a wave crest is outside the area boundaries. The sampled area maximums are then likely to happen on the area edges. This seem to agree well with the results obtained from this analysis for the 40m*40m square area.

10 Additional discussion

The results for the mean area effect shows stable values at a simulation number of 200, and agrees well with the different referenced literature. The results for the 90th percentile area effect includes a lot of variance at a simulation number of 200, and does in many cases not give a clear indication of the behavior of the area effect. However, the results for the 90th percentile area effect does indicate that the area effect is smaller at a 90th percentile level than when calculated as a mean. Hagen et al. (2018) showed that the value for the 90th percentile area effect value is smaller than the most probable maximum value for a 100 year design sea state. In this thesis, the mean area effect is given in the results and not the area effect for the most probable maximum. However, both the results presented in this thesis, and the results presented in Hagen et al. (2018) does indicate that the area effect is smaller at high percentile values. This is important, since the higher percentile values such as the 90th percentile value are commonly the value of interest when estimating extremes.

The current design practices include the use of point maximums and safety margins for airgap assessments. Another possible approach could be to use the area maximums in combinations with a smaller safety margin. Even though wave impacts can occur due to the area effect, critical structural damage may not be the case. The area of impact will probably not be very large from a crest height larger than the point maximum crest height when a safety margin is applied for the airgap. Platforms like jackets or jack-ups of are build to withstand some wave impact to the underside of the deck structure without suffering critical structural damage.

11 Conclusions

The results clearly indicates that the area effect is an important factor to consider when predicting crest maximums for any area larger than a point. The difference between area maximums and point maximums obtained from simulations are large, even for areas small in size.

The comparison analysis for the long crested extreme sea state using Gaussian and second order simulations showed that both the values obtained for the mean area effect and the mean area effect from 75th percentile value to the 100th percentile from Gaussian simulations exceeded the equivalent values obtained from second order simulations. This was the case both for the one hour simulations and for the three hour simulations. Any firm conclusions cannot be drawn based on the low total number of simulations performed. The outcome of the results may be a case of statistical deviations. A considerable larger number of simulations is needed for a firm conclusion to be drawn.

For the short crested extreme sea state analyzed, variations in the significant wave height and variations in the incoming wave directions without variations in any other parameters do not seem to affect the area effect for crest heights. Variations in the spectral peak period, variations in the directional spectrum shape factor, variations in the sea state duration and variations in the area size without variations in any other parameters clearly have influence on the magnitude of the mean area effect. Reductions in the spectral peak period and reductions in the directional spectrum shape factor increases the area effect. The area effect lowers as the sea state duration increases. Increasing the area size increases the area effect. The results for the 90th percentile area effect appears to be smaller than the mean area effect.

The analysis for the locations of the area maximum showed, for the analyzed sea state and area, that area maximums are more likely to occur along the edges of the area, and especially at the area corners, than within the area boundaries.

It has to be stressed that all results produced in this thesis are based on Gaussian and second order simulations using the JONSWAP wave spectrum. The metocean data used for a specific location in the North Sea that is no longer valid. All simulations are also done based on the deep water assumption. The results are not directly transferable to any other sea states or locations. The results produced are only meant to give a general overview of the area effect for crest heights, and to locate any trends regarding the area effect for crest heights. The general trends of the results are highly probable to give resemblance to a wide variety of sea states at different locations. In a real design situation for any location, new simulations should to be done, using correct metocean data. The validity of the simulations should also be confirmed with the use of other methods such as wave basin tests or actual wave measurements.

12 Further work

In this thesis work, Gaussian simulations are used for all analyses including short crested sea states. It would be interesting to see how the presented results for the area effect for the short crested extreme sea state would compare to results for the area effect from second order simulations. A possible shortcut for doing this would be to implement second order simulations only for the high resolution procedure, and still run Gaussian simulation for the initial simulations. The results produced are then not expected to be equivalent to the results from a full second order analysis, but merely an approximation of these. More extensive simulations are easily doable with heavier computational power.

It would also be interesting to do a more extensive study with an increase in the number of simulation for each variations in parameter, and in this way produce much more stable results for the 90th percentile area effect. The number of simulations for each variation in parameter should probably be in exceedance of 1000 to obtain stable results for the 90th percentile area effect. The 90th percentile value is normally the value of interest in a sea state with an annual exceedance probability of 10^{-2}. If the mean area effect is used to estimate the 90th percentile maximum area crest height from a 90th percentile maximum point crest height, the obtained value for the maximum area crest height is expected to be on the high side. Heavier computational power is also preferred for this.

Another matter interesting for further work, would be to look at the locations of the maximum crest heights within the area at the 90th percentile level. Since the area effect has shown to be different when calculated as the mean, and when calculated at the 90th percentile level, it can not be ruled out that the locations of the maximums also could be different.

The impact area size of possible wave impacts due to the area effect, along with analysis of possible structural damage due to area maximums hitting the deck structure are also topics for further investigation.

References

Example Metocean Report (2003). *Example Metocean Report*. Statoil, Kenneth J. Eik and Einar Nygaard, 2 edition.

Faltinsen, O. (1993). *Sea Loads on Ships and Offshore Structures Volume 1 of Cambridge Ocean Technology Series, ISSN 1746-224X Ocean Technology Sea Loads on Ships and Offshore Structures, O. M. Faltinsen*. Cambridge University Press, 1993, illustrated, reprint edition.

Forristall, G. (2006). Maximum crest heights over an area and the air gap problem. volume 2006.

Forristall, G. (2011). Maximum crest heights under a model tlp deck.

Forristall, G. (2015). Omae2015-41061 maximum crest heights over an area: Laboratory measurements compared to theory.

Forristall, G. Z. (2000). Wave crest distributions: Observations and second-order theory. *Journal of Physical Oceanography*, 30(8):1931–1943.

Greco, M. (2012). *TMR 4215: Sea Loads, Lecture Notes*.

Gunnar Lian, S. H. (2015). Measured crest height distribution compared to second order distribution. *14th International Workshop on Wave Hindcasting and Forecasting. Key West, Florida, USA, Nov 8-13, 2015*.

Hagen, i., Birknes-Berg, J., Hy Grue, I., Lian, G., Bruserud, K., and Vestbstad, T. (2018). Long-term area statistics for maximum crest height under a fixed platform deck.

Hasselmann, K., P. Barnett, T., Bouws, E., Carlson, H., E. Cartwright, D., Enke, K., A Ewing, J., Gienapp, H., E. Hasselmann, D., Kruseman, P., Meerburg, A., Muller, P., Olbers, D., Richter, K., Sell, W., and Walden, H. (1973). Measurements of wind-wave growth and swell decay during the joint north sea wave project (jonswap). *Deut. Hydrogr. Z.*, 8:1–95.

Haver, S. K. (2017). *Metocean Modelling and Predictions of Extremes*.

Knut Minsaas, H. T. W. (2004). *Kompendium TMR 4180 Marin dynamikk*. Department of marine technology NTNU.

Kvingedal, B., Bruserud, K., and Nygaard, E. (2018). Individual wave height and wave crest distributions based on field measurements from the northern north sea. *Ocean Dynamics*, 68(12):1727–1738.

Longuet-Higgins, M. (1952). On the statistical distribution of the height of sea waves. *J. Marine Res.*, 11:245–266.

Longuet-Higgins, M. S. (1963). The effect of non-linearities on statistical distributions in the theory of sea waves. *Journal of Fluid Mechanics*, 17(3):459480.

Lundberg, N. H. (2019). https://snl.no/statfjord.

Myrhaug, D. (2005). *TMR4235 Stochastic theory of sealoads*. Department of marine technology NTNU.

NORSOK STANDARD N-003 (2007). *NORSOK STANDARD N-003 Actions and action effects, Edition 2*. Standards Norway.

Pettersen, H. (2016). https://www.equinor.com/en/news/statfjord-passing-5-billion-barrels.html.

RP-C205, D. (2010). *Recomended Practice DNV RP-C205 Environmental Conditions and Environmental Loads*.

Stansberg, C. and Gudmestad, O. (Tue Dec 31 00:00:00 EST 1996). Non-linear random wave kinematics models verified against measurements in steep waves.

Stansberg, C., Gudmestad, O., and Haver, S. (2008). Kinematics under extreme waves. *Journal of Offshore Mechanics and Arctic Engineering-transactions of The Asme - J OFFSHORE MECH ARCTIC ENG*, 130.

Teigland, H. (2018). Extreme waves area effect - summer internship 2018 report (censored edition).

Torsethaugen, K. (1993). Two peak wave spectrum model. *Proceedings of the International Conference on Offshore Mechanics and Arctic Engineering - OMAE*, 2:175–180.

Tucker, M., Challenor, P., and Carter, D. (1984). Numerical simulation of a random sea: a common error and its effect upon wave group statistics. *Applied Ocean Research*, 6:118–122.

A Appendix: Maximum crest heights from analysis of area effect with variation in parameters

A.1 About appendix A

Appendix A contains the area and point maximum crest heights which forms the basis for the results in section 8. Maximum crest heights obtained for variations of the different parameters are given in separate sections below.

A.2 Maximum crest heights from analysis with variation in significant wave height

The maximum crest heights presented in this section corresponds to the results presented in section 8.2.

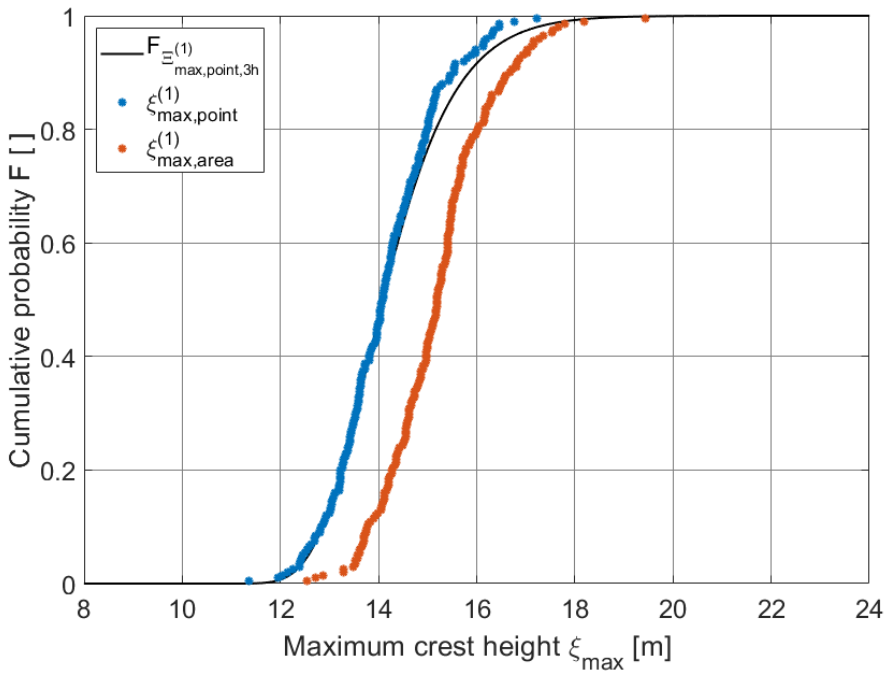

Figure A.1: *Area and point maximum crest heights from simulations with H_s = 14.90 m, along with Gaussian extreme value distribution.*

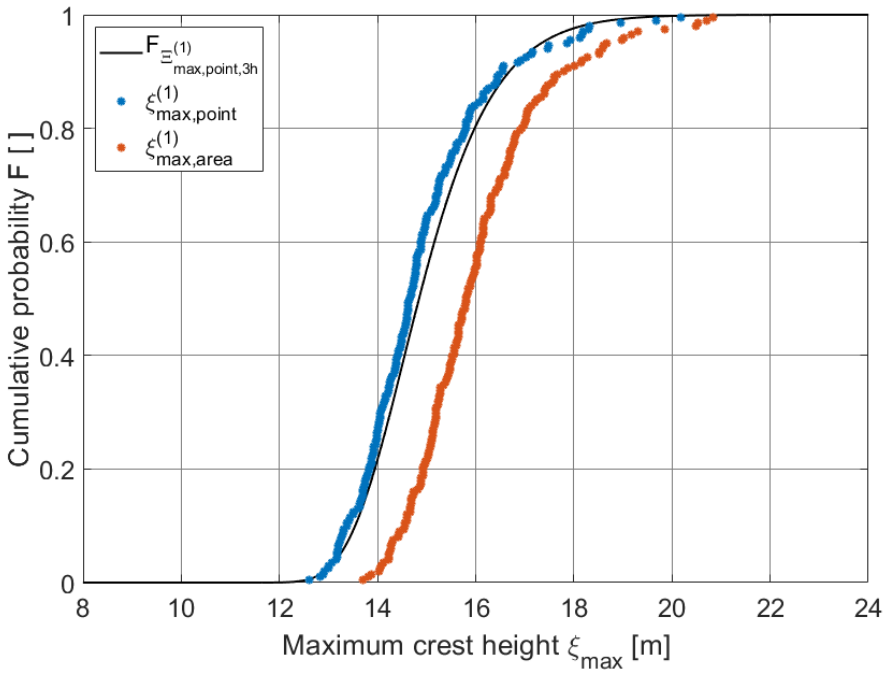

Figure A.2: *Area and point maximum crest heights from simulations with H_s = 15.70 m, along with Gaussian extreme value distribution.*

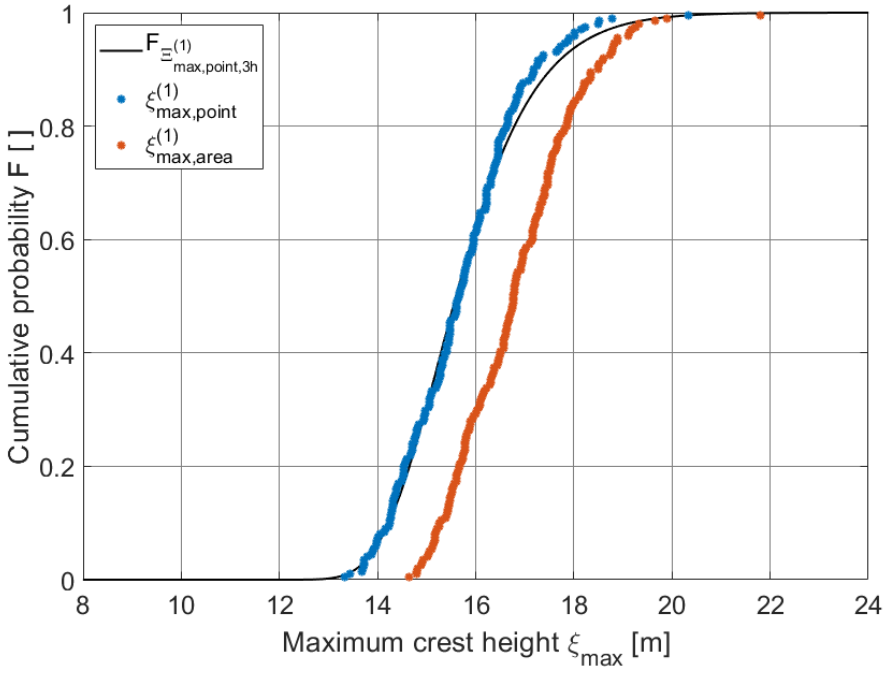

Figure A.3: *Area and point maximum crest heights from simulations with H_s = 16.50 m, along with Gaussian extreme value distribution.*

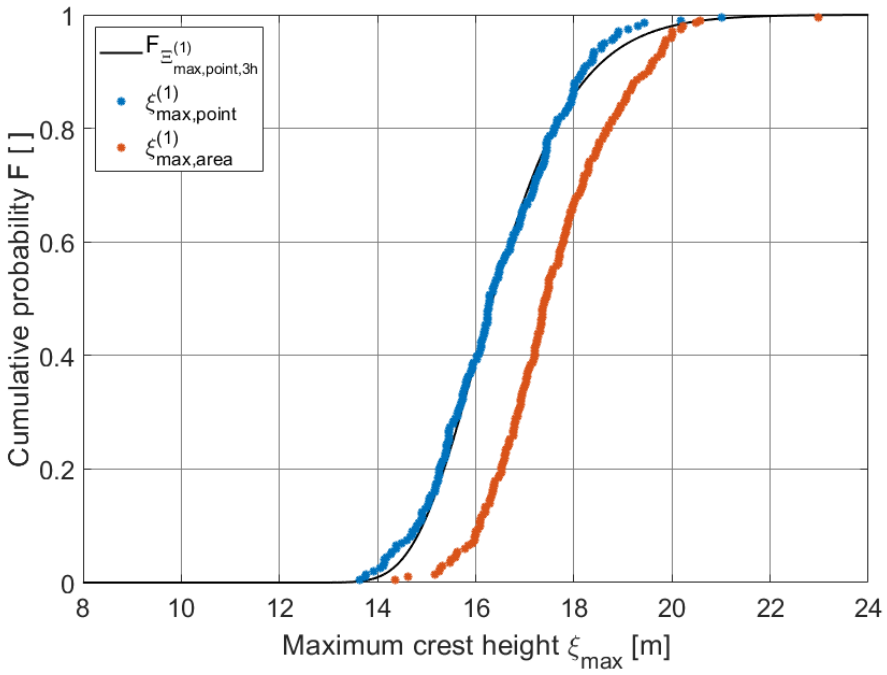

Figure A.4: *Area and point maximum crest heights from simulations with H_s = 17.30 m, along with Gaussian extreme value distribution.*

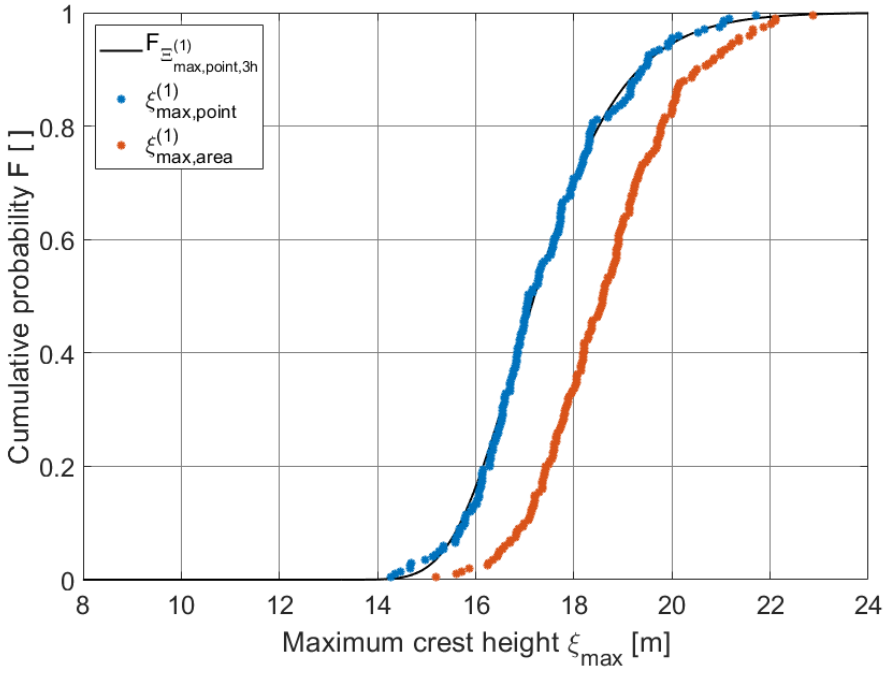

Figure A.5: *Area and point maximum crest heights from simulations with H_s = 18.20 m, along with Gaussian extreme value distribution.*

A.3 Maximum crest heights from analysis with variation in spectral peak period

The maximum crest heights presented in this section corresponds to the results presented in section 8.4.

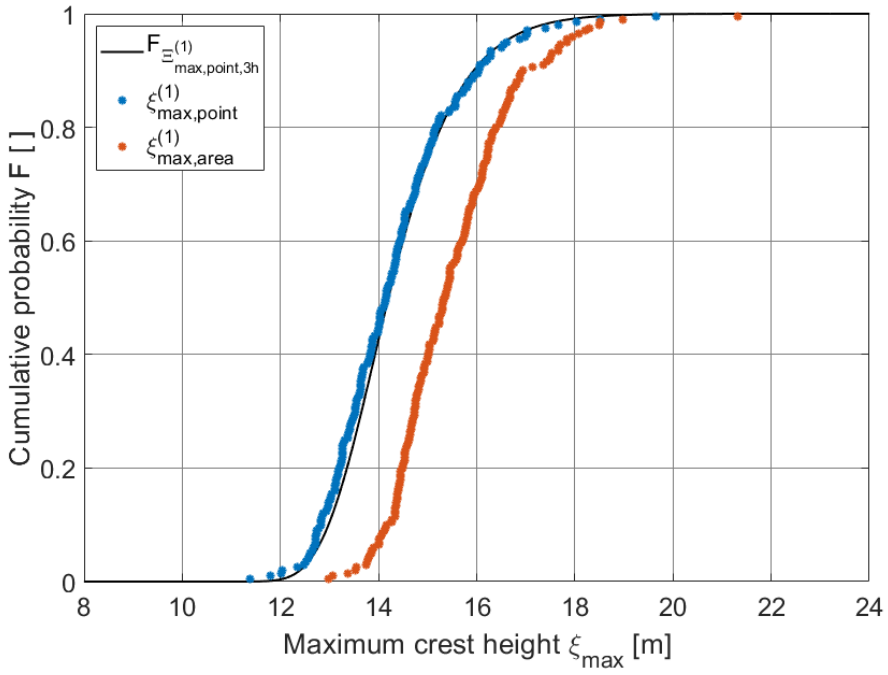

Figure A.6: *Area and point maximum crest heights from simulations with T_p = 14.00 s, along with Gaussian extreme value distribution.*

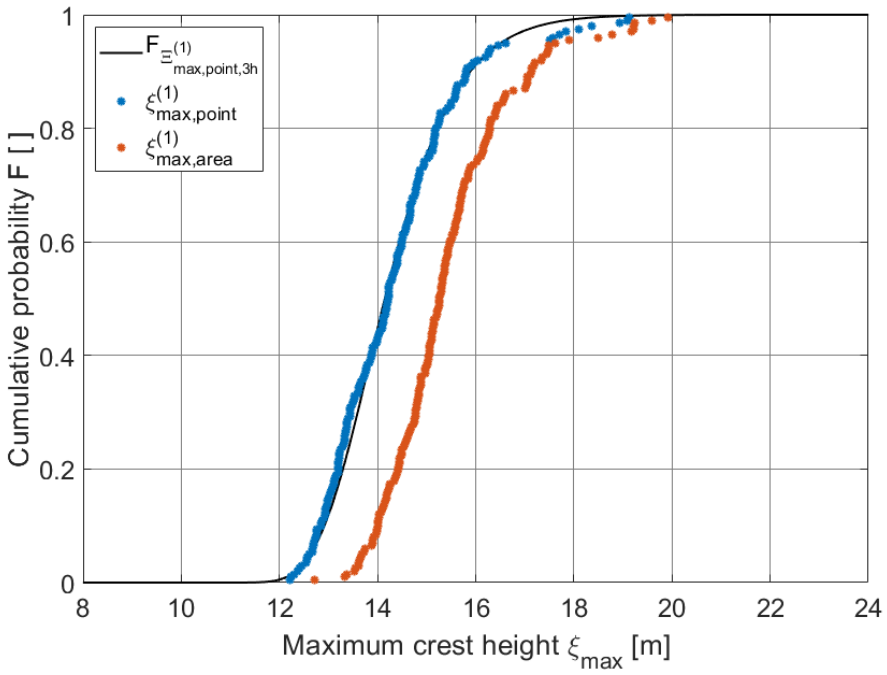

Figure A.7: *Area and point maximum crest heights from simulations with T_p = 15.00 s, along with Gaussian extreme value distribution.*

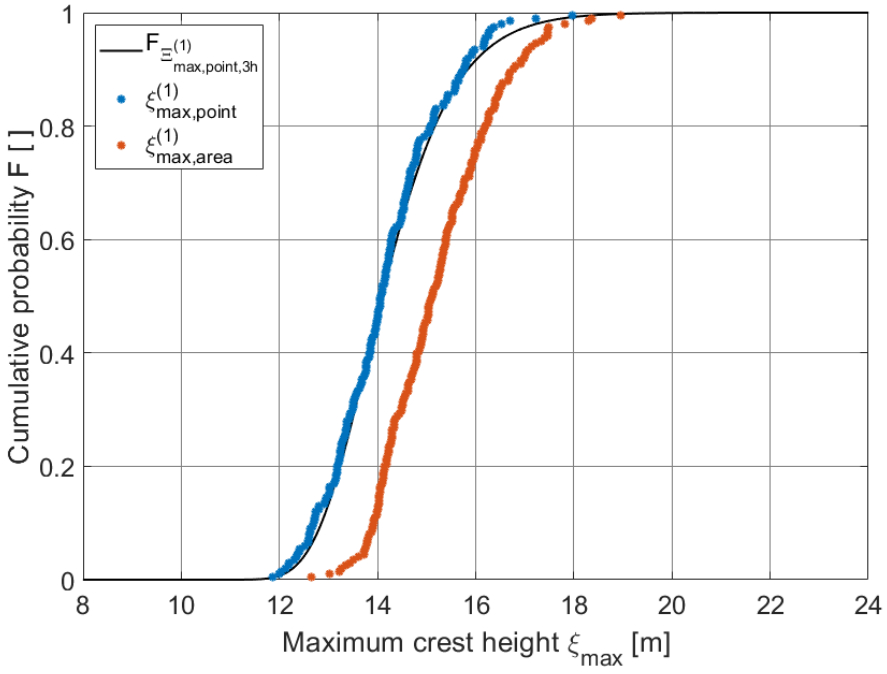

Figure A.8: *Area and point maximum crest heights from simulations with T_p = 16.00 s, along with Gaussian extreme value distribution.*

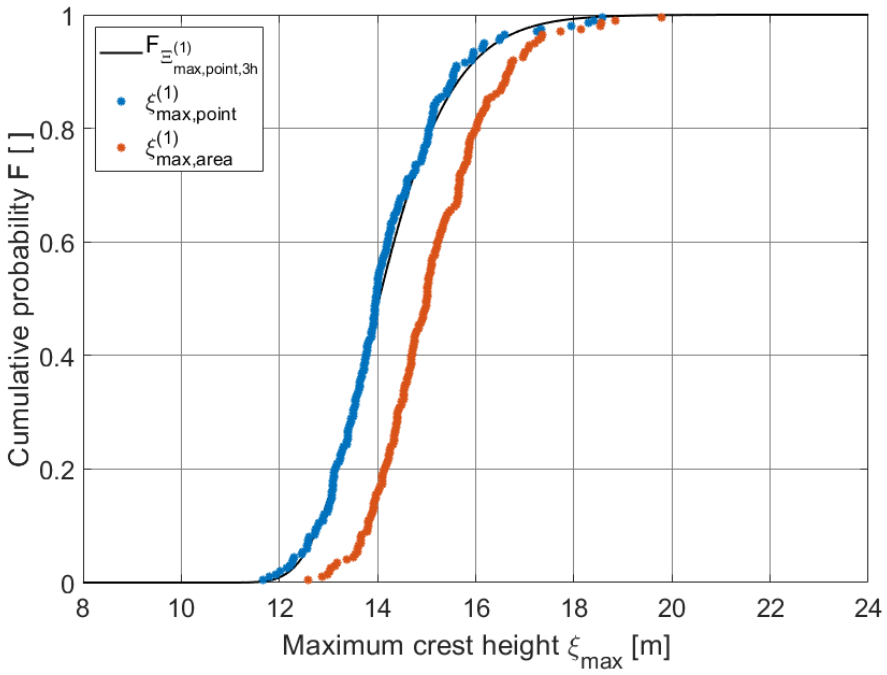

Figure A.9: *Area and point maximum crest heights from simulations with T_p = 17.10 s, along with Gaussian extreme value distribution.*

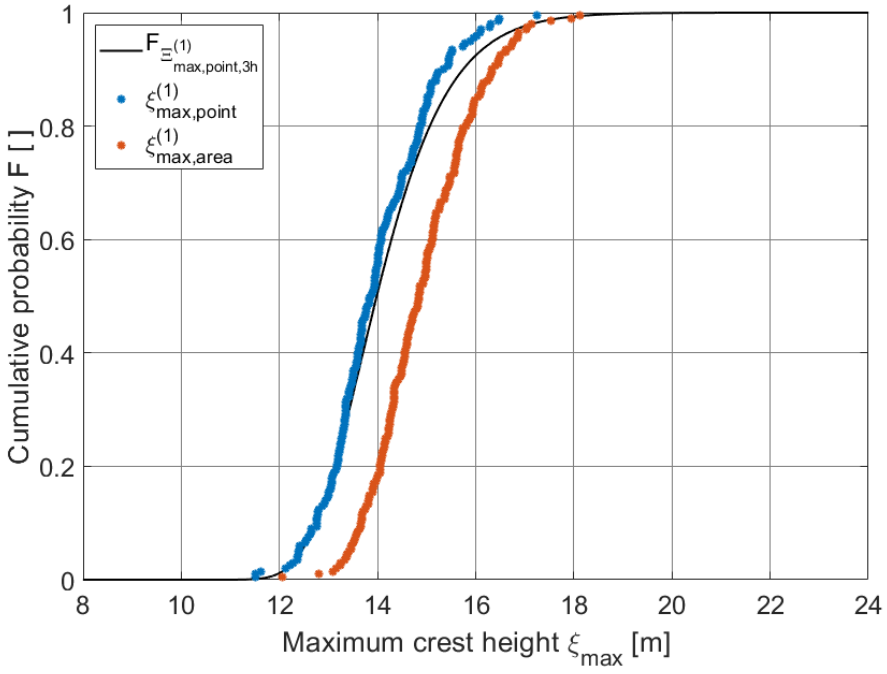

Figure A.10: *Area and point maximum crest heights from simulations with T_p = 18.20 s, along with Gaussian extreme value distribution.*

A.4 Maximum crest heights from analysis with variation in directional spectrum shape factor

The maximum crest heights presented in this section corresponds to the results presented in section 8.6.

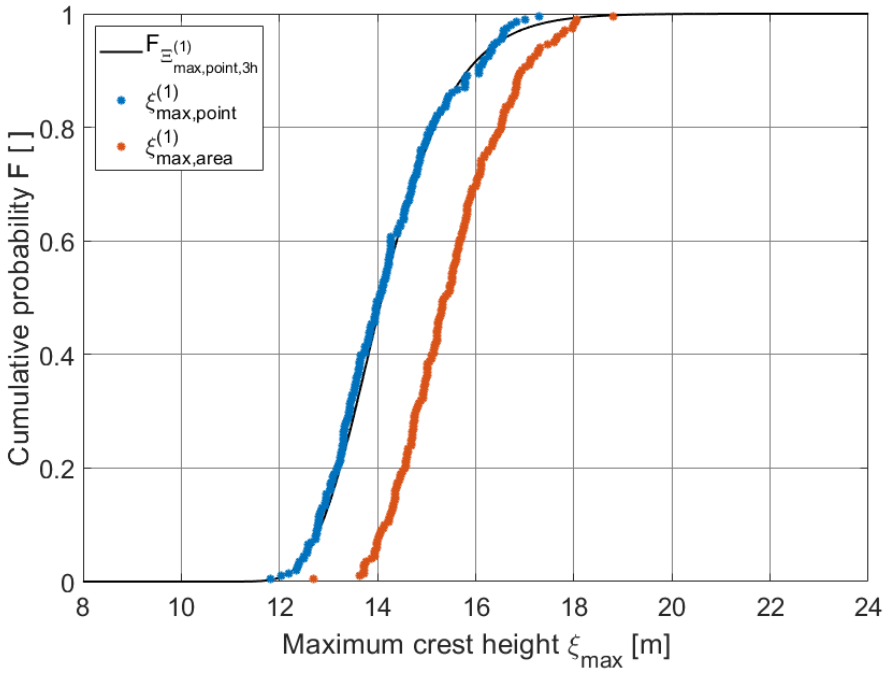

Figure A.11: *Area and point maximum crest heights from simulations with n_d = 2.00, along with Gaussian extreme value distribution.*

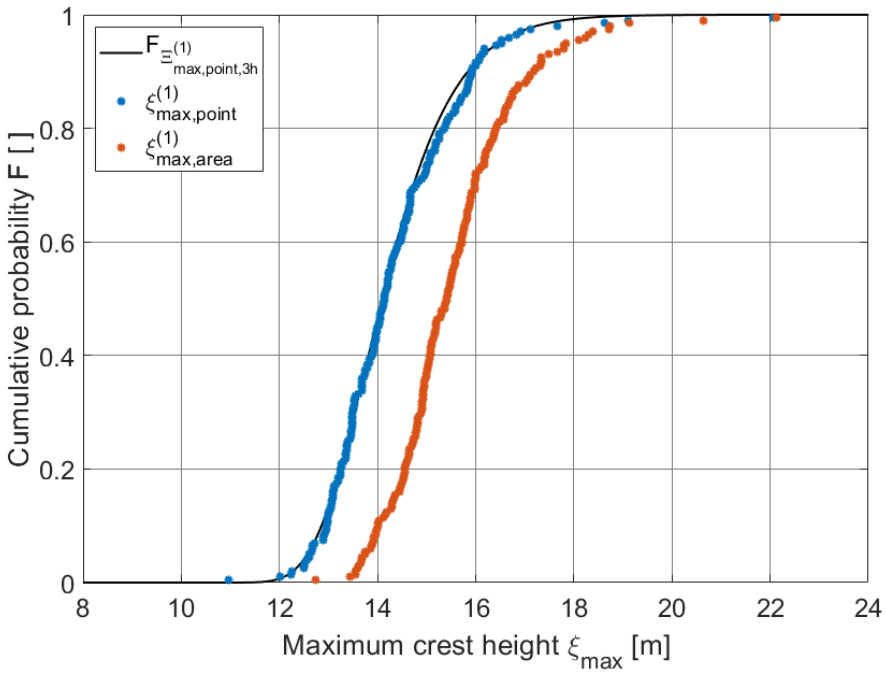

Figure A.12: *Area and point maximum crest heights from simulations with $n_d = 4.00$, along with Gaussian extreme value distribution.*

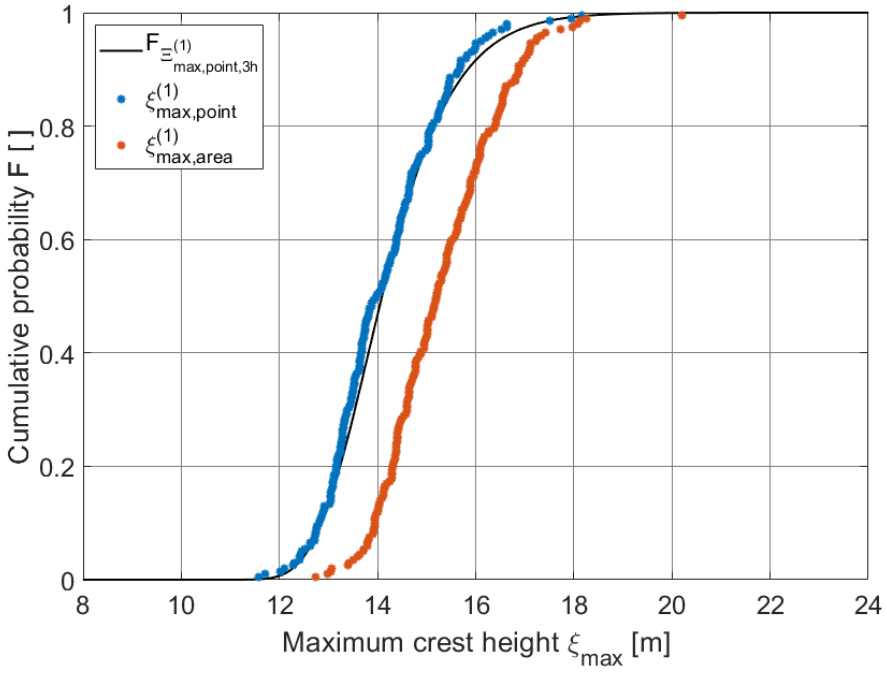

Figure A.13: *Area and point maximum crest heights from simulations with $n_d = 6.00$, along with Gaussian extreme value distribution.*

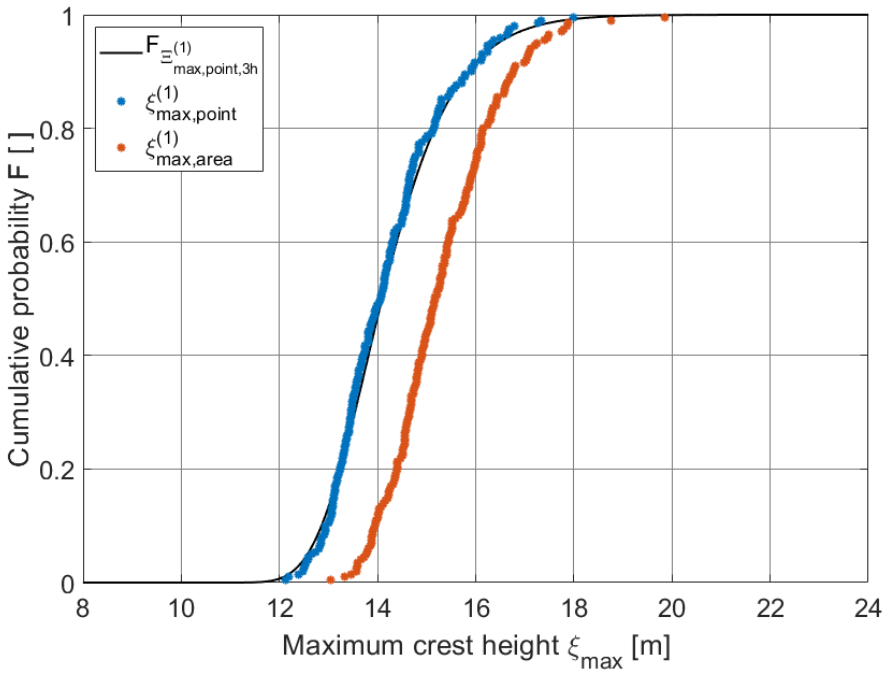

Figure A.14: *Area and point maximum crest heights from simulations with n_d = 8.00, along with Gaussian extreme value distribution.*

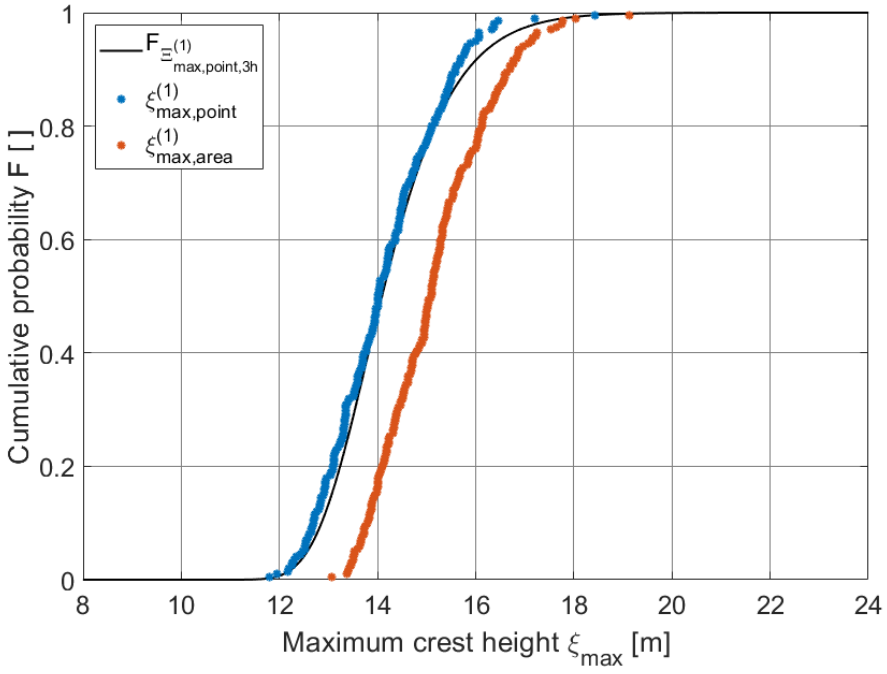

Figure A.15: *Area and point maximum crest heights from simulations with n_d = 10.00, along with Gaussian extreme value distribution.*

A.5 Maximum crest heights from analysis with variation in mean wave direction

The maximum crest heights presented in this section corresponds to the results presented in section 8.8.

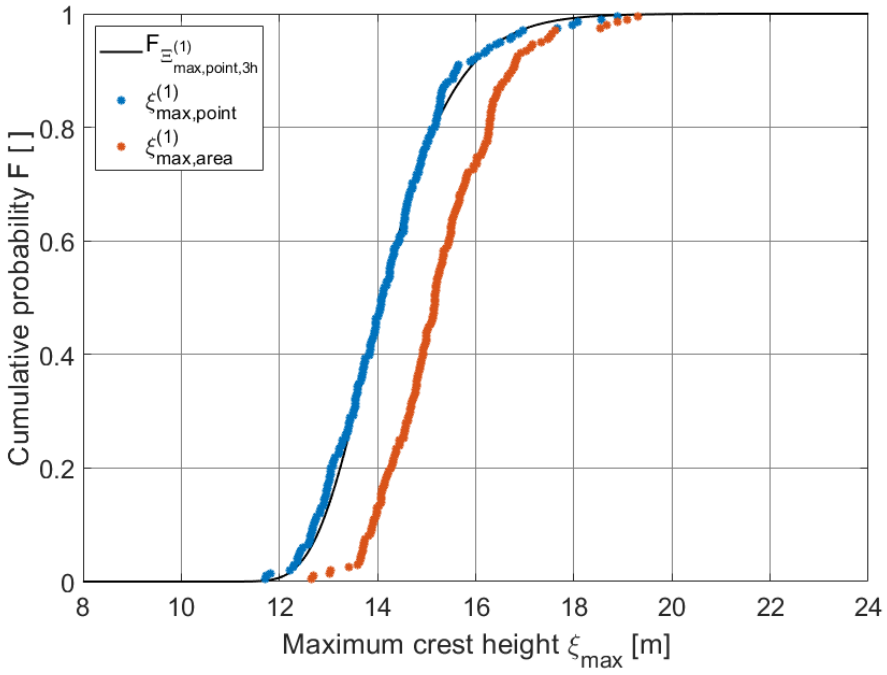

Figure A.16: *Area and point maximum crest heights from simulations with $\theta_0 = 0.00$ degrees, along with Gaussian extreme value distribution.*

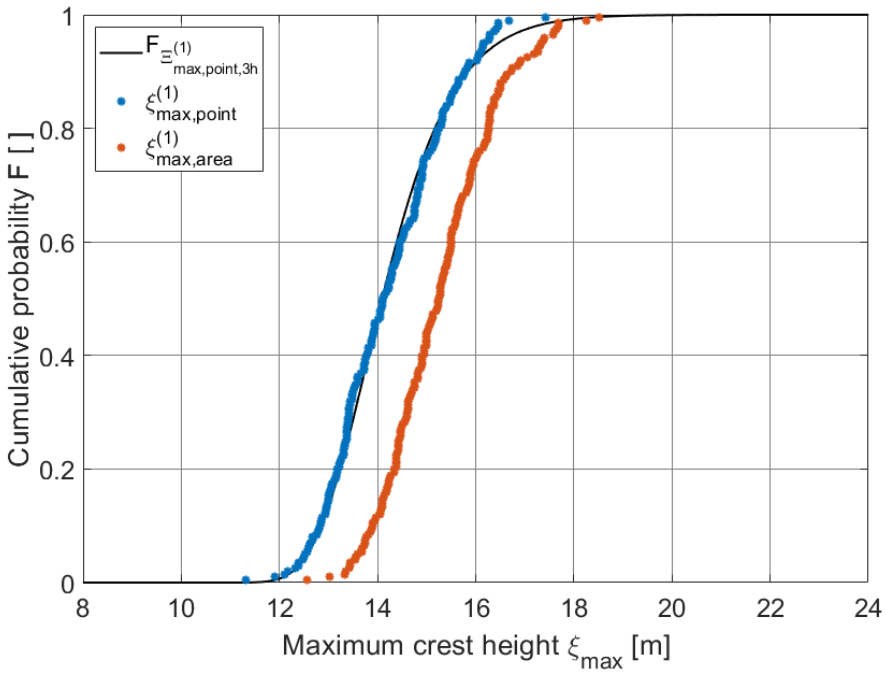

Figure A.17: *Area and point maximum crest heights from simulations with $\theta_0 = 11.25$ degrees, along with Gaussian extreme value distribution.*

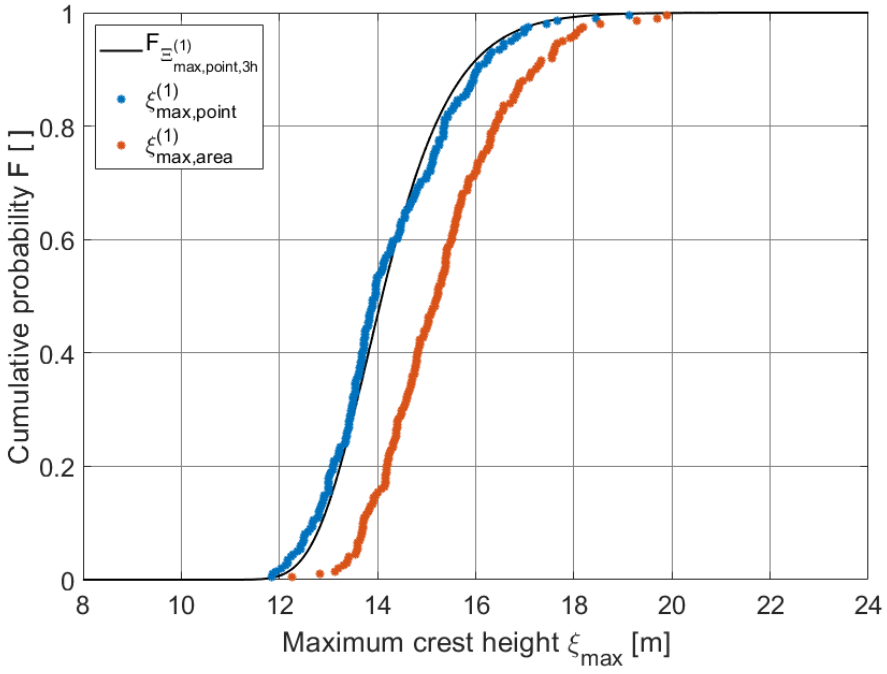

Figure A.18: *Area and point maximum crest heights from simulations with $\theta_0 = 22.50$ degrees, along with Gaussian extreme value distribution.*

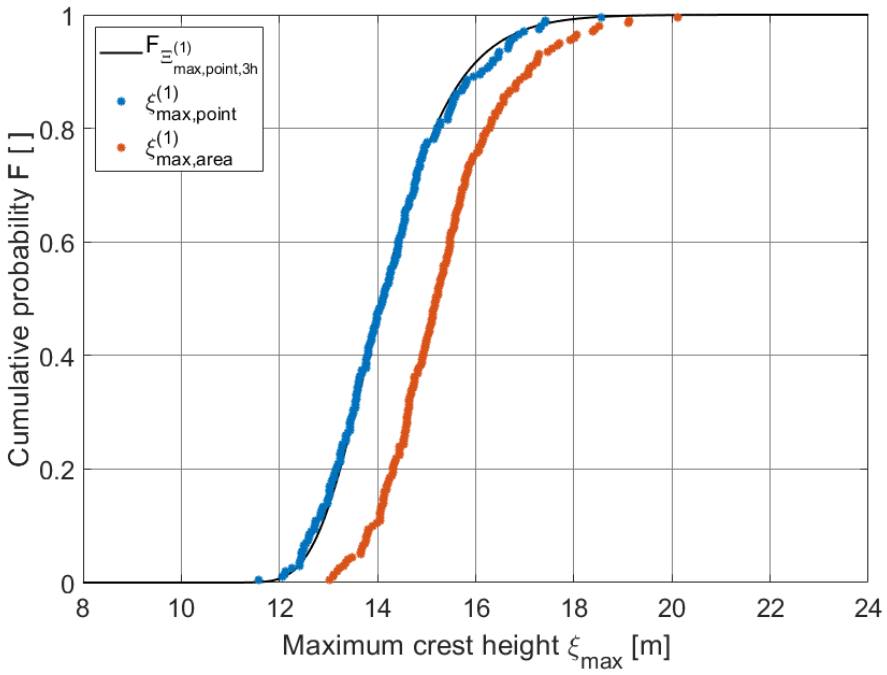

Figure A.19: *Area and point maximum crest heights from simulations with $\theta_0 = 33.75$ degrees, along with Gaussian extreme value distribution.*

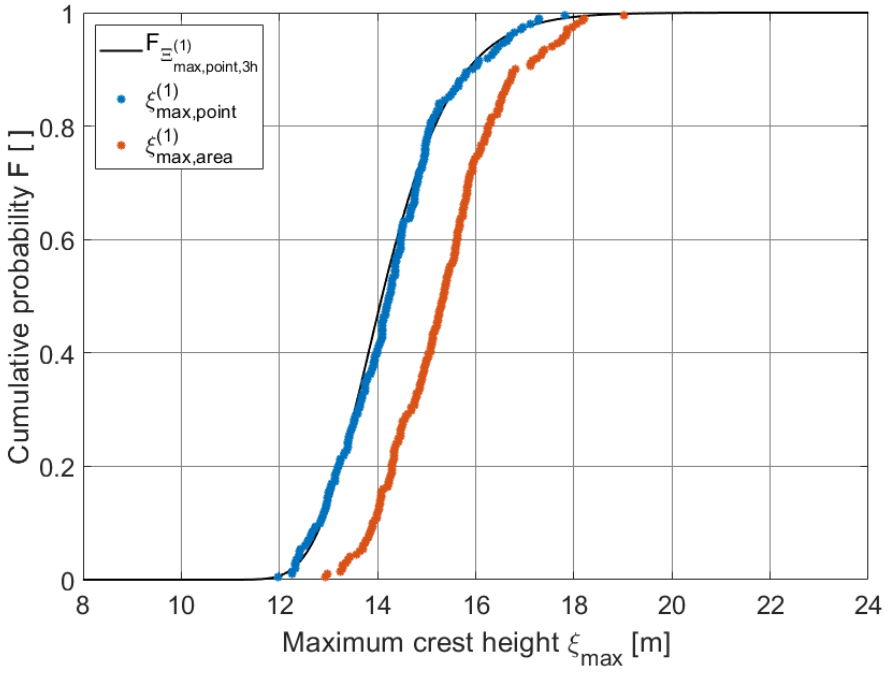

Figure A.20: *Area and point maximum crest heights from simulations with $\theta_0 = 45.00$ degrees, along with Gaussian extreme value distribution.*

A.6 Maximum crest heights from analysis with variation in simulation duration

The maximum crest heights presented in this section corresponds to the results presented in section 8.10.

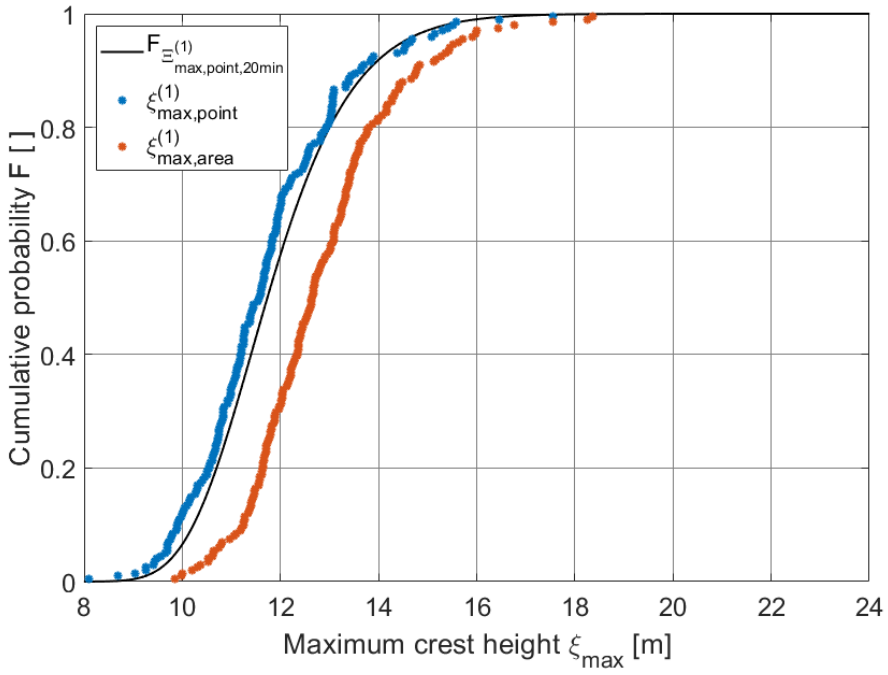

Figure A.21: *Area and point maximum crest heights from simulations with t = 1*1200 s, along with Gaussian extreme value distribution.*

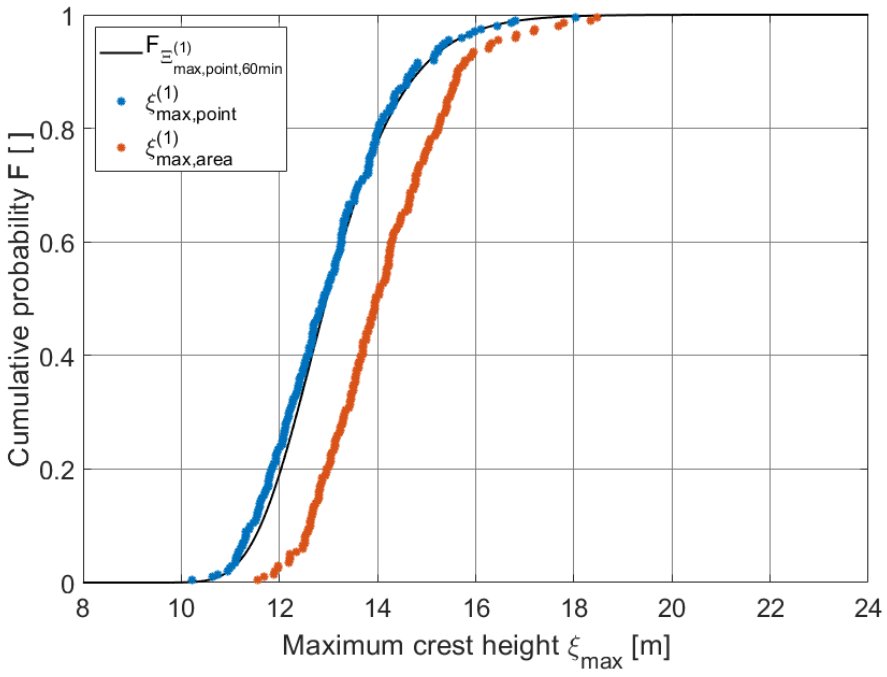

Figure A.22: *Area and point maximum crest heights from simulations with t = 3*1200 s, along with Gaussian extreme value distribution.*

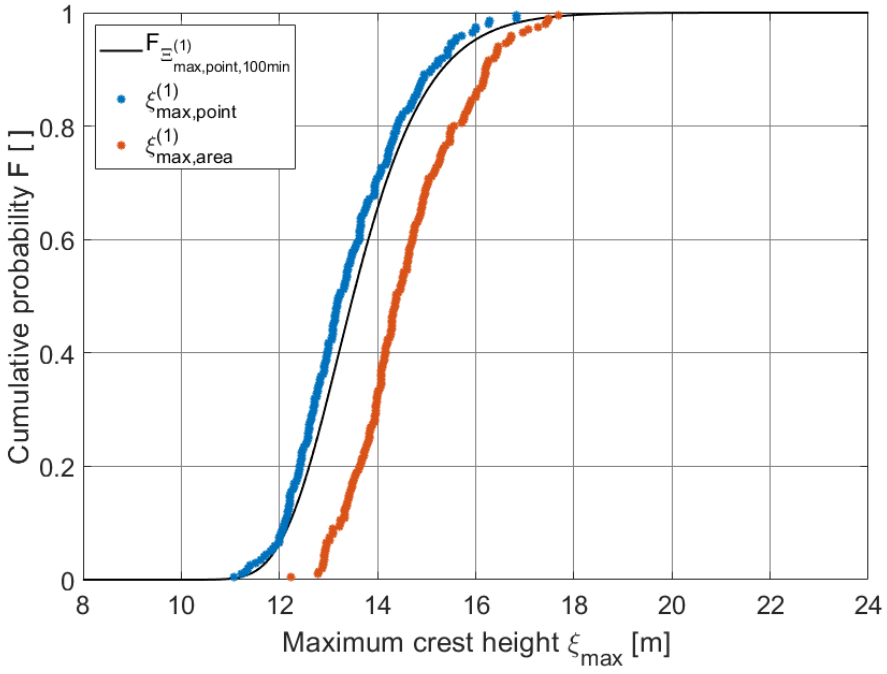

Figure A.23: *Area and point maximum crest heights from simulations with t = 5*1200 s, along with Gaussian extreme value distribution.*

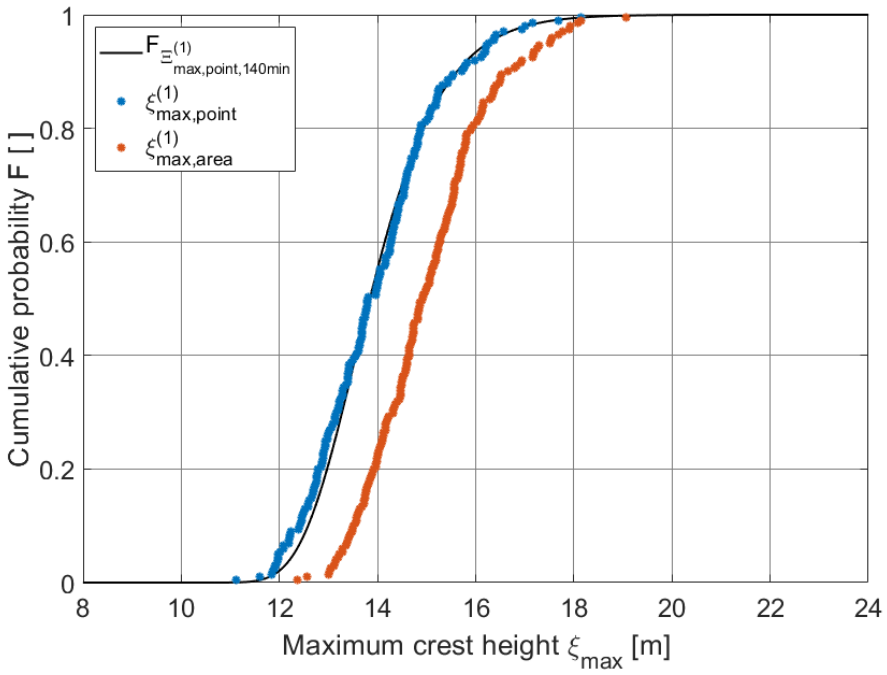

Figure A.24: *Area and point maximum crest heights from simulations with t = 7*1200 s, along with Gaussian extreme value distribution.*

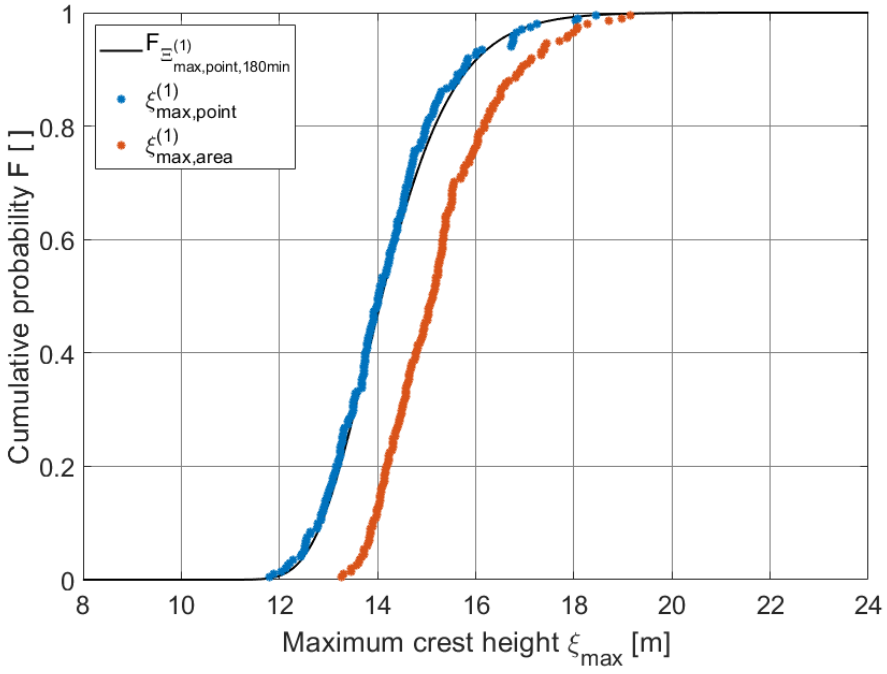

Figure A.25: *Area and point maximum crest heights from simulations with t = 9*1200 s, along with Gaussian extreme value distribution.*

A.7 Maximum crest heights from analysis with variation in square area size

The maximum crest heights presented in this section corresponds to the results presented in section 8.12.

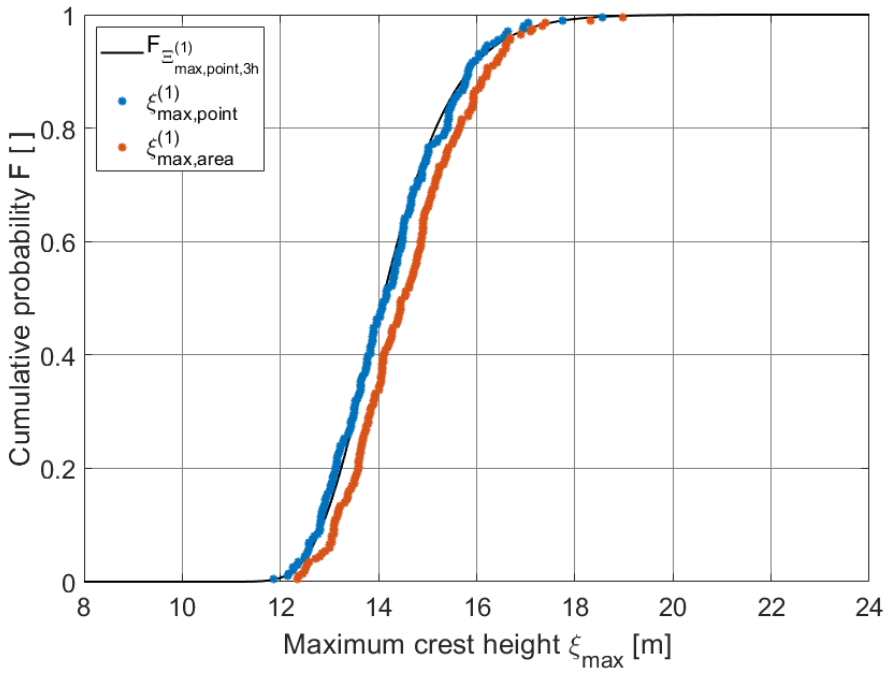

Figure A.26: *Area and point maximum crest heights from simulations with $dx, dy = 10$ m, along with Gaussian extreme value distribution.*

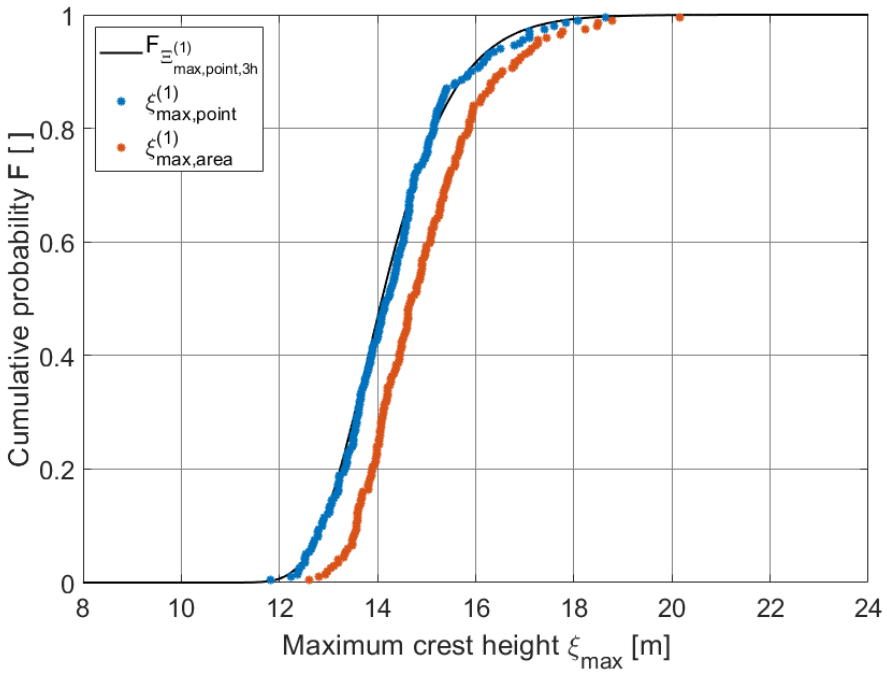

Figure A.27: *Area and point maximum crest heights from simulations with $dx, dy = 20$ m, along with Gaussian extreme value distribution.*

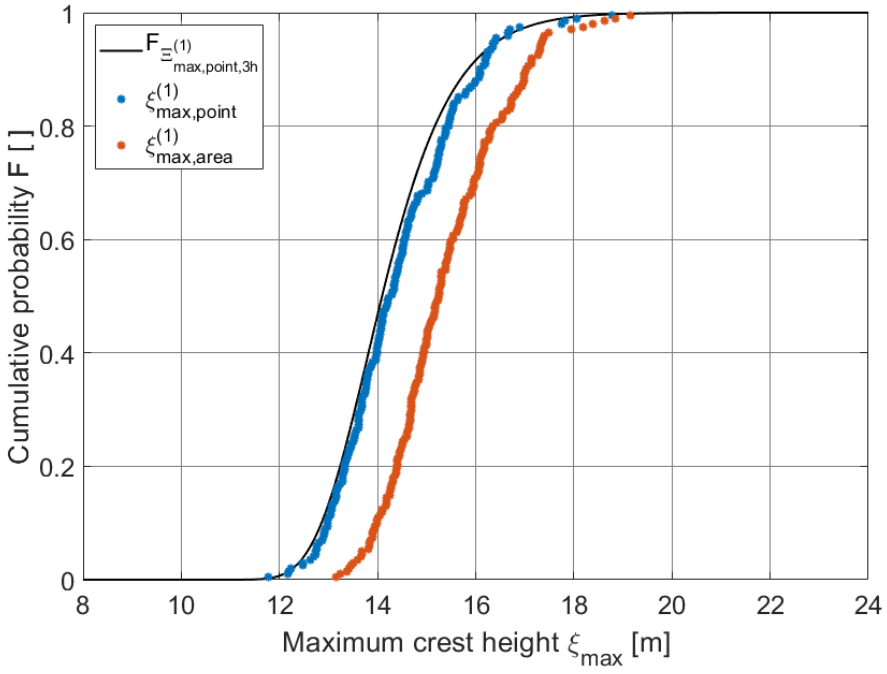

Figure A.28: *Area and point maximum crest heights from simulations with $dx, dy = 40$ m, along with Gaussian extreme value distribution.*

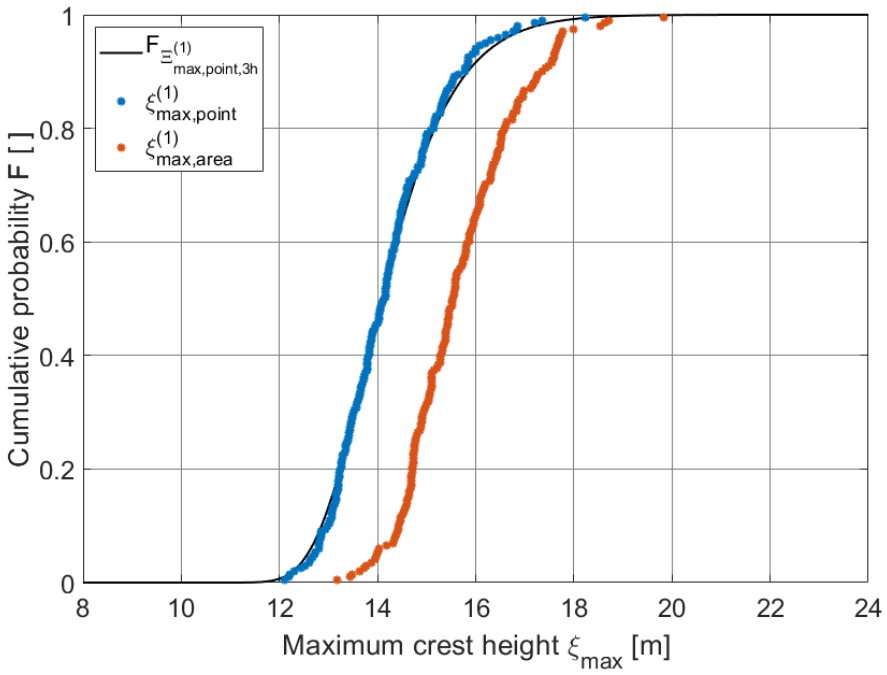

Figure A.29: *Area and point maximum crest heights from simulations with $dx, dy = 60$ m, along with Gaussian extreme value distribution.*

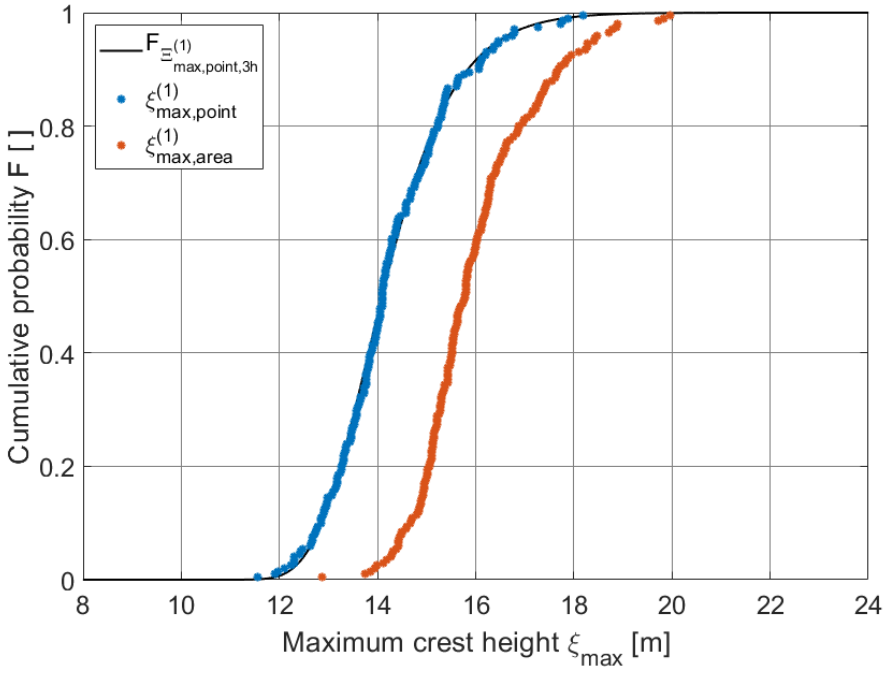

Figure A.30: *Area and point maximum crest heights from simulations with $dx, dy = 80$ m, along with Gaussian extreme value distribution.*

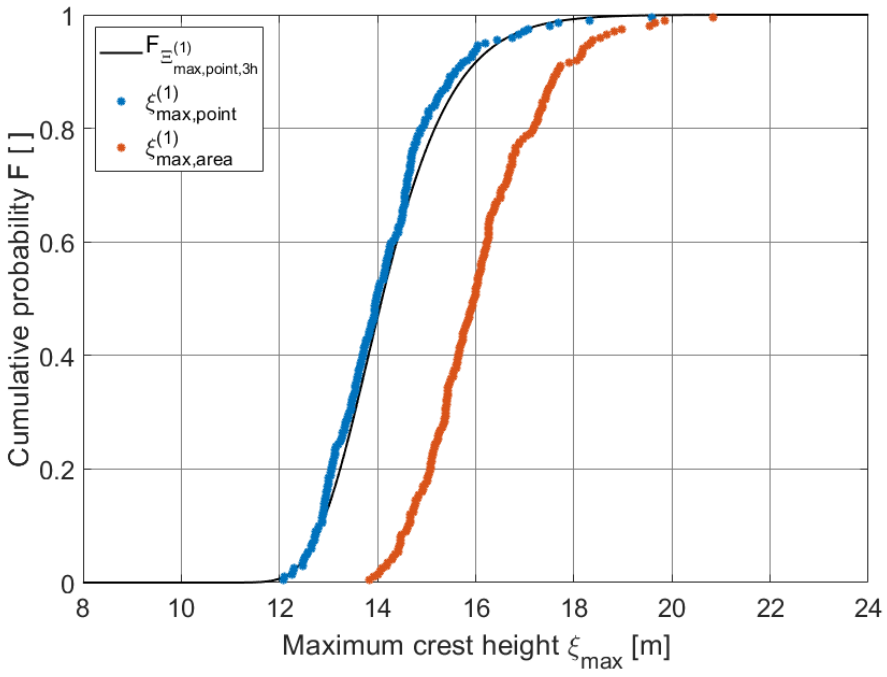

Figure A.31: *Area and point maximum crest heights from simulations with $dx, dy = 100$ m, along with Gaussian extreme value distribution.*

B Appendix: Maximum crest heights from additional analysis of area effect with variation in parameters

B.1 About appendix B

Appendix B contains the area and point maximum crest heights which forms the basis for the results in section 9. Maximum crest heights obtained for variations of the different parameters are given in separate section below. As mentioned in section 9, the JONSWAP wave spectrum is still used for this analysis. Some of the sea states analyzed does not fit well under the assumption of growing wind sea, and therefore the JONSWAP wave spectrum. It is therefore expected that the results produced include some bias at bad combinations of the significant wave height and the spectral peak period.

B.2 Maximum crest heights from additional analysis with variation in significant wave height

The maximum crest heights presented in this section corresponds to the results presented in section 9.2.

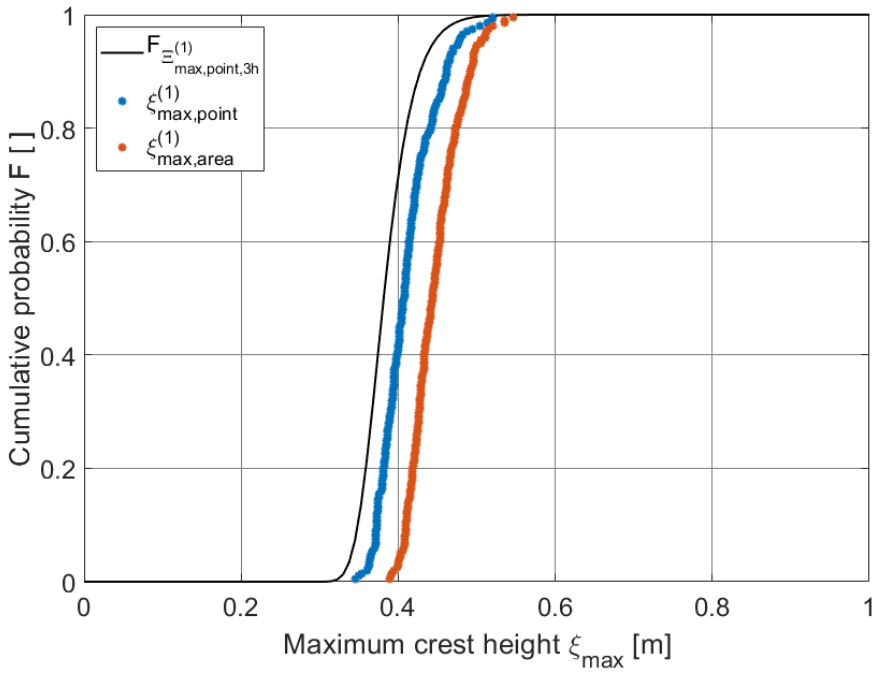

Figure B.1: *Area and point maximum crest heights from simulations with H_s = 0.40 m, T_p = 16.00 s, along with Gaussian extreme value distribution.*

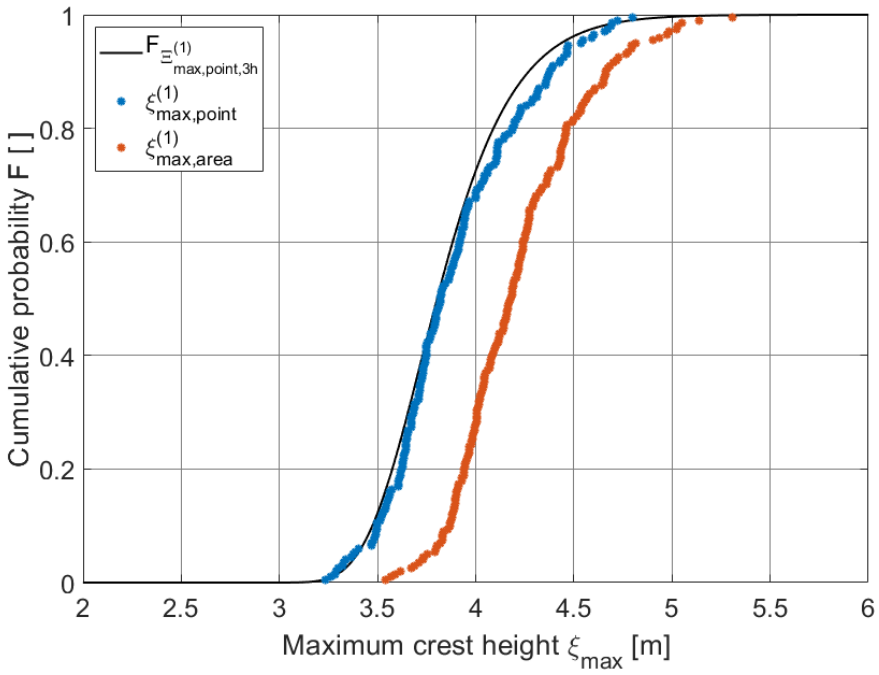

Figure B.2: *Area and point maximum crest heights from simulations with $H_s = 4.00$ m, $T_p = 16.00$ s, along with Gaussian extreme value distribution.*

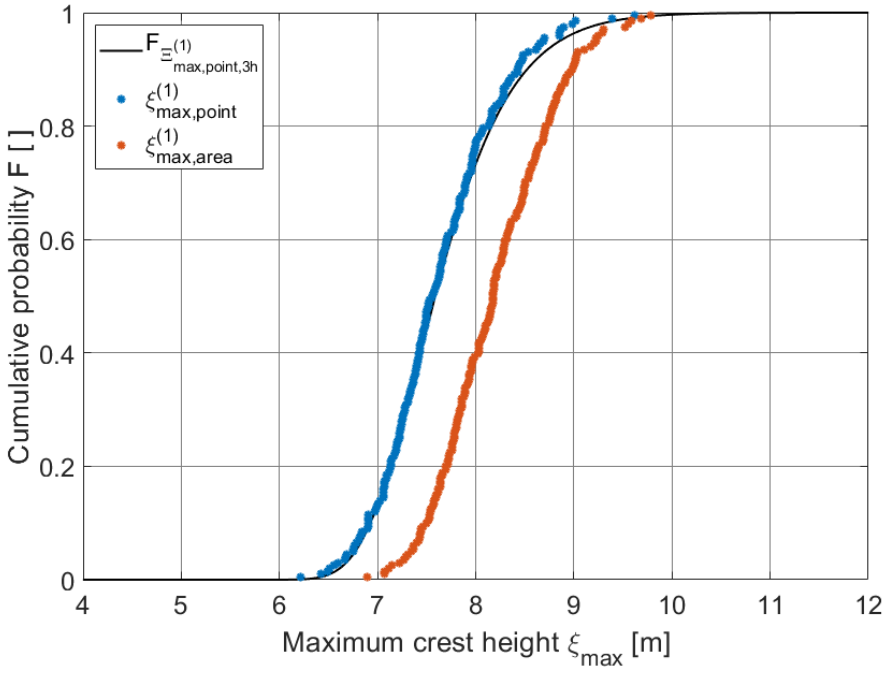

Figure B.3: *Area and point maximum crest heights from simulations with $H_s = 8.00$ m, $T_p = 16.00$ s, along with Gaussian extreme value distribution.*

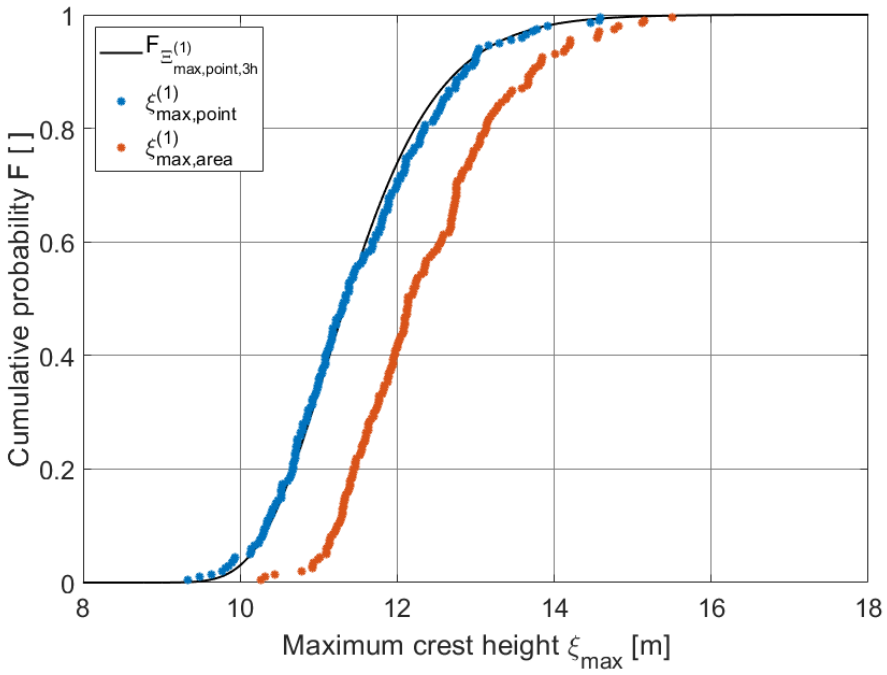

Figure B.4: *Area and point maximum crest heights from simulations with H_s = 12.00 m, T_p = 16.00 s, along with Gaussian extreme value distribution.*

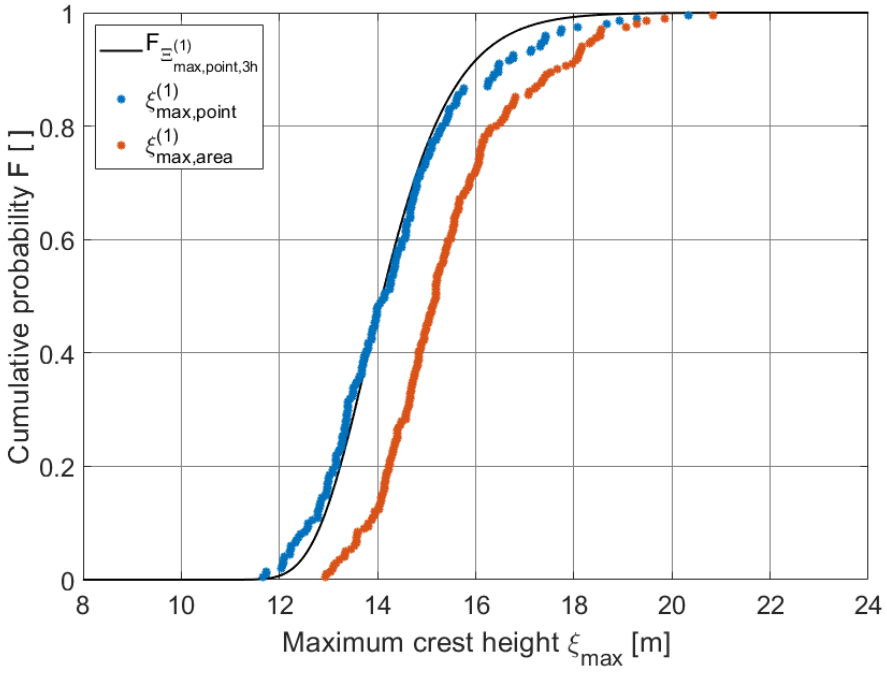

Figure B.5: *Area and point maximum crest heights from simulations with H_s = 14.90 m, T_p = 16.00 s, along with Gaussian extreme value distribution.*

B.3 Maximum crest heights from additional analysis with variation in spectral peak period

The maximum crest heights presented in this section corresponds to the results presented in section 9.4.

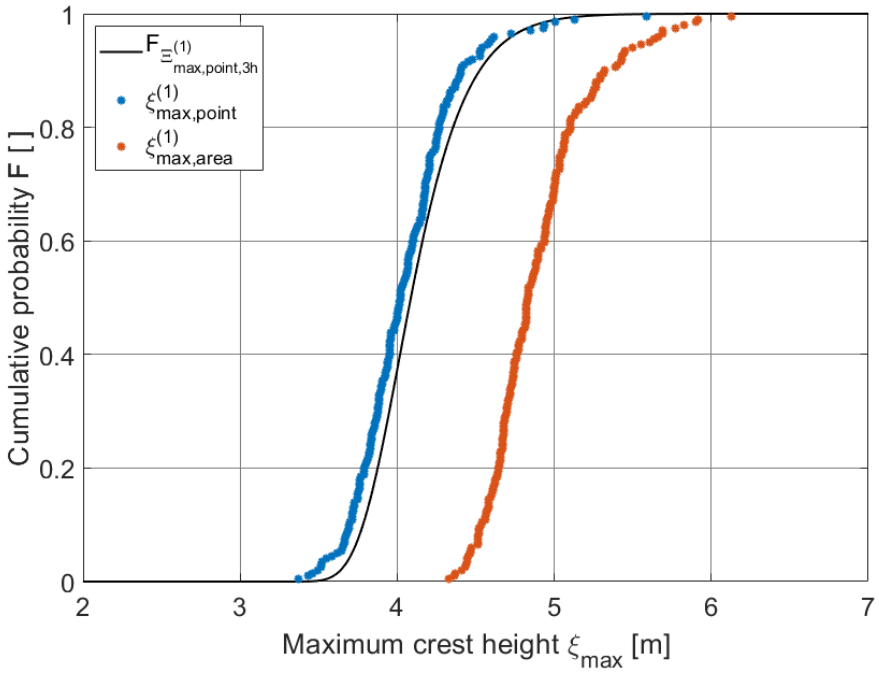

Figure B.6: *Area and point maximum crest heights from simulations with H_s = 4.00 m, T_p = 4.40 s, along with Gaussian extreme value distribution.*

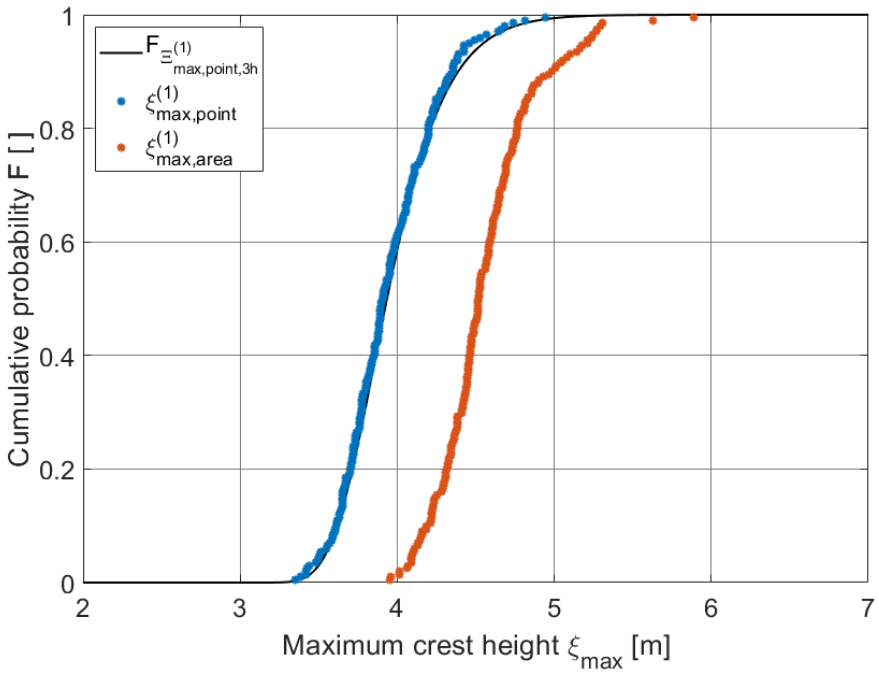

Figure B.7: *Area and point maximum crest heights from simulations with H_s = 4.00 m, T_p = 9.00 s, along with Gaussian extreme value distribution.*

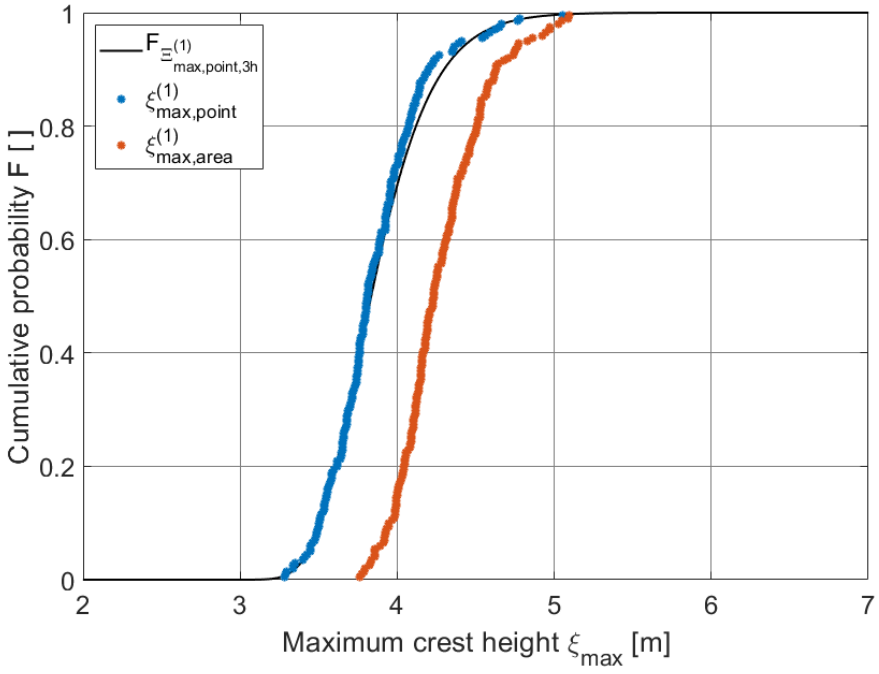

Figure B.8: *Area and point maximum crest heights from simulations with H_s = 4.00 m, T_p = 14.00 s, along with Gaussian extreme value distribution.*

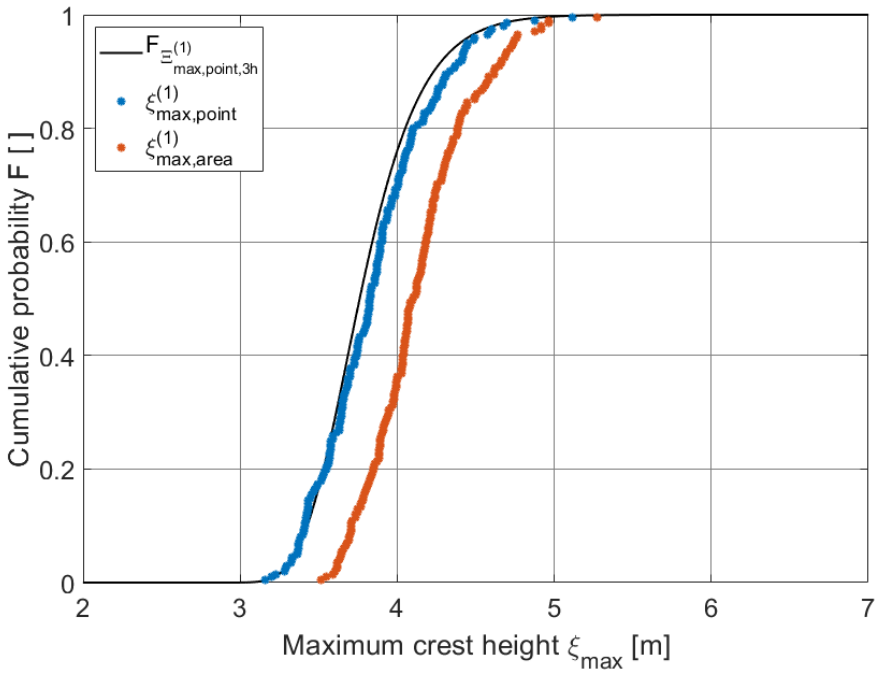

Figure B.9: *Area and point maximum crest heights from simulations with $H_s = 4.00$ m, $T_p = 19.00$ s, along with Gaussian extreme value distribution.*

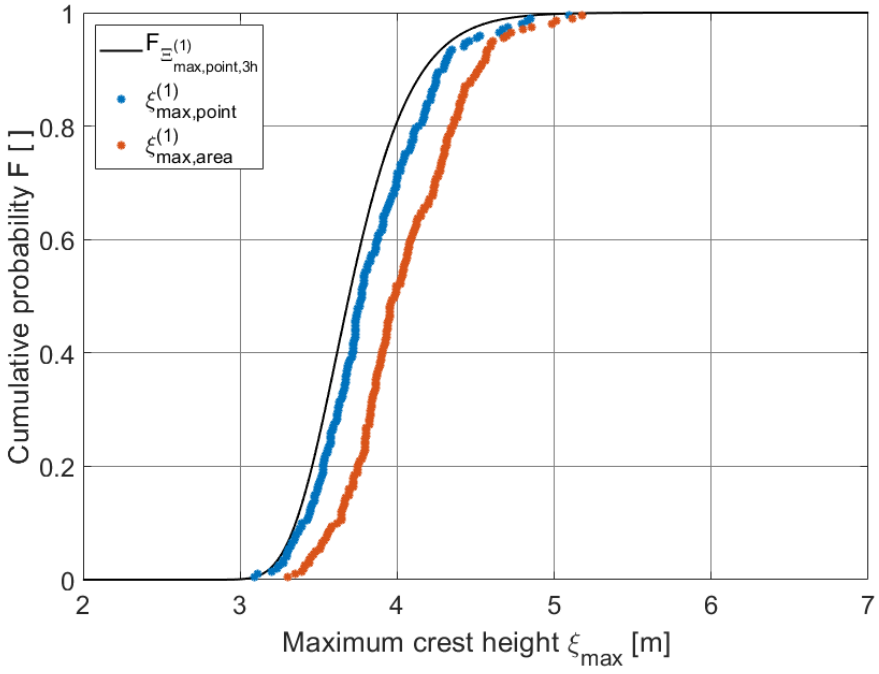

Figure B.10: *Area and point maximum crest heights from simulations with $H_s = 4.00$ m, $T_p = 24.80$ s, along with Gaussian extreme value distribution.*

B.4 Maximum crest heights from additional analysis of area maximum location

The maximum crest heights presented in this section corresponds to the results presented in section 9.6.

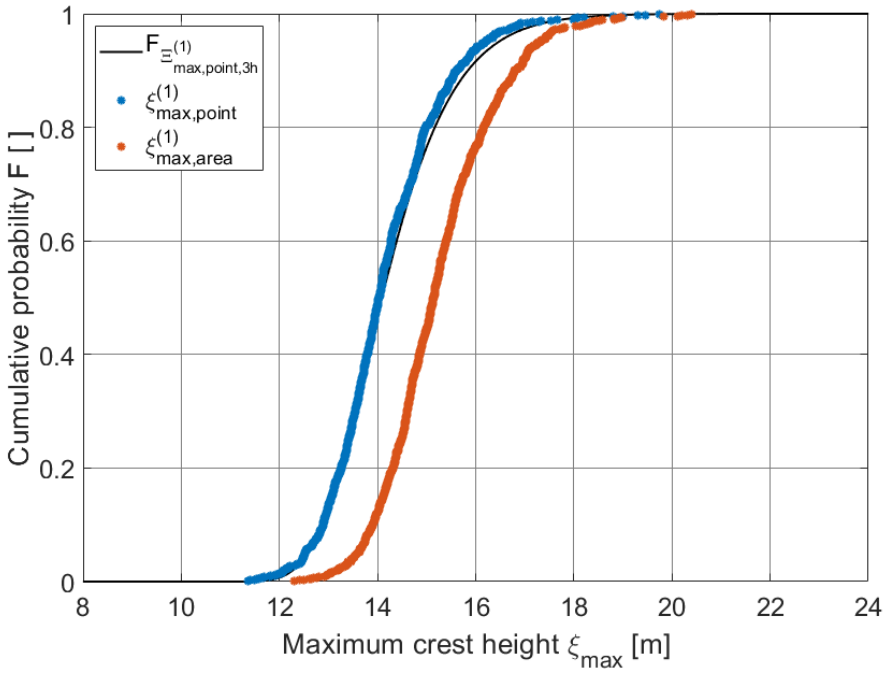

Figure B.11: *Area and point maximum crest heights from analysis of area maximum location, along with Gaussian extreme value distribution.*

C Appendix: Area effect with variation in sea state duration

C.1 About appendix C

This appendix is meant to complement the results given for the analysis with variation in sea state duration in section 8.10, and is done to give a clearer perception to why the area effect changes with sea state duration.

C.2 Area effect with variation in sea state duration

The parameters used in the simulations are the same as used in the analysis with variation in sea state duration in section 8.10 and is given in tables 39 and 49. The simulation duration will however be different. For this case, 200 simulation are done for a three hour sea state. The area maximums and the point maximums will be sampled for each time step in each of the 200 simulations. The high resolution procedure for finding maximums will not be used since the sampling is continuous. The mean of the 200 area maximums $\xi^{(1)}_{max,area,mean}$ and the mean of the 200 point maximums $\xi^{(1)}_{max,point,mean}$ at each time step are plotted as a function of sea state duration. The mean area effect $\alpha^{(1)}_{mean}$ from the 200 simulation is also calculated at each time step and plotted as a function of sea state duration. Figure C.1 shows the results from the simulations.

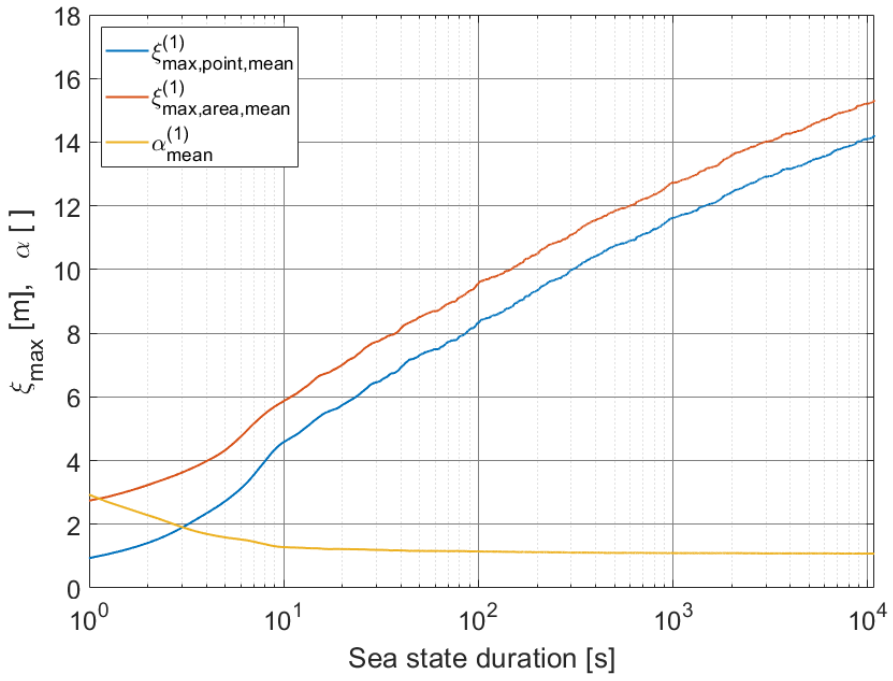

Figure C.1: *Mean of 200 area maximums, mean of 200 point maximums and mean area effect as a function of sea state duration.*

It is seen from the figure that the mean of the 200 area maximums and the mean of the 200 point maximums both increase as the sea state duration increase. However, the ratio between the mean of the 200 area maximums and the mean of the 200 point maximums decrease as the sea state duration increases, resulting in a decrease in the mean area effect when the sea state duration increases. Note that due to the logarithmic scale on the x-axis in the figure, the x-axis

starts at one second and not at zero seconds. The expected mean of the point maximums will therefore not be 0.

D Appendix: Sample of area maximum crest heights and locations for different area sizes

D.1 About appendix D

Appendix D contains a sample of maximum area crest heights and their location with variations in square area size. All simulations are done with the same parameters as used in the analysis of the area effect with variation in parameters in section 8. The parameters can be found in tables 49 and 39, with a simulation duration of one hour and variations in the area size. The area grid size used for all simulations are 5m*5m. Gaussian simulations using random wave amplitudes are used. One random simulation have been done for each variation in area size. The two figures given in each section are from the same random simulation.

D.2 Area maximum crest height for a 40m*40m area during one hour

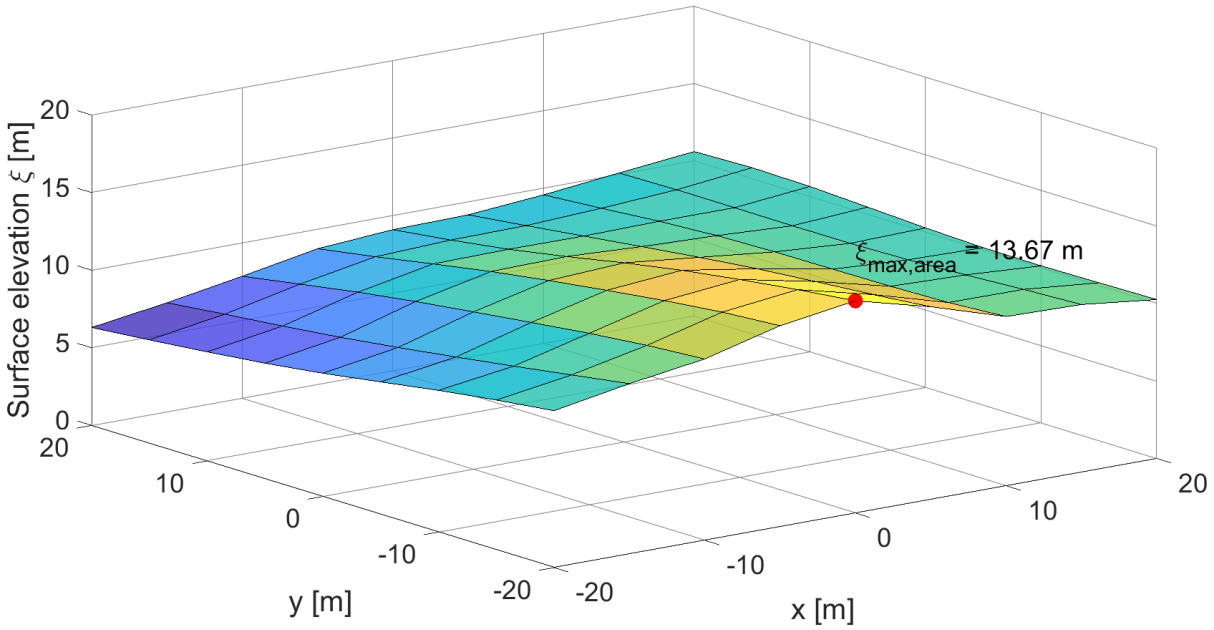

Figure D.1: *Snapshot of surface elevation process at time of area maximum from a one hour simulation of a 40m*40m square area. The red dot indicates area maximum.*

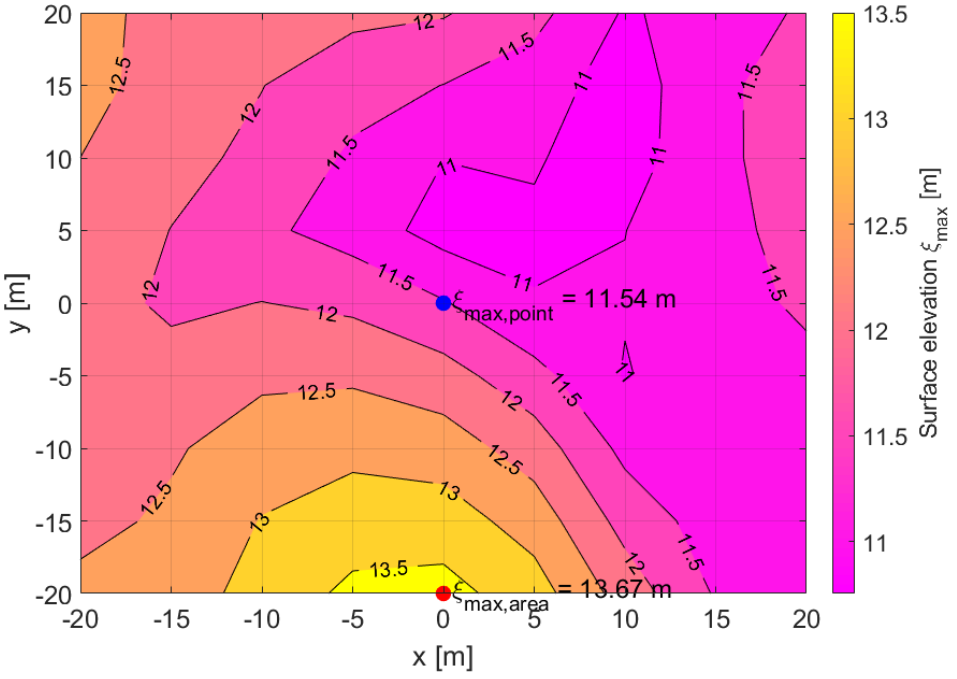

Figure D.2: *Contour plot of maximum surface elevation during one hour at all separate points from the same simulation. The blue dot indicates center point maximum and the red dot indicates area maximum.*

D.3 Area maximum crest height for a 100m*100m area during one hour

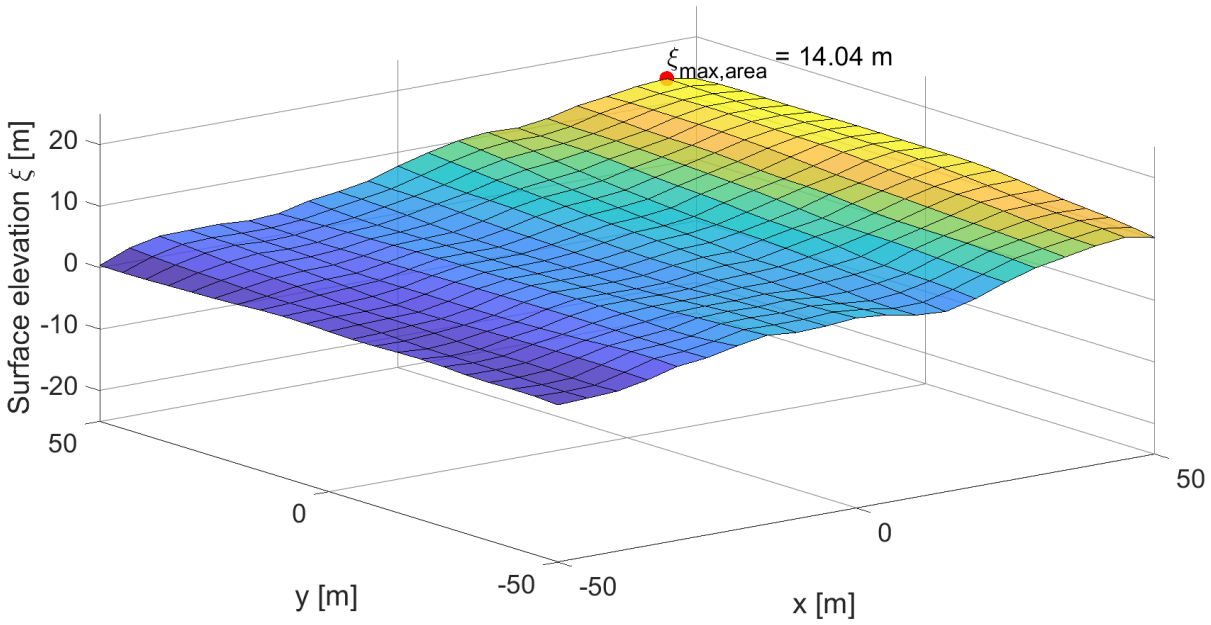

Figure D.3: *Snapshot of surface elevation process at time of area maximum from a one hour simulation of a 100m*100m square area. The red dot indicates area maximum.*

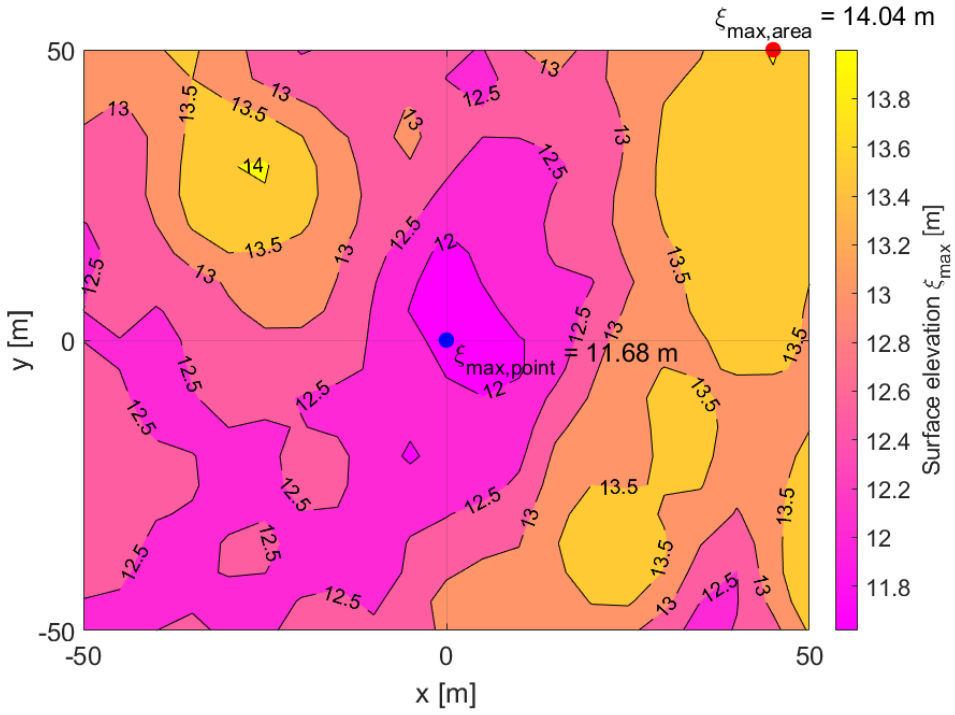

Figure D.4: *Contour plot of maximum surface elevation during one hour at all separate points from the same simulation. The blue dot indicates center point maximum and the red dot indicates area maximum.*

D.4 Area maximum crest height for a 200m*200m area during one hour

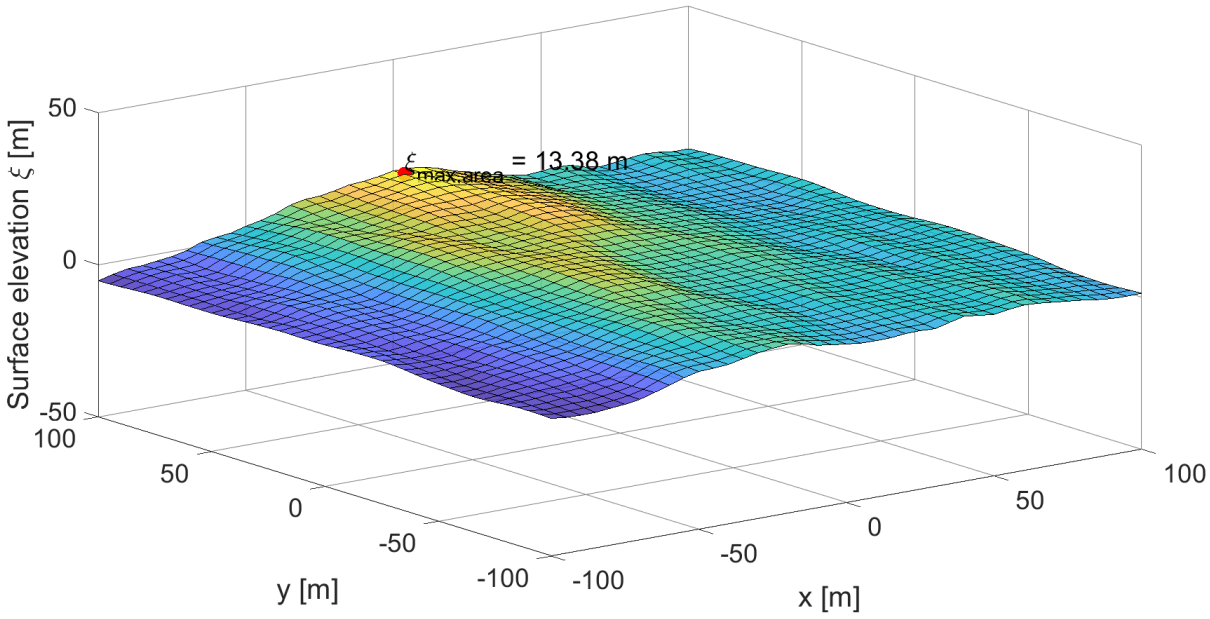

Figure D.5: *Snapshot of surface elevation process at time of area maximum from a one hour simulation of a 200m*200m square area. The red dot indicates area maximum.*

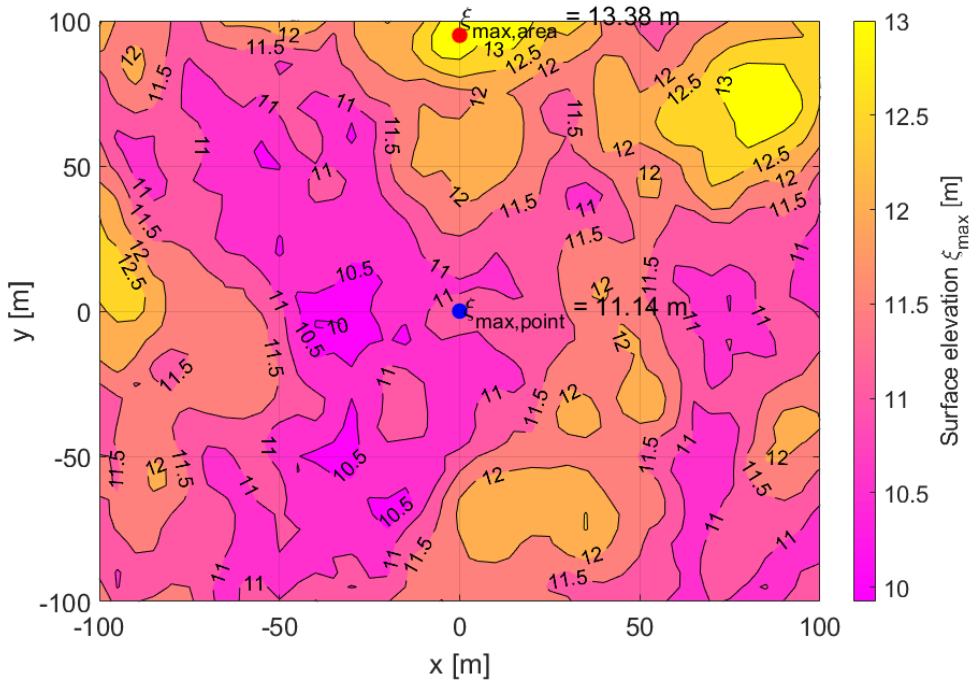

Figure D.6: *Contour plot of maximum surface elevation during one hour at all separate points from the same simulation. The blue dot indicates center point maximum and the red dot indicates area maximum.*

D.5 Area maximum crest height for a 400m*400m area during one hour

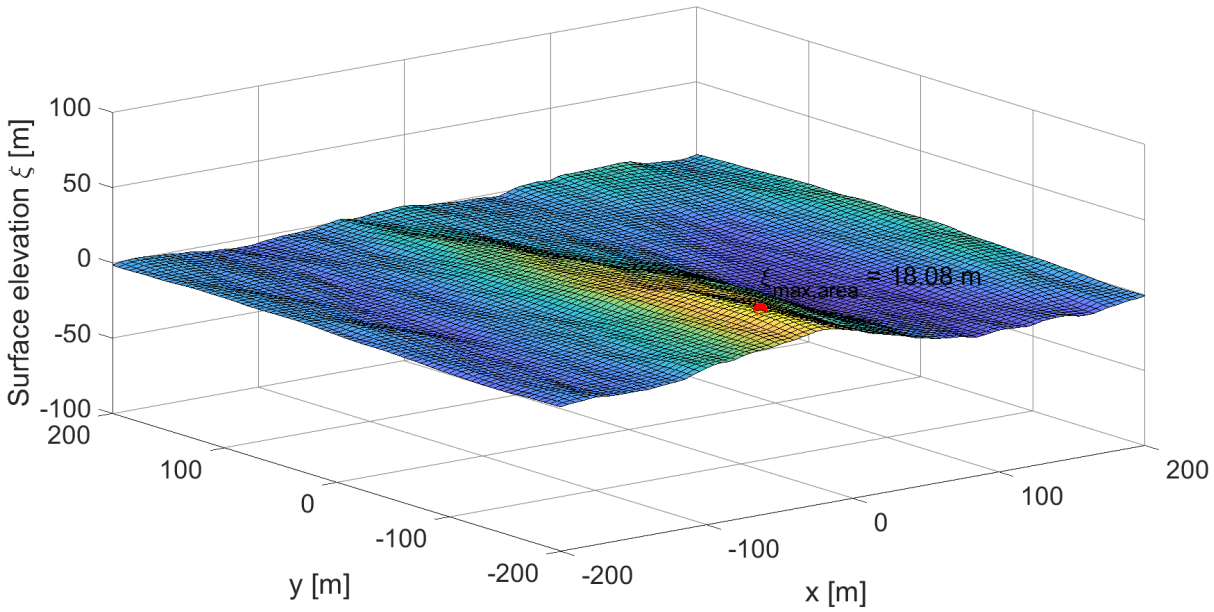

Figure D.7: *Snapshot of surface elevation process at time of area maximum from a one hour simulation of a 400m*400m square area. The red dot indicates area maximum.*

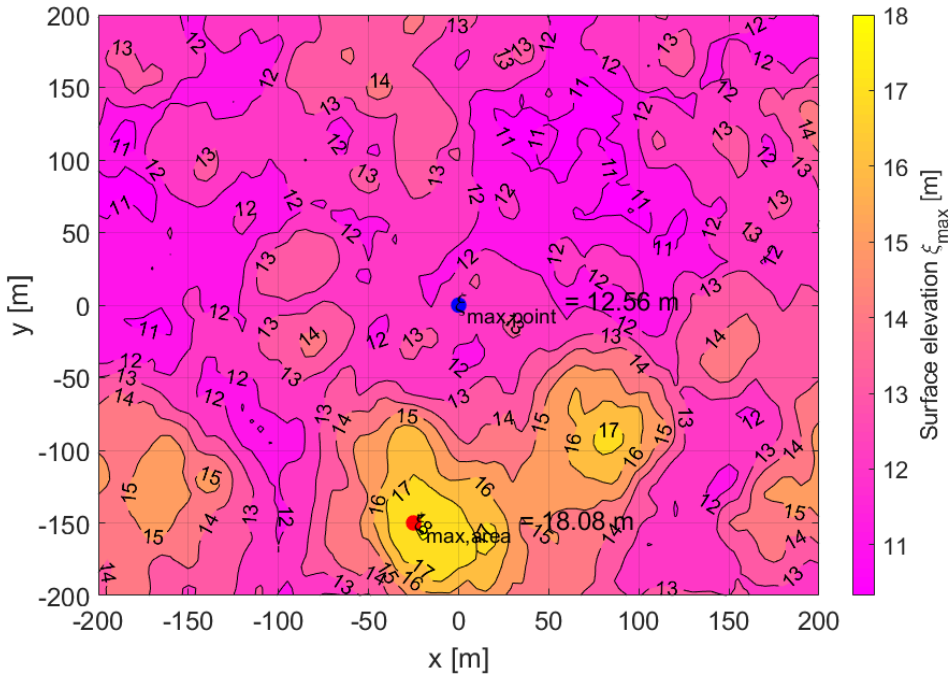

Figure D.8: *Contour plot of maximum surface elevation during one hour at all separate points from the same simulation. The blue dot indicates center point maximum and the red dot indicates area maximum.*

D.6 Area maximum crest height for a 1000m*1000m area during one hour

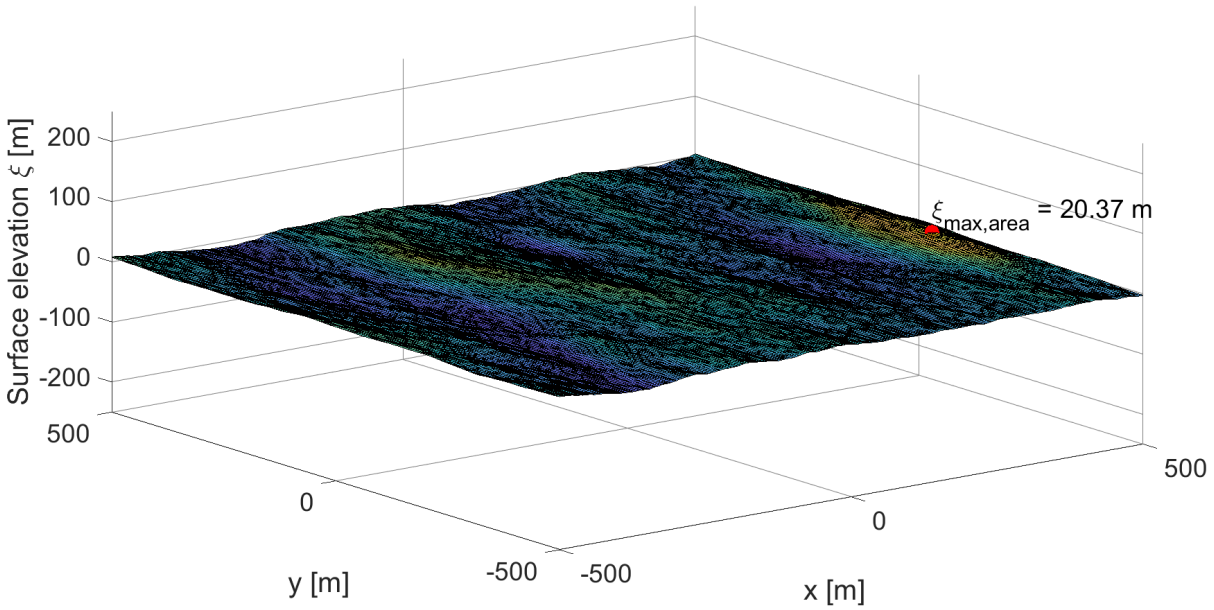

Figure D.9: *Snapshot of surface elevation process at time of area maximum from a one hour simulation of a square 1000m*1000m area. The red dot indicates area maximum.*

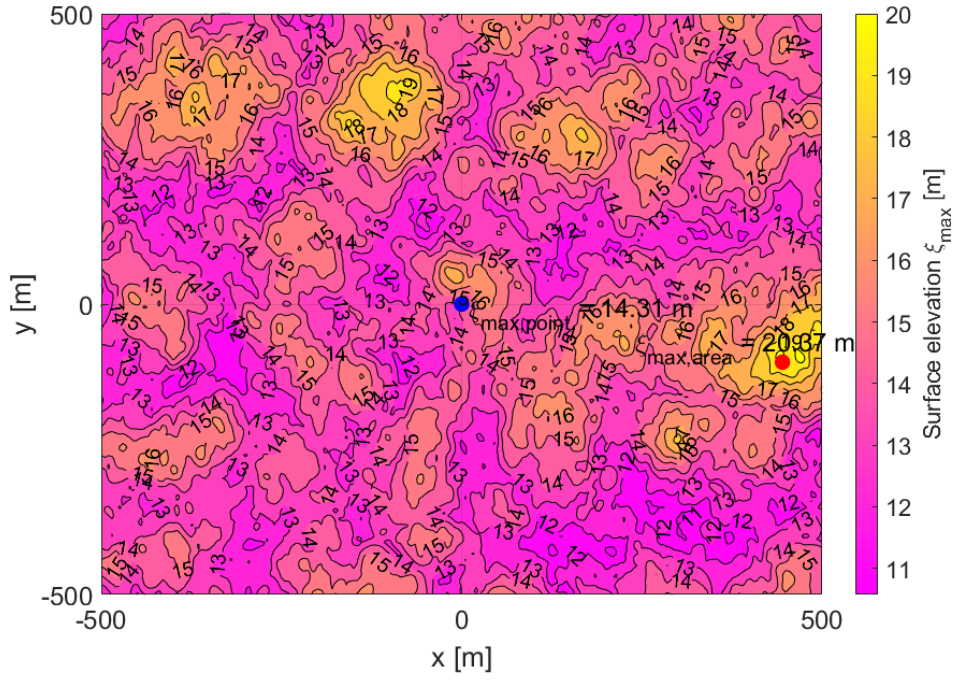

Figure D.10: *Contour plot of maximum surface elevation during one hour at all separate points from the same simulation. The blue dot indicates center point maximum and the red dot indicates area maximum.*

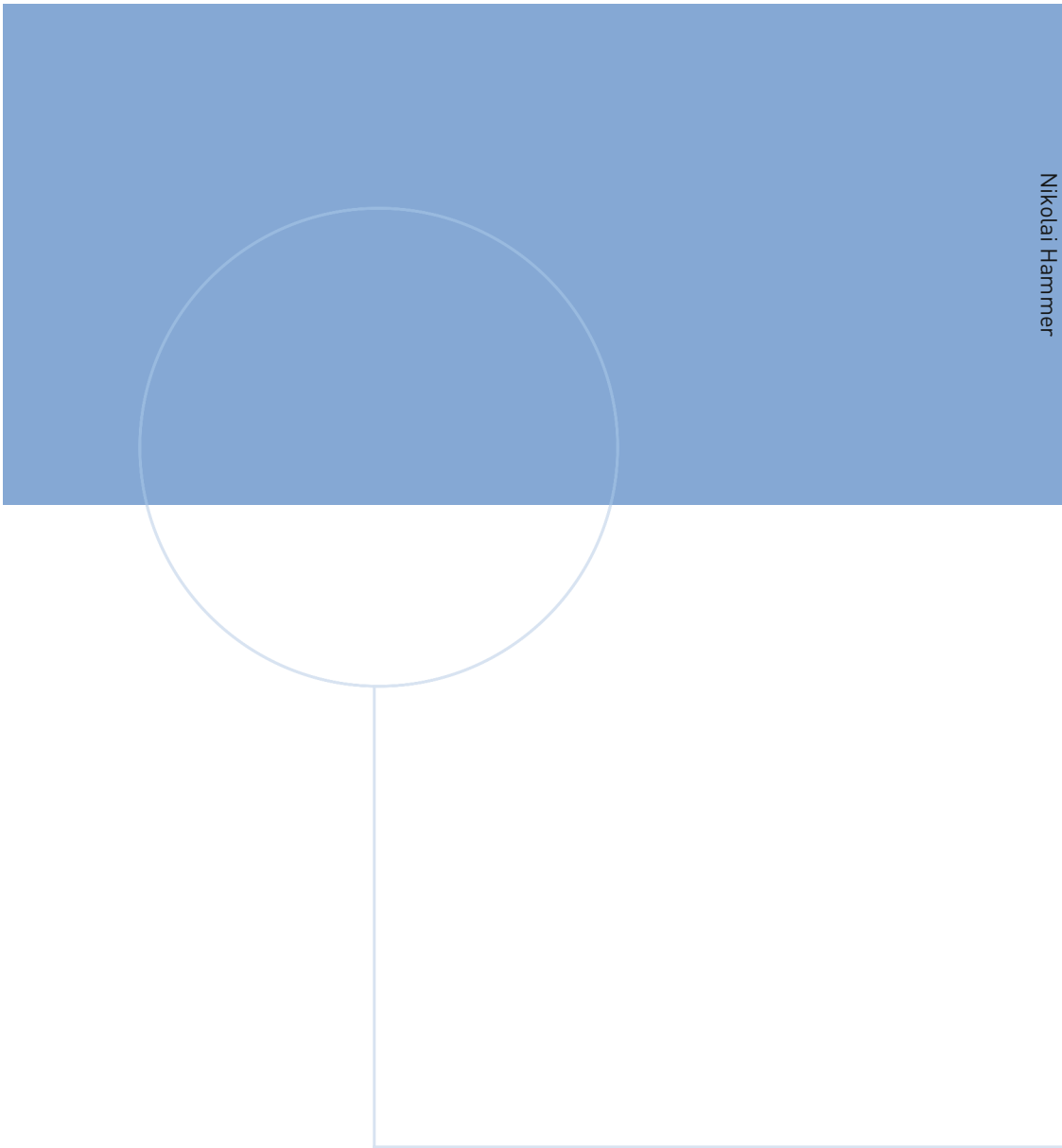

Nikolai Hammer

NTNU
Norwegian University of
Science and Technology